The University Of Sheffield.

Investigating the Control of Macrophage Function by Clearance of Apoptotic Cells using *Drosophila melanogaster*

Hannah Grace Roddie

A thesis submitted in partial fulfilment of the requirements for the degree of Doctor of Philosophy

The University of Sheffield
Faculty of Medicine, Dentistry and Health
Department of Infection, Immunity and Cardiovascular Disease

February 2018

for Grandad

And in loving memory of my Gran, Alice Roddie - the best and most loving Gran I could ever have wished for and who I will miss every day.

11/08/1927 – 31/12/2017

Acknowledgements

First of all I would like to thank my PhD supervisor Dr Iwan Evans for his encouragement, for going above and beyond to support me, and for showing me how to be a scientist! I would also like to thank him for giving me the opportunity to present my work at conferences both in Europe and the USA (I know it wasn't cheap!), and for making the lab such a fun and happy place to be. I would also like to thank Dr Simon Johnston for all of his help and support along the way, and for being a calming presence in times of need. Special thanks also to Emma Armitage for all of her help in the lab along the way.

I would also like to thank my family, and especially my Mum and Dad for their constant love and support, and for always encouraging me to aim high. Thanks also to my boyfriend Paul, for being there through the ups and the downs, and for putting up with me doing even less housework than I usually would. I'd also like to thank my best friend/sidekick Noz (sometimes referred to as Nolwenn) for all the fun and happiness she brings to my life, for being my absolute rock, and for actually enjoying fly tipping.

Thanks also to all of the members of the Evans lab, D43 and The Bateson Centre for providing a fun and stimulating environment to work in, and special thanks to Steve Renshaw, Marc Ellse and the Bateson centre for providing me with extra funding to continue my studies. I'd also like to thank Darren Robinson for training me to use the microscopes and to everyone in the fly facility for all of their help.

Abstract

Perturbed macrophage function can cause or exacerbate a wide variety of diseases, therefore understanding how the function of macrophages is controlled is of great importance. Recent studies in *Drosophila* have shown that increased numbers of engulfed apoptotic cells within macrophages inhibit their migration - an important aspect of macrophage behaviour that is fundamental to their function. Furthermore, the phagocytosis of apoptotic cells is known to have an anti-inflammatory effect on macrophages and aids in the resolution of inflammation. Therefore apoptotic cells are clearly able to regulate the function and behaviour of macrophages, however the mechanisms by which they exert these effects are incompletely understood.

Utilising the *Drosophila* embryo, which contain a population of blood cells known as hemocytes that are functionally and biochemically similar to vertebrate macrophages, it is possible to study the regulation and behaviour of these cells *in vivo*. Hemocytes are highly migratory cells, and upon wounding of the epithelium they rush to the site of injury, mimicking the vertebrate immune response. By genetically altering the number of apoptotic cells for hemocytes to clear in the embryo, we can dissect the molecular mechanisms involved in their regulation of hemocyte function.

Pathological levels of apoptosis were found to inhibit hemocyte inflammatory migrations to wounds, as well as reducing the speed at which they migrate, which were found to be due to defects in apoptotic cell clearance. We also show a role for some of the known apoptotic cell receptors in *Drosophila* during hemocyte inflammatory migrations to wounds, and highlight a previously unidentified role for the apoptotic cell receptors Scab and Simu in hemocyte retention at sites of inflammation. We propose that this may be due to defects in macrophage adhesion at wounds, and may also be due to the defective phagocytosis of cellular debris at wounds in *simu* mutants.

Abbreviations

ADP	adenosine diphosphate
AML-1	acute myeloid leukemia-1
ANOVA	Analysis of Variance
Apoe	Apolipoprotein E
Arp2/3	actin related protein 2/3
ATP	adenosine triphosphate
BAI-1	brain-specific angiogenesis inhibitor
C1q	complement component 1q
CD36	cluster of differentiation 36
Cdc	cell division control protein
cDCP-1	cleaved Death Caspase-1
CED	cell death abnormal
CM-CSF	Granulocyte-macrophage colony-stimulating factor
CNS	central nervous system
COPD	chronic obstructive pulmonary disease
Crq	croquemort
daw	*dawdle*
DCP-1	Death Caspase-1
diap1	death-associated inhibitor of apoptosis 1
DmCaBP1	*Drosophila melanogaster* calcium-binding protein 1
DNA	deoxyribonucleic acid
DOCK	dedicator of cytokinesis
dpp	*decapentaplegic*
Drpr	Draper
DUOX	dual oxidase
ECM	extracellular matrix
ELMO	engulfment and cell motility protein
Ena	Enabled
ER	endoplasmic reticulum
F-actin	filamentous actin
G-actin	globular actin
GAL4	galactose responsive transcription factor
gcm	*glial cells missing*
GEF	guanine exchange factor
GFP	green fluorescent protein
GTP	guanine triphosphate
H_2O_2	hydrogen peroxide
hid	*head involution defective*
IL	interleukin
ITAM	immunoreceptor tyrosine-based activation motif
JNK	c-Jun N-terminal kinases
JP	junctophilin

LPS	lipopolysaccharide
LRP1	Low density lipoprotein receptor-related protein 1
mbc	myoblast city
MerTK	Proto-oncogene tyrosine-protein kinase
MFGE8	milk fat globule-epidermal growth factor 8
MMP	Matrix metalloproteinase
Mys	Myospheroid
NADPH	nicotinamide adenine dinucleotide phosphate
NF-kB	nuclear factor kappa-light-chain-enhancer of activated B cells
$P2Y_2$	purinergic receptor P2Y2
PATx	PBT containing 1% Bovine Serum Albumin
PBS	phosphate buffered saline
PBT	PBS containing 0.1% Triton-X 100
PDGF	platelet-derived growth factor
PGE_2	prostaglandin E2
PI	propidium iodide
PI3K	Phosphoinositide 3 Kinase
PIP3	Phosphatidylinositol (3,4,5)- Trisphosphate
PKD2	polycyctic kidney disease 2
pnt	*pointed*
PS	phosphatidylserine
PSR	phosphatidylserine receptor
Pvf	PDGF- and VEGF- related factor
Pvr	PDGF- and VEGF-receptor related
Rac	Ras-related C3 botulinum toxin substrate
Rap	Repressor/Activator site binding Protein
Repo	reversed polarity
Rho	ras-like GTP-binding protein
RNA	ribonucleic acid
ROS	reactive oxygen species
S-1-P	sphingosine-1-phosphate
S2	Schneider 2
Scb	Scab/αPS3 integrin
SD	standard deviation
Simu	six-microns-under
Src	Proto-oncogene tyrosine-protein kinase Src
srp	*serpent*
STIM	stromal interaction molecule
Syk	spleen tyrosine kinase
TGF	transforming growth factor
TIM-4	T-Cell Immunoglobulin Mucin Receptor 4
TNF	tumor necrosis factor
TRPP	transient receptor potential polycystic
UAS	upstream activating region
upd	unpaired

UTP	uridine triphosphate
VASP	Vasodilator-stimulated phosphoprotein
VEGF	vascular endothelial growth factor
VNC	ventral nerve cord
Vps34	phosphatidylinositol 3-kinase VPS34
WAVE	Wiskott-Aldrich syndrome protein family verprolin-homolog
Zap	Zeta-chain-associated protein kinase
α/βPS	α/β position-specific integrin
βυ	beta-nu integrin

Table of contents

Table of figures

Chapter 1: Introduction

The removal of apoptotic cells, cells that have been instructed to die because they are unnecessary, diseased or injured, is an important process throughout development and in tissue homeostasis (Poon et al. 2014). Apoptotic cells that are not swiftly cleared may progress to secondary necrosis, whereby the cell membrane breaks open and the contents of the cell spills into the surrounding environment, stimulating an immune response (Elliott and Ravichandran 2010). Furthermore, the accumulation of uncleared apoptotic cells can cause chronic inflammation and can eventually lead to autoimmunity (Poon et al. 2014; Szondy et al. 2014). The clearance of apoptotic cells is carried out by phagocytes, which can be "professional" such as macrophages, or "non-professional" tissue-resident cells such as glia.

Macrophages are highly motile leukocytes that, along with apoptotic cell clearance, have a range of important functions such as the deposition of extracellular matrix, engulfment of pathogens and cellular debris, and play a part in both the initiation and resolution of inflammation (Murray and Wynn 2011). As such, perturbed macrophage function can cause or exacerbate a wide variety of diseases such as rheumatoid arthritis, chronic inflammation, cancer and lupus (Kinne et al. 2007; Li et al. 2010; Pollard 2004). It is therefore of great importance and potential benefit to understand how macrophage function is regulated.

The clearance of apoptotic cells is known to induce an anti-inflammatory phenotype in macrophages and aids in the resolution of inflammation (Szondy et al. 2017; Huynh et al. 2002; Valerie A. Fadok et al. 1998; Voll et al. 1997). Recent studies have also shown that apoptotic cells are capable of reducing the migratory capability of macrophages *in vivo*, an important aspect of their function (Berg et al. 2016; Evans et al. 2013). However how apoptotic cells affect macrophage function and behaviour *in vivo* is incompletely understood. Using the *Drosophila* embryo as a model organism I will explore the relationship between apoptotic cell clearance and macrophage function *in vivo*, and attempt to identify the mechanisms by which apoptotic cells control macrophage migration.

1.1 *Drosophila* embryonic hemocytes as a model to study macrophage biology *in vivo*

The fruit fly *Drosophila melanogaster* has played an important role in the development of our understanding of embryonic patterning and morphogenesis. It is also a well-established, genetically tractable model used to study the innate immune system (Lemaitre and Hoffmann 2007). In addition to a systemic innate immune response *Drosophila* possess a cellular arm, which consists of three main types of blood cells: crystal cells, which are required for melanisation, lamellocytes that encapsulate invading parasites, and plasmatocytes – the *Drosophila* equivalent of vertebrate macrophages, hereafter referred to simply as hemocytes (Crozatier and Meister 2007). Hemocytes have diverse functions within the organism that are similar to those of vertebrate macrophages (Wood and Jacinto 2007), one of their main roles being the detection and removal of apoptotic cells. Hemocytes also phagocytose invading pathogens, with hemocytes making up the entire cellular arm of the fly innate immune system, and are also capable of engulfing cellular debris at sites of injury or damage (Stramer et al. 2005). The similarity of hemocytes to vertebrate macrophages is demonstrated by their specification, which involves molecules related to those used in vertebrate myeloid lineages (Evans et al. 2003). For example, hemocyte specification involves the transcription factor Serpent, which is a homolog of mammalian GATA factors (Lebestky et al. 2000). Hemocytes also express many molecules related to those used in vertebrate myeloid cells such as Croquemort and Draper (Franc et al. 1996; Freeman et al. 2003) members of the CD36 and CED-1 families respectively. Hemocytes are also morphologically similar to vertebrate macrophages.

1.1.1 Hemocyte specification

Drosophila possess three different types of blood cells – crystal cells, lamellocytes and hemocytes which are all formed from the same precursors. Hemocytes are first specified in the head mesoderm of the embryo at around stage 11 of embryonic development (Tepass et al. 1994). At this stage, the transcription factor *serpent* (*srp*), which is a homolog of mammalian GATA transcription factors, is expressed in this area of the embryo and is required for haematopoesis (Rehorn et al. 1996). The expression of *srp* is in turn required for the expression of the AML-1 homolog *lozenge* (*lz*), which is a marker for the crystal cell lineage (Lebestky et al. 2000). However, it is the expression of the transcription factor *glial cells missing* (*gcm*) in hemocytes downstream of *srp* that causes their differentiation into macrophages (Lebestky et al. 2000; Bernardoni et al. 1997). An additional and related transcription factor, *gcm2*, is also

required in the differentiation of macrophages from hemocytes, and together with *gcm* is required for the expression of the hemocyte-specific gene *croquemort* (*crq)* (Alfonso and Jones 2002). Aside from the initial wave of haematopoesis in the embryo, haematopoesis also occurs in both the larval haematopoetic pockets and the lymph gland (Jung et al. 2005; Lanot et al. 2001; Gold and Brückner 2014), but have only recently been reported to occur in the adult (Ghosh et al. 2015). In larval haematopoetic pockets, embryonic-derived macrophages self-replicate in segmentally repeated patches associated with peripheral neurons (Makhijani et al. 2011). In contrast, in the lymph gland hemocyte precursors (prohemocytes) are maintained and are capable of differentiating into all three *Drosophila* blood cell types (Gold and Brückner 2014; Jung et al. 2005).

1.1.2 Hemocyte migration

A fundamental feature of macrophages essential to their proper functioning is an ability to migrate, and more specifically to respond appropriately to cues and move, or chemotax, towards areas where they are required; an attribute conserved in the highly dynamic *Drosophila* hemocytes. Hemocytes are highly migratory and respond to a variety of cues in vivo, including PDGF/Vegf homologs used to direct their developmental dispersal (Heino et al. 2001; Cho et al. 2002), tissue damage (Stramer et al. 2005; Babcock et al. 2008) apoptotic cells (Moreira et al. 2010) and even sites of cancerous growth (Pastor-Pareja et al. 2008; Cordero et al. 2010). Before developmental dispersal *Drosophila* blood cells are first specified in the embryonic head mesoderm, from where the migratory hemocytes move in a well-defined pattern along the ventral nerve cord and dorsal vessel before migrating laterally to spread throughout the entire embryo (Tepass et al. 1994; Wood et al. 2006). They are also able to migrate towards sites of injury in a process that resembles the mammalian inflammatory response (Stramer et al. 2005). Interestingly, hemocytes prioritise their embryonic developmental migrations over their wound responses in early embryogenesis (Moreira et al. 2010).

The migration of macrophages requires massive changes in the structure and organisation of the actin cytoskeleton. The process of cell migration involves several steps that are repeated in cycles to produce directional movement of the cell. To move in a given direction macrophages must first extend actin rich protrusions of the plasma membrane at the leading edge of the cell. It is thought that the main type of such a protrusion that macrophages use are lamellipodia (Rougerie et al. 2013), which are sheet-like, spreading protrusions of the plasma membrane. The migrating cell then forms integrin-mediated contacts with the substratum across which it is moving in order to produce points of adhesion upon which to generate the force to move (Lauffenburger and Horwitz 1996). Finally, the rear of the cell must detach from the

extracellular matrix and contract by involvement of both actin and myosin, allowing the cell to move forward (Lauffenburger and Horwitz 1996). The regulation and timing of these events must be tightly controlled in order for cells to migrate efficiently. For example, feedback between focal adhesions and actomyosin contraction has been shown to produce the correct balance of adhesion and contraction to produce rapid migration (Gupton and Waterman-Storer 2006).

1.1.2.1 Actin cytoskeletal rearrangements in hemocyte migration

Macrophage migration is largely mediated through the lamellipodia: broad, sheet-like protrusions at the front, or leading edge, of the cell whose dynamics are controlled through rearrangements of the actin cytoskeleton (Evans and Wood 2014). The lamellipodia was first described in migrating cultured fibroblasts by Abercrombie who observed sheet-like protrusions that contained actin filaments (Abercrombie et al. 1970; Abercrombie et al. 1971) suggesting that actin was important in cell migration. Since then it has been shown that actin polymerization at the leading edge drives the projection of the lamellipodium and in doing so allows cells to migrate (Ridley 2011). The mechanisms controlling lamellipodial-driven cell migration are complex and involve many regulators, both positive and negative, and have been extensively reviewed (Bugyi and Carlier 2010; Krause and Gautreau 2014).

Actin polymerization is the formation and lengthening of actin filaments (F-actin) from monomers of globular actin (G-actin). Branching of the actin network and the subsequent elongation of actin filaments at the leading edge produces the flat, sheet-like lamellipodia (Krause and Gautreau 2014). There are many known regulators of actin polymerization that operate to control lamellipodia projection, many of which have *Drosophila* homologs. One of the most important of these is the actin-related protein 2/3 (Arp2/3) complex (Mullins et al. 1998; Suraneni et al. 2012). The Arp2/3 complex is an actin nucleator which binds to a pre-existing actin filament and acts as a catalyst, bringing together actin monomers to produce a site where a new actin filament can branch from (Krause and Gautreau 2014). Indeed, in *Drosophila* the Arp2/3 complex activator WASH has been shown to be required for hemocyte developmental migration along the VNC from the posterior end of the embryo, and for their normal cell spreading and migration speeds (Verboon et al. 2015; Nagel et al. 2017).

Newly created actin filaments can then be extended via the action of actin elongators such as Ena/VASP and Formins (Romero et al. 2004; Breitsprecher et al. 2011). In this process G-actin monomers are added to the dynamic, so-called barbed end of the actin filament causing its elongation. This process is triggered by signalling from transmembrane receptors that sense

migratory cues, which causes the production of the phospholipid phosphatidylinositol-3,4,5-trisphosphate (PIP_3) and the activation of the Rac GTPase (Krause and Gautreau 2014). This signalling activates the SCAR/WAVE complex that then recruits the Arp2/3 complex to the leading edge, hence mediating its actin nucleating activity and inducing lamellipodial projection (Krause and Gautreau 2014). The SCAR/WAVE complex has been shown to be essential for the *in vivo* migration of *Drosophila* embryonic macrophages through its role in the formation of lamellipodia, as SCAR mutant *Drosophila* macrophages exhibit significantly reduced lamellipodia and macrophage migration speeds (Evans et al. 2013).

The growth of new filaments can be prevented by capping proteins that cover the barbed end of the filament, blocking the addition of new monomers (Cooper and Sept 2008). However, to allow for elongation this capping must be stopped. ENA/VASP proteins protect the barbed filament ends from being capped and in doing so promote elongation by recruiting profilin-actin (Barzik et al. 2005; Pasic et al. 2008). For G-actin to be able to polymerize it must have ATP bound. Profilin is a protein that causes ADP to dissociate and ATP to bind to G-actin, thus priming it for polymerization (Krause and Gautreau 2014). In *Drosophila* embryonic macrophages Ena regulates the dynamics of the lamellipodia, with Ena inactivation causing increased stability and persistence of lamellipodia whereas its overexpression decreases lamellipodia persistence but increases their protrusion speed (Tucker et al. 2011). This makes logical sense as one can imagine that lamellipodia with long filaments caused by elongation by Ena may cause fragile, less structurally sound lamellipodia than when they are shorter with a higher density of branching. This also provides a further demonstration of the requirement for fine regulation of the different components of the migratory machinery to produce optimal conditions for migration.

1.1.2.2 The role of integrins in hemocyte migration

Integrins are important during the migration of cells, as they represent the link between the extracellular matrix components on which they migrate and the intracellular actin network (Huttenlocher and Horwitz 2011). Integrin transmembrane receptors are heterodimeric in nature, with both an α subunit and a β subunit required to associate non-covalently in order to form a functioning integrin receptor. In mammals 8 different β subunits and 18 α subunits have been identified, whereas *Drosophila* possess fewer of both subunit types, with only 2 β and 5 α subunits (Bökel and Brown 2002). Integrins are essential components of cellular focal adhesions; protein complexes linking cells to the extracellular matrix that represent signalling centres mediating cellular interaction with the ECM. Therefore, integrins as well as extracellular matrix components are important players in cellular migration.

Several roles for integrins have been identified in *Drosophila* hemocyte migration. Firstly, it is known that the α integrin subunit Inflated (αPS2) is required for the penetration of hemocytes into the germband during their developmental migration in the embryo (Siekhaus et al. 2010). The PDZ-GEF Dizzy has also been found to be important in hemocyte migration, and it is thought that this is due to its ability to control integrin-dependent adhesion through Rap-1 mediated control of the βPS integrin *mys* function (Huelsmann et al. 2006). Indeed, hemocytes in *mys* mutant embryos migrate at slower speeds than controls and also have defects in hemocyte developmental migration, most notably along the ventral midline of the embryo (Comber et al. 2013). This study also shows that the α integrin subunits αPS1 and αPS3 (Scab) are required for the normal migration of hemocyte along the ventral midline by embryonic stage 13, and that this migration is delayed in mutants for these subunits (Comber et al. 2013). In this study they also go on to show that *mys* is required in hemocytes for normal contact inhibition during hemocyte migration, a factor that controls the dispersal and distribution of hemocytes in the *Drosophila* embryo (Stramer et al. 2010), with hemocytes remaining in contact with each other for longer periods of time (Comber et al. 2013). Finally they also showed that *mys* is required for the normal separation of the VNC from the epidermis (Comber et al. 2013), a process that is known to be required for the migration of hemocytes along the ventral midline (Evans et al. 2010).

1.1.2 Hemocyte developmental dispersal

Hemocytes are first specified in the head mesoderm at around stage 11 of embryonic development and by stage 12 they begin to migrate away from this area in order to become distributed throughout the entire embryo (Tepass et al. 1994). The migratory routes that hemocytes follow during embryonic development have been well characterised (Tepass et al. 1994). One such route is their penetration into the germ band during late stage 11 and stage 12, prior to germ band retraction (Tepass et al. 1994; Siekhaus et al. 2010). This transmigration of hemocytes across an epithelium requires the expression of RhoL to control the localization of the GTPase Rap1 to the cell surface, which in turn promotes integrin binding to cadherin at epithelial junctions to allow the transmigration of hemocytes through the epithelium (Siekhaus et al. 2010). This shows that the infiltration of hemocytes through the epithelium mimics that of vertebrate leukocyte transmigration through the endothelium during inflammation, and uses similar mechanisms to do so (Shimonaka et al. 2003).

The developmental dispersal of hemocytes during embryogenesis requires their expression of PDGF and vascular endothelial growth factor (VEGF) receptor-related (Pvr), and embryos mutant for *pvr* exhibit hemocyte accumulation in the head (Cho et al. 2002; Heino et al. 2001). It is also known that *Drosophila* homologs of VEGF/PDGF ligands (known as Pvfs) are expressed along developmental migration pathways in the embryo, and ectopic expression of Pvf2 is sufficient to re-route hemocyte migration, suggesting that Pvfs act as chemoattractants during the developmental dispersal of hemocytes (Cho et al. 2002). One well-characterised route of hemocyte migration during development is their dispersal along the ventral nerve cord (VNC). At stage 13 of embryonic development, hemocytes form a continuous line along the ventral midline of the embryo, and from here they migrate laterally in a highly regulated fashion to form three rows of hemocytes by stage 15 (Wood et al. 2006). This highly directional migration is regulated by the tightly controlled spatial and temporal expression of Pvf2 and Pvf3 ligands along the VNC, and a decrease in Pvf2 expression on the midline coincides with the lateral migration of hemocytes (Wood et al. 2006). Indeed, overexpression of Pvf2 along the ventral midline in *Drosophila* embryos blocks the lateral migration of hemocytes (Wood et al. 2006). Therefore the expression of chemoattractants orchestrates the developmental migration of hemocytes throughout the embryo. Interestingly Pvf2 and 3 with their receptor Pvr have also been shown to regulate cellular growth, and Pvr signalling is also required for hemocyte survival (Sims et al. 2009; Brückner et al. 2004).

As mentioned previously, the process of contact inhibition is also important for ensuring the normal dispersal of hemocytes during their developmental migration. Contact inhibition (also called contact inhibition of locomotion) is the halting of migration upon colliding with another cell that was first observed by Abercrombie in the 1950's (Abercrombie and Heaysman 1953). In the *Drosophila* embryo this process has been shown to regulate the dispersal of hemocytes along the ventral nerve cord during development and patterns their movements (Stramer et al. 2010; Davis et al. 2012). When hemocytes collide with each other their microtubules align through the lamellipodia, and forcing these microtubules to depolymerize prevents contact inhibition and causes hemocytes to clump together (Stramer et al. 2010). The actin cytoskeleton is also involved in this process, with the formation of an actin cable occurring between colliding cells at an angle perpendicular to their lamellipodia that links the two cells (Davis et al. 2015). In fact a very brief adhesion event seems to occur at the point where the actin cables from colliding cells meet, and this adhesion is required for the build-up of tension that drives contact inhibition (Davis et al. 2015).

1.1.4 Inflammatory recruitment of hemocytes

Another example of directed hemocyte migration is the inflammatory migration of hemocytes towards sites of tissue damage, which mimics the vertebrate immune response (Fig.1.1). When the epithelium of *Drosophila* embryos is wounded using a laser, there is an immediate and rapid migration of hemocytes to the site of the wound where they engulf cellular debris (Stramer et al. 2005). The earliest known chemotactic cue for this migration is the production of hydrogen peroxide (H_2O_2) from the wound site, which was first reported in zebrafish larvae (Niethammer et al. 2009) and that has subsequently been shown to also occur in *Drosophila* embryos (Moreira et al. 2010). Upon wounding, an instantaneous calcium flash occurs within epidermal cells at the wound boundary, which spreads as a wave through several rows of cells from the wound edge via gap junctions (Razzell et al. 2013). This calcium flash results in the activation of the NADPH oxidase DUOX through its EF hand calcium-binding domain and leads to the production of H_2O_2 at wounds (Razzell et al. 2013).

But how do hemocytes sense this wound chemoattractant? The inflammatory migrations of hemocytes to sites of tissue damage require the Src family kinase Src42A, which is thought to detect H_2O_2 in a manner similar to Lyn in zebrafish neutrophils (Yoo et al. 2011; Evans et al. 2015). Src42A subsequently triggers a signalling cascade within hemocytes by phosphorylating the intracellular ITAM domain of the phagocytic receptor Draper, leading to the recruitment and activation of a downstream kinase called Shark (Evans et al. 2015), itself a Zap70/Syk homolog (Ferrante et al. 1995). Interestingly, the expression of Draper by hemocytes has been shown to be regulated by the engulfment of apoptotic cells, a process that is therefore required for hemocytes to gain the ability to respond to wounds (Weavers et al. 2016). Draper expression is thought to be induced in hemocytes upon apoptotic cell engulfment by an increase in intracellular calcium that activates JNK signalling which in turn leads to the up-regulation of Draper expression (Weavers et al. 2016), a process that is also observed in phagocytosis of glia and follicle cells (Etchegaray et al. 2012; MacDonald et al. 2013).

The migration of cells towards chemotactic cues has been shown to be orchestrated by the small GTPases Rho, Rac and Cdc42, which are capable of regulating cell migration by controlling cytoskeletal rearrangements and cell-substrate adhesion downstream of transmembrane receptors detecting migratory cues (Ridley 2001). These proteins are conserved in *Drosophila* and all but one (Cdc42) have been shown to play key roles in the migration of *Drosophila* macrophages to sites of injury in vivo (Stramer et al. 2005). Another important regulator of cell chemotaxis, phosphoinositide 3-kinase (PI3K), has also been shown to be required for the inflammatory migrations of hemocytes to wounds (Wood et al. 2006).

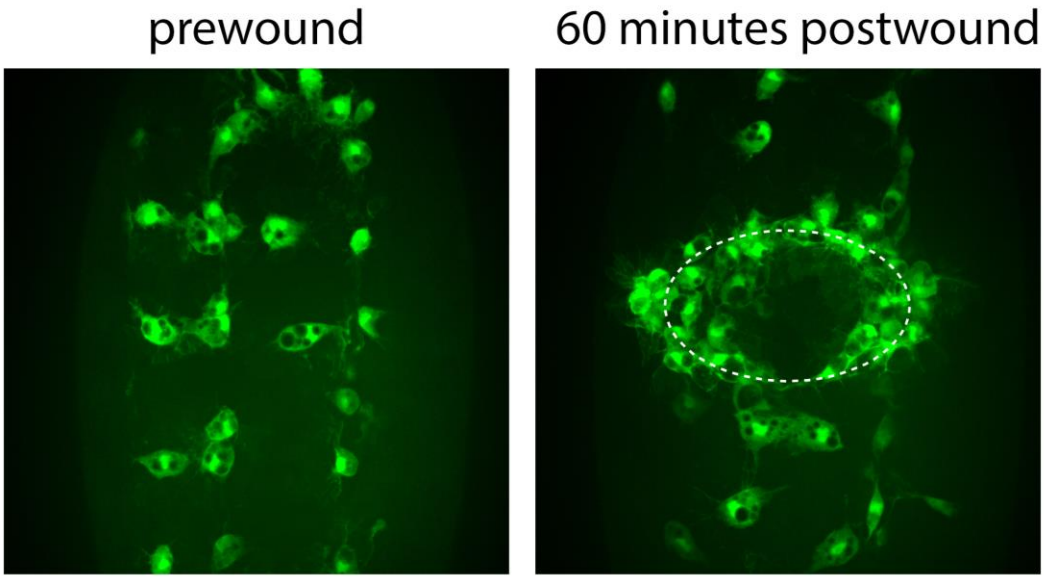

Figure 1.1: Wounding of the Drosophila embryo epithelium triggers a hemocyte inflammatory response
Upon laser ablation of the *Drosophila* embryo epithelium, hemocytes migrate to the site of tissue damage in response that mimics the vertebrate inflammatory response. The images show hemocytes on the superficial ventral nerve cord (VNC) in stage 15 embryos prior to wounding (left), as well as hemocytes at the wound 60 minutes post-wounding (right). Dashed white line represents the wound perimeter.

Altogether *Drosophila* hemocytes are morphologically, functionally and biochemically similar to vertebrate macrophages and behave in many of the same ways. Their mechanisms of migration are also highly conserved between that of vertebrate macrophages and they respond to very similar cues. As *Drosophila* are extremely genetically tractable organisms and the transparent nature of the embryo allows for high resolution imaging of cellular dynamics *in vivo*, this provides us with an excellent model to study the regulation of macrophage function *in vivo*.

1.2 Apoptotic cell clearance

Apoptosis, or programmed cell death, is a tightly regulated form of cell death that occurs when cells are no longer required or pose a threat to the health of an organism. This is in contrast to cellular necrosis when cell lysis occurs, resulting in the spilling of intracellular contents into the surrounding environment and triggering an immune response. Characteristics of apoptosis include cell shrinkage, DNA fragmentation and cellular blebbing. Cells instructed to undergo apoptosis are swiftly removed by phagocytes, a process that is known to be anti-inflammatory (Szondy et al. 2017).

In *Drosophila* apoptotic stimuli trigger apoptosis by inducing expression of the three pro-apoptotic genes *head involution defective (hid), reaper* and *grim* (White et al. 1994; White et al. 1996; Grether et al. 1995; Kornbluth and White 2005; Chen et al. 1996). The proteins encoded by these genes then act to inhibit the anti-apoptotic protein *Drosophila* IAP1 (diap1) (Goyal et al. 2000), which ultimately leads to the activation of the executioner caspases Dcp-1 (a Caspase 7 homologue) and Ice (a Caspase 3 homologue) and so induces apoptosis (Kornbluth and White 2005).

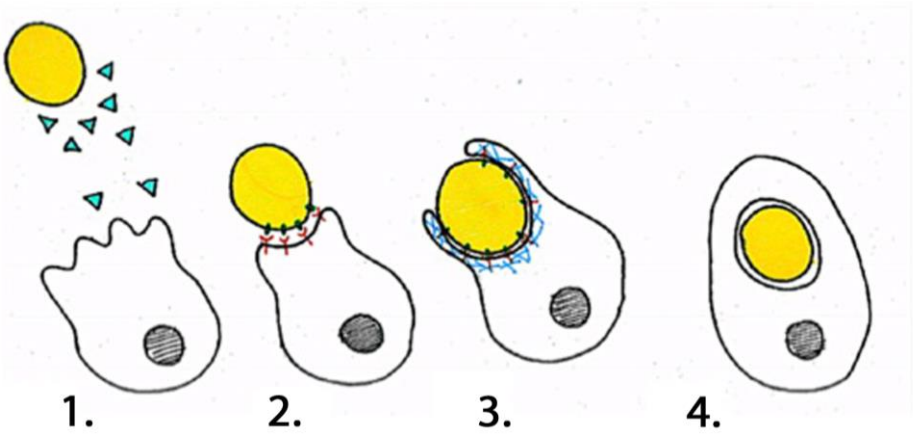

Figure 1.2: The process of apoptotic cell clearance
Stage 1 of clearance is the detection of "find-me" cues (blue triangles) released by apoptotic cells (yellow) and the subsequent chemotaxis of macrophages towards the cell. Binding to the apoptotic cells then occurs in stage 2, via phagocytic receptor binding to "eat-me" signals displayed on the surface of apoptotic cells. Stage 3 is the formation of a phagosome by extension of the membrane around the apoptotic cell, which is driven by actin rearrangements, leading to engulfment. Finally in stage 4, the engulfed apoptotic cell is processed via phagosome maturation, and eventually degraded.

One of the primary functions of macrophages is the removal and degradation of apoptotic cells, a multi-step process (Fig. 1.2) (reviewed by Fullard et al. 2009; Poon et al. 2014) beginning with the sensing of "find-me" cues secreted by apoptotic cells, which alert macrophages as to their presence and facilitate their chemotaxis towards the dying cell. The phagocyte then uses receptors expressed on its surface to recognise "eat-me" signals displayed on the cell membranes of apoptotic cells, leading engulfment of the dying cell and formation of a nascent phagosome. The internalised apoptotic cell is then processed and, after several stages of phagosome maturation, degraded (Hochreiter-Hufford and Ravichandran 2013).

1.2.1 "Find-me" signals as chemoattractants for phagocytes

In order for apoptotic cells to be cleared by professional phagocytes, the phagocytes must first be able to locate the whereabouts of the dying cells. For this to happen, it is thought that, at least in some organisms, apoptotic cells release chemotactic "find-me" cues, which phagocytes are able to sense and subsequently chemotax towards.

Several cues released by apoptotic cells that are capable of inducing chemotaxis of phagocytes have now been found, all using *in vitro* transmigration assays of monocytes and macrophages across a porous membrane towards supernatant taken from apoptotic cells (Gude et al. 2008; Truman et al. 2008; Lauber et al. 2003; Elliott et al. 2009). The first to be discovered was the phospholipid lysophosphatidylcholine (LPS), which was shown to be released by apoptotic cells upon Caspase activation and induced the transmigration of human monocytic cell lines as well as primary human macrophages (Lauber et al. 2003). Sphingosine-1-phosphate (S-1-P) and fractalkine were also found to be released by apoptotic cells and induce chemotaxis of monocytes and/or macrophages (Gude et al. 2008; Truman et al. 2008). Truman *et al.* also demonstrated that the fractalkine receptor CX3CR1 was required by macrophages to chemotax towards its ligand, and went on to show a role for fractalkine and its receptor during recruitment of macrophages to apoptotic cells in a murine model – the first time "find-me" cues had been shown to function *in vivo* (Truman et al. 2008). Finally, the nucleotides ATP and UTP were also shown to be released by apoptotic cells, and act as chemoattractant cues for monocytes and macrophages both in vitro and in vivo, and that the nucleotide receptor $P2Y_2$ was required by macrophages to migrate towards the cue (Elliott et al. 2009). It is interesting to note that although these four separate studies used similar techniques to identify potential find-me cues, the cue identified in each case was unique and non-redundant. This is potentially due to the nature of the type of cell in which apoptosis was induced and precise form of cell death, and demonstrates the diversity of cues utilised by dying cells to attract phagocytes and the complexity that this adds to the process.

1.2.2 "Eat-me" signals for the engulfment of apoptotic cells

When cells are programmed to die, they expose "eat-me" signals on the surface of their plasma membrane to facilitate their recognition by phagocytes. Perhaps the best understood "eat-me" signal is Phosphatidylserine (PS); a phospholipid that is usually a constituent of the inner leaflet of the plasma membrane, but that during apoptosis comes to be exposed on the outer leaflet (Fadok et al. 1992). PS exposure has been shown to be required for the detection and engulfment of apoptotic cells by mammalian macrophages – with a range of receptors for PS

involved, such as TIM-4 or BAI1 (Fadok et al. 2001; Hoffmann et al. 2001; Miyanishi et al. 2007; Park et al. 2007). The exposure of PS by apoptotic cells is a phenomenon that is conserved across species including *Drosophila* (van den Eijnde et al. 1998; Shklyar, Levy-Adam, et al. 2013; Tung et al. 2013).

Another "eat-me" signal is Calreticulin, a protein that is expressed in many compartments within viable cells, most notably the endoplasmic reticulum (ER) lumen where is involved in protein quality control and Ca^{2+} homeostasis, and at the cell surface (Bedard et al. 2005; Johnson et al. 2001). Increased Calreticulin expression on the surface of apoptotic cells has been observed and has been shown to be involved in the recognition and phagocytosis of apoptotic cells by mammalian macrophages via the LRP1/CD91 receptor (Gardai et al. 2005). Calreticulin is also expressed on the surface of both viable and apoptotic *Drosophila* S2 cells; when apoptosis is induced, the level of Calreticulin expression is unchanged, but it becomes clustered on the cell surface (Kuraishi et al. 2007). When the surface localisation of Calreticulin is prevented or its expression is reduced on apoptotic cells, phagocytosis of apoptotic cells is inhibited, demonstrating an important role for Calreticulin in apoptotic cell clearance in *Drosophila* (Kuraishi et al. 2007), in addition to its role in vertebrates (Gardai et al. 2005).

1.2.3 *Drosophila* apoptotic cell receptors

Several receptors for the recognition and engulfment of apoptotic cells by macrophages have been discovered in *Drosophila* (Fig. 1.3). The first to be reported was Croquemort (Crq), a CD36 superfamily protein homologue expressed specifically by *Drosophila* embryonic macrophages (Franc et al. 1996). Using *crq* null *Drosophila* embryos it was shown that Crq is required for phagocytosis of apoptotic cells and that its forced specific expression in the macrophages of *crq* null embryos rescues the phagocytic defect (Franc et al. 1999). Intriguingly, this study also showed that Crq is specifically required for apoptotic cell phagocytosis and not that of bacteria, and that the presence of apoptotic cells causes an upregulation of Crq expression on macrophages (Franc et al. 1999). More recently however, Crq has been shown to engulf bacteria, and flies mutant for *crq* have defects in microbial phagocytosis and are more susceptible to infection (Guillou et al. 2016). The identity of the ligand present for this receptor on the apoptotic surface remains unknown. Interestingly, a recent study suggests that Crq is involved in apoptotic corpse degradation, but is not essential for engulfment (Han et al. 2014).

Another phagocytic receptor is Six-microns-under (Simu), which is expressed by both macrophages and glia in *Drosophila* (Kurant et al. 2008). Again, receptor null mutant embryos were used to show that Simu is required for the binding and engulfment of apoptotic cells, both

by macrophages and glia (Kurant et al. 2008). Interestingly, when the transmembrane domain of Simu is deleted and the protein is secreted, it is still able to rescue the phenotype of the *simu* null mutant, suggesting that Simu can act either as a transmembrane receptor for apoptotic cells or can act as a secreted bridging molecule between phagocyte and apoptotic cell (Kurant et al. 2008). It has also been shown that PS is the "eat-me" signal that is recognised by Simu and to which it binds (Shklyar, Levy-Adam, et al. 2013).

Draper, which is a homologue of the *C. elegans* CED-1 and mammalian LRP1/CD91 phagocytic receptor, is also expressed in both macrophages and glia of *Drosophila* and is a receptor for apoptotic cell engulfment in *Drosophila* (Manaka et al. 2004). There is some confusion in the literature with regards to the exact role of Draper in the phagocytosis of apoptotic cells. Although one study showed that when Draper expression was inhibited in *Drosophila* embryos, the phagocytosis of apoptotic cells in both macrophages and glial cells was reduced by 30-40% in each case (Manaka et al. 2004), another showed that the physical engulfment of apoptotic particles is not affected when compared to wild type, but that the particles accumulated within the phagocytes, suggesting a role for Draper in their degradation post-engulfment (Kurant et al. 2008). These differences could be due to the different approaches used to investigate phagocytosis in vivo, with Kurant *et al*. examining phagocytosis on the ventral nerve cord in fixed mutant embryos, whereas Manaka *et al*. used double-stranded RNA against Draper and looked at phagocytosis in cells from throughout the embryo that had been dispersed (Manaka et al. 2004; Kurant et al. 2008). Kurant *et al*. suggest that Draper is acting downstream of Simu in the same phagocytic pathway, as the *draper*/*simu* double mutant phenotype resembles that of the *simu* single mutant in terms of amount and location of apoptotic particles (Kurant et al. 2008). Regardless of the exact role for Draper in apoptotic cell clearance, it is most certainly involved in apoptotic cell binding at some point in the process of apoptotic cell clearance. Despite earlier reports suggesting that PS was not an apoptotic ligand for Draper (Manaka et al. 2004), more recent reports have shown that Draper does in fact bind PS (Tung et al. 2013). Two separate *Drosophila* ER proteins, Pret-a-porter and *Drosophila melanogaster* calcium-binding protein 1 (DmCaBP1), have since been shown to be exposed on the surface of cells undergoing apoptosis and may also act as ligands for Draper during apoptotic cell phagocytosis by hemocytes (Kuraishi et al. 2009; Okada et al. 2012). The ability of Draper to bind to multiple apoptotic ligands is a striking example of the redundancy that exists in the detection of apoptotic cells.

Finally, the integrin βv has also been identified as a phagocytic receptor for apoptotic cells in *Drosophila* embryonic macrophages (Nagaosa et al. 2011). The α subunit that forms a heterodimer with this β subunit to create a functional protein has since been suggested to be αPS3, as shown by their physical interaction as well as the reduced level of apoptotic cell

phagocytosis upon reduced αPS3 expression (Nonaka et al. 2013). Similarly to Draper (Hashimoto et al. 2009), integrin αPS3/βv has also been shown to involved in bacterial detection and engulfment as well as that of apoptotic cells (Nonaka et al. 2013).

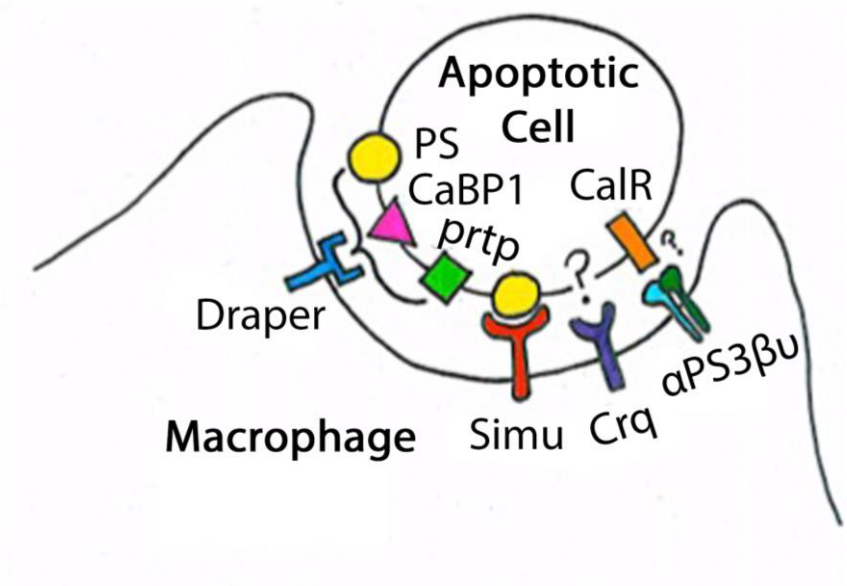

Figure 1.3: Drosophila phagocytic receptors and their apoptotic cell-derived ligands
The phagocytic receptors expressed by hemocytes and the apoptotic cell-derived "eat-me" signals to which they bind. Simu= six-microns-under; Crq= Croquemort; αPS3/βv= Integrin αPS3/βv; PS= phosphatidylserine; CaBP1= *Drosophila melanogaster* calcium-binding protein 1; prtp= pretaporter; CalR= calreticulin. Questions marks represent as yet unknown components or interactions.

1.2.3 Downstream signalling of phagocytic receptors

Drosophila possesses a number of receptors and ligands involved in the detection and engulfment of apoptotic cells, with many of these playing related roles in vertebrate cells. Downstream signalling from these phagocytic receptors has important consequences, both for the physical process of engulfment with signalling leading to the rearrangements of the actin cytoskeleton required for apoptotic cell internalisation, and the formation of the phagosome (reviewed by Penberthy and Ravichandran 2016). Indeed the detection of PS by phagocytic receptors is important for mediating the anti-inflammatory affects of apoptotic cell clearance on macrophages (Huynh et al. 2002).

The first insights into the proteins involved in the signalling pathways required for engulfment of apoptotic corpses came from studies in *C. elegans* and identified two partially redundant, conserved pathways: the CED-1/6/7 pathway and the CED-2/5/12 pathway (Ellis et al. 1991),

both of which have been shown to converge onto CED-10 (Rac1 in *Drosophila*) (Kinchen et al. 2005). These pathways are conserved in both *Drosophila* and mammals, the *Drosophila* homologs of *CED-1* and *CED-6* being *Draper* and *DCed-6* respectively, whereas the *CED-7* homolog has yet to be identified in flies. The homologs of the *CED-2/5/12* pathway in *Drosophila* are *Crk*, *mbc* (also known as *DOCK180*) and *ELMO* respectively (Kinchen 2010).

The CED-2/5/12 Pathway has been shown to activate Rac1 and hence produce the cytoskeletal rearrangements required for the engulfment of apoptotic cells. DOCK180 has been shown to bind to Rac and, along with an interaction with the adaptor protein ELMO, causes GTP to bind to Rac, hence activating the protein (Brugnera et al. 2002). The involvement of Crk in this pathway is not well understood but it has been shown to bind DOCK180 (Matsuda et al. 1996) and plays a role in the regulation and assembly of the DOCK180/ELMO complex at the plasma membrane (Akakura et al. 2005). In *C. elegans* two receptors have been shown to act upstream of the CED-2/5/12 pathway in the engulfment of apoptotic cells: PSR-1 (PS Receptor 1) and α integrin (Wang et al. 2003; Hsu and Wu 2010). No receptor for the activation of this pathway has yet to be found in *Drosophila*, however the presence of a similar integrin receptor for apoptotic cells in *Drosophila* macrophages (Nagaosa et al. 2011; Nonaka et al. 2013) suggests that this could be a candidate. As is the case in *C.* elegans, the CED-2/5/12 pathway seems distinct from that of the CED-1/6/7 pathway in *Drosophila* (van Goethem et al. 2012).

1.2.3.1 Draper-mediated signalling in hemocyte apoptotic cell clearance

In *Drosophila* the most well characterized downstream signalling events of a phagocytic receptor are those of Draper. Much of this knowledge has come from studies involving the pruning of degenerating CNS axons by glia during *Drosophila* metamorphosis, a process which is thought so be very similar to apoptotic cell clearance (Awasaki et al. 2006; Ziegenfuss et al. 2008). A high level of apoptosis occurs during the development of the CNS, as neuronal connections must become highly refined and so unnecessary and excess cells must be removed for its proper development. Both glia and macrophages carry out this clearance in *Drosophila* (Sonnenfeld and Jacobs 1995), with each expressing both Draper and Simu (Manaka et al. 2004; Kurant et al. 2008), suggesting that phagocytosis occurs via partially common mechanisms in each cell type.

The CED-1/6/7 pathway identified in *C. elegans* provided the first insight into the downstream signalling of Draper, the *Drosophila* homolog of CED-1. In this pathway it is thought that ligand binding to the CED-1 receptor causes the association of CED-6 with the intracellular NPXY domain of the receptor (Su et al. 2002), which ultimately leads to Rac1 activation and apoptotic cell engulfment (Kinchen et al. 2005). In *C. elegans* several molecules that are usually

required for endocytosis, a process not dissimilar to phagocytosis, have been shown to be required for apoptotic cell engulfment in a manner dependent on this pathway (Yu et al. 2006; Chen et al. 2013; Shen et al. 2013). These proteins have varying roles in the process but some are involved in actin cytoskeletal rearrangements, whereas others are involved in vesicle delivery to the phagocytic cup, allowing for the formation of a phagosome. This suggests that similar proteins may be involved in the process of apoptotic cell engulfment via the CED-1/6/7 pathway in *Drosophila*.

Through a series of elegant experiments involving the use of both *Drosophila* S2 cells (an embryonic macrophage cell line) and *in vivo* embryonic macrophages, Cuttell *et al*. identified a new role for Ca^{2+} homeostasis in the phagocytosis of apoptotic cells and showed that this is mediated via the CED-1/6/7 pathway (Cuttell et al. 2008). Mammalian Junctophilins (JPs) form junctions between the plasma membrane and the ER, allowing communication between the Ca^{2+} channels that exist at each of these locations (in the ER these are called Ryanodine receptors), facilitating the regulation of Ca^{2+} homeostasis within the cell (Takeshima et al. 2000). Cuttell *et al*. found that Undertaker, a *Drosophila* JP homolog, along with Rya-r44F, a *Drosophila* Ryanodine receptor, were required for apoptotic cell engulfment by macrophages and that these two proteins interact genetically with *Draper* and *CED-6* (Cuttell et al. 2008). They suggest a pathway whereby ligand binding to Draper and its associated CED-6 interaction causes store-operated extracellular Ca^{2+} entry via UTA, Rya-r44F, dSTIM (an ER localized Ca^{2+} sensor) and dOrai (a plasma membrane localized Ca^{2+}-activated Ca^{2+} channel), that this is involved in apoptotic cell engulfment (Cuttell et al. 2008). More recently PKD2, a *Drosophila* TRPP channel located at the plasma membrane that is Ca^{2+} permeable, has also been shown to fit into this pathway and is required for the phagocytosis of apoptotic cells by macrophages *in vivo* (van Goethem et al. 2012). Interestingly, this study also suggested a role for Simu in this pathway (van Goethem et al. 2012), providing further evidence for the idea that Simu and Draper interact in the same phagocytic pathway (Kurant et al. 2008).

1.2.4 Post-engulfment processing of the apoptotic corpse

Once apoptotic cells have been internalised by macrophages via phagosome formation, they must be processed for their eventual degradation via a process known as phagosome maturation. This is a complex process regulated by a plethora of proteins, which involves the progressive acidification of the phagosome through its sequential interaction with the early and late endosome intracellular compartments, before its eventual fusion to lysosomes, which contain the enzymes necessary for degradation (Vieira et al. 2002; Kinchen and Ravichandran 2008).

Much of what we now know about apoptotic phagosome maturation has come from studies conducted in *C. elegans*, but the majority of proteins involved are also conserved in *Drosophila*. The first steps involved in phagosome maturation occurs whilst the phagosome is forming, when the large GTPase Dynamin as well as the PstIns(3) kinase Vps34 are recruited to the phagosome membrane, which leads to the recruitment of inactive, GDP-bound Rab5 (Kinchen et al. 2008). Once the phagosome is fully formed, Rab5 is activated which leads to the formation of PI(3)P by the activation of Vps34 (Kinchen et al. 2008). It is thought that Rab5 activation is required for the tethering of early endosomes to phagosomes containing apoptotic cells (Lu and Zhou 2012). Indeed, dominant-negative Rab5 *Drosophila* embryonic macrophages are highly vacuolated and show a decrease in the number of acidified vacuoles, suggesting that Rab5 is also involved in phagosome maturation in *Drosophila* (Evans et al. 2013). Rab5 activation leads to the recruitment of Rab7, which is then activated by the recruitment of the HOPS complex, which eventually leads to lysosome-phagosome fusion and the degradation of the apoptotic cell (Kinchen et al. 2008; Hochreiter-Hufford and Ravichandran 2013).

A study by Evans *et al*. investigated the role of SCAR, a complex mentioned earlier that is involved in the activation of the Arp2/3 complex to produce cytoskeletal rearrangements required for cell migration, in *Drosophila* embryonic macrophages (Evans et al. 2013). Interestingly they found that mutant or dominant-negative *SCAR* macrophages contained a significantly higher number of apoptotic vacuoles compared to wild-type macrophages (Evans et al. 2013). Moreover, these mutant or dominant-negative *SCAR* macrophages contained a lower fraction of acidified phagosomes when compared to wild-type, phenocopying the dominant-negative Rab5 mutant macrophages (Evans et al. 2013). This suggests that SCAR, like Rab5, is essential for phagosome maturation post-engulfment of apoptotic cells and that its role in maturation is at an early stage, similar to that of Rab5.

1.3 Glial cell apoptotic cell clearance in *Drosophila*

Another important cell type for the clearance of apoptotic cells in *Drosophila* are the non-professional phagocytic glial cells of the central nervous system (CNS). Glial cells in *Drosophila* can be subdivided into two main groups: the midline glia and the lateral glia, the latter of which accounts for the vast majority of glia (Stork et al. 2012). During embryonic development, programmed cell death plays a critical role in the patterning and sculpting of the CNS, and large numbers of neurons undergo apoptosis in order to refine neuronal connections (Oppenheim 1991). During *Drosophila* embryogenesis, a great deal of programmed cell death

occurs in the ventral nerve cord (VNC) (Abrams et al. 1993; Rogulja-Ortmann et al. 2007), a structure considered to be the equivalent of the vertebrate spinal cord.

1.3.1 Glial cell specification

Glial cells of the *Drosophila* VNC are specified from neuroblast progenitor cells, of which there are 30 per VNC hemisegment (Bossing et al. 1996; Schmidt et al. 1997). The differentiation of neuroblasts into glial cells is dependent on the expression of the transcription factor *gcm*, and in *gcm* mutants, cells which would usually become glial cells instead differentiate into neurons (Hosoya et al. 1995; Jones et al. 1995). Conversely, ectopic expression of *gcm* in all neuroblast cells results in their differentiation into glial cells, highlighting the important role of *gcm* in the cell fate decision of cells to become glia (Hosoya et al. 1995; Jones et al. 1995). The differentiation of neuroblasts into either glia or neurons depends on the asymmetrical distribution of *gcm* RNA prior to cell division, with one progenitor cell inheriting this RNA and becoming glial cells, and the other neurons (Bernardoni et al. 1999). *gcm* then induces the expression of target genes required for glial specification such as *reversed polarity* (*repo*) (Campbell et al. 1994; Xiong et al. 1994; Halter et al. 1995), *loco* (Granderath et al. 1999) and *pointed* (*pnt*) (Klaes et al. 1994; Klambt 1993) and also the gene *tramtrack* that prevents the cells from differentiating into neurons (Giesen et al. 1997).

1.3.2 Mechanisms of apoptotic cell clearance in *Drosophila* glial cells

One aspect of glial cell function that is regulated by *repo* expression is their phagocytic capacity (Shklyar et al. 2014). Indeed, *repo* is required for glial expression of the apoptotic cell receptor Draper, and glial cells lacking *repo* are much smaller and are unable to clear apoptotic cells properly (Shklyar et al. 2014). Draper was first shown to be required for the clearance of apoptotic cells by glia in a study from 2003, where *drpr* mutants showed increased numbers of apoptotic cells within the ventral nerve cord (Freeman et al. 2003). However, more detailed analysis since then has shown that apoptotic cells actually seem to accumulate within glial cells in *drpr* mutants (Kurant et al. 2008), and seems to also be the case in hemocytes *in vivo* (Evans et al. 2015). Therefore, it seems likely that Draper may be more important physiologically for the processing of apoptotic cells post-engulfment as opposed to their actual phagocytosis as was originally reported (Manaka et al. 2004).

Apoptotic cell clearance by glial cells in *Drosophila* is also highly dependent on the apoptotic cell receptor Simu (Kurant et al. 2008). In *simu* mutant embryos, apoptotic cells accumulate outside glial cells, suggesting that Simu is required for the phagocytosis of apoptotic cells

(Kurant et al. 2008). Interestingly, the glial-specific expression of a truncated version of Simu that lacks its transmembrane domain is able to rescue defects in apoptotic cell clearance in *simu* mutants, suggesting that Simu may act as a bridging molecule (Shklyar, Levy-Adam, et al. 2013).

1.3.3 Draper signalling in glial cell phagocytosis of dying cells

In glial cells, Draper is required both for the engulfment of injured axons and the recruitment of glial projections towards injured axons in order for engulfment to occur (MacDonald et al. 2006), and it is also required for axonal pruning during pupal metamorphosis (Awasaki et al. 2006). In a hunt for molecules that interact with Draper in *Drosophila*, the non-receptor tyrosine kinase Shark was identified, whose binding to Draper requires the activity of Src42A, an Src family kinase (Ziegenfuss et al. 2008). By reducing the expression of either Shark or Src42A using RNAi, Ziegenfuss *et al.* showed that both are required for the phagocytosis of apoptotic corpses by glia and that Src42A is able to phosphorylate Draper (Ziegenfuss et al. 2008). This information points towards a model in which Src42A-mediated phosphorylation of Draper upon binding to its apoptotic ligand leads to the recruitment and binding of Shark, which ultimately leads to phagocytosis (Ziegenfuss et al. 2008). Indeed, the intracellular ITAM domain of the Draper-I isoform if required for the engulfment of degenerating axons (Logan et al. 2012), and Src42A has been shown to phosphorylate the ITAM domain of Draper, at least in the context of hemocyte inflammatory responses (Evans et al. 2015). Therefore, it may be that the ITAM domain of Draper may be phosphorylated by Src42A, not only in the context of hemocyte responses to tissue damage, but also during the phagocytosis of injured neurons. Interestingly Draper-I mediated glial cell phagocytosis of damaged axons is repressed by another isoform of Draper, Draper-II, which is also expressed in glial cells (Logan et al. 2012).

1.4 Anti-inflammatory properties of apoptotic cell clearance

To prevent the onset of chronic inflammation, inflammatory macrophages must be removed from sites of resolving inflammation, and it is thought that one mechanism of this clearance is the migration of macrophages away from sites of inflammation during resolution (Bellingan et al. 1996). In vertebrates, the first cells to be recruited to sites of tissue damage are phagocytic cells known as neutrophils, which are key players in acute inflammation and host defence (Kolaczkowska and Kubes 2013). Studies using the vertebrate zebrafish model have shown that the reverse migration of neutrophils away from sites of injury has an anti-inflammatory effect (Robertson et al. 2014; Mathias et al. 2006). Further studies using this model organism have

also suggested that neutrophils may actually be chased away from wounds by macrophages, aiding the resolution of inflammation (Tauzin et al. 2014).

In vertebrate systems it is known that the clearance of apoptotic cells by phagocytes plays a substantial and important role in the resolution of inflammation (Maderna and Godson 2003). A groundbreaking study in 1997 showed for the first time that apoptotic cells were able to induce increased production of the anti-inflammatory cytokine IL-10 in activated monocytes, and decrease their production of the pro-inflammatory cytokines IL-1β, IL-12 and TNF-α (Voll et al. 1997). Another important study published around the same time demonstrated for the first time that the phagocytosis of apoptotic cells by macrophages was able to inhibit the production of inflammatory cytokines (Fadok et al. 1998). They showed that the phagocytosis of apoptotic neutrophils by human macrophages resulted in the production of TGF-β which in turn inhibited the production of the pro-inflammatory cytokines TNF-α and IL-1β, and GM-CSF (Fadok et al. 1998). In yet another groundbreaking study from the same lab, it was shown that PS-dependent phagocytosis of apoptotic cells induced TGF-β1 secretion, which stimulated the early resolution of acute inflammation in the lungs of mice by decreasing pro-inflammatory cytokine production and reducing inflammatory cell numbers, suggesting a link between efferocytosis and inflammation resolution (Huynh et al. 2002). More recently is has been shown that the engulfment of apoptotic cells by bronchial epithelial cells in mice leads to the release of anti-inflammatory mediators such as TGF-β and PGE_2, which limit airway inflammation during exposure to allergens (Juncadella et al. 2012).

Drosophila also have homologues of some of the molecules mentioned above, or at least ones that fulfill similar roles. The *Drosophila* TGF- β superfamily member *decapentaplegic* (*dpp*) is secreted by hemocytes and helps to promote resistance to infection (Ayyaz et al. 2015). *ddp* and another TGF- β superfamily member *dawdle* (*daw)* have also been shown to be involved in regulating the *Drosophila* immune response (Clark et al. 2011). The only *Drosophila* TNF family member, *eiger*, can also be expressed in hemocytes, at least when associated with tumors (Cordero et al. 2010). Finally, the three *unpaired* (*upd*) genes *upd*, *upd2* and *upd3*, represent the *Drosophila* equivalent of interleukins (Agaisse et al. 2003), and indeed *upd3* has been shown to be expressed in hemocytes upon both aseptic and septic injury (Agaisse et al. 2003; Pastor-Pareja et al. 2008). However a link between the clearance of apoptotic cells and the regulation of such molecules has yet to be defined.

1.5 Apoptotic Cell Clearance in Disease

The defective clearance of apoptotic cells is associated with a plethora of diseases, ranging from atherosclerosis to chronic obstructive pulmonary disease (COPD) and autoimmunity (Elliott and Ravichandran 2010). Many of these diseases are chronic inflammatory conditions, highlighting a role for apoptotic cell clearance in the regulation of inflammation.

1.5.1 Atherosclerosis

Atherosclerosis is the build-up of fatty material in the walls of arteries that causes hardening and narrowing of the vessel, and is the main cause of coronary heart diease, peripheral arterial disease and ischemic stroke (Brophy et al. 2017). When these areas, also known as atherosclerotic plaques, begin to form, circulating monocytes are attracted from the bloodstream, which adhere to and subsequently transmigrate through the endothelium where they differentiate into macrophages. Here, macrophages begin to ingest the accumulating lipoprotein material in the artery wall which results in a build-up of cholesterol with macrophages which are then known as foam cells (Chistiakov et al. 2016). Foam cells eventually die via apoptosis (HEGYI et al. 1996), and the build-up of these apoptotic cells as well as apoptotic endothelial and smooth muscle cells (Van Vré et al. 2012) due to defective phagocytosis by macrophages (Schrijvers et al. 2005), drives progression of atherosclerotic plaques. The build-up of uncleared apoptotic cells in these plaques, and their subsequent necrosis, results in the formation of a necrotic core (Thorp et al. 2008), which in turn helps to drive inflammation in the plaque, leading to plaque rupture (van der Wal 1999). Interestingly, mutations in the apoptotic cell receptor MerTK has been shown to be promote the accumulation of uncleared apoptotic cells in atherosclerotic plaques in *Apoe*$^{-/-}$ mice and so drive plaque necrosis (Thorp et al. 2008). Mutations in apoptotic cell-bridging molecules have also been shown to advance the progression of atherosclerotic plaques in mice, including MFG-E8 (Ait-Oufella et al. 2007) and C1q (Bhatia et al. 2007). Therefore the normal recognition of apoptotic cells by macrophages is required to limit the rate of atherosclerotic plaque progression and represents a potential therapeutic target.

1.5.2 Chronic obstructive pulmonary disease

Chronic Obstructive Pulmonary Disease (COPD) is a chronic inflammatory condition of the lungs associated with increased numbers of apoptotic cells (Demedts et al. 2006). It has been shown that the phagocytosis of apoptotic epithelial cells by macrophages in COPD is defective (Hodge et al. 2003). Recently, the decreased ability of phagocytes to engulf apoptotic cells in COPD has been linked to the ability of cigarette smoke to downregulate the levels of the apoptotic cell-phagocyte bridging molecule MFG-E8 (Wang et al. 2017).

1.6 Experimental Aims

The efficient phagocytosis of apoptotic cells is essential in order to prevent cellular necrosis and the inflammatory response associated with this form of cell death. It is also clear that the process of engulfment of apoptotic cells by macrophages changes macrophage biology and promotes a shift in their phenotype to being anti-inflammatory that aids in the resolution of inflammation. However how apoptotic cells and their clearance affects macrophage behavior and function in vivo is incompletely understood.

The *Drosophila* embryo represents an excellent model to study this relationship in vivo, due to the high degree of genetic tractability that allows for the dissection of molecular pathways. This model also allows us to perform high-resolution imaging of macrophages in vivo due to the transparency of the embryos as well as the superficial nature of the macrophages, which can be labeled in vivo using the GAL4-UAS system.

In recent years it has been discovered that when *Drosophila* hemocytes are overloaded with apoptotic cells, either by increasing the number of apoptotic cells for hemocytes to clear or by disrupting the processing of apoptotic cells by hemocytes, their motility and ability to respond to sites of injury are perturbed (Evans and Wood, unpublished data; Evans *et al.*, 2013).

By genetically manipulating the number of apoptotic cells for macrophages to clear in the embryo we aim to study how increased numbers of apoptotic cells affect the migratory ability of macrophages. In *repo* mutants, glial cells are not specified correctly since *repo* encodes a transcription factor critical to their development (Xiong *et al.*, 1994; Halter *et al.*, 1995). Consequently, the cells of this glial lineage within the ventral nerve cord are much less able to engulf apoptotic cells - this leaves hemocytes with a greater number of apoptotic cells to clear and they become full up with corpses and appear vacuolated (Shklyar et al. 2014). This appears to lead to an attenuation of responses to wounds and hemocytes also exhibit slowed basal migration in *repo* mutants (Evans and Wood, unpublished data). Similarly in *SCAR* mutants, *Drosophila* hemocytes accumulate engulfed apoptotic cells and phenocopy the wound and basal motility defects observed in *repo* mutants (Evans *et al*., 2013). When apoptosis is prevented in theses embryos using the *Df(3L)H99* genomic deletion (White *et al.*, 1994), which relieves hemocytes of their duty to phagocytose apoptotic cells, vacuolation does not occur in *SCAR* mutant hemocytes and hemocyte lamellipodia are rescued and migration speeds almost fully restored to wild type-levels (Evans *et al*., 2013). This result suggests that apoptotic corpses somehow inhibit a SCAR-independent form of motility and turn off pro-inflammatory behaviours such as responses to wounds. However the molecular mechanisms by which

apoptotic cells exert this anti-inflammatory effect on hemocytes and how they suppress hemocyte migration are not clear.

We hypothesise that the binding of hemocytes to apoptotic cells through apoptotic cell receptors expressed on their surface, and the subsequent downstream signalling, supresses hemocyte migration in the presence of pathological levels of apoptosis. We aim to test this hypothesis by:

1) Inducing pathological levels of apoptosis in the *Drosophila* embryo using *repo* mutants to ensure that increased levels of apoptosis do indeed suppress hemocyte migrations in our hands.
2) Blocking apoptosis in *repo* mutant embryos to check for a rescue of hemocyte migrations.
3) Removing hemocyte apoptotic cell receptors in a *repo* mutant background to examine whether the binding of hemocytes to apoptotic cells is responsible for reduced hemocyte migrations.
4) Examining the activation state of candidate signaling pathways within hemocytes in a *repo* mutant background which may be responsible for suppressing hemocyte migrations.

Chapter 2: Materials and methods

2.1 Fly work

2.1.1 *Drosophila* husbandry

Fly stocks were maintained at 18°C in vials containing standard *Drosophila* medium (recipe in appendix 1). Flies were tipped to fresh vials of food every 4 weeks.

2.1.2 Fly crosses

Crosses were performed by placing appropriate male and virgin female adult flies in vials containing standard *Drosophila* medium with a pea-sized drop of yeast paste. These were then placed at 25°C and the flies tipped to fresh vials every 2 days.

2.1.3 Fly sorting

When flies required sorting based on their expression of specific balancers, or when selecting virgin females, flies were anaesthetised by placing them on CO_2 emitting pads. Selected flies were then placed in vials laid on their side to avoid anesthetised flies getting stuck in the food at the bottom. Unwanted flies were euthanised by tipping them into a bottle containing 70% IMS in water.

2.1.4 Harvesting of *Drosophila* embryos from laying cages

In order to collect embryos with a given genotype, specific male and female adult flies were placed in a laying cage with a base composed of a plate of apple juice agar with a pea-sized drop of yeast paste on the surface. The cages were then placed at 22°C and the flies were left to lay overnight. In cases where RNAi knockdown was required, cages were left at a temperature of 25°C overnight. Apple juice agar plates were then removed from the cages and the embryos rinsed off the surface using distilled water and sieved through a 40µm cell strainer (Corning). Embryos were then dechorionated by submerging in bleach for 2 minutes, followed by extensive washing in distilled water to remove the bleach.

2.1.5 Staging and sorting of *Drosophila* embryos

The embryonic stage of development of embryos was assessed by gut and amnioscerosa shape as well as and head morphology as described in the Atlas of *Drosophila* Development (Hartenstein 1993). Fluorescent balancers were selected against using a Leica M205 FA fluorescent dissection scope.

2.2 Fly stocks

The following are the details of all the stocks used in the work described in this thesis. Specific details of all the fly lines created for research can be found in appendix 2.

2.2.1 Hemocyte-specific drivers

Genotype	Chromosome	Source	References
croquemort-GAL4	3	Bloomington Stock Centre	(Stramer et al. 2005)
serpent-GAL4	2	Bloomington Stock Centre	(Brückner et al. 2004)

2.2.2 Fluorescent labels and reporter constructs

Genotype	Chromosome	Source	References
UAS-GFP	2 and 3	Bloomington Stock Centre	(Yeh et al. 1995)
UAS-nuclear red stinger	2 and 3	A gift from Brian Stramer, KCL, London	(Barolo et al. 2004)
P{srp-GMA}	2	Bloomington Stock Centre	(Bloor and Kiehart 2001)

TRE-eGFP	2	Bloomington Stock Centre	(Chatterjee and Bohmann 2012)

2.2.3 UAS constructs

Genotype		**Source**	**References**
P{TRiP.HMJ23355}attP40 (*UAS-simu RNAi*)	2	Bloomington Stock Centre	(Ni et al. 2009)
P{TRiP.JF02696}attP2 (*UAS-scb RNAi*)	2	Bloomington Stock Centre	(Ni et al. 2009)
P{TRiP.HMS01997}attP40 *(UAS-crq RNAi)*	2	Bloomington Stock Centre	(Ni et al. 2009)
P{TRiP.HMS01224}attP2 *(UAS-p38a RNAi)*	2	Bloomington Stock Centre	(Ni et al. 2009)
UAS-simu	3	A gift from Estee Kurant, University of Haifa, Israel	(Shklyar, Levy-Adam, et al. 2013)
UAS-crq	X	A gift from Natalie Franc, The Scripps Research Institute, USA	(Franc et al. 1999)

2.2.4 Mutant alleles

Genotype	Chromosome	Source	References
repo^{03702}	3	Bloomington stock centre	(Halter et al. 1995)
simu^{2}	2	A gift from Estee Kurant, University of Haifa, Israel	(Kurant et al. 2008)
crq^{KO}	2	A gift from Natalie Franc, The Scripps Research Institute, USA	(Han et al. 2014)
scb^{2}	2	Kyoto Stock Centre	(Stark et al. 1997)
scb^{01288}	2	Bloomington Stock Centre	(Stark et al. 1997)
βv^{1}	2	A gift from Nick Brown, University of Cambridge	(Devenport and Brown 2004)
draper$^{\Delta 5}$	3	A gift from Estee Kurant, University of Haifa, Israel	(Freeman et al. 2003)

2.2.5 Genomic deficiencies and miscellaneous alleles

Genotype	Chromosome	Source	References
Df(3L)H99	3	Bloomington Stock centre	(White et al. 1994)
Df(2L)BSC253	2	Bloomington Stock Centre	(Cook et al. 2012)
w^{1118}	X	Bloomington Stock Centre	(Kurkulos et al. 1991)

2.3 Live imaging of *Drosophila* embryos

2.3.1 Preparation of embryos for live imaging

Firstly, in order to mount live embryos, a short piece of double-sided sticky tape (Scotch) was placed onto a microscope slide (SGL) and two 22mm x 22mm coverslips (SLS) were stuck to this at either end Dechorionated embryos of the desired stage were then carefully mounted ventral-side-up on the section of sticky tape between the two slides using a tungsten needle. Embryos were then covered in a minimal amount of Voltalef oil/halocarbon oil (VWR) to prevent them from drying out and also to improve the quality of the imaging. Note that multiple embryos can be mounted on a single microscope slide in this way. A final 24mm x 32mm coverslip (SLS) was then carefully placed on top of the embryos with each end overlapping the two previously placed coverslips, and two spots of nail varnish placed on each end to fix it in place. Once this final coverslip had been placed, embryos were left to acclimatise in the dark at room temperature for 30 minutes before imaging.

2.3.2 Wounding of *Drosophila* embryos

In order to wound embryos to assess hemocyte inflammatory recruitment to sites of tissue damage, stage 15 embryos of the desired genotype were first prepared for live imaging as in the previous section. Using an UltraView VOX spinning disc confocal system (Perkin Elmer) with

an inverted Olympus IX81 microscope and Velocity imaging software, a pre-wound z-stack covering a depth of 25µm into the embryo was taken of the superficial hemocytes on the ventral side of the embryos with a UplanSApo 40x oil (NA=1.3) objective lens and with a z-spacing of 1µm. A wound was then made in the ventral epithelium of the embryos using a MicroPoint nitrogen ablation laser (Andor) and z-stacks were typically taken every 2 minutes for 58 minutes. At 60 minutes post-wound, another z-stack was taken, this time also using the brightfield channel, which was used to identify the wound perimeter. As all embryos wounded had hemocytes that were labelled with GFP, a 488nm laser with a GFP emission filter was always used to image the hemocytes. However, in cases where hemocytes were also labelled with nuclear red stinger, a 561nm laser with a TxRed emission filter was used in addition to GFP.

2.3.3 Random migration of hemocytes

In order to assess the migratory behaviour of hemocytes *in vivo*, embryos of the desired stage were first prepared for live imaging as previously (2.2.1). Using the same microscope set up as above (2.2.2) z-stacks covering a depth of 25µm into the embryo were taken of the superficial hemocytes on the ventral side of the embryos every 2 minutes for 60 minutes.

2.3.4 Assessing hemocyte ROS levels

2.3.4.1 Treating live embryos with ROS indicator

To assess the levels of reactive oxygen species (ROS) within hemocytes, embryos were first harvested as previously (2.1.4) and then left to sit for 30 minutes on a moist apple juice agar plate in the dark. After this time, embryos were transferred to a foil-covered glass vial containing 1ml of peroxide-free heptane with 1ml of the ROS marker dihydrorhodamine 123 (DHR 123; sigma) in PBS at a concentration of 50µM, and left on a shaker at 250rpm for 30 minutes in the dark. Using a Pasteur pipette, embryos were then immediately transferred in a minimum volume of staining solution to containing Voltalef/halocarbon oil (VWR). Embryos were then mounted on individual slides in a minimum amount of oil as previously (2.2.1). However, instead of leaving embryos to acclimatise for 30 mins, embryos were imaged immediately. Note that a maximum of 3 embryos were mounted and imaged per staining, as the ROS indicator develops rapidly.

2.3.4.2 Imaging embryos for ROS

Using lasers of wavelengths 488nm and 562nm with GFP and RFP emission filters to image DHR 123 and nuclear red stinger labelled hemocyte nuclei respectively, z-stacks covering a depth of approximately 25µm were taken of the hemocytes on the superficial surface of the VNC. This was done using a Nikon A1 inverted confocal microscope with a CFI Super Plan Fluor ELWD 40x oil objective lens (NA= 0.6), with a z-spacing of 1µm and using Nikon Elements imaging software software.

2.4 Microinjection of *Drosophila* embryos

2.4.1 Preparation of *Drosophila* embryos for injection

In preparation for injection, stage 15 dechorionated embryos were first mounted on microscope slides as previously (2.2.1), however embryos were placed in vertical lines and orientated horizontally with the anterior end pointing right. Before adding oil to the embryos, the slide was placed in a small airtight box (Tupperware) containing silica gel bags for 7 minutes in order to dehydrate the embryos. A minimal amount of Voltalef oil/halocarbon oil was then placed on the embryos at their anterior end using a tungsten needle, which gradually spreads over the entire embryo.

2.4.2 Needle pulling

15cm long 1mm glass capillaries (WPI) were placed in a Flaming/Brown P-1000 micropipette puller (Sutter) and pulled using a heat of 390 and a pulling tension of 220. The very end of the tip was then bevelled by carefully snapping using a pair of forceps while viewing the capillaries under a dissection microscope at high magnification.

2.4.3 Injecting embryos with apoptotic ‘find-me’ cues

In order to inject embryos with potential ‘find-me’ cues or apoptotic supernatant ad examine their wound responses, embryos were first prepared as in section 2.3.1. Cues were prepared and injected at the concentrations shown in sections 2.4.4. diluted in PBS. The injection solution also contained 70kDa rhodamine dextran (2.5mg/ml; molecular probes) diluted at a ratio of

1:50. Control embryos were injected with the same solution as their respective cue, except the find-me cue was replaced with an equal volume of the solvent used to make up the find-me cue stock. Injections were performed into the anterior embryo using a DigiTherm injection system (Tritech) powered by a BAMBI 35/20 silent compressor. After injection, a 24mm x 32mm coverslip was placed over the embryos and secured with nail varnish as previously (2.2.1). Once this final coverslip had been placed, embryos were left to acclimatise in the dark at room temperature for 30 minutes before imaging. Wounding was performed as in section 2.2.2.

2.4.4 Preparation of find-me cues for injection

Find-me cue	**Supplier**	**Stock diluted in**	**Stock concentration**	**Injected concentration**
Lysophosphatidylserine (LPC)	sigma	Absolute ethanol	40mM	1.6mM
Sphingosine-1-phosphate (S-1-P)	sigma	methanol	10µM	400nM
Non-hydrolysable ATP (N-H ATP)	sigma	MQH_2O	1mM	4µM

2.5 Immunostaining and imaging of fixed *Drosophila* embryos

2.5.1 Fixation of embryos

Dechorionated embryos were fixed for 20 minutes at 150 rpm on a rocker in small glass vials containing 1 ml of 4% formaldehyde (Sigma-Aldrich) in PBS and 1ml of peroxide-free heptane (Fisher Scientific), which permeabalises embryos and forms an interface on which they sit. The lower formaldehyde phase of the fixative was then removed before adding 1 ml of methanol and shaking vigorously. Embryos that had popped out of their vitelline membranes and so sunk to the bottom of the vial were then transferred to a 1.5 ml eppendorf and washed three times in 500 µl of methanol. The embryos were then stored in another 500 µl of methanol at -20°C until required (maximum 2 weeks storage time).

2.5.2 Immunostaining of *Drosophila* embryos

Following fixation and the removal of methanol, embryos were first washed three times in PBT (0.1% Triton-X 100 (Sigma) in PBS). Embryos were next blocked by incubation in PATx (1% bovine serum albumin (BSA) (Sigma) in PBT) for 20 minutes on a roller. This was repeated three times, each time replacing the PATx before incubation. Embryos were then transferred to a 500 µl eppendorf, PATx removed and embryos incubated in 250 µl of primary antibody diluted in PATx overnight on a roller at 4°C. The primary antibody solution was then removed and embryos washed 3 times in PATx before being incubated in PATx for three separate 20 minute washes on a roller at room temperature, each time replacing the PATx as before. After the final 20 minute wash, PATx was removed and replaced with 250 µl secondary antibody diluted in PATx. This was then incubated on a roller in the dark for 2 hours at room temperature. After this incubation the secondary antibody solution was removed, and embryos were again washed three times in PATX before being incubated in PATx for a further three 20-minute periods on a roller at room temperature as before. Finally, PATx was removed from the embryos and replaced with 300 µl DABCO mounting medium (Sigma; recipe in appendix 2). DABCO was left to penetrate embryos for either 1 hour at room temperature or 24 hours at 4°C before mounting for imaging. Immunostained embryos were stored in DABCO in the dark at 4°C. Details of primary and secondary antibodies can be found below.

2.5.3 Antibodies used for Immunostaining

Primary antibodies used:

Antibody	Supplier	Code	Dilution	Diluted In
Rabbit anti-GFP	Abcam	ab290	1:500	PATX
Mouse anti-GFP	Abcam	ab1218	1:100	PATX
Rabbit anti-cDCP1	Cell Signaling	95785	1:500	PATX

Secondary antibodies used:

Antibody	Supplier	Code	Dilution	Diluted In
Goat anti-rabbit Alexa Fluor 488	Molecular probes	a11034	1:200	PATX
Goat anti-rabbit Alexa Fluor 568	Molecular probes	a11036	1:200	PATX
Goat anti-mouse FITC	Stratech	115-095-146	1:200	PATX
Goat anti-mouse Alexa Fluor 488	Molecular probes	a11029	1:200	PATX

2.5.4 Mounting fixed embryos for imaging

Fixed embryos of the desired embryonic stage were mounted using the same microscope slide set-up as for live imaging (section 2.2.1; Fig. 2.1), however fixed embryos were mounted in a small drop of DABCO instead of oil, and only single embryos were mounted per slide.

2.5.5 Imaging DCP-1 stained embryos

Using lasers of wavelengths 488nm and 562nm with GFP and RFP emission filters to image GFP labelled hemocytes and cDCP-1 labelled apoptotic cells respectively, z-stacks covering a depth of approximately 15µm were taken of the hemocytes on the superficial surface of the VNC. This was done using a Nikon A1 inverted confocal microscope with a CFI Plan Apochromat VC 60x oil objective lens (NA= 1.4), a zoom of 1.6 and z-spacing of 0.25µm, with Nikon Elements software. These stacks were taken at both the anterior and posterior ends of each embryo, allowing imaging of the majority of each embryo.

2.5.6 Imaging hemocytes on the VNC in stage 13 embryos

Fixed and Immunostained stage embryos with GFP-labelled hemocytes were mounted as in 2.4.3 and imaged using the same microscope set-up as in section 2.2.4.2.

2.6 *Drosophila* S2 cell work

2.6.1 Cell culture

Drosophila S2 cells (a gift from David Strutt, University of Sheffield) were cultured in Schneider's *Drosophila* medium (Gibco) supplemented with 10% heat-inactivated fetal bovine serum (Sigma –Aldrich) and 1% Penicillin-Streptomycin (Gibco) in a 25°C humidified incubator.

2.6.2 Assessment of Caspase activation post apoptosis induction

2.6.2.1 Induction of apoptosis

In order to work out the timing of apoptosis post-UV treatment, 150µl of S2 cells at a concentration of $1x10^6$ cells/ml in S2 media were first seeded to each of 9 wells of a 96-well cell culture plate, and left to adhere at for 2 hours at 25°C. The media was then removed from the wells and replaced with 100µl PBS. With the lid of the plate removed, cells were then irradiated with 100 mJ/cm^2 UV using a Stratalinker 2400 UV crosslinker. As a control, 3 of the wells were covered with aluminium foil during this treatment to prevent them from being exposed to UV. PBS was then removed from the wells and replaced with 100µl of S2 media containing 5 µM CellEvent Caspase -3/7 green detection reagent (Invitrogen) and propidium iodide (BIOlegend) (2µg/ml). As a further control, 3 of the UV-treated wells also contained the pan-caspase inhibitor Z-VAD-FMK (ApexBio) at a concentration of 100µM in order to prevent the activation of caspases.

2.6.2.2 Imaging

Time-lapse imaging of Caspase activation and PI staining in UV-treated cells prepared as above was then performed. Imaging was done with a Nikon Ti-E with Intensilight fluorescent illumination with ET/sputtered series fluorescent filters 49002 (Chroma), and a CFI Plan Apochromat λ 20X, N.A.0.75 objective lens with Perfect Focus system. Images were captured every 15 minutes for approximately 14 hours using NIS-Elements software (Nikon).

2.6.3 Collection of apoptotic cell supernatant for injection

To induce apoptosis of S2 cells, 1.2 x 10^7 cells suspended in Schneider's *Drosophila* medium were first plated to 60mm cell culture dishes (Sigma-Aldrich) and left to adhere for 3 hours at 25°C. The media was then carefully removed from the dishes and replaced with 2ml of PBS. With the lid of the cell culture dishes removed, cells were then irradiated with 100 mJ/cm^2 UV using a Stratalinker 2400 UV crosslinker. PBS was then removed and replaced with 2ml of fresh Schneider's *Drosophila* medium before the dishes were returned to the 25°C incubator. As a control, one of the dishes of cells was treated in exactly the same way as above but without treating with UV irradiation. Cells were then left for 13 hours before the cell supernatant was transferred to a 15ml falcon tube and put on ice. These were then centrifuged at 1000xg for 3 minutes at 4°C. The supernatant from this was then transferred to a fresh 15ml falcon tube and the centrifugation repeated. The supernatant of this was then removed and placed on ice until ready for injection.

2.7 Image processing and analysis

All image processing and analysis was performed using Fiji (ImageJ).

2.7.1 Analysis of hemocyte wound responses

Hemocyte responses to wounds at 60-minutes post-wounding (and other timepoints as required) were analysed by first blinding all post-wound images using a Python script obtained from the Whitworth Laboratory (University of Cambridge). The brightfield channel image was then used to locate the wound perimeter, which was drawn around using the polygon selection tool in Fiji. The area of the wound was then measured and the wound perimeter drawn on every z-slice of

the GFP channel. 15 z-slices (15µm depth) were then counted from and including the first non-wound hemocyte (i.e. those that are not touching the wound perimeter in any way) to come into focus in the stack, and every slice after this was deleted. The number of hemocytes at the wound was then counted by scrolling through the z-stack and identifying hemocytes within or with any part of them touching the wound perimeter, and marking them using the multi-point tool in Fiji as they were counted. The density of hemocytes at the wound was then quantified by dividing the number of hemocytes present at the wound by the wound area for each embryo. This was then normalised to control embryo hemocyte densities. Wounds with an area of less than 1500 μm^2 were not used.

2.7.2 Analysis of time-lapse movies of hemocytes responding to wounds

In order to gain a better insight into the dynamics of hemocyte responses to wounds, the 60-minute time-lapse movies of hemocytes responding to the wounds taken as part of the wounding assay were sometimes analysed. The movies were first prepared for analysis by creating a maximum projection of the GFP channel. The corresponding post-wound image was then opened and the brightfield channel used to identify the wound perimeter as above. This selection was then added to the manager in Fiji and transferred onto the maximum projection movie in order to visualise the location of the wound. A number of analyses were then performed in these processed movies:

2.7.2.1 Percentage responders

To analyse the percentage of hemocytes that respond to the wound at any given point during the 60-minute time-lapse movie, each hemocyte present at the first time point (t=0) was tracked over the duration of the movie. If any part of the hemocyte came into contact with the wound perimeter during the course of the movie, then it was counted as having responded. The percentage of hemocytes actively responding to the wound was then calculated for each embryo. This was done by subtracting the number of hemocytes already at the wound at t=0 by the total number of hemocytes tracked (giving us the number of hemocytes with the potential to actively respond to the wound), and then dividing the number of hemocytes who responded to the wound by this number, and finally multiplying by 100.

2.7.2.2 Percentage of hemocytes leaving the wound

Hemocytes were tracked in the wounding movies as above, however this time every hemocyte that was present at the wound at any point during the movie, but who left at any point (i.e. no single part of the hemocyte was touching the wound perimeter) was counted. The percentage of

hemocytes leaving the wound per embryo was then calculated by dividing the number of hemocytes deemed to have left the wound by the number of hemocytes that were already at or responded to the wound during the movie (i.e. the number there at t=0 plus the number that were to deemed to have responded), and multiplying by 100.

2.7.3 Pre-wound hemocyte density on the VNC

The density of hemocytes in pre-wound images was analysed by first counting 15 z-slices (15µm depth) from and including the first hemocyte to come into focus in the z-stack, and deleting all subsequent slices. A maximum projection of the remaining slices was then created and the number of hemocytes counted using the multi-point tool in Fiji. The area of the embryo was then measured by using the polygon selection tool to draw around the embryo boundary, which was defined as the area where the auto-fluorescence from the vitelline membrane ends. Finally, hemocyte density was calculated by dividing the number of hemocytes by the embryo area and then multiplying this by 100

2.7.4 Stage 13 hemocyte density on the VNC

The density of hemocytes on the VNC in stage 13 embryos was analysed as above but using fixed embryos.

2.7.4 Analysis of hemocyte random migration speeds

In order to analyse the random migratory behaviour of hemocytes, maximum projection time-lapse movies were first created using the GFP channel. Hemocyte migrations were then tracked using the manual tracking plug-in in Fiji, which involved tracking each individual hemocyte over the course of the movie by clicking on the centre of the hemocyte at each time point. The ImageJ chemotaxis plugin was then used to calculate the speed of migration for each hemocyte tracked and an embryo average was also calculated. It must be noted that only hemocytes on or close to the midline were analysed, as those located more laterally are capable of migrating down the sides of the embryo, which would cause hemocyte velocity readings to be inaccurate as they may appear to be migrating very little, when in fact they may be migrating in a different plane of view.

2.7.5 Analysis of apoptotic cell clearance

In order to assess the engulfment of apoptotic cells by hemocytes, the two channels of each stack were first separated and de-speckled. 41 z slices were then counted from and including the slice in which the first hemocyte came into focus, which represents a depth of 10μm, and all remaining slices removed from both channels. The green and red channels of each stack were then re-merged to allow engulfed apoptotic cells to be seen within hemocytes. For each hemocyte that is fully in view in both the XY and Z planes, the number of engulfed apoptotic cells is quantified by scrolling through the stack and counting the number of red cDCP-1 punctae that are located fully within the hemocytes. This data is then used to calculate the average number of engulfed apoptotic cells per hemocyte per embryo. Untouched apoptotic cells were quantified by counting the number of red cDCP-1 punctae that are located within the above z-stacks but are in no way touching hemocytes.

2.7.6 Analysis of embryo ROS

In order to analyse the levels of DHR 123 ROS indicator fluorescence, 15 z-slices from and including the first nuclear red stinger labelled hemocyte nuclei to come into focus were counted and all other slices deleted for all channels. Maximum projections of each channel were then made and merged. Hemocyte ROS levels were then assessed by measuring the mean gray value of the green channel in a 6 μm diameter circle centred over each hemocyte nuclei. Background ROS levels were assessed using the same method except random areas of the embryo not containing hemocyte nuclei measured.

2.7.7 Analysis of Caspase activation and PI staining post-UV irradiation of *Drosophila* S2 cells

In order to analyse the activation of Caspases, and also PI staining of cells post-UV irradiation, each channel was first separated and despeckled in Fiji. A mask was then created of both the red and green channels before watershedding each. These masks were then used to quantify the number of cells Caspase (green channel) or PI (red channel) positive cells at each timepoint. In order to estimate the percentage of cells positive for each marker, the brightfield channel was then used to estimate the total number of cells in view. This was done by setting a zoom of 150% and counting the number of cells in the top right-hand section of the image at the first

timepoint. As the top right-hand corner at this zoom represents approximately one ninth of the entire image, the number counted in this area was multiplied by nine to get an estimate of the overall cell number. Finally, this was used to calculate the percentage of cells positive for each marker at each timepoint.

2.8 Experimental Repeats

At least three experimental repeats were done for every experiment, each on separate days.

2.9 Statistical analysis

All statistical analysis was performed using Prism software (GraphPad Prism 7). A non-parametric Mann-Whitney U test was performed when comparing two sets of data. When multiple comparisons between data sets were required a Kruskal-Wallis one-way ANOVA with Dunn's multiple comparison test was used. Data was deemed to be statistically significant if $p<0.05$.

Chapter 3: Overloading macrophages with apoptotic cells affects their function and behaviour

3.1 INTRODUCTION

Programmed cell death during embryonic development, and the subsequent removal of these dying cells by phagocytes is a fundamental and essential process that occurs in all multi-cellular organisms. During embryonic development, programmed cell death plays a critical role in the patterning and sculpting of the central nervous system, and large numbers of neurons undergo apoptosis in order to refine neuronal connections (Oppenheim 1991). During *Drosophila* embryogenesis, a great deal of programmed cell death occurs in the ventral nerve cord (VNC) (Abrams et al. 1993; Rogulja-Ortmann et al. 2007), a structure widely-considered to be the equivalent of the vertebrate spinal cord.

Apoptotic cells can first be observed in the VNC at stage 11 of *Drosophila* embryonic development, and from here the number increases until around stage 14, when there is a plateau in apoptosis that continues until the end of embryogenesis (Rogulja-Ortmann et al. 2007). In order to prevent secondary necrosis of apoptotic cells, and to prevent their contents from spilling into the surrounding environment, they must be swiftly and efficiently cleared by phagocytes. In the central nervous system (CNS) of *Drosophila* embryos, apoptotic cells are efficiently cleared by glial cells – which operate as non-professional phagocytes (Freeman et al. 2003; Kurant et al. 2008). In order for glia to perform this essential role, they must first acquire the ability to recognise and engulf apoptotic cells.

Glial cells in *Drosophila* can be subdivided into two main groups: the midline glia and the lateral glia, the latter of which accounts for the vast majority of glia (Stork et al. 2012). The specification of lateral glia requires the transcription factor Glial cells missing (Gcm) (Jones et al. 1995; Hosoya et al. 1995). Gcm then induces the expression of target genes in lateral glia such as *reversed polarity* (*repo*), a transcription factor expressed in all lateral glial cells that is required for their normal function and differentiation (Campbell et al. 1994; Xiong et al. 1994; Halter et al. 1995). In fact in *repo* mutants there are normal numbers of glia but their morphology is abnormal and their volume is significantly decreased (Shklyar et al. 2014). As well as being required for normal morphology, *repo* is also important in regulating the phagocytic capacity of glial cells in the CNS (Shklyar et al. 2014). *repo* is required for the

expression of the apoptotic cell receptor Draper (Drpr) and for normal expression levels of another apoptotic cell receptor, Simu, in glial cells, and in *repo* mutant embryos increased numbers of apoptotic cells can be found in the VNC due to the decreased ability of glia to clear apoptotic cells (Shklyar et al. 2014). Interestingly, restoring expression of Simu and Drpr specifically in glial cells in *repo* mutants rescues their defective phagocytosis of apoptotic cells (Shklyar et al. 2014). Therefore, *repo* is required for the normal expression of the apoptotic cell receptors Drpr and Simu on glial cells, important effectors of apoptotic cell clearance.

On the ventral side of the embryo, macrophages migrate on the surface of the VNC in close contact with glial cells. Prior to the VNC becoming fully ensheathed by surface glial cells by approximately stage 16 of embryonic development (Schwabe et al. 2005), which seals the VNC from coming into direct contact with macrophages, it seems that these two phagocytic cell types work in concert to clear apoptotic neurons in this location. This seems true as in *repo* mutants, where glial cell specification is disrupted and they are much less able to phagocytose apoptotic cells, macrophages seem to increase their clearance of apoptotic cells in this area, suggesting that they are clearing those that would otherwise have been cleared by glial cells (Shklyar et al. 2014). This study also suggests that, unlike in control embryos, macrophages can occasionally be found within the VNC in *repo* mutant stage 16 embryos, which demonstrates that the sealing of the VNC by surface glia is perhaps disrupted in *repo* mutants (Shklyar et al. 2014). Together this suggests that prior to the ensheathment of the VNC (i.e. before around stage 16 of embryonic development), macrophages are able to clear apoptotic cells of the CNS together with glia.

There are a multitude of chronic inflammatory diseases where the clearance of apoptotic cells by macrophages is perturbed, including atherosclerosis, COPD and autoimmune diseases such as Systemic lupus erythematosus (SLE) (Poon et al. 2014). To better understand how the build-up of apoptotic cells affects macrophage function and behaviour *in vivo*, we sought to use *Drosophila* as a model organism to study this. In *Drosophila*, the build-up of engulfed apoptotic cells within macrophages in *SCAR* mutant embryos caused by defective corpse processing, results in their migration speeds being slowed, which can be partially rescued by blocking apoptosis (Evans et al. 2013), suggesting that apoptotic cells have the ability to affect macrophage migration, an essential aspect of macrophage function. Therefore, we aim to further examine how pathological levels of apoptosis affects macrophage function *in vivo* by genetically increasing the number of apoptotic cells for macrophages to clear in the *Drosophila* embryo. We hypothesise that *repo* mutant embryos represent a good model to study this as macrophages in such mutants have been reported to phagocytose increased numbers of apoptotic cells (Shklyar et al. 2014). We aim to study how macrophage migration and

inflammatory responses to wounds are affected in *repo* mutants and hypothesise that both of these migratory behaviours are perturbed in these embryos.

3.2 RESULTS

3.2.1 Macrophages clear increased numbers of apoptotic cells in the absence of normal glial cell specification

As we wished to study how pathological levels of apoptosis affect macrophage function and behaviour *in vivo*, we first needed to find a way of increasing the number of apoptotic cells for hemocytes to clear in the *Drosophila* embryo. We hypothesised that as hemocytes on the superficial VNC seem to work in concert with glial cells to clear apoptotic cells, then disrupting glial cell specification may lead to an increased number of apoptotic cells for hemocytes to clear. Therefore, we hypothesised that *repo* mutant embryos may represent a good model in which macrophages are overloaded with apoptotic cells. As this was being looked in to, a study by Shklyar *et al.* examining the developmental regulation of glial cell phagocytosis was published, which briefly noted that there is an increased volume of apoptotic cells per macrophage in *repo* mutant embryos (Shklyar et al. 2014). This supported our hypothesis and so we sought to examine apoptotic cell clearance in more detail in these mutants. To do this control and $repo^{03702}$ null mutant (Halter et al. 1995) embryos in which hemocytes were labelled using *UAS-GFP* expression under the control of the hemocyte specific *crq-GAL4* driver, were fixed and immunostained for cleaved DCP-1 (a downstream effector caspase cleaved during apoptosis (Song et al. 1997)) to label apoptotic cells and also for GFP to visualise hemocytes (Fig. 3.1 A-B'). To quantify the engulfment of apoptotic cells by hemocytes in these embryos, the number of cleaved DCP-1 particles found within the hemocytes on the VNC was counted. When we analysed engulfment in this way we found that hemocytes in $repo^{03702}$ mutants contained on average over double the number of corpses of those in control embryos (n=6 and 5 embryos for control (*w;;crq-GAL4,UAS-GFP*) and $repo^{03702}$ mutants (*w;;*$repo^{03702}$*,crq-GAL4,UAS-GFP*), respectively; p=0.0043 via Mann-Whitney test) (Fig. 3.1 C). We also counted the number of apoptotic cells that remained untouched by hemocytes in these embryos as a measure of the level of uncleared apoptotic cells and found that, although there was a trend towards an increase in the number untouched by hemocytes in the space between the epithelium and developing CNS in $repo^{03702}$ mutant embryos, this was not statistically significant compared to controls (n=4 and 9 embryos for control and $repo^{03702}$ mutants respectively; p=0.106 via Mann-Whitney test; Fig. 3.1 D). This data shows that hemocytes in *repo* mutants contain increased numbers of apoptotic cells, presumably because many of the glial cells can no longer phagocytose apoptotic cells efficiently, leaving more to be cleared by the hemocytes. We term this an increased

"apoptotic cell burden", as there is no evidence that there are enhanced levels of apoptotic cell death in *repo* mutants (Shklyar et al. 2014). This suggested to us that *repo*^{03702} mutants represent a useful model to understand how increased numbers of apoptotic cells affect macrophage function *in vivo*, particularly as hemocytes do not express *repo* (Xiong *et al.*, 1994; Armitage and Evans, unpublished data) and their initial specification at least should be unperturbed in this genetic background, as supported by the fact that the expression of hemocyte-specific genes *serpent* and *croquemort* seem normal in *repo* mutants.

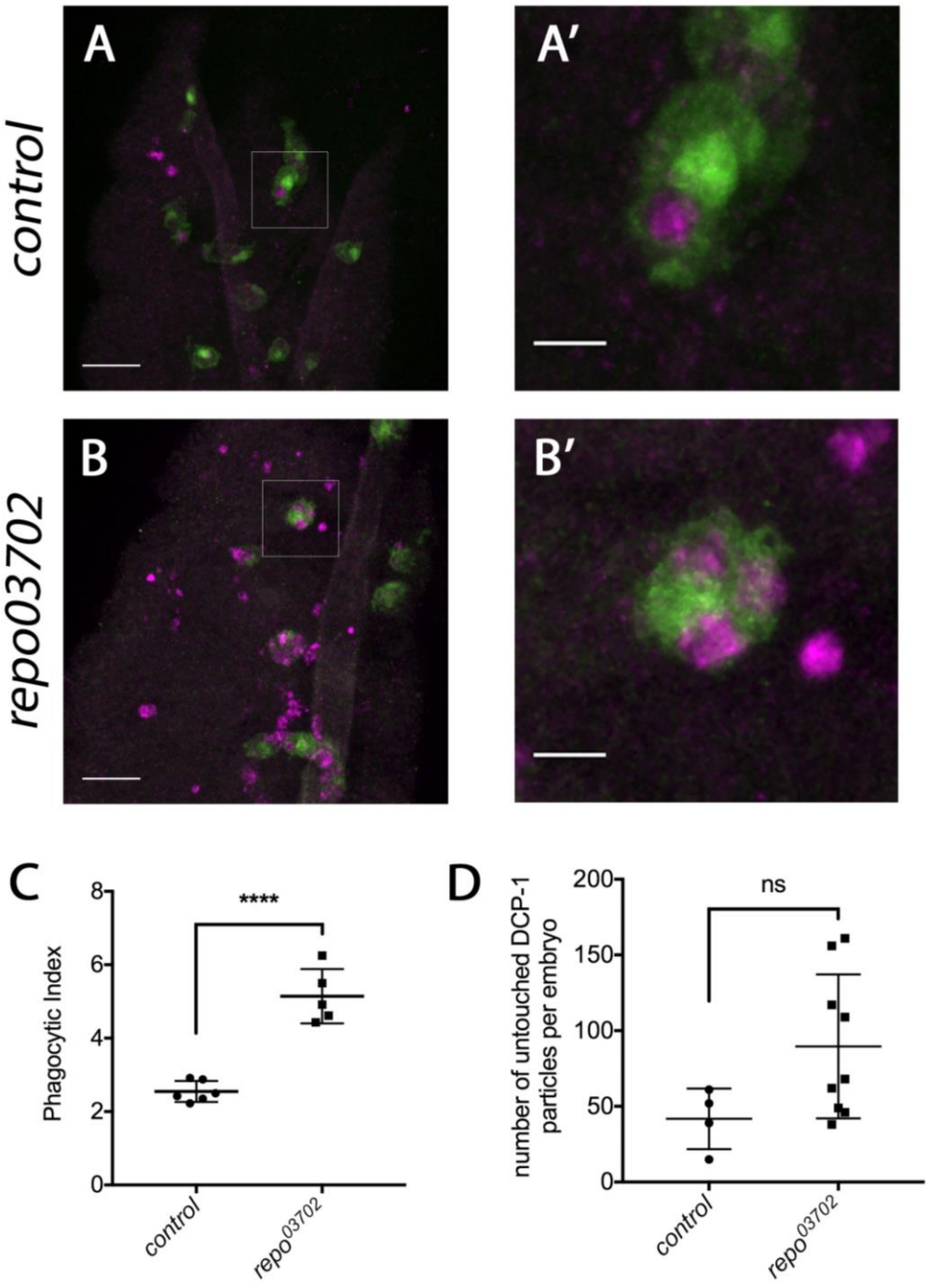

Figure 3.1: DCP-1 staining in *repo*^{03702} mutants reveals an accumulation of apoptotic cells within hemocytes
(A and B) Representative projections from confocal stacks of hemocytes (in green; crq>GFP) and apoptotic cells (in magenta; DCP-1) superficial to the VNC in control and *repo*^{03702} fixed stage 15 embryos, showing greatly increased numbers of apoptotic cells within hemocytes in *repo*^{03702} mutants. Scale bars represent 20µm. (A' and B') Zoomed images from A and B demonstrating the accumulation of apoptotic cells within hemocytes in *repo*^{03702} mutants. Scale bars represent 5µm. (C) Scatterplot of the average number of DCP-1 particles engulfed per hemocyte, per embryo (referred to as the 'phagocytic index' (PI)). Lines and error bars represent mean±SD; n=6 and 5 embryos analysed for controls and *repo*^{03702} mutants respectively. (D) Scatterplot of the number of DCP-1 particles that remain uncleared by hemocytes in control and *repo*^{03702} mutant embryos. Lines and error bars represent mean±SD; n=4 and 9 embryos analysed for control and *repo*^{03702} mutants respectively.
Asterisks indicate statistical significance as determined by Mann-Whitney test; ****p < 0.0001 and ns = not significant.

3.2.2 Macrophage inflammatory responses to wounds are decreased in *repo* mutants

As we found that the engulfment of apoptotic cells by hemocytes is increased in *repo*^{03702} mutants, and it is known that the engulfment of apoptotic cells by vertebrate macrophages induces an anti-inflammatory phenotype (Szondy et al. 2017), we sought to examine hemocyte inflammatory responses to wounds in *repo*^{03702} mutant embryos. To do this we wounded control (*w;;crq-GAL4,UAS-GFP*) and *repo*^{03702} mutant (*w;;repo*^{03702}*,crq-GAL4,UAS-GFP*) stage 15 embryos at the ventral epithelium using an ablation laser, and analysed the inflammatory response of hemocytes by quantifying the density of hemocytes at wounds 60 minutes post-wounding. In control embryos, hemocytes respond by robustly migrating to the wound and at 60 minutes post-wound there is a high density of hemocytes at the wound site (Fig. 3.2 A). In contrast, hemocytes in *repo*^{03702} mutants exhibit a decrease in their inflammatory migrations to wounds (Fig. 3.2 A, B), and at 60 minutes post-wound the density of hemocytes at the wound is significantly decreased by approximately 50% when compared to controls (n=23 and 17 embryos for controls and *repo*^{03702} mutants respectively; p<0.0001 via Mann-Whitney test) (Fig. 3.2 B). This shows that hemocyte inflammatory responses to wounds are reduced in *repo*^{03702} mutants where there are increased numbers of apoptotic cells engulfed by hemocytes, suggesting that increased exposure to or engulfment of apoptotic cells by hemocytes may be reducing their ability to mount an inflammatory response.

The *repo*^{03702} allele represents the strongest loss-of-function allele currently available (Halter et al. 1995), and since the previous phenotypes were all found in *repo*^{03702} homozygous embryos it was of paramount importance to confirm that these were specifically due to loss of *repo* function and not a second site mutation elsewhere on chromosome 3. To address this embryos trans-heterozygous for both the *repo*^{03702} mutation and a deficiency removing the *repo* gene

(*Df(3R)BSC638*) were wounded and hemocyte wound responses analysed (Armitage and Evans, unpublished data). This showed that there was a decrease in hemocyte wound responses at 60 minutes post-wounding, which was similar to *repo*^{03702} mutant homozygotes, with approximately a 50% reduction in hemocyte density at wounds compared to controls, showing that it is indeed the *repo*^{03702} mutation that is causing hemocyte inflammatory responses to be reduced in *repo*^{03702} mutant embryos. Hemocytes in these trans-heterozygous embryos also appear highly vacuolated, suggesting that the *repo*^{03702} mutation also causes there to be increased numbers of apoptotic cells within hemocytes (data not shown).

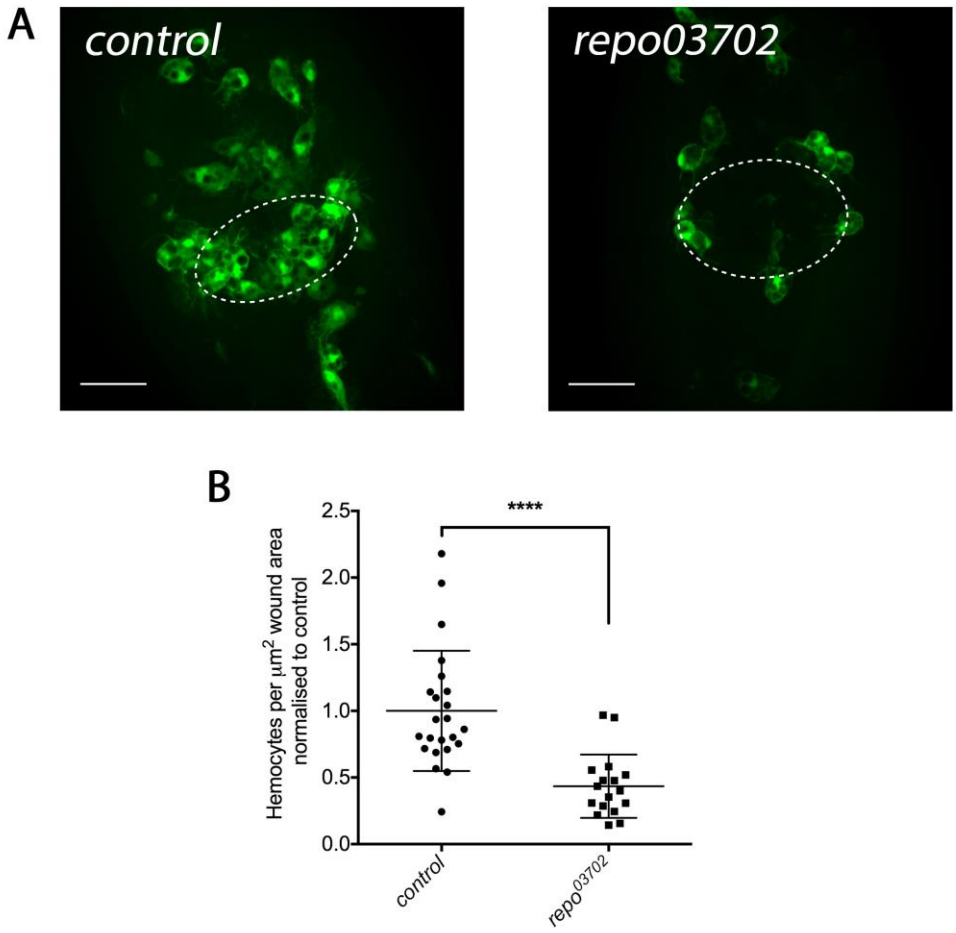

Figure 3.2: Hemocyte inflammatory migrations to wounds are perturbed in *repo*^{03702} mutants
(A) Representative stills of GFP-labeled hemocyte responses to wounds at 60 minutes post-wound in control and *repo*^{03702} mutant stage 15 embryos. (B) Scatterplot of hemocyte wound responses per embryo shown as the number of hemocytes per μm^2 wound area at 60 minutes post-wounding normalized to the control average. Lines and error bars represent mean±SD; n=23 embryos for controls and n=17 for *repo*^{03702} mutants.
White dashed ovals represent wound perimeter; scale bars represent 20μm; asterisks indicate statistical significance as determined by Mann-Whitney test; ****p < 0.0001.

3.2.3 Total number of macrophages in *repo* mutant embryos is unchanged, however less reach the ventral nerve cord

When wounding *repo* mutant embryos, we noticed that there seemed to be fewer hemocytes on the ventral nerve cord (VNC) around the wounding area compared to controls. Therefore we decided to analyse this by counting the number of hemocytes present in the pre-wound images taken as part of the wounding assay in control (*w;;crq-GAL4,UAS-GFP*) and *repo*^{03702} mutant (*w;;repo*^{03702}*,crq-GAL4,UAS-GFP*) embryos (Fig. 3.3 A), and calculating hemocyte density by normalising according to the area of the embryo in the field of view. We found that the density of hemocytes in these pre-wound images was indeed reduced in *repo*^{03702} mutants, with approximately a 40% decrease compared to control embryos (n=23 and 15 for control and *repo*^{03702} mutants respectively; p<0.0001 via Mann-Whitney test) (Fig 3.3 B). This suggests that the wound response defect observed in *repo* mutants may be due to decreased numbers of hemocytes in the wound vicinity prior to wounding.

In light of this result, we wondered whether there was perhaps a decrease in the total numbers of hemocytes in *repo* mutants. To examine this we flattened embryos whose hemocytes were labelled using the nuclear-specific marker *UAS-nuclear red stinger* that was specifically expressed in hemocytes using *crq-GAL4*. Flattening of the embryos then allowed us to count the number of red nuclei in the entire embryo and therefore the total number of hemocytes (Fig. 3.3 C). We found that, compared to control embryos (*w;;crq-Gal4,UAS-nuclear red stinger*), there was no difference in the total numbers of hemocytes in the whole embryo in *repo*^{03702} mutants (*w;;repo*^{03702}*,crq-Gal4,UAS-nuclear red stinger*; n=10 and 13 embryos for controls and *repo* mutants respectively; p=0.455 via Mann-Whitney test; Fig. 3.3 D), with both genotypes having around 700 hemocytes per embryo which is in line with published data (Brückner et al. 2004). This was also the case in *repo*^{03702}*/Df(3R)BSC638* trans-heterozygotes (Armitage and Evans, unpublished data). This shows that the decreased number of hemocytes in pre-wound images in *repo*^{03702} mutants is not due to a decrease in overall numbers of hemocytes in the embryo.

If not for decreased numbers of hemocytes in the embryo, we wondered what might possibly be the reason for decreased numbers of hemocytes on the ventral midline at stage 15 of development (Fig. 3.3 A, B). So, we next hypothesised that the decreased numbers were due to defects in the developmental dispersal of hemocytes. Hemocytes have been shown to migrate along well characterised routes through the embryo during embryonic development, to eventually become dispersed throughout the entire embryo (Tepass et al. 1994). By embryonic stage 13, a continuous line of hemocytes usually forms on the ventral midline of the embryo, and this line is formed by the migration of hemocytes from both the anterior and posterior ends of the embryo (Wood et al. 2006; Tepass et al. 1994). Therefore, we first decided to assess developmental dispersal by checking for this line of hemocytes on the ventral embryo. We did this by fixing and staining control (*w;;crq-GAL4,UAS-GFP*) and $repo^{03702}$ (*w;;*$repo^{03702}$*,crq-GAL4,UAS-GFP*) embryos for GFP and imaging stage 13 embryos laterally, in the plane of focus that allows us to see the hemocytes along the ventral midline (Fig. 3.3 F). We then calculated the percentage of embryonic segments that contained hemocytes in this location, as a measure of the extent to which the hemocytes had managed to migrate along the midline. When we did this, we found that hemocytes in $repo^{03702}$ mutant embryos could be found in 100% of segments, which was also true for controls (n=15 and 17 embryos for controls and $repo^{03702}$ mutants respectively; $p>0.999$ via Mann-Whitney test) (Fig. 3.3 E). We also quantified the number of hemocytes in the central 5 segments at the VNC in stage 13 embryos (Fig. 3.3 G). This quantification showed that as well as in stage 15, stage 13 $repo^{03702}$ mutant embryos also have decreased numbers of hemocytes in this area compared to controls (n=13 embryos for both controls and $repo^{03702}$ mutants; $p<0.0001$ via Mann-Whitney test) (Fig. 3.3 H). Altogether this data suggests that fewer hemocytes are reaching the superficial VNC area of the embryo in *repo* mutants. One explanation may be due to hemocytes being preoccupied by clearing the increased numbers of apoptotic cells elsewhere in these embryos, as apoptosis can be observed from as early as embryonic stage 11 in the *Drosophila* CNS (Rogulja-Ortmann et al. 2007). Hemocytes also migrate slower in *repo* mutants (see Fig. 3.9), therefore fewer hemocytes may be present on the VNC at both stage 13 and 15, as they simply cannot get there as quickly as in controls. Since hemocytes do not migrate more rapidly than controls in the absence of apoptosis (Evans et al., 2013; see also figure 3.10 below), it seems less likely that engulfment restricts migration speeds per se, though of course larger hemocytes that are full of apoptotic cells as in *repo* mutants, may find it more difficult to move through more spatially constricted regions, for example during entry into the germband (Ratheesh et al. 2015).

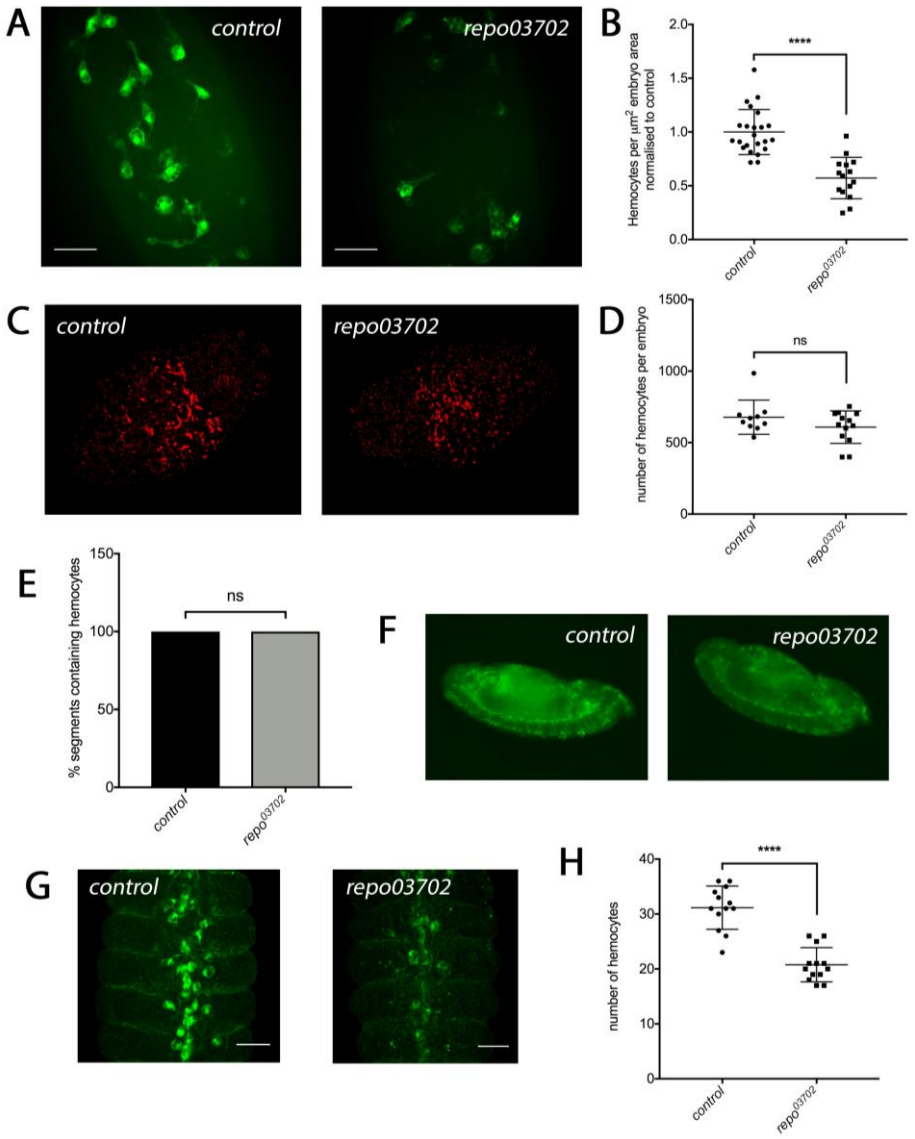

Figure 3.3: Hemocyte numbers on the VNC in stage 15 embryos are reduced in *repo*^{03702} mutants, but total numbers are not affected

(A) Representative pre-wound stills of GFP-labeled hemocytes on the superficial VNC in control and *repo*^{03702} mutant stage 15 embryos. (B) Scatterplot of hemocyte densities in stage 15 pre-wound images shown as the number of hemocytes per µm^2 embryo area normalized to the control average. Lines and error bars represent mean±SD; n=23 embryos for controls and n=15 for *repo*^{03702} mutants. (C) crq>redst labeled hemocyte nuclei in control and *repo*^{03702} mutant squashed stage 15 embryos embryos, showing the total number of hemocytes in the embryos. (D) Scatterplot of the total number of hemocytes per embryo. (E) Quantification of the % of embryonic segments containing hemocytes on the superficial VNC. (F) GFP-labeled hemocytes in immunostained control and *repo*^{03702} mutant embryos. (G) GFP-labeled hemocytes on the VNC in immunostained control and *repo*^{03702} mutant stage 13 embryos. (H) Scatterplot of the number of hemocytes on the VNC in stage 13 embryos. Lines and error bars represent mean±SD; n=10 and 13 embryos for controls and *repo*^{03702} mutants respectively.

3.2.4 The percentage of hemocytes migrating to wounds is decreased in *repo* mutants

As there are decreased numbers of hemocytes in the area of the embryo typically ablated in the wounding assay, we wanted to assess whether the decreased wound response seen in *repo* mutants was due simply to there being less hemocytes in the surrounding area. To do this we made time-lapse movies of hemocytes as they responded to wounds in $repo^{03702}$ mutant (*w;;*$repo^{03702}$*,crq-GAL4,UAS-GFP*) and control (*w;;crq-GAL4,UAS-GFP*) embryos, and calculated the percentage of hemocytes present in the frame of view at the beginning of the movie that actively migrated to the wound. When we did this, we found that the percentage of hemocytes responding to wounds at any point during the wounding movie was significantly decreased in $repo^{03702}$ mutants when compared to controls (n=7 and 9 embryos for controls and $repo^{03702}$ mutants respectively; p=0.0003 via Mann-Whitney test; Fig. 3.4 A, B). The percentage of hemocytes that are at or migrate to the wound that subsequently leave was also analysed. We found that hemocytes in $repo^{03702}$ mutants are no more likely to leave the wound than in controls (n=7 and 9 embryos for controls and $repo^{03702}$ mutants respectively; p>0.999 via Mann-Whitney test; Fig. 3.4 C), suggesting that the decreased wound response in $repo^{03702}$ mutants is not due to hemocytes migrating to and then leaving the wound. Together this data suggests that the defective wound responses of hemocytes in *repo* mutants are unlikely to be due solely to a decrease in hemocyte density in the surrounding area, as the hemocytes that are present in this area in these mutants are still much less likely to migrate to wounds. It is possible that a certain number of hemocytes need to migrate to wounds in order to relay a signal that attracts further hemocytes to the wound. However, we have found that a reduction in hemocytes in the wounding area does not always correlate with a decrease in the % of those responding to wounds (for example in *crq* mutants; Chapter 6, Figure 6.4), therefore this is unlikely to be the case.

3.2.5 Absence of JNK signalling in hemocytes does not correlate with failure to migrate to wounds

In $repo^{03702}$ mutants, hemocytes contain on average over double the number of apoptotic corpses seen in control hemocytes (see Figure 3.1). We hypothesised that this may induce stress signalling in hemocytes, which might in turn affect the ability of macrophages to mount an inflammatory response to wounds. One well-known stress signalling pathway is the JNK pathway, which controls essential cellular processes such as proliferation, apoptosis and inflammation (Johnson and Nakamura 2007). Further to this, a study by Weavers *et al.* showed that corpse engulfment by hemocytes induces JNK signalling within the hemocytes, and that

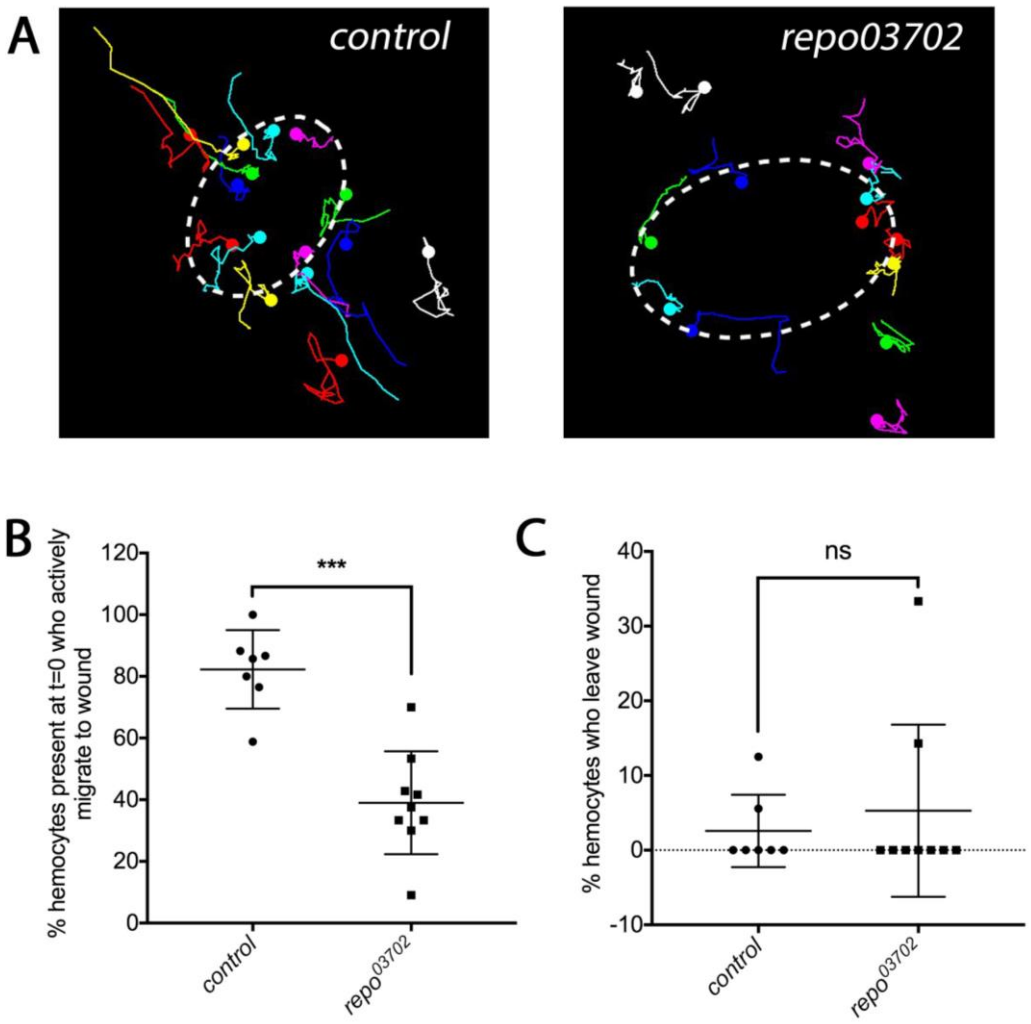

Figure 3.4: The percentage of hemocytes migrating to wounds during the 58-minute time period post-wounding is reduced in *repo*^{03702} mutants

(A) Representative tracks of hemocyte wound responses over 58 minutes from the time of wounding in control and *repo*^{03702} mutant stage 15 embryos. Coloured lines represent the course of migration of each hemocyte tracked and coloured dots show the final position of hemocytes at 58 minutes post-wound. (B) Scatterplot of the % of hemocytes present at t=0 minutes post-wound who actively migrate to the wound at any point during the wounding movie. Lines and error bars represent mean±SD; n=7 movies analysed for control embryos, n=9 for *repo*^{03702} mutants. (C) Scatterplots of the % of hemocytes present at t=0 minutes post-wound who are at and then migrate away from the wound at any point during the wounding movie. Lines and error bars represent mean±SD; n=7 movies analysed for control embryos, n=9 for *repo*^{03702} mutants. White dashed ovals represent wound perimeter; scale bars represent 20μm; asterisks indicate statistical significance as determined by Mann-Whitney test; ***$p < 0.001$ and ns = not significant.

this is required for subsequent inflammatory responses to wounds (Weavers et al. 2016). They also showed that most hemocytes in stage 14 control embryos have active JNK signalling due to the engulfment of apoptotic corpses (Weavers et al. 2016). Therefore we sought to examine the activation of JNK signalling in hemocytes in *repo*^{03702} mutants to see whether abnormal activation might explain their lack of a wound response. To do this we used flies carrying *TRE-eGFP* - a JNK signalling transgenic reporter construct that results in GFP expression induction in cells where JNK signalling is active (Chatterjee and Bohmann 2012). When we examined hemocytes in stage 15 embryos for active JNK signalling, we found that approximately 3% of hemocytes exhibit active JNK signalling in control embryos (*w;TRE-eGFP;crq-Gal4,UAS-nuclear red stinger*), whereas this increased to around 7% in *repo* mutants (*w;TRE-eGFP;repo*^{03702}*,crq-Gal4,UAS-nuclear red stinger*; Fig. 3.5 A, B), and although this increase in the percentage of GFP-positive hemocytes was only very slight, this was significantly different from controls (n=16 and 13 embryos for controls and *repo*^{03702} mutants respectively; p=0.0264 via Mann-Whitney test; Fig. 3.5 B). As an internal control to confirm that *TRE-eGFP* construct was indeed present and functionally correctly, we examined the dorsal side of the embryo, where JNK signalling is required for dorsal closure (Sluss et al. 1996). Here we found very strong GFP expression in the most dorsal epithelia in both control and *repo* mutant embryos (data not shown), confirming that the TRE-eGFP construct was functional in these embryos. Furthermore, Together this data suggests that, in contrast to published data (Weavers et al. 2016), JNK signalling is generally not active in hemocytes in stage 15 embryos and very minor differences in the numbers of JNK positive cells per embryo (a difference of on average only one extra JNK-positive cell per embryo) seem unlikely to account for the phenotypes associated with *repo* loss-of-function.

Imaging JNK signalling activation in hemocytes during wounding using the *TRE-eGFP* reporter, we assessed whether hemocytes activate JNK signalling in response to wounds and whether this is a pre-requisite for their inflammatory migrations, which may be perturbed in *repo*^{03702} mutants. In this case time-lapse wounding movies were recorded for 120 minutes instead of the usual 60 minutes to allow time for GFP to be expressed upon JNK signalling activation. We were confident that this was enough time to visualise JNK signalling activation as by 60 minutes post-wound GFP expression was observed in the epithelial cells around the periphery of the wound (Fig. 3.5 C', D'), which was extremely bright by 120 minutes. This also acts as a further control to ensure that the TRE-eGFP reporter is functional as it is known that JNK signalling becomes active in cells at the edge of wounds in *Drosophila* (Rämet et al. 2002). When we observed these time-lapse wounding movies we noticed that very few hemocytes migrating to wounds in control embryos became GFP-positive during their response to wounds over 60 or 120 minutes, and that the same was true for hemocytes in *repo*^{03702} mutants (Fig. 3.5 C-D';), suggesting that JNK signalling is not activated in hemocytes upon their migration to

wounds. We also observed that active JNK signalling in hemocytes prior to wounding does not preclude migration to wounds, as GFP-positive hemocytes were observed responding to wounds. This data suggests that JNK signalling is not activated upon hemocyte migration to wounds, and that this is not a pre-requisite for hemocytes to be able to respond to wounds. Therefore the *repo* mutant inflammatory response defect is unlikely due to deregulated JNK signalling in hemocytes.

3.2.6 ROS levels are unaffected in *repo* mutant embryos

Engulfment of apoptotic cells by macrophages has been shown to induce a shift in macrophage phenotype to a more anti-inflammatory state, and results in the secretion of anti-inflammatory cytokines and inhibition of pro-inflammatory cytokine production (Voll et al. 1997; Valerie A. Fadok et al. 1998; Szondy et al. 2017). Therefore, another possible explanation for a decrease in the inflammatory response of hemocytes in *repo* mutants may be that the engulfment of increased numbers of apoptotic cells is shifting the phenotype of hemocytes to a more anti-inflammatory state. One important mediator of this are Reactive Oxygen Species (ROS), whose increased presence is associated with the promotion and function of 'M1' type macrophages, which are considered to be pro-inflammatory (Tan et al. 2016). The ROS hydrogen peroxide (H_2O_2) is also known to be the chemoattractive cue produced at wounds that forms a gradient mediating hemocyte migration to sites of tissue damage (Moreira et al. 2010), therefore changes in embryo ROS levels may affect the ability of hemocytes to respond to wounds. With this in mind we sought to stain $repo^{03702}$ mutant (*w;;*$repo^{03702}$*,crq-GAL4,UAS-nuclear red stinger*) and control (*w;;crq-GAL4,UAS-nuclear red stinger*) embryos for ROS. To do this we used the ROS indicator Dihydrorhodamine 123 (DHR 123) to stain live, stage 15 embryos. DHR 123 is oxidised by ROS within cells, causing it to localise to mitochondria and become fluorescent. When the degree of DHR 123 fluorescence in hemocytes on the superficial surface of the VNC was analysed compared to embryo background levels, we found that these were no different in $repo^{03702}$ embryos when compared to controls (n=9 and 10 embryos analysed for control and $repo^{03702}$ respectively; p=0.905 via Mann-Whitney test; Fig. 3.6 A, B). The levels of DHR 123 fluorescence in the background (i.e. levels extracellular to hemocytes) of $repo^{03702}$ mutant embryos were also no different to controls (n=9 and 10 embryos for control and $repo^{03702}$ respectively; p=0.604 via Mann-Whitney test; Fig. 3.6 A, C). This data therefore suggests that the decrease in hemocyte inflammatory responses in *repo* mutants cannot be explained by differing levels of hemocyte ROS levels, or indeed levels extracellular to hemocytes in the embryo.

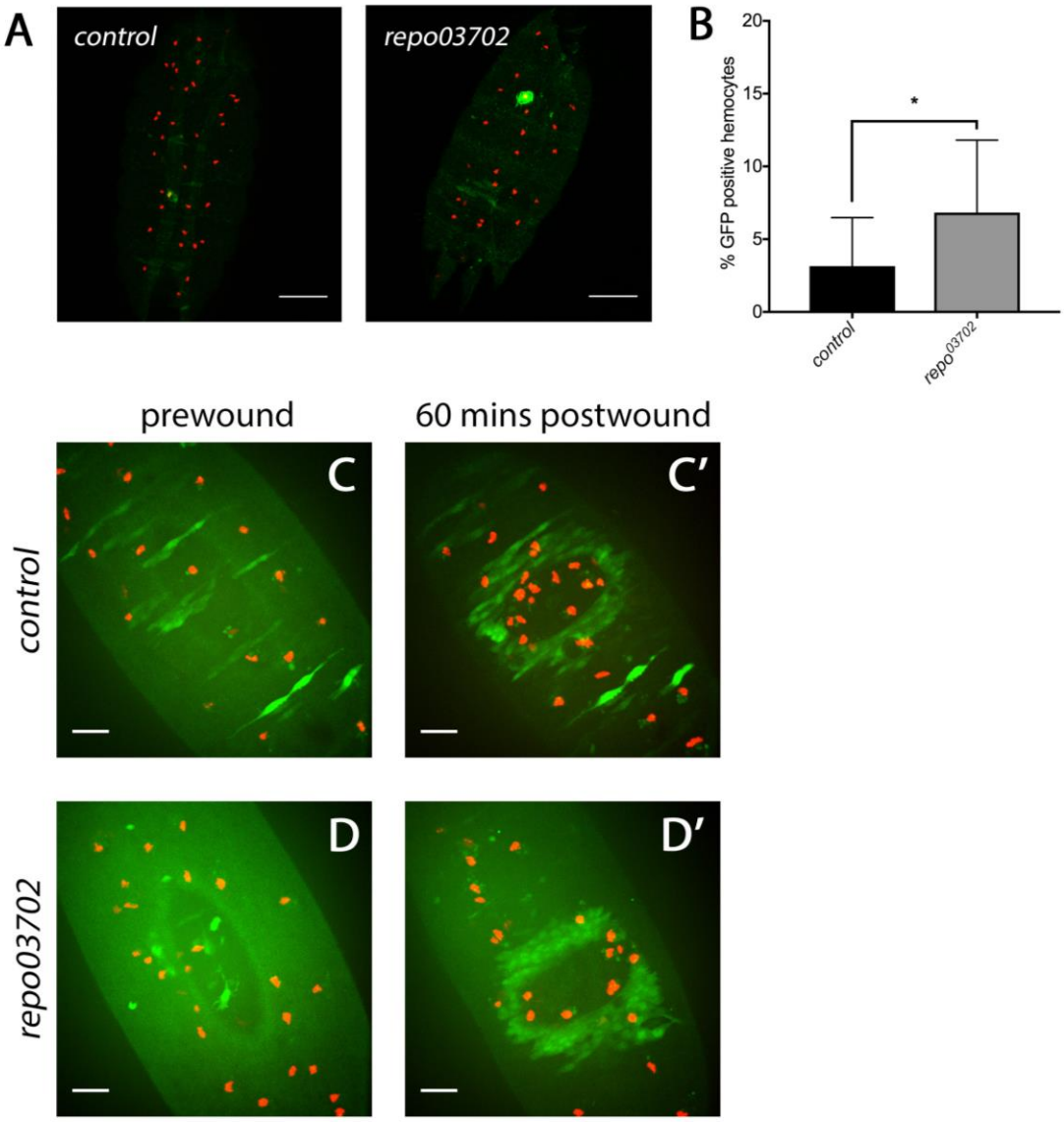

Figure 3.5: Very few hemocytes exhibit active JNK signalling at the VNC in Drosophila embryos and its activity does not correlate with hemocyte migrations to wounds
(A) Representative projections from confocal stacks of stage 15 embryos (whose hemocyte nuclei are shown in red; crq>nuclear red stinger) fixed and stained for GFP to label cells expressing the *TRE-eGFP* JNK signalling reporter construct, showing very minimal numbers of GFP labelled hemocytes in control and *repo*^{03702} mutants. (B) Quantification of the percentage of hemocytes on the VNC with active JNK signalling. Data represented as mean+SD; n=16 and 13 embryos for controls and *repo*^{03702} mutants respectively. (C and D) Representative pre-wound and 60 minute post-wound (C' and D') stills of nuclear red stinger labelled hemocytes on the VNC in embryos carrying the *TRE-eGFP* JNK signalling reporter construct, showing that hemocytes in control and *repo*^{03702} mutant stage 15 embryos do not activate JNK signalling in the 60 minute time period following wounding. Note the expression of GFP in the epithelial cells surrounding the wound in C' and D'.

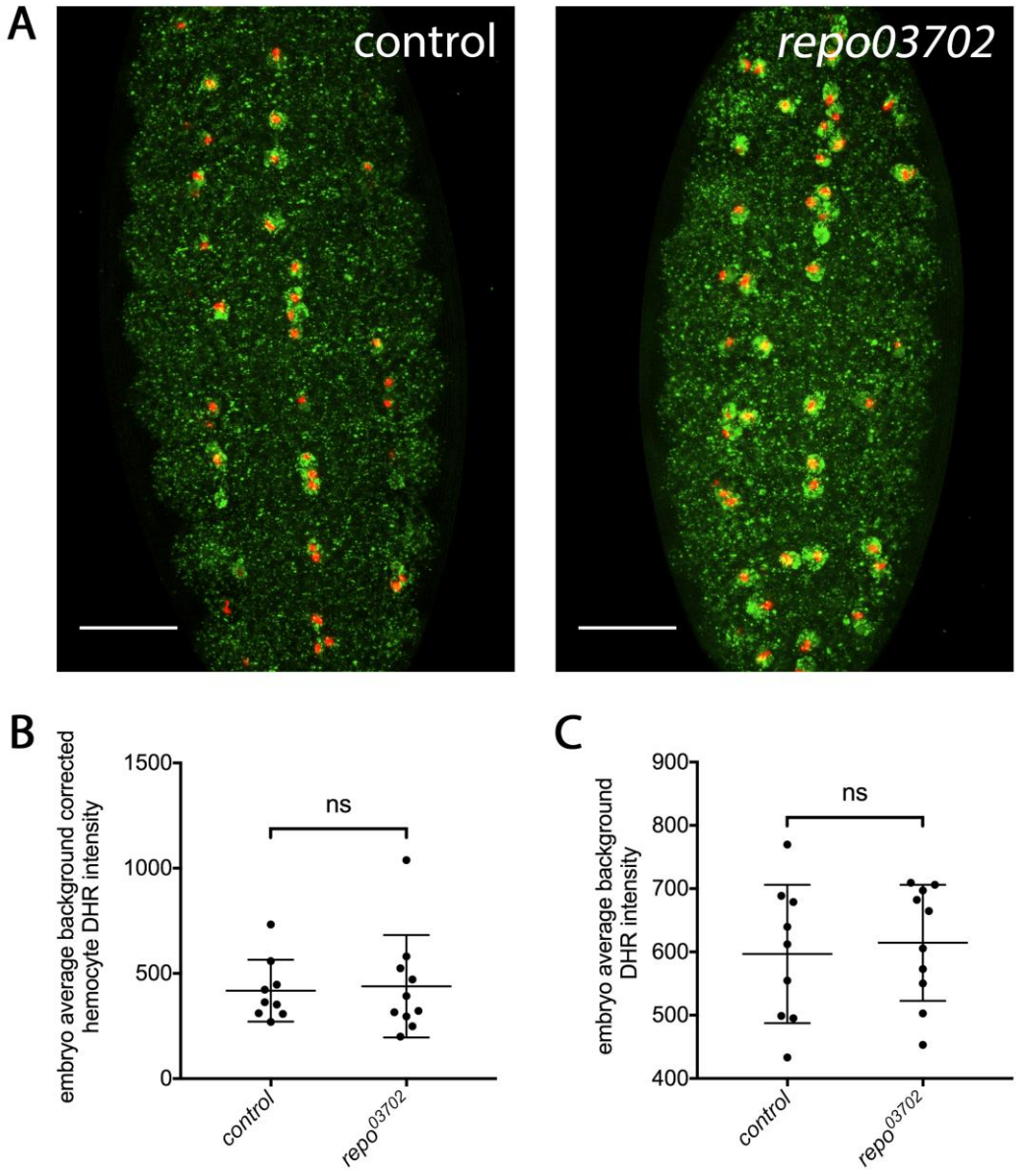

Figure 3.6: Hemocyte ROS levels are unchanged in *repo*^{03702} mutants
(A) Representative projections from confocal stacks of live stage 15 embryos (whose hemocyte nuclei are shown in red) treated with the ROS indicator DHR 123 (green), showing similar levels of ROS in hemocytes compared to the rest of the embryo in *repo*^{03702} compared to control. (B) Scatterplot of embryo average background corrected hemocyte DHR 123 indicator intensities. Lines and error bars represent mean±SD; n=9 and 10 embryos for controls and *repo*^{03702} mutants respectively. (C) Scatterplot of embryo average DHR 123 indicator background intensity. Lines and error bars represent mean±SD; n=9 and 10 embryos for controls and *repo*^{03702} mutants respectively.
Scale bars represent 20μm; asterisks indicate statistical significance as determined by Mann-Whitney test; ns= not significant.

3.2.7 Removal of individual apoptotic cell receptors fails to rescue hemocyte inflammatory responses

Another hypothesis was that hemocyte migration to wounds is decreased in *repo* mutants due to increased downstream signalling from apoptotic cell receptors in hemocytes. To examine this we analysed hemocyte wound responses in embryos mutant for both one of the known apoptotic cell receptors (Croquemort, Scab, Simu or Beta-nu Integrin) and $repo^{03702}$ (Fig. 3.7 A), with the idea that doing so may prevent downstream signalling from that particular receptor and so rescue inflammatory responses. No double mutant combination tested ($crq^{KO};repo^{03702}$ (*w;*$crq^{KO};repo^{03702}$*,crq-GAL4,UAS-GFP*), $scb^{2};repo^{03702}$ (*w;*$scb^{2};repo^{03702}$*,crq-GAL4,UAS-GFP*), $simu^{2};repo^{03702}$ (*w;*$simu^{2};repo^{03702}$*,crq-GAL4,UAS-GFP*)and $\beta v^{1};repo^{03702}$ (*w;* $\beta v^{1};repo^{03702}$*,crq-GAL4,UAS-GFP*)) was able to rescue *repo*-dependent (*w;;*$repo^{03702}$*,crq-GAL4,UAS-GFP*) hemocyte wound responses (Fig. 3.7 B). This suggests that downstream signalling from any one of these apoptotic cell receptors is unlikely to be responsible for dampening hemocyte inflammatory responses, though of course removal of clearance receptors may also exacerbate the problem in *repo* mutants. It still may be the case that there is redundancy in the function of apoptotic cell receptors and that you may need to remove multiple receptors to fully block downstream signalling from apoptotic cells receptors. Note that we did not examine the apoptotic cell receptor Drpr in these experiments, as the *drpr* and *repo* mutations are on the same chromosome, and despite a large mapping distance between these loci we have been unable to recover *draper*$^{\Delta 5}$,$repo^{03702}$ recombinants, potentially suggesting synthetic lethality between the alleles used.

3.2.8 p38 MAPK signalling in hemocytes is not responsible for decreased inflammatory responses in *repo* mutants

As macrophages fail to migrate normally to sites of tissue damage in $repo^{03702}$ mutants we wondered whether this was perhaps due to the decreased ability of hemocytes to prioritise chemotactic cues. In *Drosophila* embryos a hierarchy of cue prioritisation by hemocytes seems to exist, with apoptotic cells at the top, then development chemoattractants and finally wound cues (Moreira et al. 2010). Vertebrate neutrophils have also been shown to prioritise migratory cues, as they favour migration towards bacterial and necrotic cell-derived fMLP over endogenous IL-8 (Campbell et al. 1997). It has been shown that the p38 MAPK and PI3K/Akt signaling pathways are responsible for determining the hierarchy of responsiveness towards chemotactic cues, with p38 MAPK signalling mediating response to so-called ‘end target’ chemoattractants such as fMLP, whereas PI3K/Akt signaling mediates the response to ‘intermediate’ ones (Heit et al. 2002). In *Drosophila* PI3K signalling has been shown to be

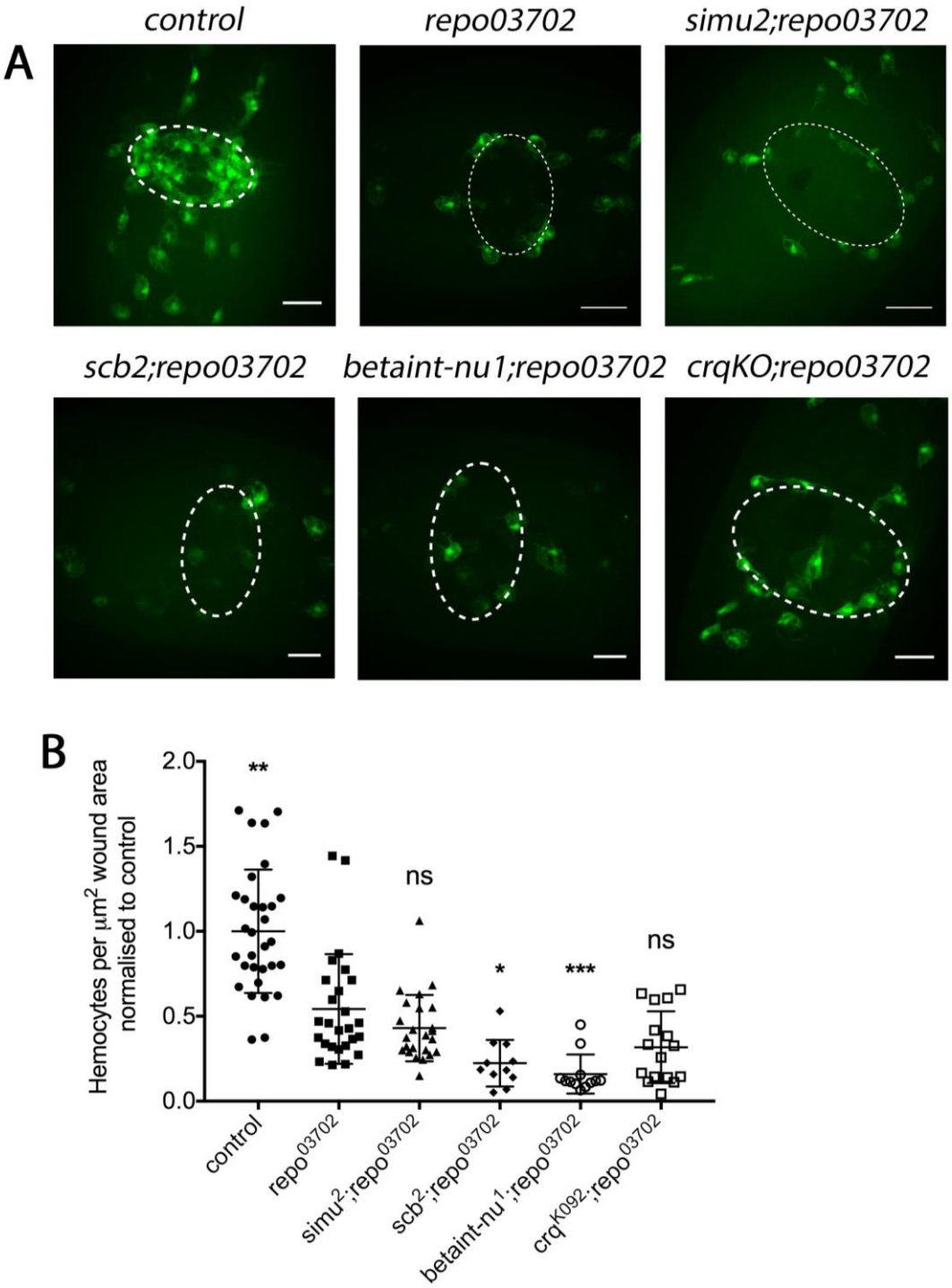

Figure 3.7: Removing either of the apoptotic cell receptors *Simu, Crq, Scab* or *βv* integrin is unable to rescue repo^{03702} mutant inflammatory responses

(A) Representative stills of GFP-labeled hemocyte responses to wounds at 60 minutes post-wound in control and *repo^{03702}* mutant stage 15 embryos, as well as *simu^{2}; repo^{03702}*, *scb^{2};repo^{03702}, βv^{1};repo^{03702}* and *crq^{KO};repo^{03702}* double mutants. (B) Scatterplot of hemocyte wound responses per embryo shown as the number of hemocytes per µm^2 wound area at 60 minutes post-wounding normalized to the control average. Lines and error bars represent mean±SD; n=31, 26, 24, 11, 12 and 16 embryos per the above genotypes respectively. White dashed ovals represent wound perimeter; scale bars represent 20µm; asterisks indicate statistical significance compared to *repo^{03702}* mutants as determined by Kruskal-Wallis one-way ANOVA test; ***p < 0.001, **p<0.01, *p<0.05 and ns = not significant.

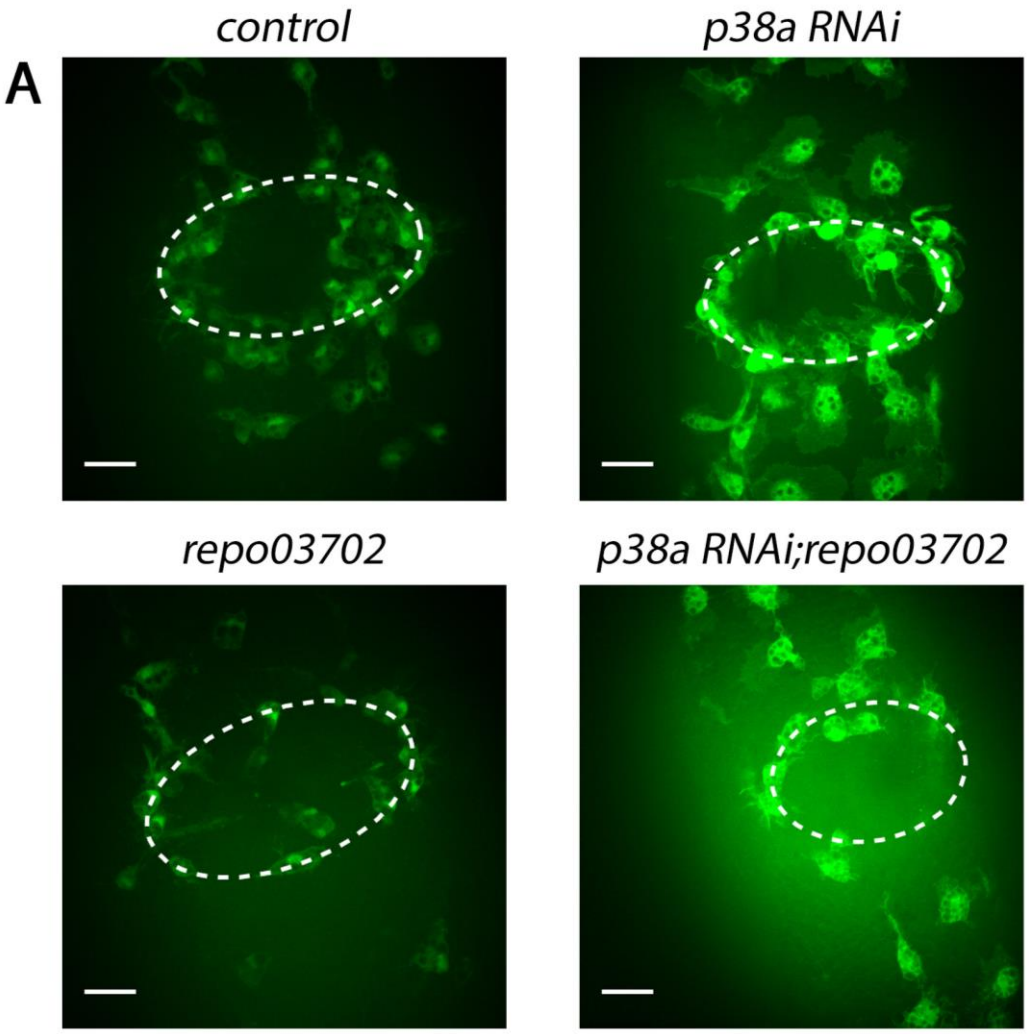
A
control
p38a RNAi
repo03702
p38a RNAi;repo03702

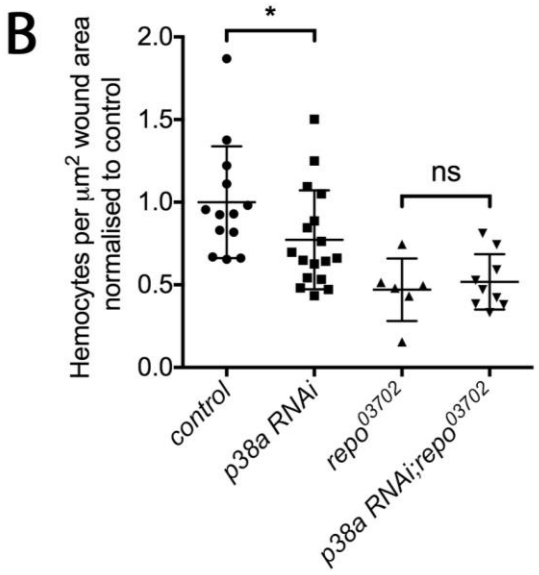
B
Hemocytes per µm2 wound area normalised to control
2.0
1.5
1.0
0.5
0.0
*
ns
control
p38a RNAi
repo03702
p38a RNAi;repo03702

Figure 3.8: Hemocyte-specific RNAi knockdown of p38a MAPK is unable to rescue *repo*^{03702} mutant hemocyte inflammatory responses
(A) Representative stills of GFP-labeled hemocyte responses to wounds at 60 minutes post-wound in control stage 15 embryos as well as those in which p38a expression had been knocked down specifically in hemocytes using *UAS-p38a RNAi* expression under the control of the *crq-GAL4 driver* (*p38a RNAi*), *repo*^{03702} mutants and *p38a RNAi;repo*^{03702} embryos.
(B) Scatterplot of hemocyte wound responses per embryo shown as the number of hemocytes per μm^2 wound area at 60 minutes post-wounding normalized to the control average. Lines and error bars represent mean±SD; n=13, 17, 6 and 9 embryos per the above genotypes respectively. White dashed ovals represent wound perimeter; scale bars represent 20μm; asterisks indicate statistical significance as determined by Mann-Whitney test;*p<0.05 and ns = not significant.

required for hemocyte migration to wounds, but not for their developmental migration in response to Pvfs (Wood et al. 2006). As apoptotic cells seem to represent an important cue for macrophage migration in the *Drosophila* embryo, we hypothesised that p38 MAPK signalling is responsible for determining this hierarchy, and that hemocytes in *repo* mutants are utilising p38 MAPK signalling to migrate towards apoptotic cells rather than wounds. To test this, we reduced the expression of one of three *Drosophila* p38 MAPK proteins, p38a, specifically in hemocytes in *repo*^{03702} using RNAi-mediated knockdown to see whether this was able to rescue *repo* mutant wound responses. Compared to *repo*^{03702} mutants alone (*w;;repo*^{03702}*;crq-GAL4,UAS-GFP*) *p38a RNAi;repo*^{03702} embryos (*w;UAS-p38a RNAi;crq-GAL4,UAS-GFP*) showed similar defects in hemocyte inflammatory responses (n=6 and 9 embryos for *repo*^{03702} and *p38a RNAi;repo*^{03702} respectively; p>0.999 via Mann-Whitney test; Fig. 3.8 A, B). Interestingly, compared to control embryos (*w;;crq-GAL4,UAS-GFP*), those in which *p38a RNAi* is expressed specifically in hemocytes (*w;p38a RNAi;crq-GAL4,UAS-GFP*) show a slight but significant decrease in hemocyte inflammatory responses to wounds (n=13 and 17 embryos for controls and *p38a RNAi* embryos respectively; p=0.0313 via Mann-Whitney test; Fig. 3.8 A, B). Altogether this data suggests that p38a MAPK is required by hemocytes for their normal inflammatory responses in *Drosophila*, but that p38a MAPK signalling in hemocytes in *repo* mutants is not the factor causing a reduction in inflammatory responses. However, as we have not tested the other p38 MAPK proteins (p38b and p38c), and as there seems to be some redundancy in their function at least in host defence (Chen et al. 2010), we cannot conclusively conclude that p38 MAPK signalling in hemocytes in *repo* mutants is not causing hemocyte inflammatory migrations to be perturbed.

3.2.9 Macrophage basal migration speeds are reduced in *repo* mutants

In *repo* mutants, where there are increased numbers of apoptotic cells for hemocytes to clear, we observed that hemocyte inflammatory migrations to wounds were perturbed. We therefore

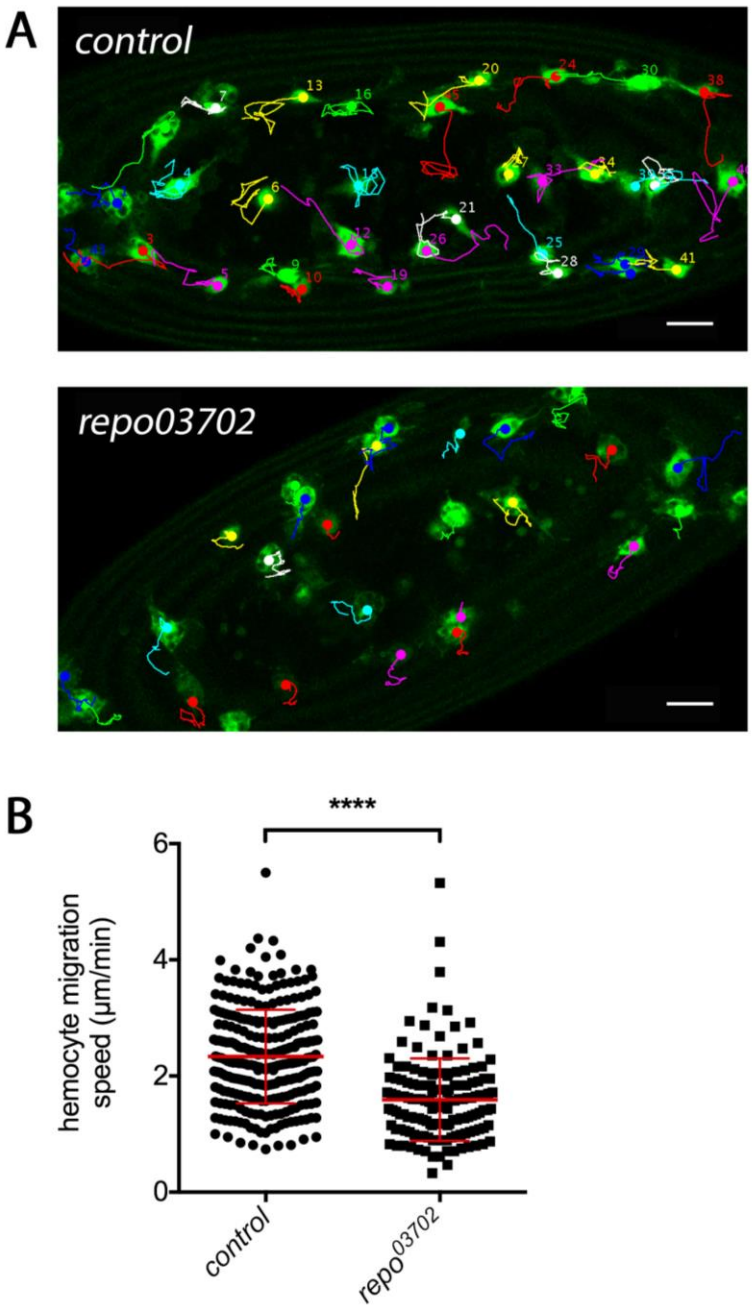

Figure 3.9: Hemocyte random migration speeds are reduced in *repo*^{03702} mutant embryos
(A) Representative tracks of GFP-labeled hemocytes migrating on the superficial VNC over a 30-minute time period in control and *repo*^{03702} mutants. Coloured lines represent the course of migration of each hemocyte tracked and coloured dots show the final position of hemocytes.
(B) Scatterplot of the mean migration speeds of individual hemocytes. Lines and error bars represent mean±SD; n=280 and 147 hemocytes tracked for controls and *repo*^{03702} mutants respectively.
Scale bars represent 20µm; asterisks indicate statistical significance as determined by Mann-Whitney test; ****$p < 0.0001$.

wanted to see how other essential hemocyte behaviours were affected in *repo* mutants. One such behaviour is the ability of hemocytes to migrate around within the embryo, a fundamental aspect of hemocyte function that allows them to perform the vast majority of their essential roles such as depositing matrix, and patrolling for pathogens and indeed apoptotic cells. It has previously been shown that the accumulation of apoptotic cells within hemocytes causes their migration to be slowed, such as in SCAR mutants that have defects in processing apoptotic cells once engulfed (Evans et al. 2013), and similarly in *drpr* mutants, which also seem to have defects in apoptotic cell processing (Evans et al. 2015). As hemocytes in *repo* mutants have increased numbers of engulfed apoptotic cells, we hypothesise that their migration may be slowed. To examine this we made 60-minute time-lapse movies of hemocytes migrating on the superficial surface of the VNC in $repo^{03702}$ mutant (*w;;*$repo^{03702}$*,crq-GAL4,UAS-GFP*) and control (*w;;crq-GAL4,UAS-GFP*) embryos. We then tracked hemocyte migrations using the manual tracking plugin in Fiji, which allowed us to calculate hemocyte migration speeds (Fig. 3.9). When we did this we found that hemocytes migrated significantly more slowly in $repo^{03702}$ mutants when compared to those in control embryos (n=280 and 147 hemocytes for control and $repo^{03702}$ respectively; $p<0.0001$ via Mann-Whitney test; Fig 3.9). This shows that hemocyte migration speeds are reduced in *repo* mutants, which may be a consequence of their increased engulfment of, or exposure to, apoptotic cells.

3.2.10 Removal of apoptosis rescues macrophage migration speeds in *repo* mutants

In order to clarify whether it is indeed increased numbers of apoptotic cells in *repo* mutants that is causing the slowed migration of hemocytes, we sought to remove apoptosis from these embryos to see what effect this would have on hemocyte migration. To do this we used the genomic deletion mutant *Df(3L)H99*, which removes the three pro-apoptotic genes *hid*, *reaper* and *grim* and in doing so prevents all apoptosis in the embryo (White et al. 1994). When we analysed random migration (Fig 3.10 A), we once again observed that hemocytes in *repo* (*w;srp-GAL4,UAS-GFP/srp-GAL4,UAS-nuclear red stinger;*$repo^{03702}$) mutants were significantly slower than those in control (*w;srp-GAL4,UAS-GFP/srp-GAL4,UAS-nuclear red stinger*) embryos, and we also found that hemocytes in *Df(3L)H99* (*w;srp-GAL4,UAS-GFP/srp-GAL4,UAS-nuclear red stinger;Df(3L)H99*) embryos migrated at slightly higher speeds when compared to controls (n=6 embryos analysed for both controls and *Df(3L)H99*; p=0.0152; Fig 3.10 B). Most interestingly, we were able to show that by removing apoptosis in a *repo* mutant background using the *H99* deletion (*w;srp-GAL4,UAS-GFP/srp-GAL4,UAS-nuclear red stinger;*$repo^{03702}$*,Df(3L)*H99), *repo* mutant hemocyte migration speeds could be partially rescued (n=9 and 8 embryos for $repo^{03702}$ and $repo^{03702}$*,Df(3L)H99* mutants respectively;

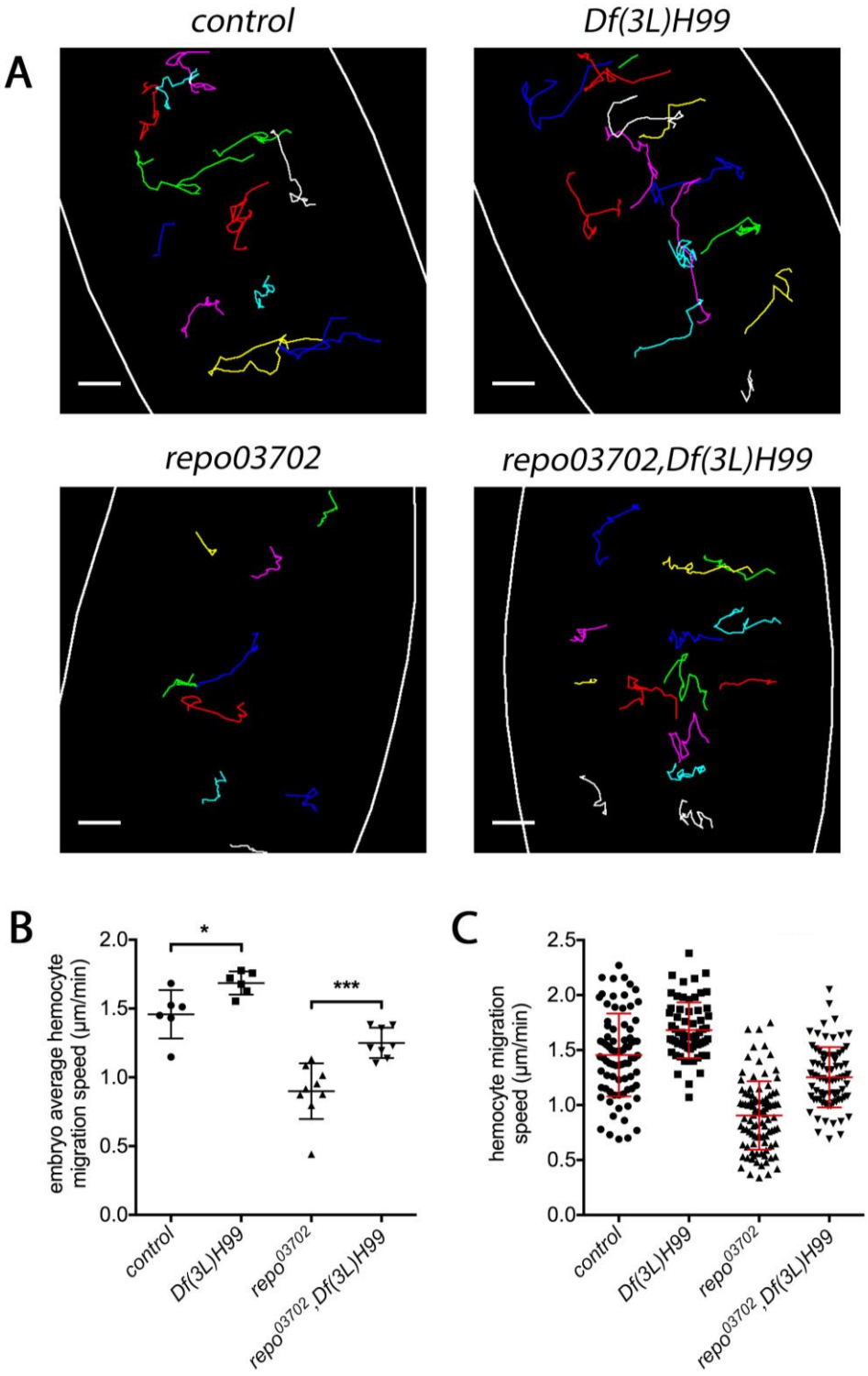
A
control
Df(3L)H99
repo03702
repo03702,Df(3L)H99
B
embryo average hemocyte migration speed (µm/min)
2.0
1.5
1.0
0.5
0.0
*
***
control
Df(3L)H99
repo03702
repo03702 ;Df(3L)H99
C
hemocyte migration speed (µm/min)
2.5
2.0
1.5
1.0
0.5
0.0
control
Df(3L)H99
repo03702
repo03702 ;Df(3L)H99

Figure 3.10: Blocking apoptosis using the *Df(3L)H99* genomic deletion rescues hemocyte migration speeds in *repo*^{03702} mutants
(A) Representative tracks of hemocytes migrating on the superficial VNC over a 60-minute time period in control, *Df(3L)H99*, *repo*^{03702} and *repo*^{03702},*Df(3L)H99* mutant embryos. Coloured lines represent the course of migration of each hemocyte tracked and the white outline represents the edge of the embryo. (B) Scatterplot of embryo average hemocyte migration speeds. Lines and error bar represent mean±SD; n=6, 6, 9 and 8 embryos per the above genotypes respectively. (C) Scatterplot of the mean migration speeds of individual hemocytes. Lines and error bars represent mean±SD; n=80, 65, 97 and 78 hemocytes tracked for each of the above genotypes respectively.
Scale bars represent 20μm; asterisks indicate statistical significance as determined by Mann-Whitney test; ****p < 0.0001, ***p<0.001 and *p<0.05.
p=0.0002; Fig 3.10 B).

This shows that a build-up of apoptotic cells in *repo* mutants slows hemocyte migrations, but is unable to completely explain the migratory defect observed. Finally, this data also shows that hemocytes that have never come into contact with apoptotic cells migrate at slightly increased speeds compared to controls. Together this data suggests that there is a possible correlation between the number of apoptotic cells engulfed by hemocytes and the speed at which they migrate, although this would need to be tested further to prove.

3.2.11 Removal of apoptosis is unable to rescue *repo* mutant wound responses

As the removal of apoptosis using the *Df(3L)H99* deletion was able to rescue hemocyte migration speeds in *repo*^{03702} mutants, we wanted to check whether this was also able to rescue *repo*^{03702} hemocyte inflammatory responses. However, it has previously been shown that *Df(3L)H99* mutant embryos have reduced hemocyte inflammatory responses due to a lack of *drpr* expression in hemocytes, caused by them having never engulfed apoptotic cells (Weavers et al. 2016). To confirm this result and as a control for our experiment, we wounded *Df(3L)H99* (*w;srp-GAL4,UAS-GFP/srp-GAL4,UAS-nuclear red stinger;Df(3L)H99*) embryos alongside the other genotypes. When we analysed the wound response in *Df(3L)H99* embryos, in contrast to published data, we found that there was no difference in the density of hemocytes at wounds 60 minutes post-wound when compared to controls (*w;srp-GAL4,UAS-GFP/srp-GAL4,UAS-nuclear red stinger*) (n=15 and 7 embryos for controls and *Df(3L)H99* mutants respectively; p=0.630 via Mann-Whitney test; Fig. 3.11 A, B). This data suggests that hemocytes do not need to be exposed to apoptotic cells in order to mount a normal inflammatory response as previously published (Weavers et al. 2016). A possible explanation for this is that in order to produce flies with both the *Df(3L)H99* deletion and the *repo*^{03702} mutation, we had to recombine these two elements as both are located on chromosome 3. During the process of recombination it is

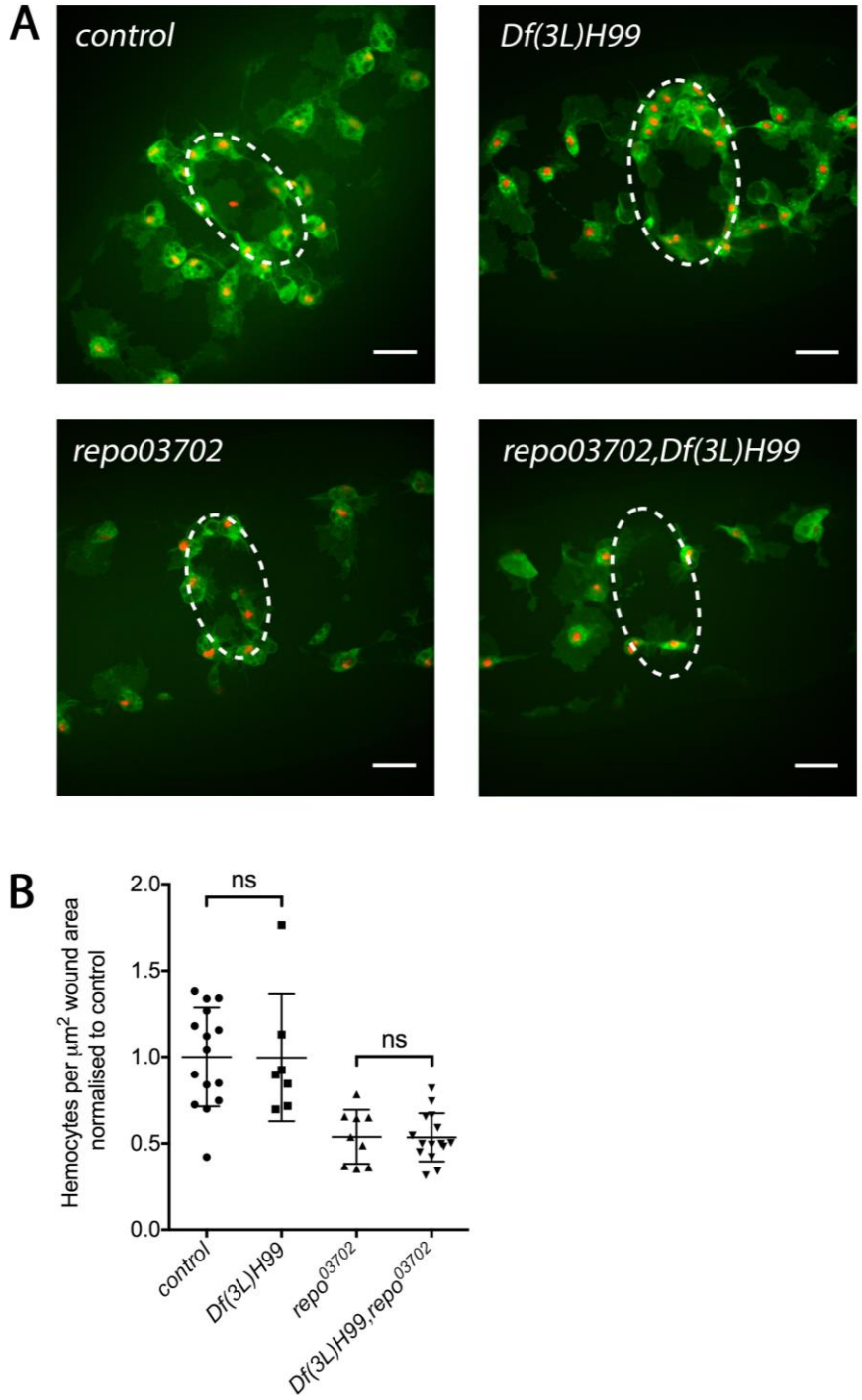

Figure 3.11: Blocking apoptosis using the *Df(3L)H99* genomic deletion is unable to rescue macrophage wound responses at 60-minutes post-wound in *repo^{03702}* mutants

(A) Representative stills of GFP and nuclear red stinger labeled hemocyte responses to wounds at 60 minutes post-wound in control, *Df(3L)H99*, *repo^{03702}*, and *repo^{03702},Df(3L)H99* mutant stage 15 embryos. (B) Scatterplot of hemocyte wound responses per embryo shown as the number of hemocytes per µm^2 wound area at 60 minutes post-wounding normalized to the control average. Lines and error bars represent mean±SD; n=15, 7, 9 and 15 embryos per genotype for the above genotypes respectively.

White dashed ovals represent wound perimeter; scale bars represent 20µm; asterisks indicate statistical significance as determined by Mann-Whitney test; ns= not significant.

possible that a second site mutation responsible for the published wound phenotype in *Df(3L)H99* was removed, or a suppressor mutation generated/recombined in. In order to address this, we have wounded and analysed hemocyte inflammatory responses in the original (unrecombined) *Df(3L)H99* line used in the study by Weavers *et al.* and were also able to obtain wound response defects as published (Weavers *et al.*, 2017; Armitage and Evans, unpublished data). However, wounding of trans-heterozygotes containing this original line and one of two deletions that also remove the pro-apoptotic genes *hid*, *rpr* and *grim (Df(3L)H99/Df(3L)cat* or *Df(3L)H99/Df(3L)BSC775*) did not produce a wound response defect (Armitage and Evans, unpublished data). This supports the idea that a second site mutation contributes to the *Df(3L)H99* published phenotypes, but without a molecular lesion this is impossible to prove. However, even using the recombined *Df(3L)H99* chromosome we sometimes observe a mild wound response defect (for an example see Chapter 4, Figure 4.13), although it seems likely that this decreased wound response is due solely to a decrease in hemocyte numbers in the wounding area in *Df(3L)H99* embryos, as the percentage of hemocytes that migrate to the wound is always similar to controls.

My analysis also showed that the removing apoptosis from $repo^{03702}$ mutant embryos using the *Df(3L)H99* deletion was unable to rescue the wound response defect observed in *repo* mutants (n=9 and 15 embryos for $repo^{03702}$ and $repo^{03702}$*,Df(3L)H99* respectively; p<0.999 via Mann-Whitney test; Fig. 3.11 A, B). This suggests that the decreased wound response in *repo* mutants is not due to the increased numbers of apoptotic cells alone, and that another defect unrelated to apoptosis is sufficient to impair wound responses.

3.2.12 The percentage of hemocytes responding to wounds in *repo* mutants cannot be rescued by removing apoptosis

In order to check that the lack of a rescue in wound responses in *repo* mutants by the removal of apoptosis was not due to hemocytes migrating to the wound and then leaving again, we examined the behaviour of hemocytes as they responded to these wounds. To do this the percentage of hemocytes present in the first time frame of the time-lapse wounding movies that migrate to the wound at any point during the movie was first analysed (termed % responders). Firstly, this revealed that although there was a trend towards there being an increased percentage of hemocytes responding to wounds in *Df(3L)H99* embryos (*w;srp-GAL4,UAS-GFP/srp-GAL4,UAS-nuclear red stinger;Df(3L)*H99) when compared to controls (*w;srp-GAL4,UAS-GFP/srp-GAL4,UAS-nuclear red stinger*), this was not statistically significant (n=9 and 4 wounding movies analysed for control and *Df(3L)H99* embryos respectively; p=0.0545 via Mann-Whitney test; Fig. 3.12 A-E). This analysis also showed that, compared to $repo^{03702}$

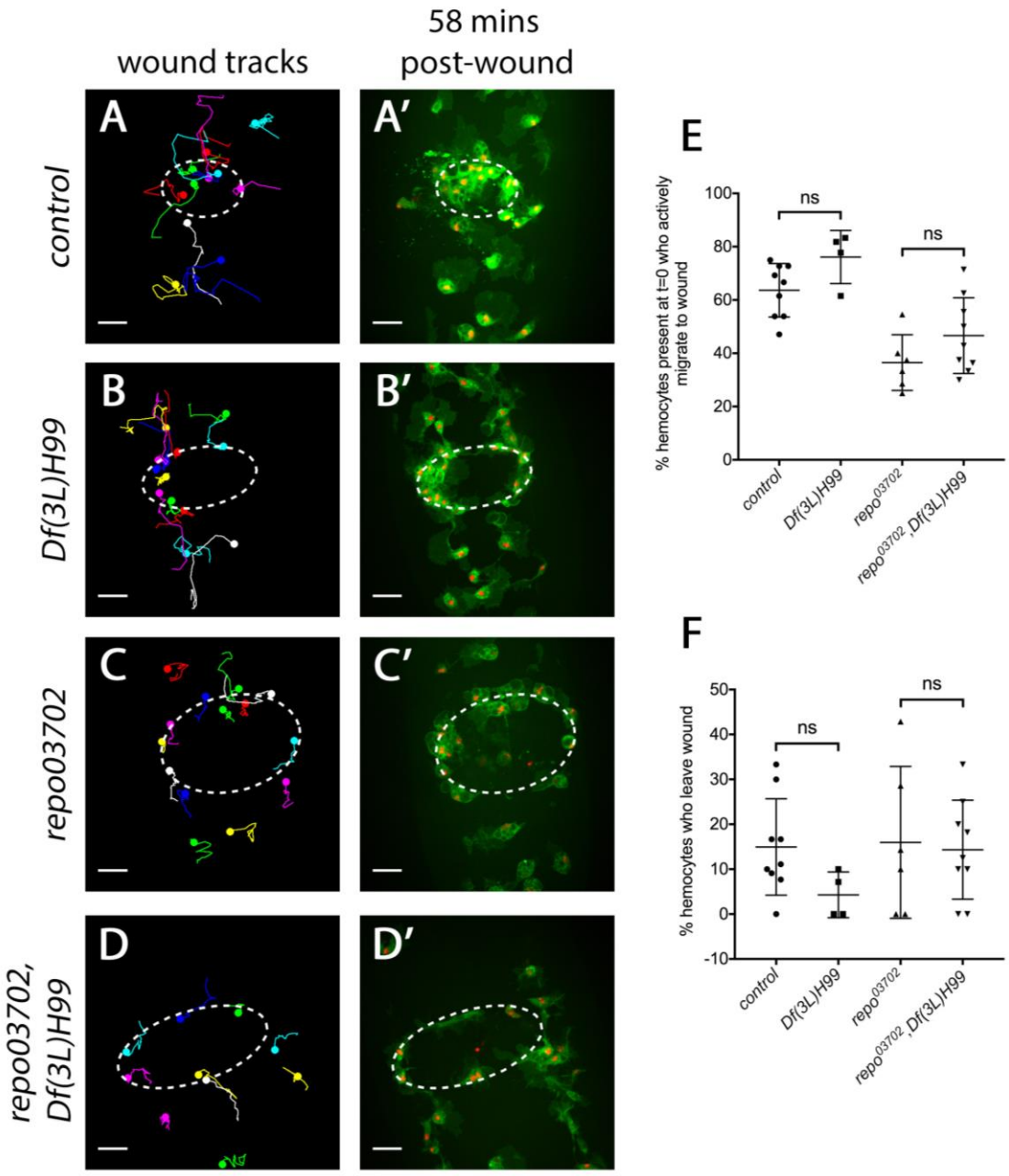

Figure 3.12: Blocking apoptosis using the *Df(3L)H99* genomic deletion is unable to rescue the percentage of hemocytes migrating to the wound in *repo^{03702}* mutants

(A-D) Representative tracks of hemocyte wound responses over 58 minutes from the time of wounding in control, *Df(3L)H99*, *repo^{03702}*, and *repo^{03702},Df(3L)H99* mutant stage 15 embryos. Coloured lines represent the course of migration of each hemocyte tracked and coloured dots show the final position of hemocytes at 58 minutes post-wound. (A'-D') Corresponding representative stills of GFP and nuclear red stinger labeled hemocyte responses to wounds at 58 minutes post-wound in control, *Df(3L)H99*, *repo^{03702}*, and *repo^{03702},Df(3L)H99* mutant stage 15 embryos. (E) Scatterplot of the % of hemocytes present at t=0 minutes post-wound who actively migrate to the wound at any point during the first 58 minutes post-wounding. Lines and error bars represent mean±SD; n=9, 4, 6 and 9 movies analysed for each of the above genotypes respectively. (F) Scatterplots of the % of hemocytes present at t=0 minutes post-wound who are present at and then migrate away from the wound at any point during the above wounding movie. Lines and error bars represent mean±SD.

White dashed ovals represent wound perimeter; scale bars represent 20μm; asterisks indicate statistical significance as determined by Mann-Whitney test; ns = not significant.

mutants alone (*w;srp-GAL4,UAS-GFP/srp-GAL4,UAS-nuclear red stinger;repo*^{03702}), those in which apoptosis had been blocked using the *Df(3L)H99* deletion (*w;srp-GAL4,UAS-GFP/srp-GAL4,UAS-nuclear red stinger;repo*^{03702}*,Df(3L)H99*) had a slightly higher average percentage of hemocytes responding to wounds, however, this was not significantly different (n=6 and 9 wounding movies analysed for *repo*^{03702} and *repo*^{03702}*,Df(3L)H99* mutants respectively; p=0.171 via Mann-Whitney test; Fig. 3.12 A-E). Whilst analysing the wounding movies in this way we also quantified the percentage of hemocytes that migrated away from the wound at any point during the wounding movie, as a way of assessing hemocyte retention at wounds. When we did this we found that although lower, the percentage of hemocytes leaving wounds in *Df(3L)H99* embryos (4.3% ± 5.1) was statistically similar to that of controls (15% ± 10.1) (n=9 and 4 wounding movies analysed for control and *Df(3L)H99* embryos respectively; p=0.0560; Fig. 3.12 F). Similarly, we found that the percentage of hemocytes leaving wounds in *repo*^{03702}*;Df(3L)H99* embryos (14.3% ± 11) was similar to that of *repo*^{03702} mutants (16% ± 16.9) (n= and 6 wounding movies analysed *repo*^{03702}*,Df(3L)H99* and *repo*^{03702} mutants respectively; p>0.999 via Mann-Whitney test; Fig. 3.12 F).

Together this data suggests that blocking apoptosis in a *repo*^{03702} mutant background using the *Df(3L)H99* deletion is unable to rescue the percentage of hemocytes migrating to wounds, thus providing further evidence that *repo*^{03702} mutant wound response phenotpyes are due to another defect that is unrelated to apoptosis. It also shows once again that there is no defect in hemocyte retention at wounds in *repo*^{03702} mutants, therefore the wound response defect in *repo*^{03702} mutants is likely due to a decreased ability of hemocytes to migrate to wounds. Furthermore, the recruitment of hemocytes to wounds is normal in *Df(3L)H99* embryos and there is also no defect in wound retention in the absence of apoptosis. This provides further evidence that the pre-exposure of hemocytes to apoptotic cells is not required for hemocytes to migrate to wounds.

3.3 DISCUSSION

The work presented in this chapter has provided a new line of evidence showing that a build-up of apoptotic cells within hemocytes causes their migration speeds to be decreased - this is in addition to data that has already been published (Evans et al. 2013). It also reveals that hemocytes in *repo* mutant embryos have an inflammatory response defect that is unrelated to increased numbers of apoptotic cells within hemocytes, but this does not rule out a role for apoptotic cells in dampening hemocyte inflammatory responses. Finally, this work shows that

the developmental dispersal of hemocytes along the VNC is slightly disrupted in *repo* mutants, with decreased numbers reaching this area.

3.3.1 The use of *repo* mutants to induce pathological levels of apoptosis

By analysing the clearance of apoptotic cells by hemocytes in *repo* mutant embryos we were able to show that apoptotic cell engulfment by hemocytes is greatly increased. This analysis adds a further level of detail to the study by Shklyar *et al.*, which focused mainly on the glial-specific defects in apoptotic cell clearance of *repo* mutants (Shklyar et al. 2014). As a result of this, we were able to confirm that apoptotic cell clearance is perturbed in *repo* mutants and we are therefore able to use *repo* mutants as a model to study how increased numbers of apoptotic cells affects macrophage function and behaviour *in vivo*. This model is particularly useful to understand how macrophage function is altered in pathologies associated with increased numbers of apoptotic cells that are engulfed efficiently by macrophages, such as at sites of inflammation.

3.3.2 Apoptosis-dependent perturbation of hemocyte wandering migration

We found that macrophage migration speeds in *repo* mutants were reduced (Fig. 3.9) and that this could be partially rescued by blocking apoptosis in the embryo (Fig. 3.10), suggesting that the presence of increased numbers of apoptotic cells in *repo* mutants contributes to their slowed migration. This result is in line with a previous study in which showed that the accumulation of apoptotic cells within macrophages causes their migration to be slowed (Evans et al. 2013). However, there are several explanations as to why increased numbers of apoptotic cells may slow macrophage migrations in *repo* mutants.

Firstly, apoptotic cells within phagosomes may be capable of signalling through receptors for apoptotic cells and may be acting to reduce the migration of macrophages. This makes sense if you use the analogy of having eaten a big meal and needing time to digest before exerting yourself physically. Despite testing to see whether removing apoptotic cell receptors would rescue macrophage inflammatory responses in *repo* mutants, we did not examine whether this would rescue their migration, therefore this remains to be tested in future.

Macrophages full of apoptotic cells may also migrate more slowly due to their increased load, or they may be simply physically larger which restricts their migration through the tightly-confined space between the epithelium and the VNC (Evans et al. 2010). A study from as far

back as 1966 suggested that the phagocytosis of bacteria or latex beads was able to slow leukocyte migration speeds (Bryant et al. 1966). Macrophages from a zebrafish model of lysosomal storage disease are unable to digest phagocytosed material properly which results in a build-up of undigested lysosomal material and macrophages appear larger with an increased number of vacuoles (Berg et al. 2016). Interestingly, engulfed apoptotic cells accumulate in these macrophages, which slows their general migration and abolishes their ability to migrate to chemotactic cues (Berg et al. 2016), suggesting that increased loads within macrophages impairs their migration. The increased numbers of phagosomes within macrophages in *repo* mutants may also mean that the amount of cell membrane available for the cellular protrusions required for cell migrations is decreased, resulting in slowed migration. Alternatively, perhaps components required for migration are being sequestered on the inside of cells in phagosomes, as many components required for migration are also required for phagocytosis.

3.3.3 What is causing hemocyte inflammatory responses to be decreased in *repo* mutants?

My analysis showed that although hemocyte migration speeds can be partially rescued by removing apoptosis in *repo* mutants, their inflammatory migrations to wounds cannot. Therefore, the defective inflammatory responses observed in *repo* mutants cannot be explained by the presence of increased numbers of engulfed apoptotic cells within hemocytes or in their surroundings. Again, there are many possible explanations as to why this might be the case.

It is known that upon wounding of the epithelium in *Drosophila* embryos, an instantaneous wave of calcium travels from the wound, through epithelia, to several rows of cells back from the wound edge (Razzell et al. 2013). This calcium flash travels through epithelial cells via gap junctions and is required for the production of the wound attract H_2O_2, and so disrupting this wave results in reduced hemocyte inflammatory responses (Razzell et al. 2013). Work in our lab has shown that, as well as calcium flashes occurring in the ventral epidermis upon wounding of *Drosophila* embryos, a calcium wave also occurs through the VNC (Armitage and Evans, unpublished data), showing that calcium flashes also occur in tissues below the epidermis. It is possible that in *repo* mutants, where glial cell specification is disrupted and they exhibit altered morphology (Shklyar et al. 2014), glial cells do not form proper junctions between each other and the calcium flash, and subsequently H_2O_2 production, may be disrupted leading to a reduction in hemocyte inflammatory responses. Therefore, live calcium imaging in the VNC upon wounding should be performed in a *repo* mutant background to examine whether this is disrupted.

Another explanation may be that the substrate on which hemocytes are migrating in *repo* mutants may be disrupted. The sealing of the VNC is performed by Repo-positive surface glia which form intercellular septate junctions to ensheath and insulate the VNC (Schwabe et al. 2005; Carlson et al. 2000). This cell layer acts as the substrate on which macrophages migrate on the ventral embryo. In *repo* mutants, the proper specification of glial cells is disrupted and their phagocytic function and morphology are severely affected, with glial cells having a much-reduced volume (Shklyar et al. 2014). Therefore, the cell layer ensheathing the VNC may not be properly formed in *repo* mutants. This is supported by the fact that usually, at late stages of embryogenesis, macrophages cannot enter the CNS due to this physical barrier (Kurant et al. 2008; Shklyar et al. 2014). In *repo* mutants however, macrophages can be seen inside the VNC (Shklyar et al. 2014), suggesting that this barrier is not properly formed. The disruption of proper glial cell specification in *repo* mutants also leads to a reduction in the amount of the ECM protein Trol on the VNC (Comber 2014). As chemoattractants are known to activate integrins which bind to components of the ECM to aid cellular chemotaxis (Laudanna et al. 2002), it may be that reduced levels of ECM proteins in *repo* mutants result in a decrease in the ability of hemocytes to chemotax towards migratory cues such as those emanating from wounds. Indeed, the ECM component laminin has been shown to be required for the normal inflammatory recruitment of hemocytes to wounds in *Drosophila* embryos. However, this is thought to be due to their slowed migration (Sánchez-Sánchez et al. 2017). It is also known that the degradation of ECM components by chemotaxing cells through the action of matrix metalloproteinases (MMPs) are involved in creating chemokine gradients by cleaving chemokines which have bound to ECM components (Van Lint and Libert 2007). The products of the breakdown of ECM components themselves also have chemotactic properties, and have been associated with inflammatory conditions such as COPD (O'Reilly et al. 2008). Therefore, it is possible that reduced levels of ECM components in *repo* mutants alters the production of chemokine gradients and thus affects hemocyte inflammatory recruitment. Of course, the levels and expression patterns of other ECM proteins on the VNC in *repo* mutants would first have to be analysed before this hypothesis could be followed-up, although a genome-wide microarray comparison of *repo* and control embryos did in fact reveal a significant reduction in expression of the ECM component *papilin* in *repo* mutant embryos (data not shown).

Homozygous $repo^{03702}$ mutants are embryonic lethal due to defective glial cell function (Xiong et al. 1994). Therefore, stress signalling within tissues in *repo* mutants may be increased, which in turn may affect macrophage function. To address this, we attempted to examine some common pathways often up-regulated in stressed tissues, and found that both JNK signalling and oxidative stress were not increased in macrophages in *repo* mutants. We also tested whether a reduction in p38 signalling within macrophages by macrophage-specific RNAi knockdown of p38a could rescue the inflammatory response of *repo* mutants. This was originally performed as

before we showed that removing apoptosis was unable to rescue hemocyte inflammatory responses, we hypothesised that, as in neutrophils, p38 signalling was involved in the prioritisation of chemotactic cues (Heit et al. 2002) by macrophages which may have explained the wound response defect. Knockdown of p38 signalling in hemocytes was unable to rescue the *repo* mutant inflammatory response defect, but caused a small but significant reduction in hemocyte inflammatory responses in a control background (Fig. 3.8). Therefore it is unlikely that p38 activation in hemocytes is responsible for their inflammatory defects. However, there are a range of other stress signalling pathways that could be acting to disrupt hemocyte function in *repo* mutants, that could be examined in the future. These could include oxidative stress pathways, NF kappa B signalling, MAPK signalling, AKT or PI3K signalling, among others, of which PI3K signalling has already been shown to be required for hemocyte migration to wounds (Wood et al. 2006).

3.4 CONCLUSIONS

The data presented in this chapter adds further evidence to an increasing body of data that suggests increased numbers of engulfed apoptotic cells within macrophages causes their migration to be slowed. It also reveals a role for proper glial cell specification in controlling the general migration and developmental dispersal of macrophages, as well as their inflammatory migrations to wounds, at least when macrophages are in close proximity to glial cells. In contrast to published data (Weavers et al. 2016), we also show that the engulfment of apoptotic cells by hemocytes does not seem to be a prerequisite for them to be able to migrate to sites of tissue damage.

Chapter 4: Regulation of macrophage behaviour and function by inefficient clearance of apoptotic cells

4.1 INTRODUCTION

An important step in the clearance of apoptotic cells is the binding of the phagocyte to the dying cell through receptor-ligand interactions. In *Drosophila*, one such receptor for apoptotic cells that has been identified is Six-microns-under (Simu) (Kurant et al. 2008), which is a member of the Nimrod family of conserved proteins that also includes the apoptotic cell receptors Draper (CED-1), Jedi-1 and MEGF10 (Freeman et al. 2003; Wu et al. 2009; Hamon et al. 2006; Kurant et al. 2008), and is a homologue of the apoptotic cell receptor Stabilin-1 (Park et al. 2009). Simu is expressed in all three phagocytic cell types in *Drosophila* embryos: ectodermal cells, glia and macrophages, and has been shown to bind specifically to apoptotic cells (Kurant et al. 2008). More recently, Simu has been shown to bind to phosphatidylserine (PS) (Shklyar, Levy-Adam, et al. 2013), a well-recognised 'eat-me' signal exposed on the surface of apoptotic cells which acts as a ligand for many apoptotic cell receptors (Segawa and Nagata 2015).

Using *simu* null mutant embryos Kurant *et al.* were able to show that Simu is required for the phagocytosis of apoptotic cells by both glia and macrophages in *Drosophila* embryos, and in such embryos there are greatly increased numbers of apoptotic cells that remain uncleared by both macrophages and glia (Kurant et al. 2008). They were also able to confirm that the overall morphology and scavenging behaviour of glia and macrophages in *simu* null mutants was normal, but that these cells are unable to recognize and engulf apoptotic particles (Kurant et al. 2008). Interestingly, the SIMU protein lacks an intracellular signalling domain, and a truncated version of SIMU lacking its transmembrane domain can rescue the apoptotic cell clearance defects seen in *simu*^{2} mutants, suggesting that Simu can act as both a soluble and tethered bridging molecule between phagocytes and apoptotic cells (Kurant et al. 2008). Finally, as Simu lacks an intracellular signalling domain, it is likely to work in concert with other co-receptors in order to facilitate the engulfment of apoptotic cells. Kurant *et al.* provide evidence that Simu works upstream of the phagocytic receptor Draper in the phagocytosis of apoptotic cells, as embryos mutant for both *simu* and *drpr* have similar defects in the clearance of dying cells as *simu* mutants alone (Kurant et al. 2008). However, it remains quite possible that other receptors are also capable of interacting with Simu in the recognition and engulfment of apoptotic cells,

or that it mediates engulfment through other mechanisms such as inducing membrane curvature through membrane clustering.

The apoptotic cell receptor Draper has also been shown to have a seemingly separate function as a damage receptor required for macrophage inflammatory migrations to wounds in *Drosophila* (Evans et al. 2015). It has been shown that H_2O_2 produced at sites of tissue damage acts as a migratory cue for macrophages (Moreira et al. 2010) and that the Src family kinase Src42a is responsible for macrophage detection of this cue (Evans et al. 2015). Active Src42a then phosphorylates Draper on its ITAM domain which in turn leads to the recruitment of a Syk-related kinase named Shark, which induces the migration of macrophages towards wounds (Evans et al. 2015). Interestingly, macrophage Draper expression has been shown to be induced by the engulfment of apoptotic cells in *Drosophila*, and macrophages within embryos in which apoptosis has been genetically blocked have low levels of Draper expression and are less able to migrate to wounds (Weavers et al. 2016).

In the previous chapter we showed that macrophages engulf increased numbers of apoptotic cells in *repo* mutants, where glial cell phagocytic function is disrupted. By blocking apoptosis in *repo* mutant embryos we were able to show that this build-up of apoptotic cells caused macrophage migration speeds to be slowed. However, the macrophage inflammatory response defect observed in *repo* mutants could not be rescued by removing apoptosis, suggesting that other unknown mechanisms must be in play that are preventing macrophages from migrating to wounds in these mutants. In order to further examine how increased numbers of apoptotic cells affect the function of macrophages *in vivo,* we sought to further examine how this might be controlled. We hypothesised that perhaps apoptotic cells are capable of exerting their effects on macrophage function prior to being engulfed and therefore sought to find a way of increasing the number of uncleared apoptotic cells in *Drosophila* embryos. As receptors for apoptotic cells are required for their engulfment by phagocytes, we further hypothesised that embryos mutant for such receptors may exhibit an accumulation of uncleared apoptotic cells. As discussed above, Simu functions as a receptor for apoptotic cells and removing this single receptor leads to a significant build-up of un-cleared apoptotic cells (Kurant et al. 2008). Furthermore, as macrophages superficial to the VNC in the *Drosophila* embryo clear apoptotic cells in concert with glial cells, it seemed that mutants for this receptor may be most likely to have increased numbers of uncleared apoptotic cells in the vicinity of macrophages in this area. Therefore, we set out to use *simu* mutant embryos as a model to study the effects of pathological levels of uncleared apoptotic cells on macrophage function and behaviour.

4.2 RESULTS

4.2.1 Impairing the ability of hemocytes and glia to engulf apoptotic cells leads to an accumulation of uncleared apoptotic cells

It has previously been shown that *simu*^{2} homozygous mutant embryos have increased numbers of uncleared apoptotic cells in the vicinity of macrophages on the VNC (Kurant et al. 2008), therefore ahead of using *simu*^{2} mutants to test the effect of uncleared apoptotic cells on hemocyte behaviour we first confirmed these results. To do this control and *simu*^{2} mutant embryos whose hemocytes were labelled using *UAS-GFP* expression under the control of the hemocyte specific *crq-GAL4* driver, were fixed and immunostained for cleaved DCP-1 (a downstream effector caspase cleaved during apoptosis (Song et al. 1997)) to label apoptotic cells and also for GFP to visualise hemocytes (Fig. 4.1 A-B'). The number of untouched apoptotic cells surrounding hemocytes on the VNC in stage 15 embryos was then quantified by counting the number of cleaved DCP-1 positive particles that remained untouched by hemocytes. When comparing the average number of untouched apoptotic cells per embryo between the two genotypes we found that *simu*^{2} mutant embryos had 10 times more particles than controls (n=7 embryos for both control and *simu*^{2}; p=0.0006 via Mann-Whitney test; Fig. 4.1 C), suggesting that *simu*^{2} mutants have a severe defect in their ability to clear apoptotic cells efficiently. As part of this analysis, the engulfment of apoptotic cells by hemocytes was also quantified by counting the number of cleaved DCP-1 particles found within the hemocytes on the VNC in these embryos. Surprisingly, when engulfment was compared between control and *simu*^{2} mutants, we found that hemocytes in *simu*^{2} mutants had engulfed over double that of control hemocytes (n= 6 and 5 embryos for control and *simu*^{2} respectively; p=0.0173 via Mann-Whitney test; Fig 4.1 D). This result suggests that hemocytes lacking the Simu apoptotic cell receptor are still capable of phagocytosing apoptotic cells, and suggests that there is redundancy in the genes required to engulf apoptotic cells. It is possible that the increased number of engulfed apoptotic cells observed in *simu* mutant macrophages may be due to defects in phagosome maturation, as seems to be the case in both *drpr* and *crq* mutants (Kurant et al. 2008; Evans et al. 2015; Han et al. 2014). However when considering these two results together it is obvious that hemocytes in *simu* mutants are much less efficient at engulfing apoptotic cells than in controls as there is a significant accumulation of apoptotic cells that remain untouched. Overall, analysis of apoptotic cell clearance in *simu* mutants has revealed that there is an accumulation of untouched apoptotic cells in these mutants, and therefore we can use *simu* mutant embryos as a model to study how inefficient clearance apoptotic cells affect macrophage function.

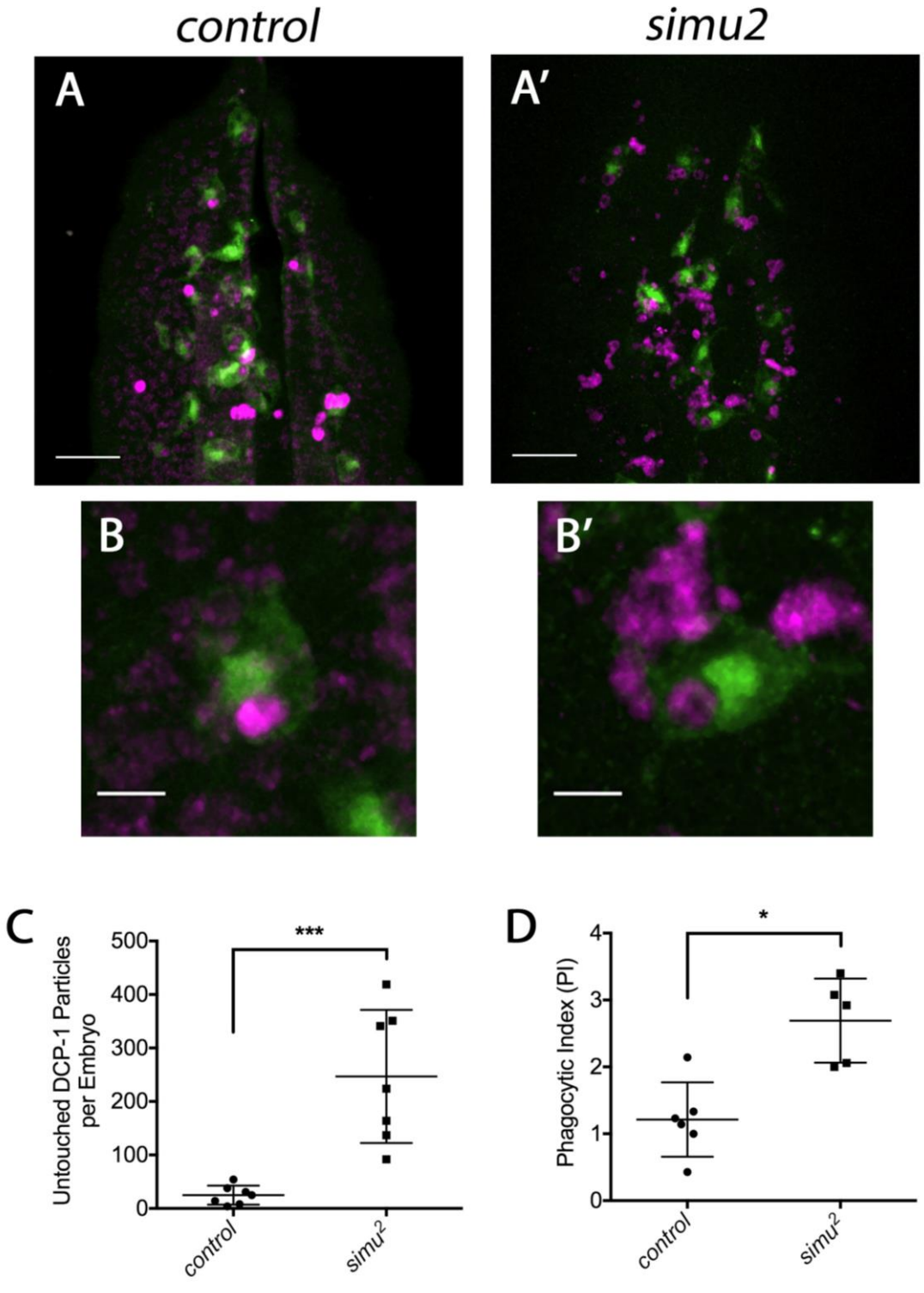
control
simu2
A
A′
B
B′
C
Untouched DCP-1 Particles per Embryo
500
400
300
200
100
0
***
control
simu2
D
Phagocytic Index (PI)
4
3
2
1
0
*
control
simu2

Figure 4.1: DCP-1 staining in *simu*^{2} mutants reveals an accumulation of uncleared apoptotic cells
(A and A') Representative projections from confocal stacks of hemocytes (in green) and apoptotic cells (in magenta; DCP-1) superficial to the VNC in control and *simu*^{2} fixed stage 15 embryos, showing increased numbers of apoptotic cells in *simu*^{2} mutants. Scale bars represent 20µm. (B and B') Zoomed images from A and B demonstrating the accumulation of apoptotic cells surrounding hemocytes in *simu*^{2} mutants. Scale bars represent 5µm. (C) Scatterplot of the number of DCP-1 particles that remain untouched by hemocytes in control and *simu*^{2} mutant embryos. Lines and error bars represent mean±SD; n=7 embryos analysed for each genotype. Asterisks indicate statistical significance as determined by Mann-Whitney test; ***$p < 0.001$ and *$p<0.05$. (D) Scatterplot of the average number of DCP-1 particles engulfed per hemocyte, per embryo (referred to as the 'phagocytic index' (PI)). Lines and error bars represent mean±SD; n=6 embryos and n=96 hemocytes for controls and n=5 embryos and n=64 hemocytes for *simu*^{2} mutants.

4.2.2 Macrophage inflammatory responses to wounds are decreased in *simu* mutants

As we discovered that there are defects in apoptotic cell clearance in *simu*^{2} mutant embryos, we wanted to examine what effect this might have on the ability of hemocytes to respond to wounds. To do this we wounded the ventral epithelium of control (*w;;crq-GAL4,UAS-GFP*) and *simu*^{2} mutant embryos (*w;simu*^{2}*;crq-GAL4,UAS-GFP*), and examined the density of hemocytes present at the wound site 60 minutes post-wounding (Fig. 4.2 A). When we did this we found that there was a significantly decreased density of hemocytes at wounds in *simu*^{2} mutants compared to controls (n=23 and 15 embryos for control and *simu*^{2}, respectively; $p<0.0001$ via Mann-Whitney test), with *simu* mutants showing approximately a 50% decrease (Fig. 4.2 B). This therefore suggests that hemocyte inflammatory responses in *simu*^{2} mutants are perturbed.

4.2.3 *simu* trans-heterozygotes phenocopy *simu* mutant wound response defects

In order to confirm that the wound response defect observed in *simu*^{2} mutants was due specifically to the mutation in the *simu* gene, rather than other mutations on the *simu*^{2}-bearing chromosome, we wounded embryos which were trans-heterozygous for the *simu*^{2} mutation and a genetic deletion, *Df(2L)BSC253* (*w;simu*^{2}*/ Df(2L)BSC253;crq-GAL4,UAS-GFP*), a deletion of approximately 180bp between segments 34E1 to 34F3 that removes the entire *simu* gene . When we did this and analysed the density of hemocytes at the wound 60-minutes post-wounding, we found that there was a very similar defect in wound responses to *simu*^{2} mutants with approximately a 50% reduction in hemocyte wound density compared to controls (n=19 and 16

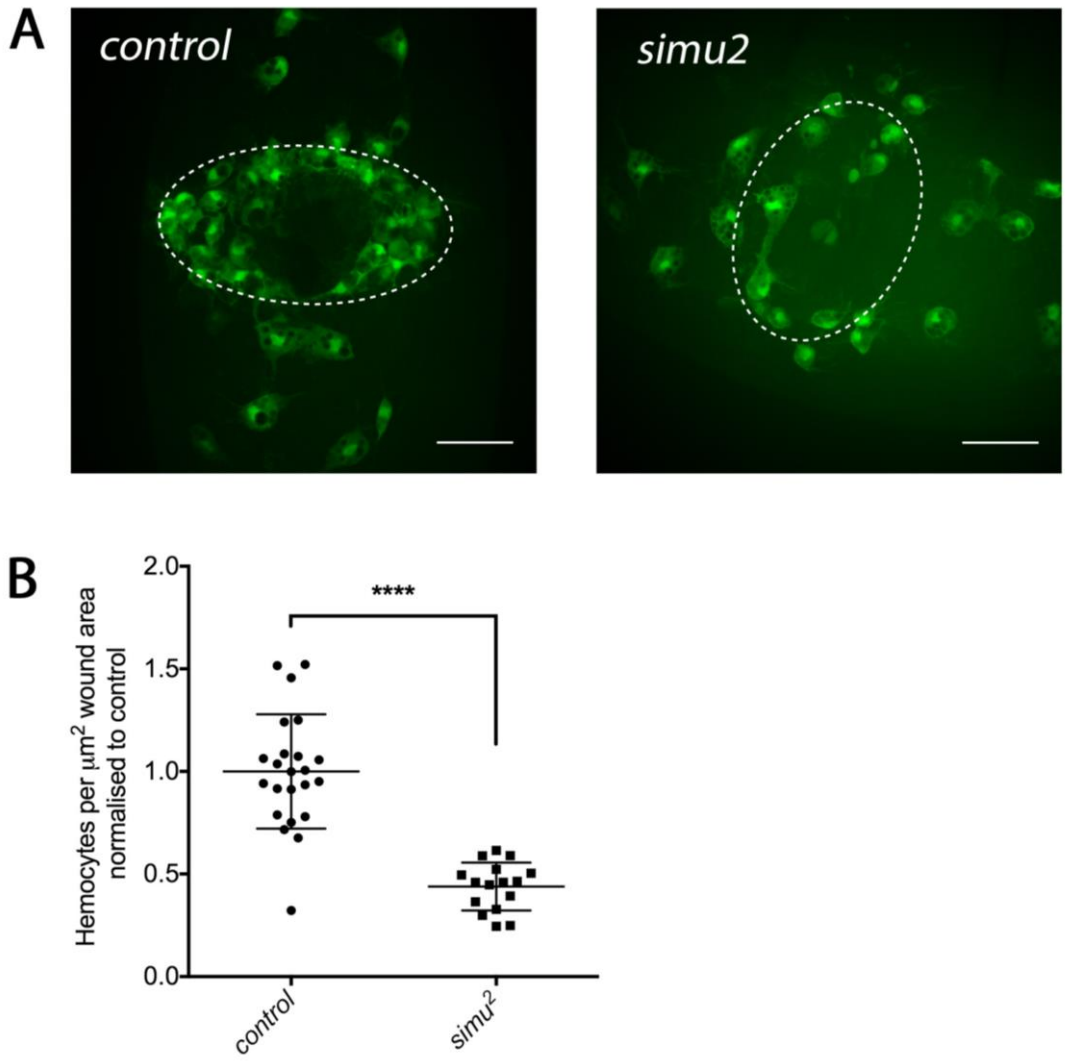

Figure 4.2: Hemocyte inflammatory migrations to wounds are perturbed in *simu* mutants
(A) Representative stills of GFP-labelled hemocyte responses to wounds at 60 minutes post-wound in control and *simu*^{2} mutant stage 15 embryos. (B) Scatterplot of hemocyte wound responses per embryo shown as the number of hemocytes per µm^2 wound area at 60 minutes post-wounding normalized to the control average. Lines and error bars represent mean±SD; n=23 embryos for controls and n=16 for *simu*^{2} mutants.
White dashed ovals represent wound perimeter; scale bars represent 20µm; asterisks indicate statistical significance as determined by Mann-Whitney test; ****p < 0.0001.

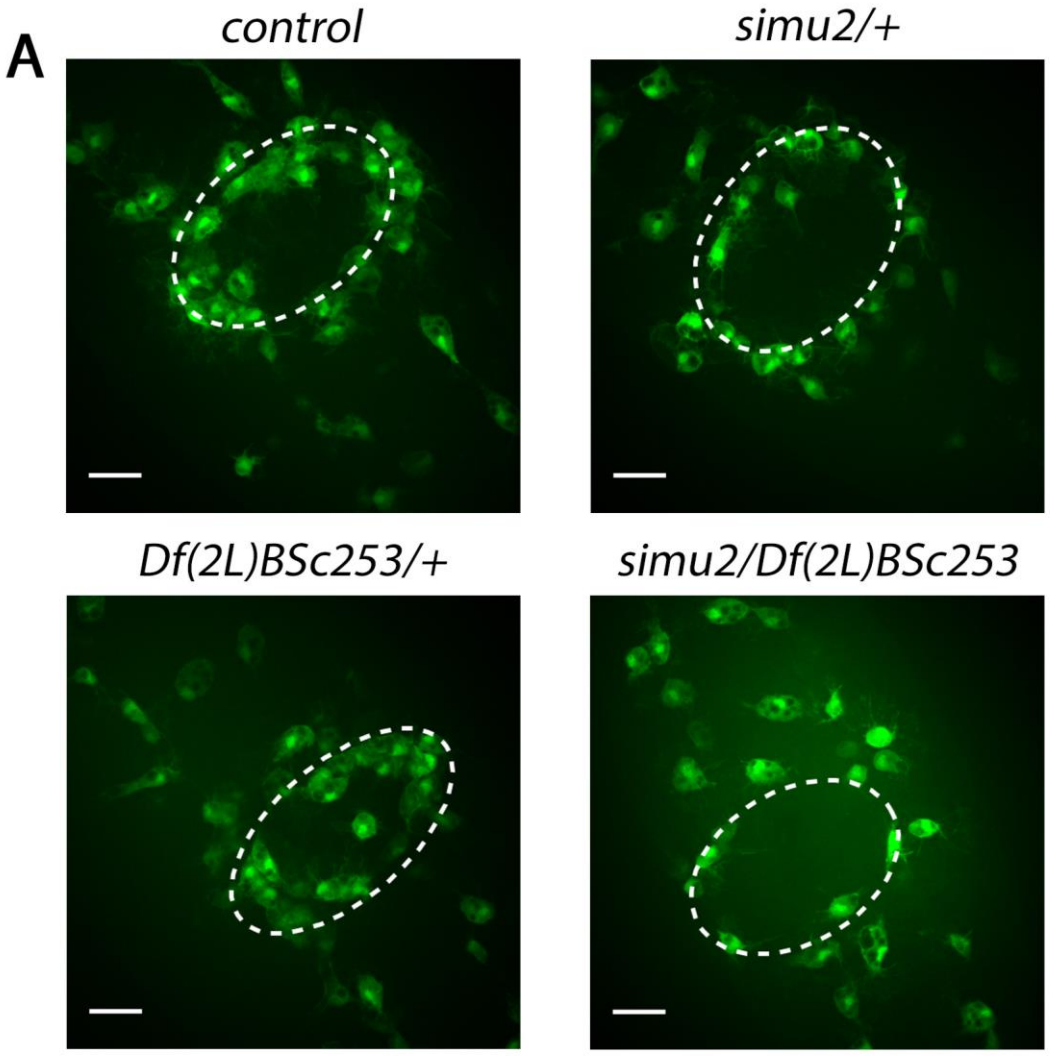
A
control
simu2/+
Df(2L)BSc253/+
simu2/Df(2L)BSc253

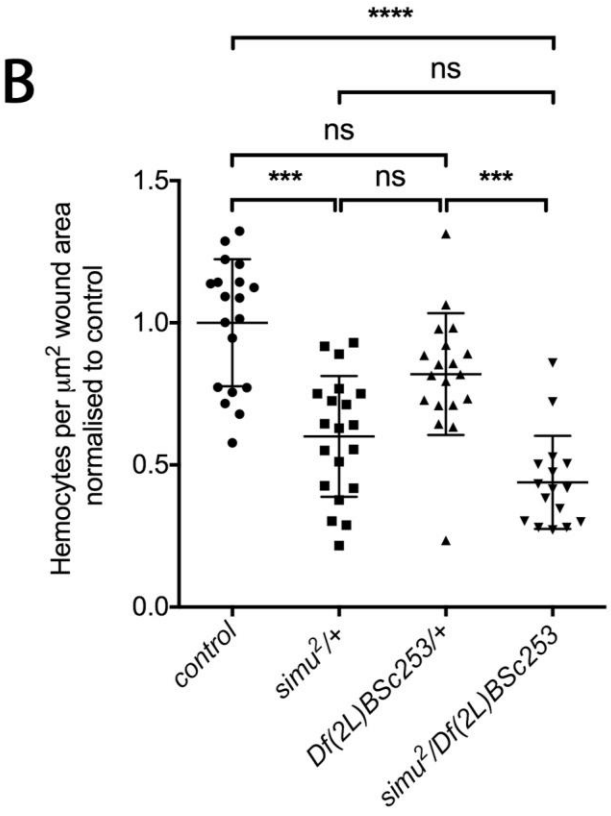
B
****
ns
ns
***
ns
***
Hemocytes per µm2 wound area
normalised to control
1.5
1.0
0.5
0.0
control
simu2/+
Df(2L)BSc253/+
simu2/Df(2L)BSc253

Figure 4.3: Hemocyte inflammatory migrations to wounds are perturbed in *simu*^{2}/deficiency transheterozygotes
(A) Representative stills of GFP-labelled hemocyte responses to wounds at 60 minutes post-wound in control, *simu*^{2} heterozygote, *Df(2L)BSc253* heterozygote and *simu*^{2}/*Df(2L)BSC253* transheterozyogte stage 15 embryos. (B) Scatterplot of hemocyte wound responses per embryo shown as the number of hemocytes per μm^2 wound area at 60 minutes post-wounding normalized to the control average. Lines and error bars represent mean±SD; n=19, 20, 19 and 16 embryos for each of the above genotypes respectively.
White dashed ovals represent wound perimeter; scale bars represent 20μm; asterisks indicate statistical significance as determined by a Kruskal-Wallis one-way ANOVA test; ****p < 0.0001, ***p < 0.001 and ns= not significant.

embryos for control and *simu*^{2}*/ Df(2L)BSC253* respectively; p<0.0001 via Kruskal-Wallis ANOVA with Dunn's multiple comparisons test; Fig. 4.3 A, B), suggesting that the causative mutation is in *simu* or another gene close by that is also removed by the deficiency. RNAi and rescue data shown in Figures 4.4 and 4.5 provide further support that the mutation in *simu* is responsible for the defective wound response phenotype. Interestingly, *simu* appears haploinsufficient as both *simu*^{2}/+ and *Df(2L)BSC253*/+ heterozygotes exhibit a decrease in wound responses compared to controls although the latter is not statistically significant (n=19, 20 and 19 embryos for control, *simu*^{2}/+ and *Df(2L)BSC253*/+ respectively; p=0.0002 for *simu*^{2}/+ and p=0.481 for *Df(2L)BSC253*/+ via Kruskal-Wallis ANOVA with Dunn's multiple comparisons test; Fig. 4.3 A, B). Since the *simu*^{2}*/Df(2L)BSC253* trans-heterozygotes do not show a significantly stronger wound response defect when compared to *simu*^{2}/+ heterozygotes, we speculate that being heterozygous for the *simu*^{2} allele is enough to produce a strong wound response defect.

4.2.4 *simu* is required cell-autonomously by hemocytes for their normal inflammatory migrations to wounds

As hemocytes in *simu*^{2} mutants exhibit a defect in their inflammatory responses to sites of tissue damage, we wanted to assess whether there is a cell autonomous requirement for *simu* in hemocyte responses to wounds. In order to do this, embryos in which *simu* expression was reduced specifically in hemocytes using *UAS-simu RNAi* (*w;UAS-simu RNAi;crq-GAL4,UAS-GFP*) were wounded and hemocyte responses to wounds were quantified and compared to controls (*w;;crq-GAL4,UAS-GFP*) (Fig. 4.4 A, B). At 60 minutes post-wounding, the density of hemocytes at wounds was significantly reduced by approximately 25% when compared to control embryos (n=13 and 17 embryos for control and *simu RNAi* respectively; p=0.0003 via Mann-Whitney test; Fig. 4.4 A, B). This defect in hemocyte inflammatory responses is 25% less

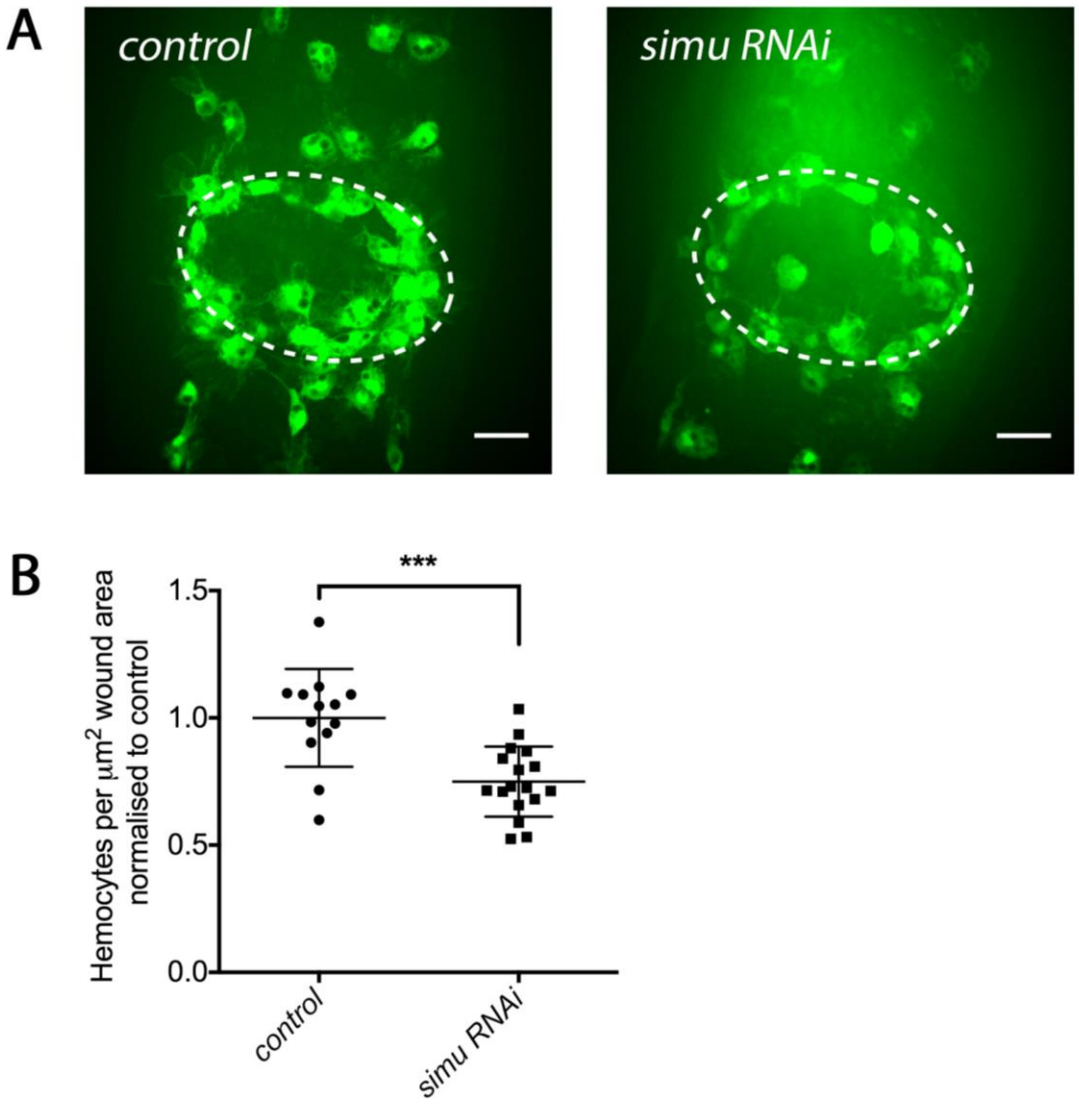

Figure 4.4: Hemocyte-specific RNAi knockdown of *simu* results in a wound response defect

(A) Representative stills of GFP-labeled hemocyte responses to wounds at 60 minutes post-wound in control stage 15 embryos and those in which *simu* expression has been reduced specifically in hemocytes using RNAi knockdown. (B) Scatterplot of hemocyte wound responses per embryo shown as the number of hemocytes per μm^2 wound area at 60 minutes post-wounding normalized to the control average. Lines and error bars represent mean±SD; n=13 embryos for controls and n=17 for *simu* RNAi.

White dashed ovals represent wound perimeter; scale bars represent 20µm; asterisks indicate statistical significance as determined by Mann-Whitney test; ***$p < 0.001$.

severe than that observed in *simu*^{2} homozygous embryos, which could possibly be explained by the incomplete knockdown of *simu* by RNAi. Alternatively, if the inflammatory defect observed in *simu*^{2} mutants is due to the accumulation of uncleared apoptotic cells caused by the loss of *simu* in both glia and hemocytes then perhaps the loss of *simu* solely in hemocytes causes this accumulation to be reduced. This seems likely as there is no noticeable accumulation of apoptotic cells in *simu RNAi* embryos when compared to controls (data not shown). However, this data does suggest that Simu is required in part to be expressed by hemocytes for their normal inflammatory migrations to sites of tissue damage.

4.2.5 Re-expression of *simu* in hemocytes partially rescues inflammatory responses

In order to further validate this result, we also wounded *simu*^{2} mutant embryos in which *simu* expression had been rescued specifically in hemocytes using the GAL4-UAS system. When hemocyte inflammatory responses to wounds were quantified we found that re-expression of *simu* in hemocytes was able to significantly rescue *simu* mutant wound responses (*w;simu*^{2}*,srp-GAL4,UAS-nuclear red stinger/simu*^{2}*;crq-GAL4,UAS-GFP/+* compared to *w;simu*^{2}*,srp-GAL4,UAS-nuclear red stinger/simu*^{2}*;UAS-simu/crq-GAL4,UAS-GFP*) although this rescue appears to be relatively weak (n=16 and 18 embryos for *simu*^{2} and *simu*^{2}*,UAS-simu* respectively; p=0.0167 via Mann-Whitney test; Fig. 4.5 A, B). Together with the previous result showing that RNAi-mediated knockdown of *simu* specifically in hemocytes results in a wound response defect, the evidence suggests that Simu is required specifically in hemocytes for their normal inflammatory migrations to wounds.

4.2.6 Hemocyte numbers on the VNC are reduced in *simu* mutants

As we observed a reduction in the number of hemocytes present at wounds in *simu*^{2} mutant embryos at 60 minutes post-wounding, we wanted to check that this was not due simply to a decrease in the number of hemocytes available to respond in the vicinity of the wound. To do this we counted the number of hemocytes present in the pre-wound images and calculated their density in this area of the embryo. Comparing *simu*^{2} mutants with controls (*w;simu*^{2}*;crq-GAL4,UAS-GFP* with *w;;crq-GAL4,UAS-GFP*), we found that there was a slight but significant decrease (n=23 and 13 embryos for control and *simu*^{2} respectively; p=0.04 via Mann-Whitney test) in the density of hemocytes present prior to wounding (Fig. 4.6 A, A', D). However, the severity of the wounding defect is much greater than the decrease in hemocyte numbers,

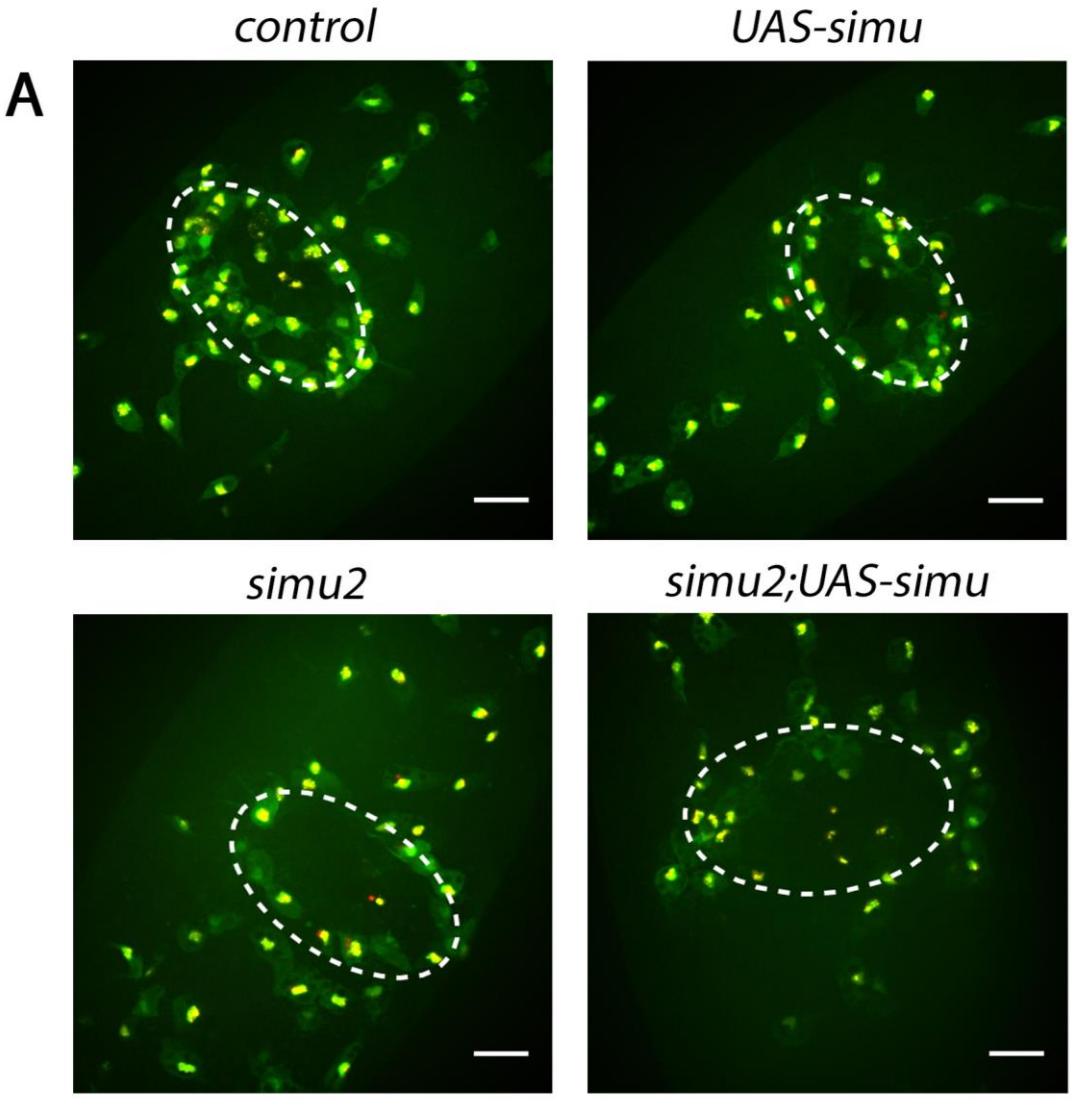
A
control
UAS-simu
simu2
simu2;UAS-simu

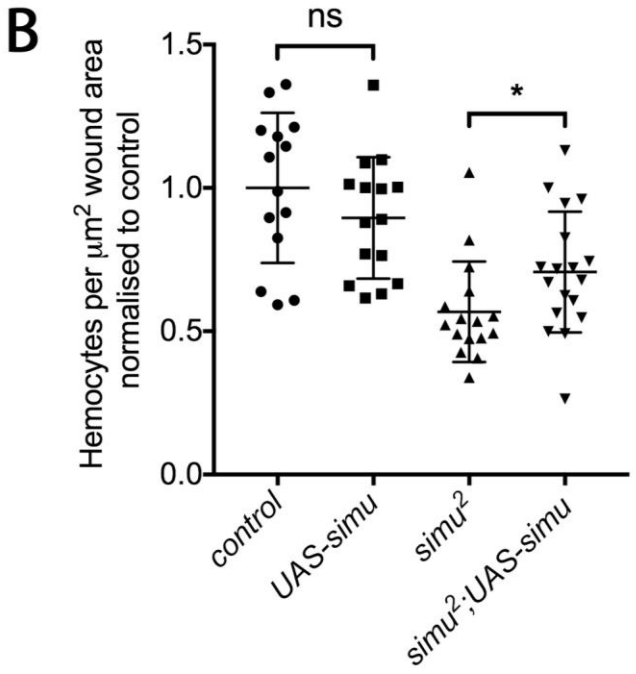
B
ns
*
Hemocytes per µm2 wound area normalised to control
1.5
1.0
0.5
0.0
control
UAS-simu
simu2
simu2;UAS-simu

Figure 4.5: Hemocyte-specific re-expression of simu in *simu^2* mutants partially rescues hemocyte inflammatory responses to wounds

(A) Representative stills of GFP-labelled hemocyte responses to wounds at 60 minutes post-wound in control and *simu^2* mutant stage 15 embryos, and in those in which *UAS-simu* has been expressed specifically in hemocytes in a control and *simu^2* mutant background.

(B) Scatterplot of hemocyte wound responses per embryo shown as the number of hemocytes per μm^2 wound area at 60 minutes post-wounding normalized to the control average. Lines and error bars represent mean±SD; n=14 embryos for controls, n=15 for *UAS-simu*, n=16 for *simu^2* and n=18 for *simu^2;UAS-simu*.

White dashed ovals represent wound perimeter; scale bars represent 20μm; asterisks indicate statistical significance as determined by Mann-Whitney test; *p < 0.05 or ns= not significant.

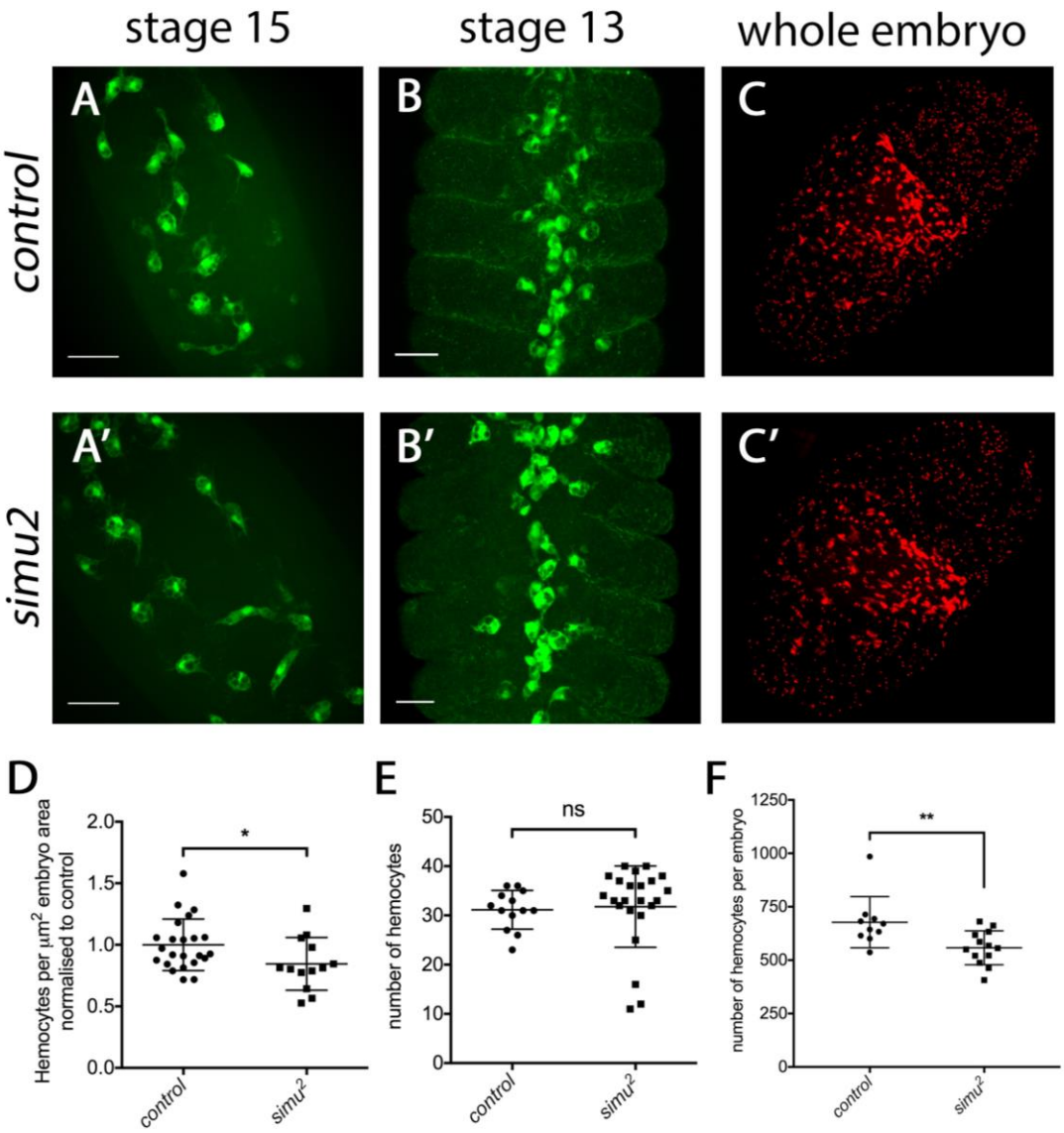

Figure 4.6: Hemocyte numbers on the VNC and total numbers in embryos
(A and A') Representative pre-wound stills of GFP-labelled hemocytes on the superficial VNC in control and *simu*^{2} mutant stage 15 embryos. (B and B') Projections from confocal stacks of GFP-labelled hemocytes on the superficial VNC in control and *simu*^{2} fixed stage 13 embryos. (C and C') nuclear red stinger labelled hemocyte nuclei in control and *simu*^{2} mutant squashed stage 15 embryos embryos, showing the total number of hemocytes in the embryos. (D) Scatterplot of hemocyte densities in stage 15 pre-wound images shown as the number of hemocytes per µm^2 embryo area normalized to the control average. Lines and error bars represent mean±SD; n=23 embryos for controls and n=13 for *simu*^{2} mutants. (E) Scatterplot of hemocyte numbers on the VNC in stage 13 fixed embryos. Lines and error bars represent mean±SD; n=13 and 23 embryos controls and *simu*^{2} mutants respectively. (F) Scatterplot of the total number of hemocytes per embryo. Lines and error bars represent mean±SD; n=10 and 13 embryos for controls and *simu*^{2} mutants respectively.
Scale bars represent 20µm; asterisks indicate statistical significance as determined by Mann-Whitney test; **$p < 0.01$, *$p < 0.05$, and ns= not significant.

suggesting that the wound response defect cannot be explained simply by there being fewer hemocytes around.

In order to check whether there were a similar number of hemocytes in *simu*^{2} mutants compared to controls, we sought to quantify total hemocyte number in the embryos. To examine this we flattened embryos whose hemocytes were labelled using the nuclear-specific marker *UAS-nuclear red stinger* that was specifically expressed in hemocytes using the crq-GAL4 driver. Flattening of the embryos then allowed us to count the number of red nuclei in the entire embryo and therefore the number of hemocytes in *simu*^{2} mutants (*w;simu*^{2}*;crq-GAL4,UAS-nuclear red stinger*) and controls (*w;;crq-GAL4,UAS-nuclear red stinger*) (Fig. 4.6 C, C'). Surprisingly, when we did this we found that, compared to control embryos, *simu*^{2} mutants contained approximately 20% fewer hemocytes (n=10 and 13 for control and *simu*^{2} respectively; p=0.0055 via Mann-Whitney test; Fig. 4.6 F), suggesting that *simu* may be involved in the normal proliferation or specification of hemocytes. However, there is not sufficient evidence for this as the clustering of hemocytes in specific locations and/or differences in *crq*-driven *nuclear red stinger* expression levels may also cause a reduction in the total number of macrophages counted. More detailed analysis perhaps using light-sheet microscopy would need to be performed in order to identify a role for *simu* in hemocyte specification or proliferation.

In order to try to establish whether the decreased number of hemocytes on the VNC was due to a development migration defect, or whether it may solely be due to a decrease in overall hemocyte numbers, we examined hemocytes on the VNC in stage 13 embryos, comparing controls (*w;;crq-GAL4,UAS-GFP*) with *simu*^{2} mutants (*w;simu*^{2}*;crq-GAL4,UAS-GFP*) (Fig. 4.6 B, B'). By stage 13 of embryonic development hemocytes usually form a continuous line along the midline of the ventral embryo (Tepass et al. 1994). When we quantified the number of hemocytes in the central 5 embryonic segments on the ventral midline in stage 13 control and *simu*^{2} mutant embryos, we found that there was no significant difference (n=13 and 23 embryos for control and *simu*^{2} respectively; p=0.145 via Mann-Whitney test; Fig. 4.6 E).

Altogether this data suggests that hemocyte numbers on the VNC in stage 15 embryos are slightly reduced in *simu*^{2} mutants, and that there may be a slight reduction in total hemocyte numbers also, but that further analysis would need to be performed in order to confirm this. It is possible that altering *simu* expression may also alter expression of the apoptotic cell receptor and hemocyte-specific driver *crq*. Therefore, as total hemocyte numbers were counted using marker expression under the control of the *crq-GAL4* driver, this may result in an artificial decrease in hemocyte numbers. A more detailed analysis could be performed using alternative hemocyte-specific drivers such as *srp* or *pxn*.

4.2.7 The percentage of hemocytes responding to wounds is reduced in *simu* mutants

In order to rule out that the inflammatory defect observed in *simu*^{2} mutants is not solely due to decreased numbers of hemocytes at the VNC, we sought to characterise the ability of hemocytes to respond to wounds in more detail. To do this we made time-lapse movies of hemocytes as they responded to wounds in *simu*^{2} mutant (*w;simu*^{2}*;crq-GAL4,UAS-GFP*) and control embryos (*w;;crq-GAL4,UAS-GFP*) over a 58 minute time period, and calculated the percentage of hemocytes present in the frame of view at the beginning of the movie that actively migrated to the wound (Fig. 4.7). We found that compared to controls, 33% fewer hemocytes migrated to wounds in *simu*^{2} mutants (Fig. 4.7 C). This shows that although there are slightly fewer hemocytes in the wound vicinity in *simu* mutants, a significantly decreased proportion of these are able to migrate to wounds (n=7 and 9 embryos for control and *simu*^{2} respectively; p=0.0006 via Mann-Whitney test). It is possible that a certain number of macrophages are required to migrate to the wound in order to relay an amplification signal that leads to the recruitment of more hemocytes. However, in *crq* mutants (see Chapter 6, Fig. 6.4), despite there being fewer hemocytes in the wound vicinity, the percentage that migrate to the wound is no different to controls, suggesting that this is not the case. Therefore it seems likely that hemocytes in *simu* mutants have a reduced ability to respond to sites of tissue damage.

4.2.8 Macrophage JNK signalling is normal in *simu* mutants

A study by Weavers *et al.* showed that JNK signalling within *Drosophila* embryonic hemocytes is required for their inflammatory responses to wounds, and also showed that most hemocytes in stage 14 control embryos have active JNK signalling due to the engulfment of apoptotic corpses (Weavers et al. 2016). As shown in the previous chapter (Chapter 5, Figure 3.5), we found that control stage 15 embryos carrying the TRE-eGFP JNK signalling reporter construct (Chatterjee and Bohmann 2012) contained very few GFP-positive hemocytes, showing that few hemocytes on the VNC had active JNK signalling. In the previous chapter we also found that hemocytes do not seem to require active JNK signalling in order to respond to wounds, and that hemocytes do not seem to activate JNK signalling when mounting an immune response to wounds.

Given that previous studies implicate JNK signalling in control of hemocyte fate (Weavers et al. 2016) and that JNK could equally activate stress signalling in the embryo (Johnson and Nakamura 2007) that might also affect hemocyte behaviour, we investigated JNK signalling in a *simu*^{2} mutant background. Therefore to address whether hemocyte JNK signalling activation

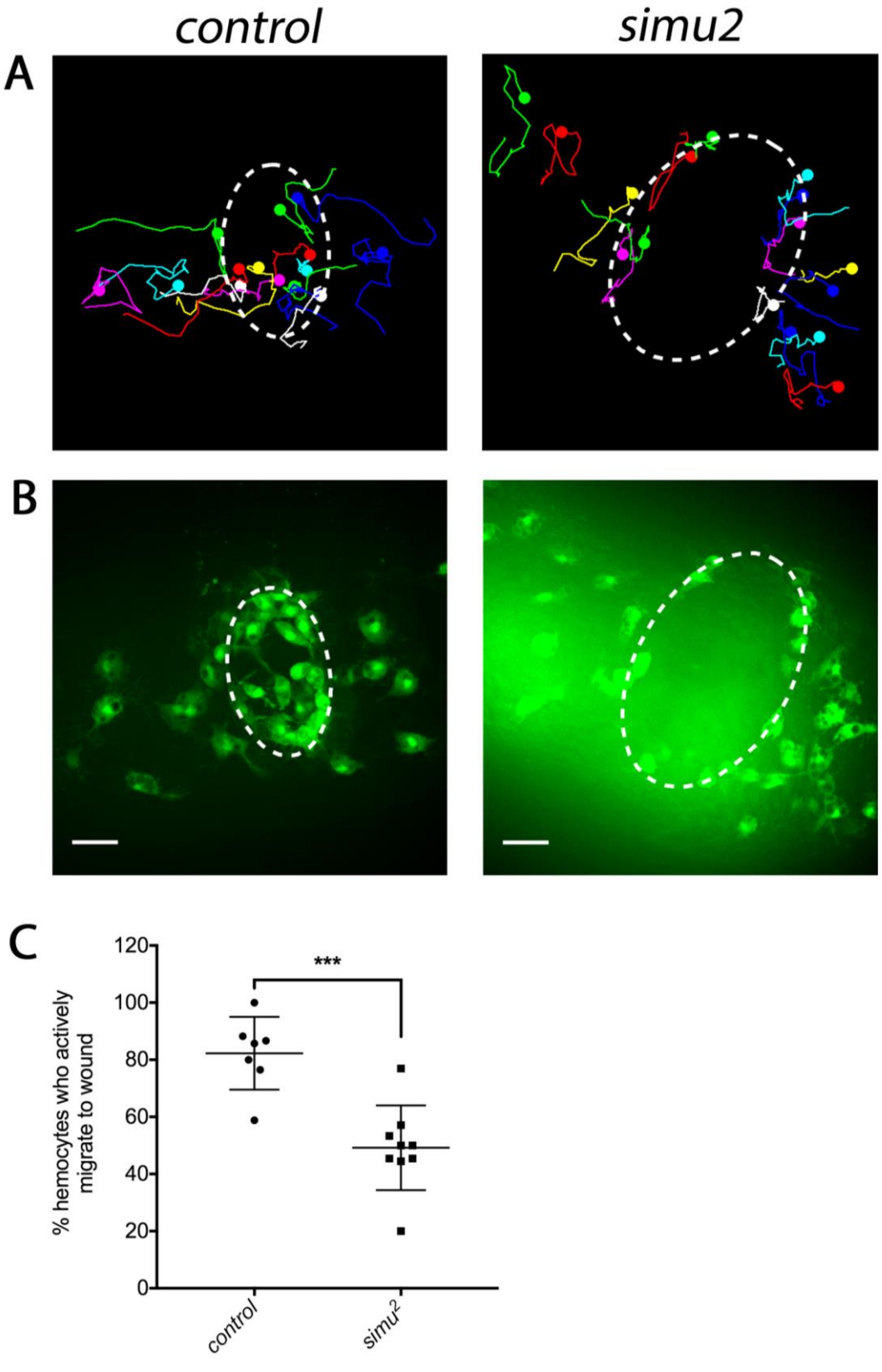
control
simu2
A
B
C
***
% hemocytes who actively migrate to wound
120
100
80
60
40
20
0
control
simu2

Figure 4.7: The percentage of hemocytes migrating to wounds during the 58-minute time period post-wounding is reduced in *simu*^{2} mutants
(A) Representative tracks of hemocyte wound responses over 58 minutes from the time of wounding in control and *simu*^{2} mutant stage 15 embryos. Coloured lines represent the course of migration of each hemocyte tracked and coloured dots show the final position of hemocytes at 58 minutes post-wound. (B) Corresponding stills of GFP-labelled hemocytes at wounds 58 minutes post-wounding in control and *simu*^{2} embryos. (C) Scatterplot of the % of hemocytes present at t=0 minutes post-wound who actively migrate to the wound at any point during the wounding movie. Lines and error bars represent mean±SD; n=7 movies analysed for control embryos, n=9 for *simu*^{2} mutants.
White dashed ovals represent wound perimeter; scale bars represent 20μm; asterisks indicate statistical significance as determined by Mann-Whitney test; ***p < 0.001.

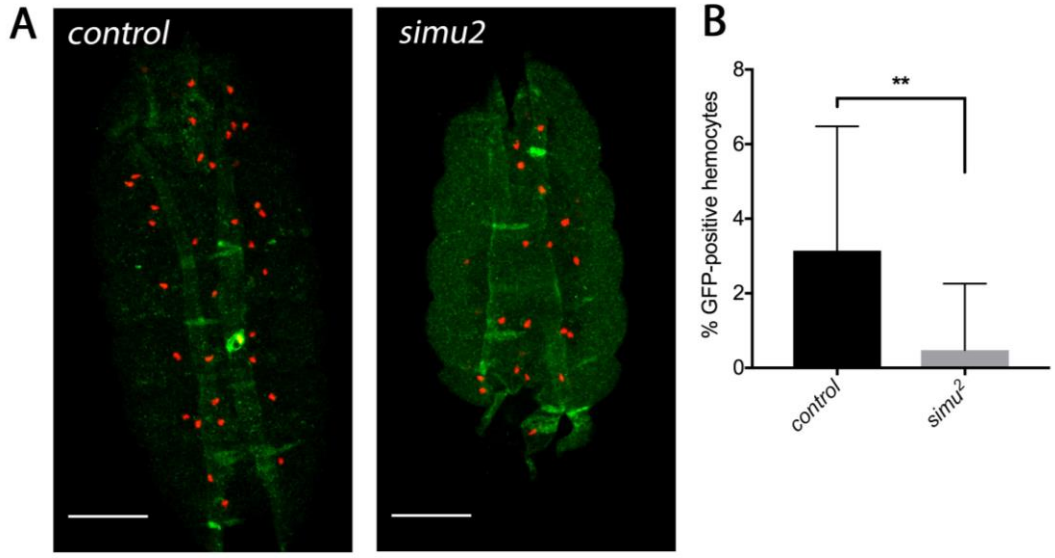

Figure 4.8: Very few hemocytes exhibit active JNK signalling at the VNC in control and *simu* mutant embryos
(A) Representative projections from confocal stacks of stage 15 embryos (whose hemocyte nuclei are shown in red) fixed and stained for GFP to label cells expressing the *TRE-eGFP* JNK signalling reporter construct, showing very minimal numbers of GFP labelled hemocytes in control and *simu*^{2} mutants. (B) Quantification of the percentage of hemocytes on the VNC in stage 15 embryos with active JNK signalling. Data represented as mean+SD; n=16 and 14 embryos for controls and *simu*^{2} mutants respectively. Control data is the same as in Fig. 3.5, Chapter 3 as these experiments were carried out in parallel.
Scale bars represent 100μm; asterisks indicate statistical significance as determined by Mann-Whitney test; **p < 0.01.

was abnormal in *simu*^{2} mutant embryos, we compared JNK activation in *simu*^{2} mutant (*w;TRE-eGFP,simu*^{2}*;crq-GAL4,UAS-nuclear red stinger*) and control (*w;TRE-eGFP;crq-GAL4,UAS-nuclear red stinger*) embryos (Fig. 4.8 A, B). To do this we again used flies carrying the TRE-eGFP ubiquitous JNK signalling reporter construct and examined stage 15 embryos for GFP-positive hemocytes; we found that *simu*^{2} mutants contained slightly fewer hemocytes with active JNK signalling than in controls (n=16 and 14 embryos for control and *simu*^{2} respectively; p=0.004 via Mann-Whitney test; Fig. 4.8 B). However, as GFP-positive hemocytes only made up about 3% of the total hemocytes on the VNC in control embryos, and this was reduced by 2.5% in *simu*^{2} mutants, it seems unlikely that this difference would explain the 50% decrease in hemocyte wound responses observed in *simu*^{2} mutants.

4.2.9 Macrophage ROS levels are decreased in *simu* mutants

As in the previous chapter, we hypothesised that the decrease in inflammatory responses of hemocytes in *simu*^{2} mutants may be due to a shift in the inflammatory state of hemocytes caused by the presence of increased numbers of apoptotic cells. As ROS are an important mediator of vertebrate macrophage polarisation (Tan et al. 2016), we further hypothesised that hemocyte ROS levels may be altered in *simu*^{2} mutants. Furthermore, changes in ROS levels in *simu* mutant embryos may alter the ability of hemocytes to respond to wounds, as the ROS H_2O_2 is the chemotactic signal produced at wounds (Moreira et al. 2010). To examine ROS levels in embryos, *simu*^{2} mutant (*w;simu*^{2}*;crq-GAL4,UAS-nuclear red stinger*) and control (*w;;crq-GAL4,UAS-nuclear red stinger*) embryos were treated with the ROS indicator Dihydrorhodamine 123 (DHR 123), which is oxidised by ROS within cells, causing it to localise to mitochondria and produce green fluorescence (Fig. 4.9 A). When the degree of DHR 123 fluorescence in hemocytes on the superficial surface of the VNC was analysed compared to embryo background levels, we found that this was significantly decreased in *simu*^{2} mutant hemocytes when compared to controls (n=9 and 10 embryos for control and *simu*^{2} respectively; p=0.001 via Mann-Whitney test; Fig. 4.9 A, B). However the overall levels of DHR 123 fluorescence in the background (i.e. levels extracellular to hemocytes) of *simu*^{2} mutant embryos was no different to controls (n=9 and 11 embryos for control and *simu*^{2} respectively; p=0.604 via Mann-Whitney test; Fig. 4.9 A, C). Interestingly, this data suggests that hemocyte ROS levels are reduced in *simu*^{2} mutants, but that the levels of ROS extracellular to hemocytes in embryos are no different to controls. Decreased ROS levels in hemocytes in *simu*^{2} mutants represent a potential mechanism to explain the reduced inflammatory responses of hemocytes in *simu*^{2} mutants, as reduced macrophage ROS production is a known marker of ‘M2’ type anti-inflammatory macrophages (Tan et al. 2016).

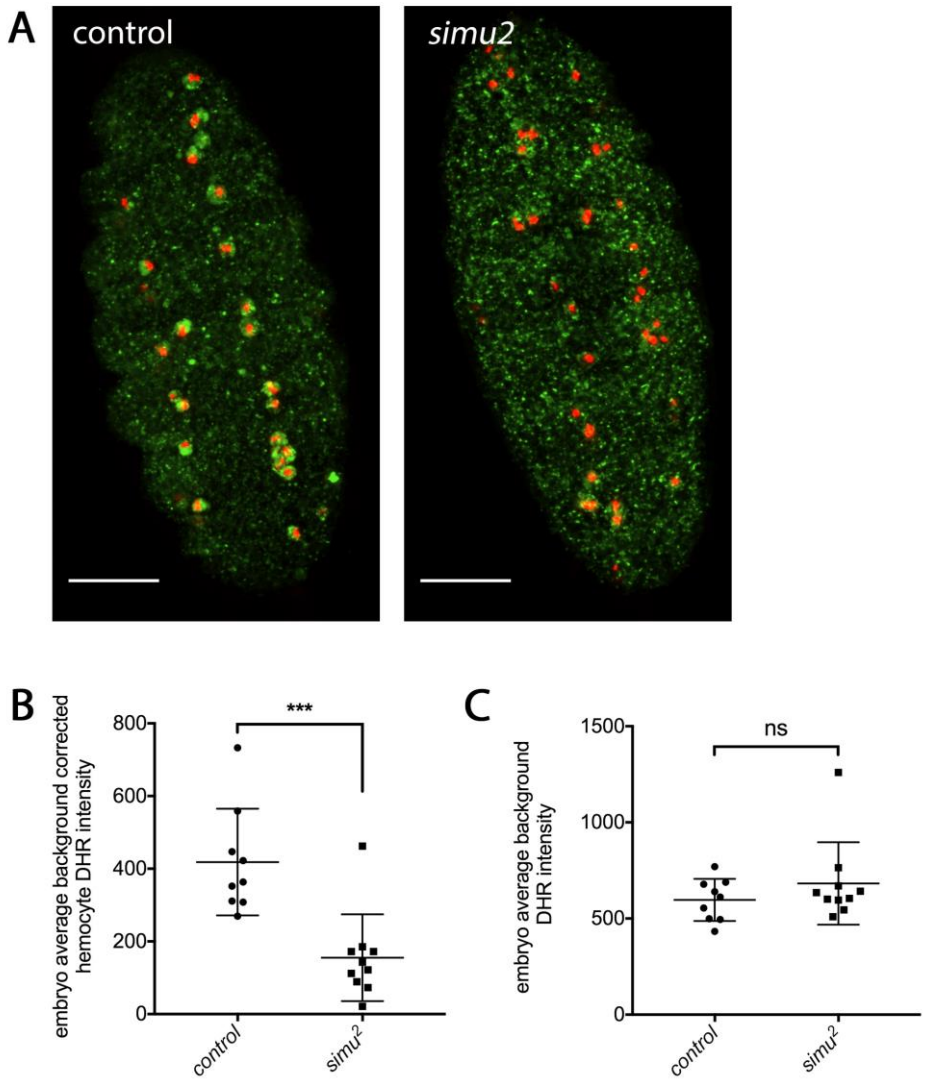

Figure 4.9: Hemocyte ROS levels are decreased in *simu*^{2} mutants
(A) Representative projections from confocal stacks of live stage 15 embryos (whose hemocyte nuclei are shown in red) treated with the ROS indicator DHR 123 (green), showing reduced levels of ROS in hemocytes compared to the rest of the embryo in *simu*^{2} compared to control. (B) Scatterplot of embryo average background corrected hemocyte DHR 123 indicator intensities. Lines and error bars represent mean±SD; n=9 and 10 embryos for controls and *simu*^{2} mutants respectively. (C) Scatterplot of embryo average DHR 123 indicator background intensity. Lines and error bars represent mean±SD; n=9 and 11 embryos for controls and *simu*^{2} mutants respectively. Control data is the same as in Fig. 3.6, Chapter 3 as these experiments were carried out in parallel.
Scale bars represent 100µm; asterisks indicate statistical significance as determined by Mann-Whitney test; ***$p < 0.001$ and ns= not significant.

4.2.10 Macrophage basal migration speeds are decreased in *simu* mutants

In *repo*^{03702} mutant embryos where there is a build up of apoptotic cells inside hemocytes, we observed that hemocytes migrate a lot more slowly than in control embryos (Chapter 3, Fig. 3.9). Therefore, we wanted to see whether an accumulation of apoptotic cells that remained mostly unengulfed, as is the case in *simu*^{2} mutants, was also able to affect hemocyte migration speeds. To do this we tracked the basal migrations of hemocytes in control (*w;;crq-GAL4,UAS-GFP*) and *simu*^{2} mutant embryos (*w;simu*^{2}*;crq-GAL4,UAS-GFP*) over a 60-minute time period using the Fiji manual tracking plug-in, and then calculated their average migration speeds (Fig. 4.10 A-C). In *simu*^{2} mutant embryos we found that hemocyte basal migration speeds were significantly lower than those of hemocytes in control embryos (n=7 and 8 embryos for controls and *simu*^{2} mutants respectively; p=0.0003 via Mann-Whitney test; Fig. 4.10 A, B), suggesting that Simu is required for normal hemocyte migration speeds in *Drosophila* embryos. These slower migration speeds are unlikely to explain the wound response defect in *simu*^{2} mutants as in *mys* mutant embryos, where macrophage migration speeds are significantly slowed, hemocyte numbers at wounds 60-minute post-wounding are normal (Comber et al. 2013). In the previous chapter we showed that defects in apoptotic cell clearance reduce hemocyte migrations speeds (Fig. 3.9), and this has also previously been demonstrated in *SCAR* mutants (Evans et al. 2013).Therefore it is possible that the build-up of apoptotic cells in *simu*^{2} mutants is causing migration speeds to be reduced.

4.2.11 Simu is not required cell-autonomously by hemocytes for their general migratory behaviour

In order to examine whether Simu is required cell-autonomously in hemocytes for their normal migration, we performed RNAi-mediated knock-down of *simu* specifically in hemocytes by expressing *UAS-simu RNAi* under the control of the *crq-GAL4* driver, and examined hemocyte migrations in these embryos (*w;UAS-simu RNAi;crq-GAL4,UAS-GFP*) compared to controls (*w;;crq-GAL4,UAS-GFP*). After calculating average hemocyte speeds as previously, we found that there was no difference between basal migration speeds in control embryos and embryos in which hemocytes expressed a RNAi construct targeting *simu* (n= 8 and 10 embryos for control and *simu RNAi* respectively; p=0.408 via Mann-Whitney test; Fig. 4.11 A, B). Therefore it is likely that Simu is not required cell-autonomously in hemocytes for them to migrate at normal speeds. However, as discussed previously, RNAi knockdown of *simu* in hemocytes may be incomplete, resulting in low levels of *simu* expression that may be sufficient for normal macrophage migration.

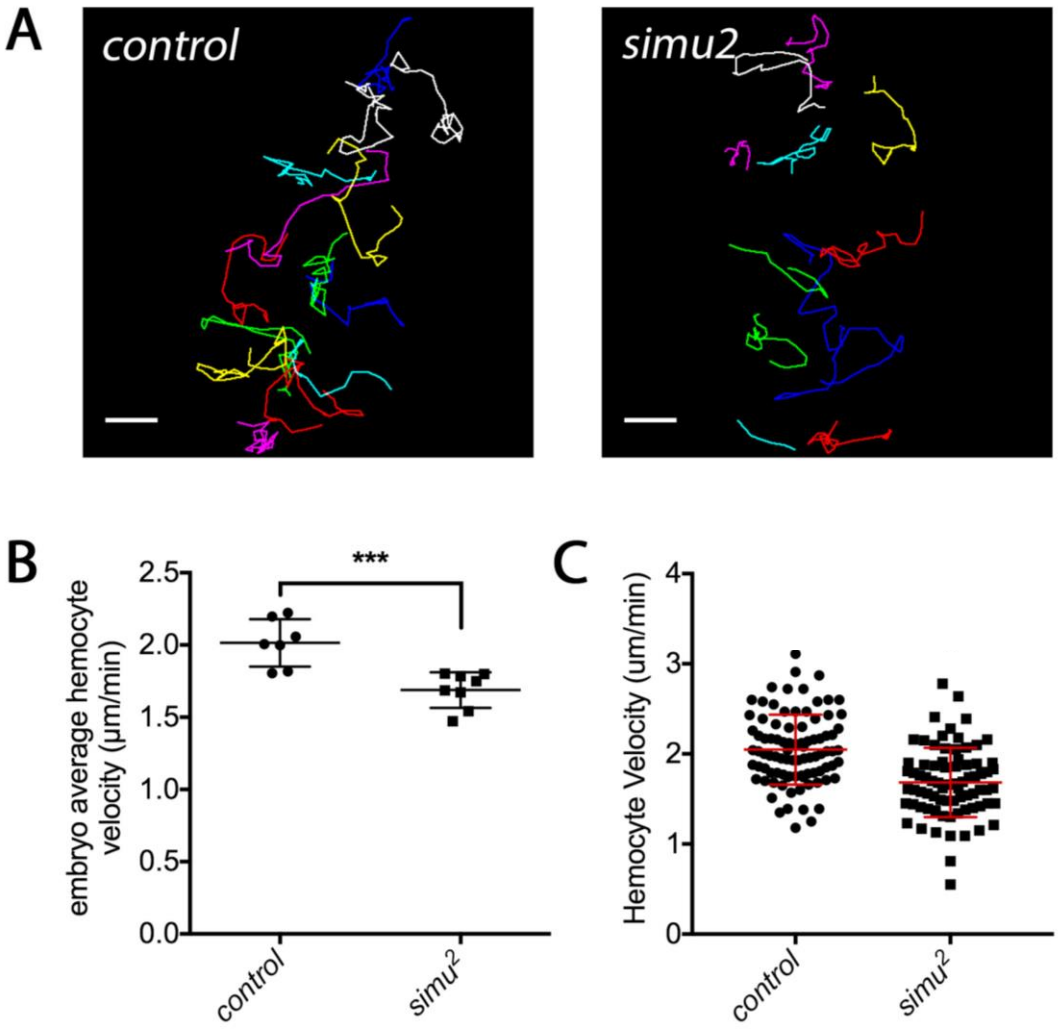

Figure 4.10: Hemocytes migrate at reduced speeds in *simu*^{2} mutants
(A) Representative tracks of hemocytes migrating on the superficial VNC over a 60-minute time period in control and *simu*^{2} mutants. Coloured lines represent the course of migration of each hemocyte tracked and coloured dots show the final position of hemocytes. (B) Scatterplot of embryo average hemocyte migration speeds. Lines and error bar represent mean±SD; n=7 and 8 embryos for controls and *simu*^{2} mutants respectively. (C) Scatterplot of the mean migration speeds of individual hemocytes. Lines and error bars represent mean±SD; n=90 and 78 hemocytes tracked for controls and *simu*^{2} mutants respectively.
Scale bars represent 20μm; asterisks indicate statistical significance as determined by Mann-Whitney test; ***$p < 0.001$ and ****$p < 0.0001$.

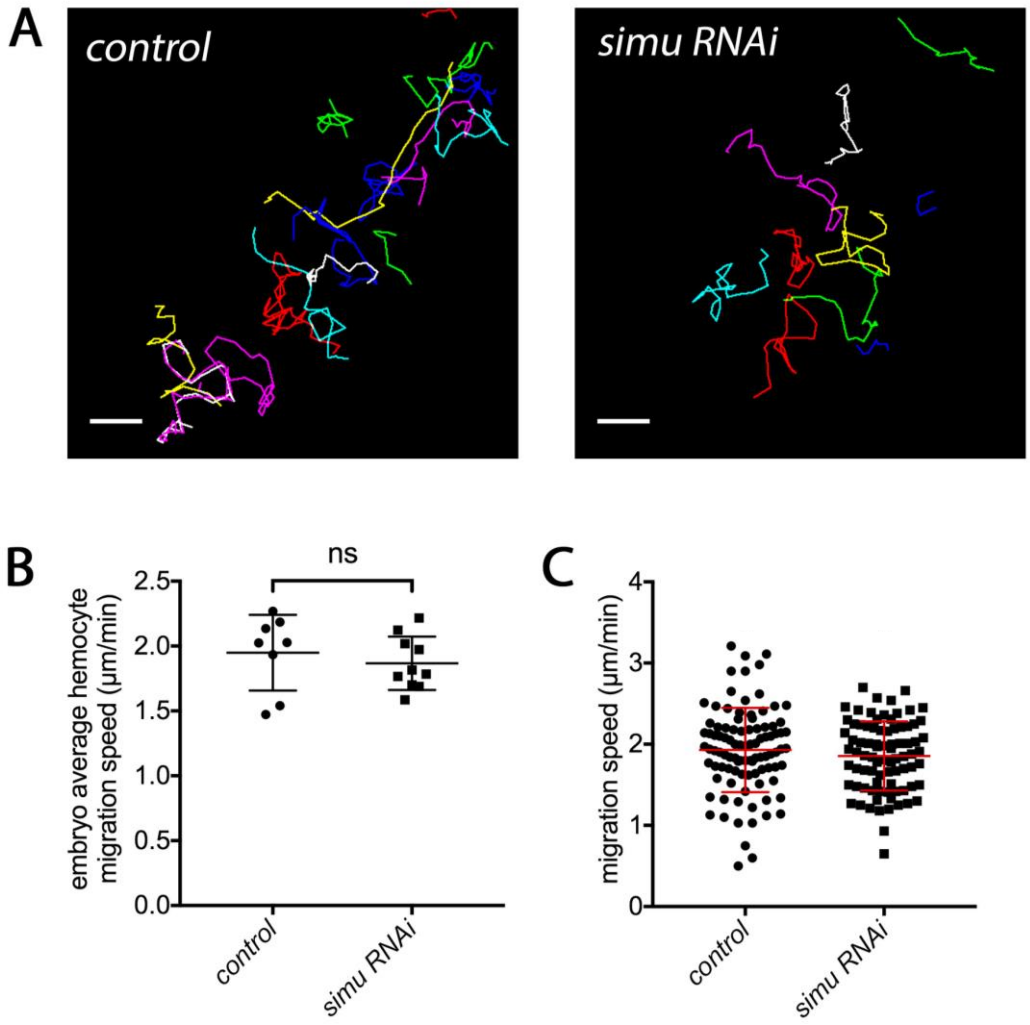

Figure 4.11: Macrophage-specific RNAi knockdown of *simu* has no affect on macrophage migration speeds

(A) Representative tracks of hemocytes migrating on the superficial VNC over a 60-minute time period in control stage 15 embryos and those in which *simu* expression has been reduced by RNAi knockdown specifically in hemocytes. Coloured lines represent the course of migration of each hemocyte tracked and coloured dots show the final position of hemocytes. (B) Scatterplot of embryo average hemocyte migration speeds. Lines and error bar represent mean±SD; n=8 and 10 embryos for controls and *simu RNAi* respectively. (C) Scatterplot of the mean migration speeds of individual hemocytes. Lines and error bars represent mean±SD; n=97 and 84 hemocytes tracked for control and simu RNAi embryos respectively.

Scale bars represent 20µm; statistical significance determined by Mann-Whitney test; ns= not significant.

Together this data suggests that Simu expression must be completely lost in the entire embryo in order to affect hemocyte migration. I hypothesise that this is because in *simu*^{2} mutants neither glial cells nor hemocytes can efficiently engulf apoptotic cells, which leads to the build up of uncleared apoptotic cells observed in these mutants, and it is this build-up that causes hemocyte migrations to be slowed. However, when *simu* expression is knocked-down specifically in hemocytes, glial cells are presumably still able to clear apoptotic cells efficiently and there may be a reduction in the accumulation of uncleared apoptotic cells, which seems likely as there is no noticeable accumulation of apoptotic cells in *simu RNAi* embryos when compared to controls (data not shown). Therefore it is possible that the accumulation of apoptotic cells in *simu* mutants causes hemocyte migration speeds to be decreased.

4.2.12 Removal of apoptosis rescues *simu* mutant hemocyte migration speeds

As we hypothesised that the build up of apoptotic cells in *simu*^{2} mutants may be causing hemocyte migration speeds to be reduced, we sought to remove apoptosis from *simu*^{2} mutant embryos using the widely-used *Df(3L)H99* genomic deletion as described in the previous chapter, which blocks all developmental apoptosis in the embryo (White et al. 1994). Time-lapse movies were then made of hemocytes labelled using UAS-GFP expression under the control of crq-GAL4 migrating on the VNC at stage 15 in *simu*^{2} mutant embryos (*w;simu*^{2}*;crq-GAL4,UAS-GFP*) and in *simu* mutant embryos that also had the *Df(3L)H99* deficiency (*w;simu*^{2}*;Df(3L)H99,crq-GAL4,UAS-GFP*), to see whether removing apoptosis might rescue the slowed migration of hemocytes seen in *simu*^{2} mutants. After tracking and analysing their migration we found that hemocytes in *simu*^{2}*;Df(3L)H99* embryos did indeed migrate at significantly higher speeds than those in *simu*^{2} mutants (n=8 and 10 embryos for *simu*^{2} and *simu*^{2}*;Df(3L)H99* respectively; p=0.0062 via Mann-Whitney test; Figure 4.12 A, B). We were also able to show that hemocytes in *Df(3L)H99* embryos (*w;;Df(3L)H99,crq-GAL4,UAS-GFP*) migrate at similar velocities to those in controls (*w;;crq-GAL4,UAS-GFP*), indicating that removing apoptosis does not affect hemocyte migration speeds (n=7 and 9 embryos for control and *Df(3L)H99* respectively; p=0.252 via Mann-Whitney; Fig. 4.12 A, B). Together this data suggests that it is the increased numbers of apoptotic cells in *simu*^{2} mutants that causes hemocytes to migrate more slowly, thus providing further evidence that apoptotic cells are able to alter the migration of hemocytes *in vivo*.

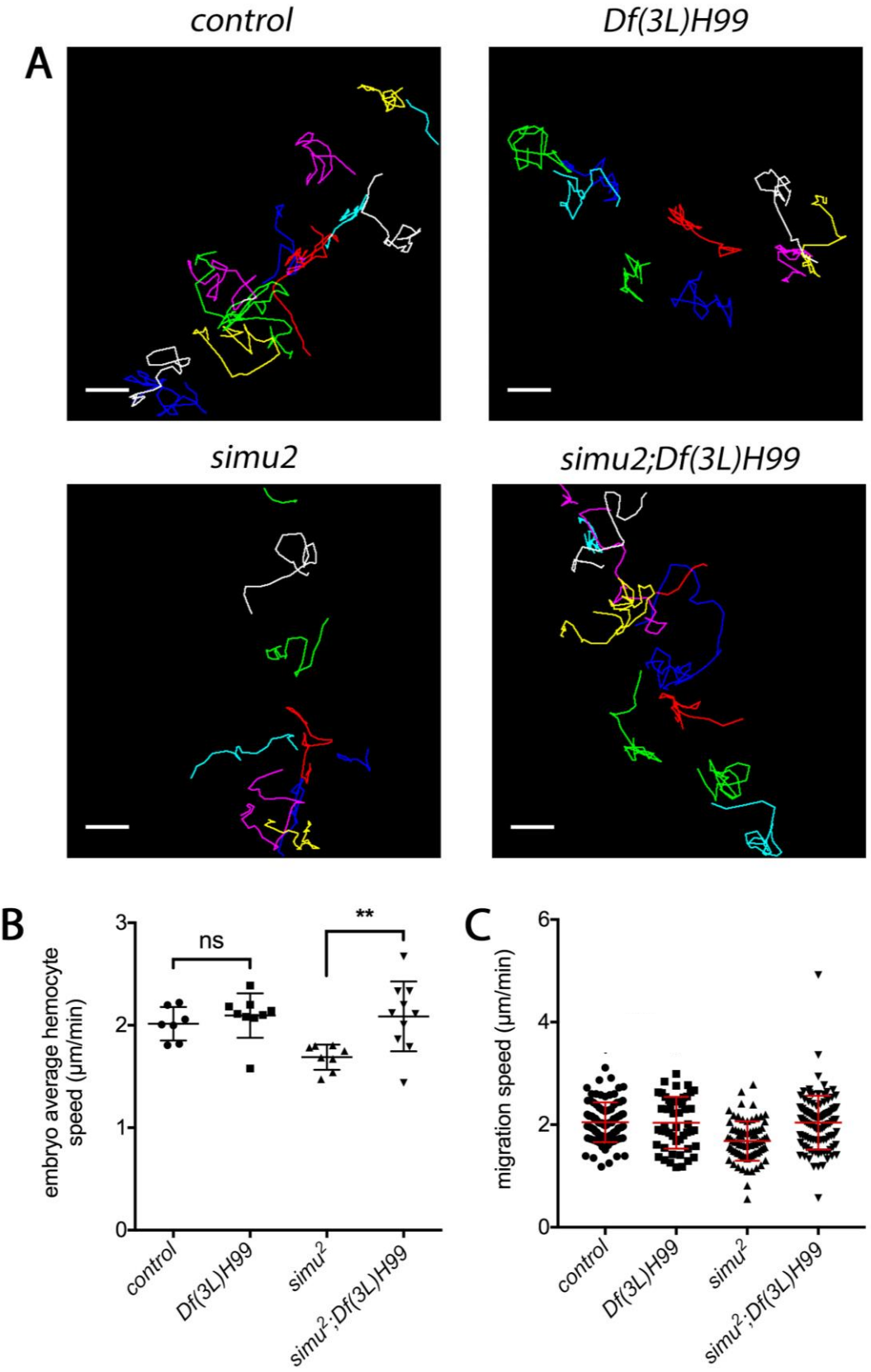
A
control
Df(3L)H99
simu2
simu2;Df(3L)H99
B
embryo average hemocyte speed (μm/min)
ns
**
control
Df(3L)H99
simu2
simu2;Df(3L)H99
C
migration speed (μm/min)
control
Df(3L)H99
simu2
simu2;Df(3L)H99

Figure 4.12: Blocking apoptosis using the *Df(3L)H99* genomic deletion rescues macrophage migration speeds in *simu*^{2} mutants
(A) Representative tracks of hemocytes migrating on the superficial VNC over a 60-minute time period in control, *Df(3L)H99*, *simu*^{2}, and *simu*^{2} mutant stage 15 embryos.. Coloured lines represent the course of migration of each hemocyte tracked and coloured dots show the final position of hemocytes. (B) Scatterplot of embryo average hemocyte migration speeds. Lines and error bar represent mean±SD; n=7, 9, 8 and 10 embryos analysed per genotype for the above genotypes respectively. (C) Scatterplot of the mean migration speeds of individual hemocytes. Lines and error bars represent mean±SD; n=90, 50, 78 and 108 hemocytes tracked per genotype for the above genotypes respectively.
Scale bars represent 20μm; asterisks indicate statistical significance as determined by Mann-Whitney test; **p < 0.01, ****p < 0.0001 and ns= not significant.

4.2.13 Removal of apoptosis in *simu* mutants is unable to rescue hemocyte wound responses at 60 minutes post-wound

In light of the previous result, we then sought to test whether removing apoptosis in *simu*^{2} mutants was also able to rescue hemocyte inflammatory response defects. To examine this we wounded both *simu*^{2} mutants (*w;simu*^{2}*;crq-GAL4,UAS-GFP*) and *simu*^{2}*;Df(3L)H99* double mutants (*w;simu*^{2}*;Df(3L)H99,crq-GAL4,UAS-GFP*), analysing hemocyte density at wounds 60 minutes post-wounding (Fig 4.13). We found that *simu*^{2}*;Df(3L)H99* hemocyte wound densities were similar and not significantly different to those in *simu*^{2} mutants alone (n=18 and 19 embryos for *simu*^{2} and *simu*^{2}*;Df(3L)H99* respectively; p=0.298 via Mann-Whitney test; Fig 4.13 A, B). As per previous publications there was a mild impairment of the inflammatory response in *Df(3L)H99* homozygotes compared to controls (n=22 and 26 for control and *Df(3L)H99* respectively; p=0.0387 via Mann-Whitney test; Fig. 4.14 A, B; Weavers et al. 2017)). These results suggest that it is not apoptotic cells in *simu*^{2} mutants that are causing hemocyte migrations to wounds to be perturbed, at least by this form of analysis, and that removal of apoptotic cells does not rescue responses even to the level of mildly-affected *Df(3L)H99* homozygotes.

4.2.14 Removal of apoptosis does not rescue prewound hemocyte numbers in *simu* mutants

In order to confirm that the lack of a rescue in wound responses in *simu* mutants by the removal of apoptosis was not due to differences in hemocyte numbers in the surrounding area, we also analysed pre-wound hemocyte densities as previously. We found that compared to *simu*^{2}

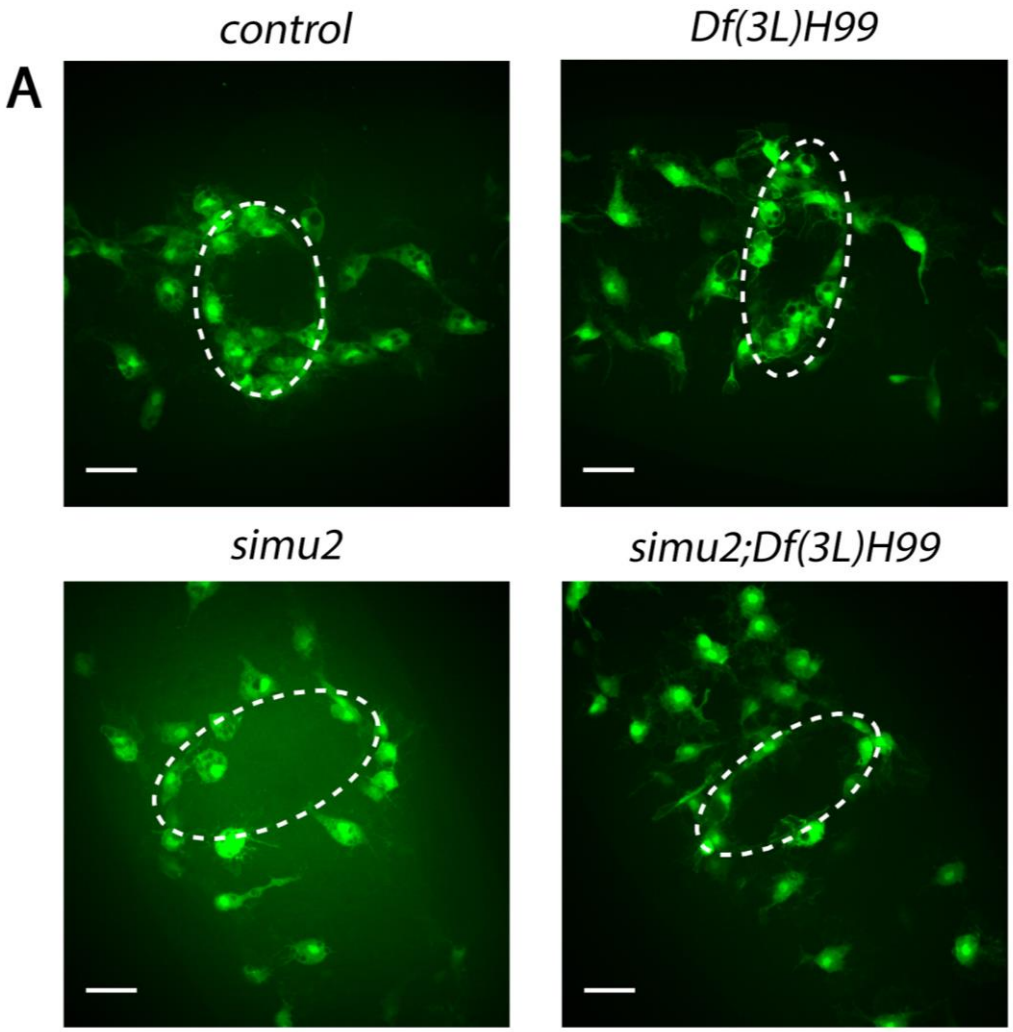
A
control
Df(3L)H99
simu2
simu2;Df(3L)H99
B
Hemocytes per µm² wound area normalised to control
2.0
1.5
1.0
0.5
0.0
*
ns
control
Df(3L)H99
simu²
simu²;Df(3L)H99

Figure 4.13: Blocking apoptosis using the *Df(3L)H99* genomic deletion is unable to rescue macrophage wound responses at 60-minutes post-wound in *simu*^{2} mutants
(A) Representative stills of GFP-labelled hemocyte responses to wounds at 60 minutes post-wound in control, *Df(3L)H99*, *simu*^{2}, and *simu*^{2}*;Df(3L)H99* mutant stage 15 embryos. (B) Scatterplot of hemocyte wound responses per embryo shown as the number of hemocytes per μm^{2} wound area at 60 minutes post-wounding normalized to the control average. Lines and error bars represent mean±SD; n=22, 26, 18 and 19 embryos per genotype for the above genotypes respectively.
White dashed ovals represent wound perimeter; scale bars represent 20μm; asterisks indicate statistical significance as determined by Mann-Whitney test; *$p < 0.05$ and ns= not significant.

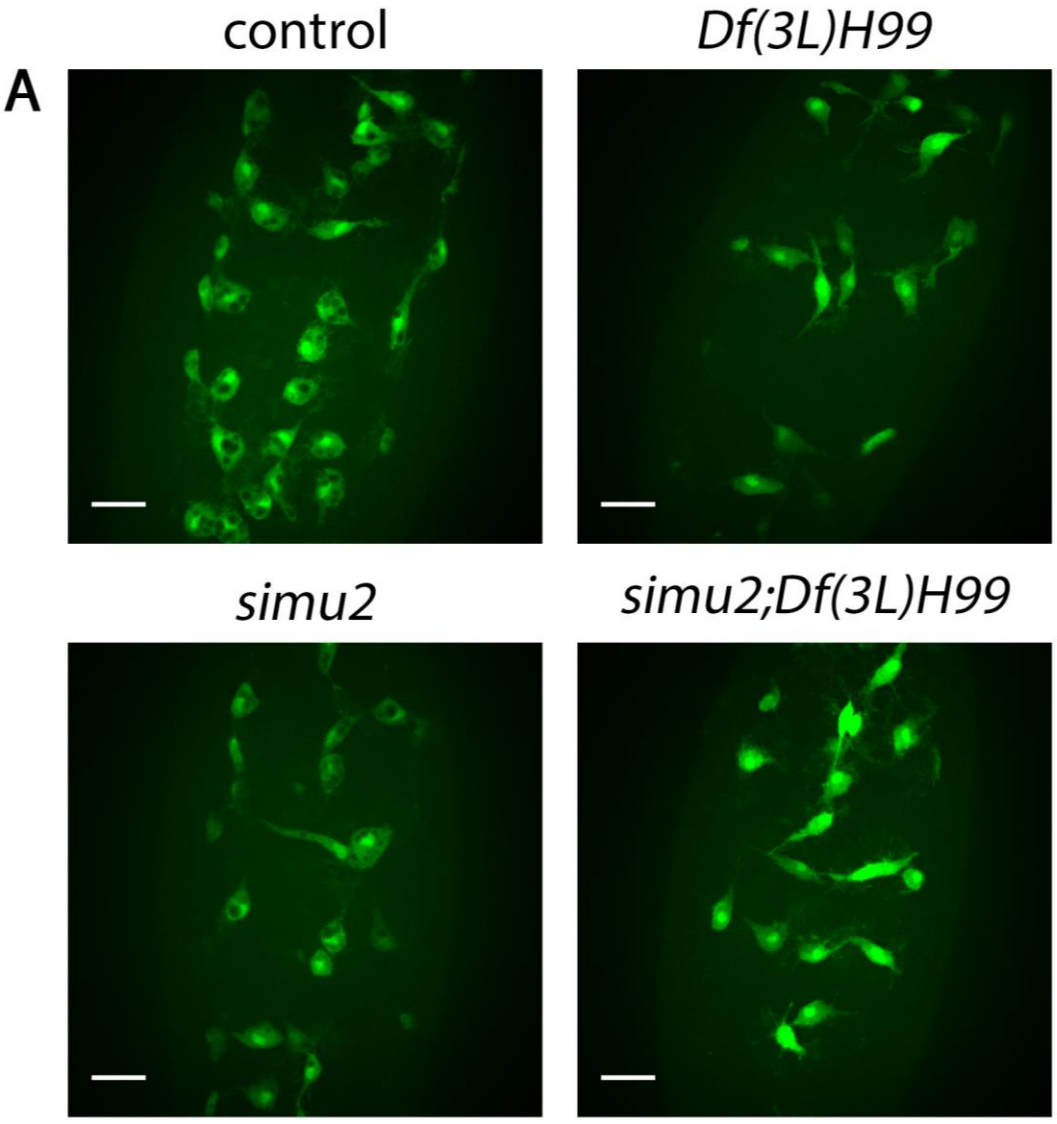
A
control
Df(3L)H99
simu2
simu2;Df(3L)H99

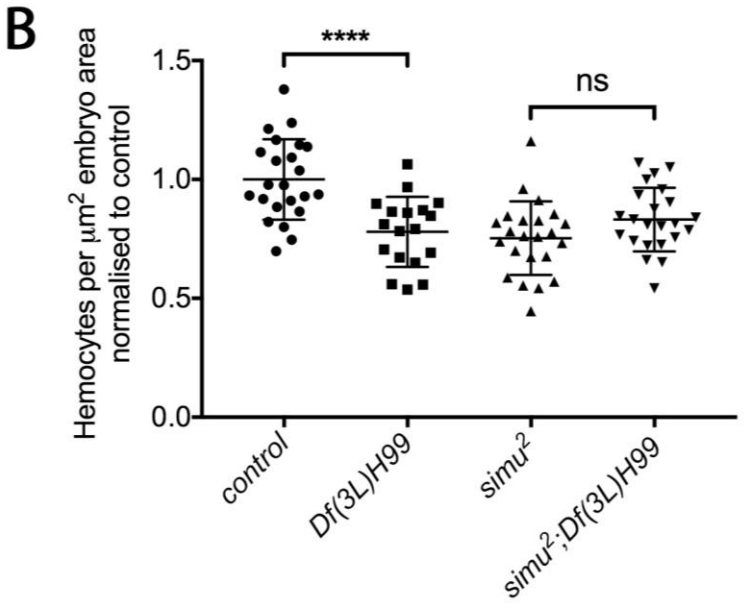
B
Hemocytes per µm² embryo area normalised to control
1.5
1.0
0.5
0.0
****
ns
control
Df(3L)H99
simu²
simu²;Df(3L)H99

Figure 4.14: Blocking apoptosis using the *Df(3L)H99* genomic deletion is unable to rescue pre-wound macrophage numbers in *simu*^{2} mutants
(A) Representative pre-wound stills of GFP-labelled hemocytes on the superficial VNC in control, *Df(3L)H99*, *simu*^{2}, and *simu*^{2}*;Df(3L)H99* mutant stage 15 embryos. (B) Scatterplot of hemocyte densities in stage 15 pre-wound images shown as the number of hemocytes per μm^2 embryo area normalized to the control average. Lines and error bars represent mean±SD; n=23, 18, 23 and 23 embryos per genotype for the above genotypes respectively.
Scale bars represent 20μm; asterisks indicate statistical significance as determined by Mann-Whitney test; ****p < 0.0001 and ns= not significant.

mutants alone (*w;simu*^{2}*;crq-GAL4,UAS-GFP*) those in which apoptosis had been blocked using the *Df(3L)H99* genomic deletion (*w;simu*^{2}*;Df(3L)H99,crq-GAL4,UAS-GFP*) had similar numbers of hemocytes in the pre-wound images (n=23 embryos for both *simu*^{2} and *simu*^{2}*;Df(3L)H99*; p=0.0952 via Mann-Whitney test; Fig. 4.14 A, B). Therefore it is unlikely that the lack of rescue in inflammatory responses is not down to there being fewer hemocytes in *simu*^{2}*;Df(3L)H99* embryos. Surprisingly we also found that, when compared to controls (*w;;crq-GAL4,UAS-GFP*), *Df(3L)H99* embryos (*w;;Df(3L)H99,crq-GAL4,UAS-GFP*) have decreased hemocyte densities in this area (n=23 and 18 embryos for control and *Df(3L)H99* respectively; p<0.0001 via Mann-Whitney test; Fig. 4.14 A, B). This suggests that the slight wound response defect seen in *Df(3L)H99* embryos may be due to a reduction in the number of hemocytes in the surrounding area.

4.2.15 The percentage of hemocytes that migrate to the wound is partially rescued by removing apoptosis in *simu* mutants

Whilst examining the time-lapse wounding movies taken as part of the wounding assay, we noticed that hemocyte responses to wounds in *simu*^{2}*;Df(3L)H99* double mutant embryos seemed more pronounced than those in *simu*^{2} mutants: it seemed as though the initial migration of hemocytes to wounds in *simu*^{2}*;Df(3L)H99* mutants might be more effective than in *simu*^{2} mutants. Therefore to examine this further the percentage of hemocytes present in the first time frame of the time-lapse wounding movies that migrate to the wound at any point during the movie was analysed (termed % responders). Interestingly, we found that the percentage of hemocytes responding to wounds in *simu*^{2}*;Df(3L)H99* embryos was significantly higher than in *simu*^{2} mutant embryos, (n=25 and 18 embryos for *simu*^{2} and *simu*^{2}*;Df(3L)H99* respectively; p=0.0190 via Mann-Whitney test; Fig 4.15 A, B). This result was particularly interesting as it suggested that hemocytes in *simu*^{2} mutants lacking apoptosis were better able to respond to wounds than those in *simu*^{2} mutants. To determine whether the slight wound response defect

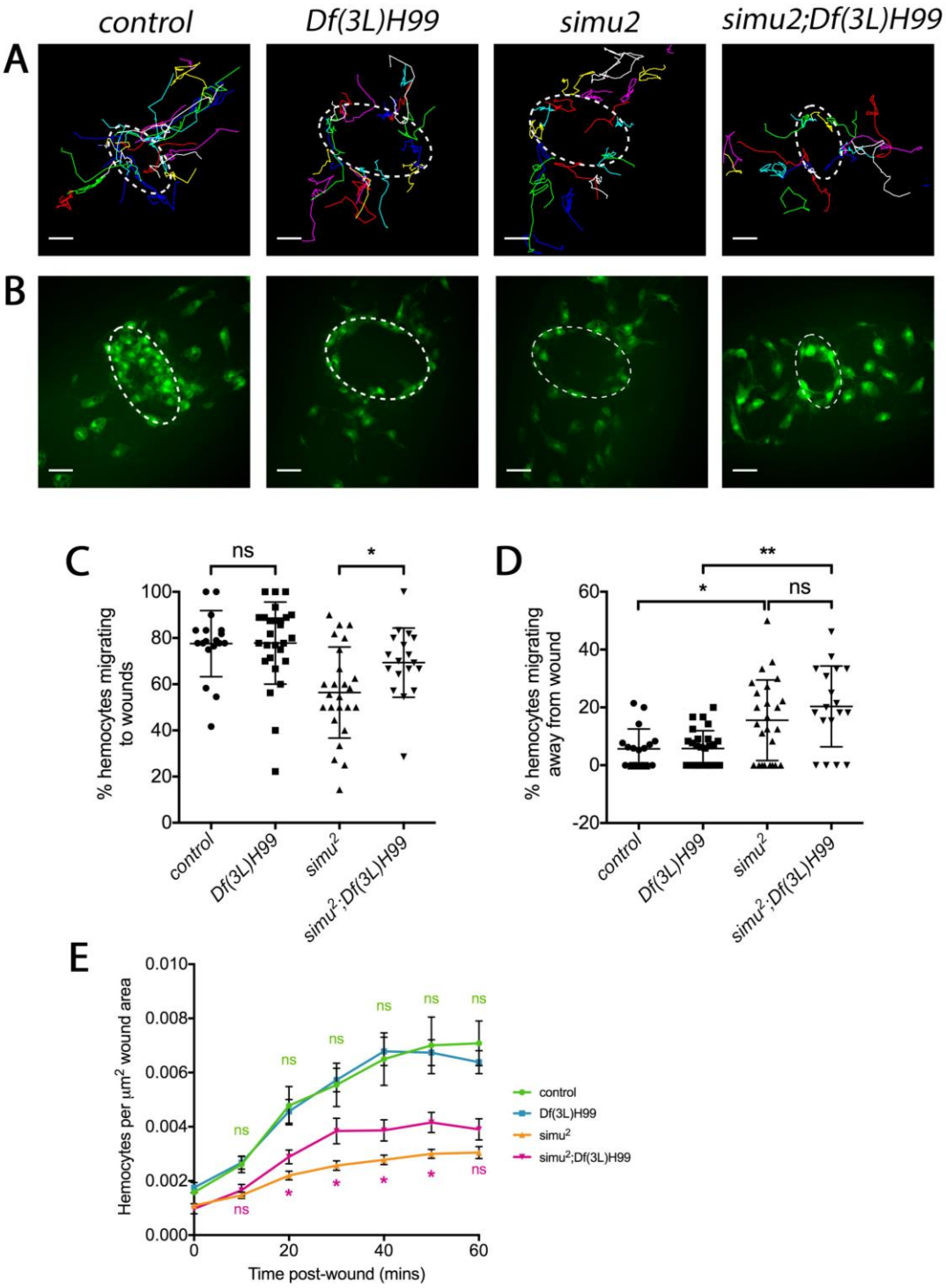
control
Df(3L)H99
simu2
simu2;Df(3L)H99
A
B
C
ns
*
% hemocytes migrating to wounds
100
80
60
40
20
0
control
Df(3L)H99
simu2
simu2;Df(3L)H99
D
**
*
ns
% hemocytes migrating away from wound
60
40
20
0
-20
control
Df(3L)H99
simu2
simu2;Df(3L)H99
E
Hemocytes per µm2 wound area
0.010
0.008
0.006
0.004
0.002
0.000
0
20
40
60
Time post-wound (mins)
ns
*
control
Df(3L)H99
simu2
simu2;Df(3L)H99

Figure 4.15: Blocking apoptosis using the *Df(3L)H99* genomic deletion rescues the percentage of hemocytes migrating to wounds during the 60-minute time period post-wounding in *simu*^{2} mutants
(A) Representative tracks of hemocyte wound responses over 58 minutes from the time of wounding in control, *Df(3L)H99*, *simu*^{2}, and *simu*^{2} mutant stage 15 embryos. Coloured lines represent the course of migration of each hemocyte tracked. (B) Corresponding representative stills of GFP-labelled hemocyte responses to wounds at 58 minutes post-wound in control, *Df(3L)H99*, *simu*^{2}, and *simu*^{2}*;Df(3L)H99* mutant stage 15 embryos. (C) Scatterplot of the % of hemocytes present at t=0 minutes post-wound who actively migrate to the wound at any point during the wounding movie. Lines and error bars represent mean±SD; n=18, 27, 25 and 18 movies analysed per genotype for the above genotypes respectively. (D) Scatterplots of the % of hemocytes present at t=0 minutes post-wound who migrate away from the wound at any point during the wounding movie. Lines and error bars represent mean±SD; n=18, 27, 25 and 18 movies analysed per genotype for the above genotypes respectively. (E) Line graph of the number of hemocytes per μm^2 wound area at specified time-points in minutes post-wounding. Data points and error bars represent mean±SD; n= 6, 16, 10 and 10 movies analysed per genotype for the above genotypes respectively.
White dashed ovals represent wound perimeter; asterisks indicate statistical significance as determined by Mann-Whitney (B and D) or by a Kruskal-Wallis one-way ANOVA test (C); *p < 0.05, **p < 0.01 and ns=not significant.

observed in *Df(3L)H99* embryos was due simply to decreased numbers of hemocytes in the wounding area, we also examined the % of hemocytes migrating to wounds in *Df(3L)H99* embryos compared to controls. This analysis showed that the % of hemocytes responding to wounds in *Df(3L)H99* was no different to controls (n=18 and 27 embryos for control and *Df(3L)H99* respectively; p=0.796 via Mann-Whitney test; Fig. 4.15 A, B), suggesting hemocytes in *Df(3L)H99* embryos are just as able to respond to wounds as those in controls, and that the wound response defect observed is likely due solely to decreased numbers of hemocytes in the wounding location.

One explanation for the discrepancy between hemocyte numbers at the wound at 60 minutes and the percentage responders in *simu*^{2}*;Df(3L)H99* embryos may be that hemocytes are leaving the wound, a process termed "resolution", at a higher rate. An emerging idea in the field of inflammation is that resolution is controlled, at least in part, by retention signals (Nourshargh et al. 2016). In light of this and our own observations of hemocyte behaviour at wounds, we also examined the percentage of hemocytes that migrated away from the wound at any point during the wounding movie, as a way of assessing hemocyte retention at wounds. We found that in *simu*^{2} mutants a greater percentage of hemocytes leave the wound during the 60 minute time-frame postwound when compared to controls (n=18 and 25 for control and *simu*^{2} respectively; p=0.0465 via Kruskal-Wallis ANOVA; Fig 4.15 C). We also found that, when compared to *Df(3L)H99* embryos, a greater percentage of hemocytes migrated away from the wound in *simu*^{2}*;Df(3L)H99* embryos (n=27 and 18 embryos for *Df(3L)H99* and *simu*^{2}*;Df(3L)H99* respectively; p=0.0015 via Kruskal-Wallis ANOVA; Fig 4.15 C).

Together this suggests that, regardless of the levels of apoptosis present, hemocytes in *simu*^{2} mutant embryos do indeed have defects in their retention at wounds; to our knowledge this is the first time that a gene has been shown to be involved in hemocyte retention at wounds in *Drosophila* embryos.

In order to gain a better understanding of how hemocytes respond to wounds in *simu*^{2} mutants, and how this is affected by the removal of apoptosis, the density of hemocytes present at wounds over time was analysed. This was done by calculating the density of hemocytes at wounds immediately after wounding (t=0), and at 10-minute intervals thereafter up to and including 60 minutes post-wounding. In contrast to published data (Weavers et al. 2016), this analysis showed that the pattern of hemocyte wound recruitment over time in *Df(3L)H99* embryos is almost identical to controls, suggesting that there is no defect in hemocyte wound recruitment over time in *Df(3L)H99* embryos. In *simu*^{2} mutants, however, there is an extremely minimal increase in hemocyte densities over time (Fig. 4.14 D), however when apoptosis is removed in *simu*^{2} mutants (*simu*^{2}*;Df(3L)H99*), there is significantly increased hemocyte recruitment compared to *simu*^{2} mutants at 20, 30, 40 and 50 minutes post-wound (Fig. 4.14 D).

Taken together, this analysis suggests that hemocyte recruitment to wounds is improved in *simu*^{2} mutants when apoptosis is blocked, suggesting that to some extent, apoptotic cells play a role in preventing hemocytes from migrating to wounds in *simu*^{2} mutants. However, hemocyte recruitment in *simu*^{2}*;Df(3L)H99* embryos remains much lower than controls at every timepoint, demonstrating that Simu is needed for normal hemocyte responses to wounds. As Simu has no intracellular signalling domain (Kurant et al. 2008) it is not possible for Simu to act alone as a receptor for wounds, however it may work in concert with other damage receptors, the only known one of which is Draper (Evans et al. 2015). Altogether this data shows that there is no defect in hemocyte wound recruitment over time in *Df(3L)H99* embryos when compared to controls.

4.2.16 Simu may act in a separate pathway to Draper during hemocyte inflammatory responses

It has previously been reported that Simu acts upstream of Draper in the same genetic pathway during glial phagocytosis of apoptotic cells (Kurant et al. 2008). As it is known that Draper is required cell-autonomously by hemocytes for their inflammatory responses to wounds in

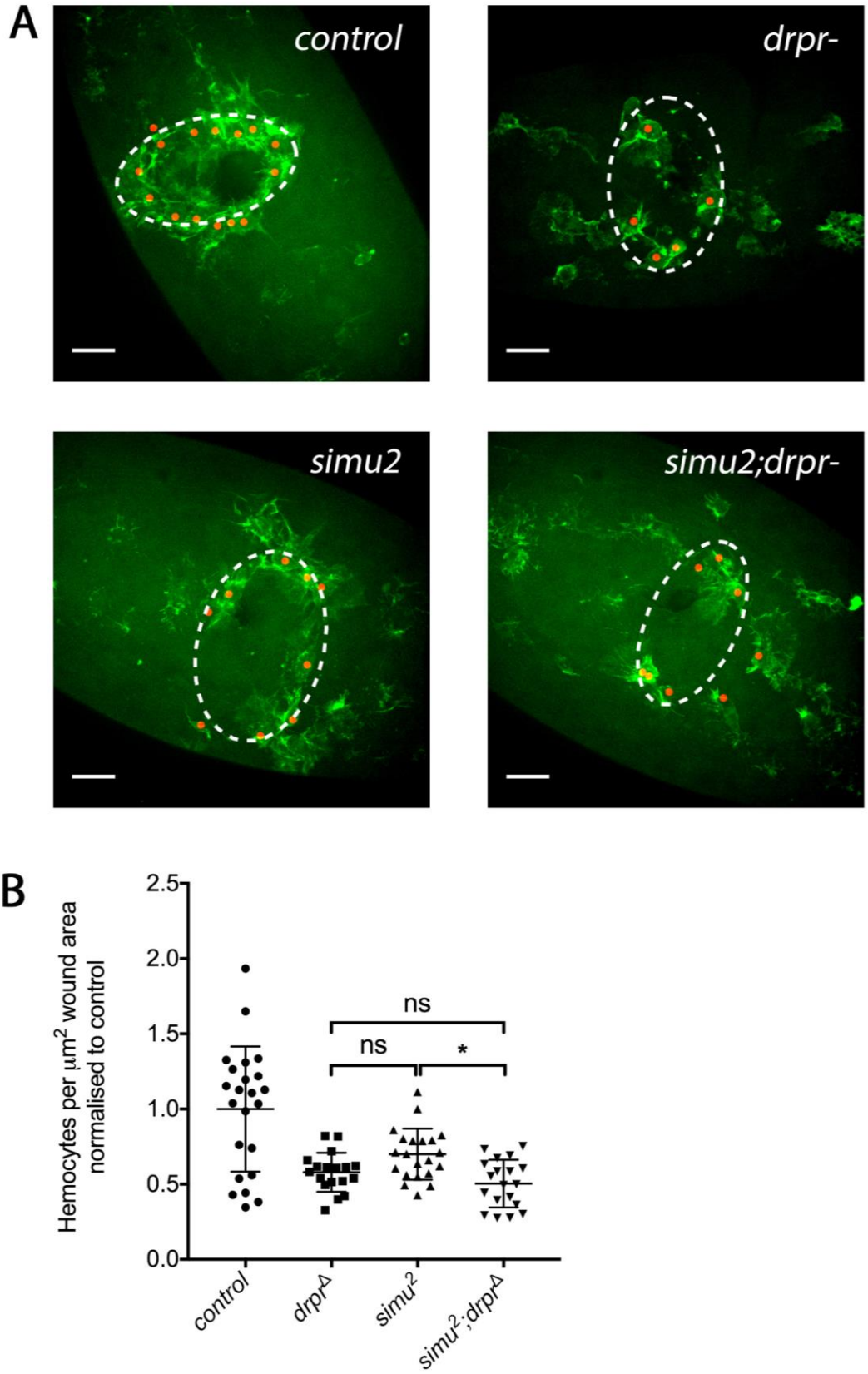
A
control
drpr-
simu2
simu2;drpr-
B
Hemocytes per µm2 wound area normalised to control
2.5
2.0
1.5
1.0
0.5
0.0
ns
ns
*
control
drpΔ
simu2
simu2;drpΔ

Figure 4.16: Wound phenotypes of *simu^{2};drpr$^{\Delta 5}$* double mutants compared to *simu^{2}* and *drpr$^{\Delta 5}$* single mutants
(A) Representative stills of *srp-GMA* labelled hemocyte responses to wounds at 60 minutes post-wound in control, *simu^{2}*, *drpr$^{\Delta 5}$* and *simu^{2};drpr$^{\Delta 5}$* double mutant stage 15 embryos. Manually drawn red dots indicate the location of hemocyte cell bodies to aid in identifying individual hemocytes. (B) Scatterplot of hemocyte wound responses per embryo shown as the number of hemocytes per μm^{2} wound area at 60 minutes post-wounding normalised to the control average. Lines and error bars represent mean±SD; n=23, 18, 21 and 19 embryos per genotype for the above genotypes respectively.
White dashed ovals represent wound perimeter; scale bars represent 20μm; asterisks indicate statistical significance as determined by Kruskal-Wallis one-way ANOVA with Dunn's multiple comparison test; *p < 0.05 and ns= not significant.

Drosophila (Evans et al. 2015), we hypothesised that Simu may also be required upstream of Draper during hemocyte inflammatory migrations to wounds. To test this we wounded embryos that were mutant for both *simu^{2}* and *drpr$^{\Delta 5}$*, (*w;simu^{2},p{srp-GMA}; drpr$^{\Delta 5}$*) and compared hemocyte inflammatory responses with those of *simu^{2}* (*w;simu^{2},p{srp-GMA}*) and *drpr$^{\Delta 5}$* (*w;p{srp-GMA}; drpr$^{\Delta 5}$*) single mutant embryos as well as controls (*w;p{srp-GMA}*) (Fig. 4.16 A, B). Firstly, this analysis showed that the wound response defect in *simu^{2}* mutants is no more severe than that of *drpr$^{\Delta 5}$* mutants (n=18 and 21 embryos for *simu^{2}* and *drpr$^{\Delta 5}$* respectively; p=0.315 via Kruskal-Wallis ANOVA; Fig. 4.16 A, B). It also revealed that the wound response in *simu^{2};drpr$^{\Delta 5}$* double mutants was slightly decreased when compared to *simu^{2}* mutants alone (n=21 and 19 embryos for *simu^{2}* and *simu^{2};drpr$^{\Delta 5}$* respectively; p=0.0177 via Kruskal-Wallis ANOVA) but that this was not the case compared to *drpr$^{\Delta 5}$* mutants (n=18 and 19 embryos for *drpr$^{\Delta 5}$* and *simu^{2};drpr$^{\Delta 5}$* respectively; p=0.8578 via Kruskal-Wallis ANOVA) (Fig. 4.16 A, B). This additive effect suggests that Simu may be acting in a separate genetic pathway to Draper during hemocyte inflammatory responses, although as the wound response defect in *simu^{2};drpr$^{\Delta 5}$* is no different to *drpr$^{\Delta 5}$* mutants, this would certainly need further investigation.

4.2.17 Simu is required for the engulfment of cellular debris by hemocytes at wounds

As hemocytes are statistically more likely to migrate away from wounds in *simu^{2}* mutants, suggesting a requirement for Simu in hemocyte retention at wounds, we sought to examine its role in this process. Work in our lab and others has shown that Caspase active-positive/apoptotic cells can seldom be found at the wound, at least during the 60 minutes after the wound has been induced (Abreu-Blanco et al. 2012; Weavers et al. 2017a; Armitage and Evans, unpublished data), however PS exposure is high at wounds suggesting high levels of necrotic cellular debris

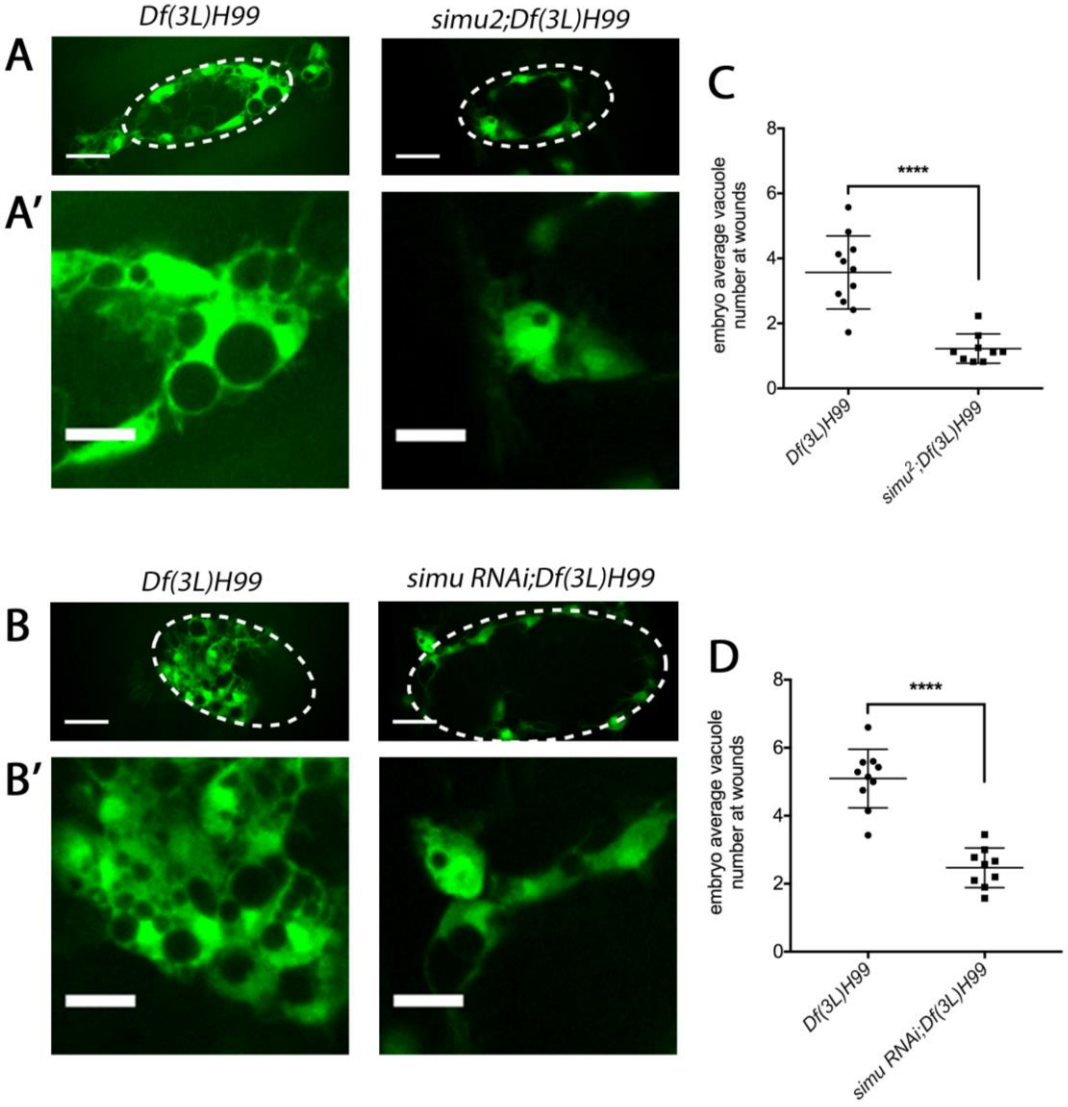

Figure 4.17: Simu is required in hemocytes for normal levels of hemocyte vacuolation at wounds

(A and B) Representative individual slices from stills of GFP-labelled hemocytes at wounds in order to observe vacuoles within hemocytes. Scale bars represent 20μm. (A' and B') Zoomed sections of images from A and B demonstrating the decreased vacuolation of hemocytes at wounds in *simu*^{2}*;Df(3L)H99* mutants or embryos in which *simu* expression has been reduced specifically in hemocytes by RNAi-mediated knockdown in a *Df(3L)H99* background (*UAS-simu RNAi;Df(3L)H99*), compared to their respective *Df(3L)H99* controls. Scale bars represent 10μm. (C and D) Scatterplots of the average number of vacuoles per hemocyte at wounds 60-minute post-wounding per embryo. Lines and error bars represent mean±SD; (n=11 and 9 embryos for *Df(3L)H99* and *simu*^{2}*;Df(3L)H99* respectively; (D) n=10 and 9 embryos for *Df(3L)H99* and *UAS-simu RNAi;Df(3L)H99* respectively.

White dashed ovals represent wound perimeter; asterisks indicate statistical significance as determined by Mann-Whitney test; ****$p < 0.0001$.

(Armitage and Evans, unpublished data). As PS acts as the ligand for Simu on apoptotic cells, we hypothesised that Simu also acts as a receptor for necrotic cells and that this interaction acts as a retention signal at wounds.

In *Df(3L)H99* embryos hemocytes contain no vacuoles, as there are no apoptotic bodies for them to engulf (see Fig. 4.14 A), however when *Df(3L)H99* embryos are wounded, hemocytes at the wound become highly vacuolated. Therefore as wounds induced in embryos are sterile, the vacuolation seen in hemocytes at wounds in *H99* embryos is likely due to the engulfment of necrotic cellular debris. To test whether Simu is required for the engulfment of necrotic cells, we quantified the number of vacuoles in hemocytes present at the wound at 60-minutes post-wound in *Df(3L)H99* and *simu*^{2}*;Df(3L)H99* embryos (the same post wound images collected for wound response analysis in Fig. 4.13), as any vacuoles present will be due to engulfment at wounds. This analysis showed that, compared to hemocytes at wounds in *Df(3L)H99* embryos, those in *simu*^{2}*;Df(3L)H99* embryos contained significantly fewer vacuoles (n=11 and 9 embryos for *Df(3L)H99* and *simu*^{2}*;Df(3L)H99* respectively; $p<0.0001$ via Mann-Whitney test; Fig. 4.17 A-C). Therefore it seems that Simu is required for the efficient engulfment of cellular debris by hemocytes at wounds. This is the first time that Simu has been shown to be involved in the clearance of necrotic cells in addition to apoptotic cells.

In order to assess whether Simu is required cell-autonomously in hemocyte engulfment of cellular debris at wounds, the vacuolation of hemocytes at wounds in *Df(3L)H99* embryos and in those in which RNAi-mediated knockdown of *simu* had been performed specifically in hemocytes in a *Df(3L)H99* background was analysed. As before, hemocytes at wounds in *Df(3L)H99* embryos were highly vacuolated (Fig. 4.17 D, D'). In contrast, however, wound hemocytes contained substantially fewer vacuoles in *Df(3L)H99* embryos in which hemocyte *simu* was targeted by *RNAi* (n=10 and 9 embryos for *Df(3L)H99* and *simu RNAi;Df(3L)H99* respectively; $p<0.0001$ via Mann-Whitney test; Fig. 4.17 D-F). This suggests that Simu is required cell-autonomously in hemocytes for engulfment of debris at wounds.

4.3 DISCUSSION

4.3.1 Modulation of macrophage inflammatory and basal migrations by apoptotic cells

Analysis of macrophage wandering migrations in *simu* loss-of-function mutant embryos showed that macrophage migration speeds were reduced (Fig. 4.10), but that Simu was not required cell-autonomously for normal hemocyte migrations (Fig. 4.11). By blocking apoptosis in *simu* mutants using the *Df(3L)H99* genomic deletion that removes the three pro-apoptotic genes *hid*, *grim* and *reaper* (White et al. 1994) it was possible to show that this slowed migration was indeed due to apoptotic cells, be it directly or indirectly, as their removal resulted in a rescue of macrophage migration speeds (Fig. 4.12). Macrophages in *simu* mutants also showed a reduced ability to migrate to sites of tissue damage - a defect that could be partially improved by blocking apoptosis in the embryo. Therefore it is clear that apoptotic cells disrupt hemocyte migratory behaviour *in vivo*, however the mechanisms by which they do so are yet to be discovered.

There are many potential hypotheses as to how apoptotic cells affect macrophage migratory behaviour. Firstly, it may well be the case that apoptotic cells are secreting chemotactic 'find-me' cues that are capable of slowing or antagonising typical macrophage migrations. As hemocytes in *simu* mutants seem to become surrounded by multiple uncleared apoptotic cells (Fig. 4.1) it is likely that they are receiving cues that are trying to direct their migration in multiple different directions all at once. This may be confusing the hemocytes, and instead their migration may be stalling. Some evidence for this kind of behaviour comes from a study using *Dictyostelium discoideum*, in which the migratory speed of cells were slowed when the cells were exposed to chemotactic gradients which were quickly being altered both spatially and temporally, leading to what they call 'cell trapping' (Meier et al. 2011). It has also been shown that hemocytes have a hierarchical response to chemotactic cues in the *Drosophila* embryo, with apoptotic cells seemingly placed at the top of the hierarchy followed by development migration cues and finally wound chemoattractants (Moreira et al. 2010). Therefore, as uncleared apoptotic cells accumulate in the area surrounding hemocytes in *simu* mutants (Fig. 4.1), it may be that they are being inundated with the find-me cues being released by apoptotic cells, and are prioritising these over those diffusing from the wound. However, these hypotheses would be difficult to test as the find-me cues released by apoptotic cells in *Drosophila* remain to be identified (see Chapter 5), therefore blocking them is not currently feasible. A possible experiment to test the role of find-me cues in modulating macrophage migratory behaviour would be to inject embryos with known vertebrate find-me cues such as the nucleotides ATP

and UTP, sphingosine-1-phosphate and lysophosphatidylcholine (Elliott et al. 2009; Gude et al. 2008; Lauber et al. 2003), which have the potential to also act as 'find-me' cues in *Drosophila*. This approach is explored in Chapter 5.

In *simu* mutants, there is a highly significant increase in the number of apoptotic cells that remain untouched by hemocytes (a measure of uncleared apoptotic cells), but there is also an increase in the number of engulfed apoptotic cells (Fig. 4.1). Therefore in order to attempt to address whether apoptotic cells are capable of modulating hemocyte inflammatory responses prior to their engulfment by hemocytes, an experiment was performed whereby apoptosis was induced throughout the embryo by heat treating embryos carrying *heat shock-hid* genomic construct (Armitage and Evans, unpublished data). These embryos were then wounded at a time-point after caspase activation, but before the apoptotic cells had begun to be engulfed by hemocytes, and it was found that hemocyte inflammatory responses were greatly reduced in such embryos (Armitage and Evans, unpublished data), adding strength to the hypothesis that uncleared apoptotic cells dampen macrophage inflammatory responses. Therefore, it is possible that uncleared apoptotic cells in *simu* mutants are capable of dampening hemocyte inflammatory responses, but the increased engulfment of apoptotic cells in these mutants cannot be ruled out as also having an affect on hemocyte inflammatory migrations. For example, the defective processing of apoptotic cells in SCAR mutant hemocytes causes their migration to be slowed (Evans et al. 2013), as does the build-up of apoptotic cell material in macrophages from a zebrafish model of lysosomal disorders (Berg et al. 2016). In dendritic cells, which patrol their environment and engulf antigens, the capture of antigens is associated with a decrease in their migration speeds caused by the recruitment of myosin IIA to the front of the cells (Chabaud et al. 2015). Together, this provides evidence that phagocyte migration can be slowed during the process of phagocytosis and also by the build-up of apoptotic cells within hemocytes, two potential explanations as to why macrophage migratory behaviour may be perturbed in *simu* mutants.

Another explanation is that macrophages in *simu* mutants may be in contact with apoptotic cells through binding of other apoptotic cell receptors such as Draper, Croquemort, Scab or Beta-nu integrin (Manaka et al. 2004; Franc et al. 1999; Nagaosa et al. 2011; Nonaka et al. 2013). Therefore the binding of apoptotic cells, either from within hemocytes or extracellularly, may be inducing downstream signalling from apoptotic cell receptors, which may perturb their migratory behaviour. In order to examine whether hemocyte-apoptotic cell interactions may be important in the suppression of hemocyte immune responses, an attempt was made to block so-called 'eat-me' signals on the surface apoptotic cells to prevent their interactions with hemocytes. The most well-characterised eat-me signal exposed on the surface of apoptotic cells is phosphatidylserine (PS) (Segawa and Nagata 2015), which has been shown to be a ligand for

both Simu and Draper and may well also be a ligand for the other known apoptotic cell receptors in *Drosophila* (Shklyar, Levy-Adam, et al. 2013; Tung et al. 2013). Therefore AnnexinV, a protein that binds to and masks PS, was injected prior to wounding in control and *simu* mutant embryos, to examine whether this might result in a rescue of inflammatory responses in *simu* mutants. However, it was found that the injection of AnnexinV was unable to rescue hemocyte migrations to wounds in *simu* mutants (Armitage and Evans, unpublished data). This suggests that the binding of hemocytes to the apoptotic eat-me' signal PS does not preventing hemocytes from migrating to wounds in *simu* mutants. It is also possible that other eat-me signals may still be binding to apoptotic cell receptors in this case. For example, Calreticulin and Pret-a-porter have both been shown to be exposed on the surface of apoptotic cells in *Drosophila* (Gardai et al. 2005; Kuraishi et al. 2007; Kuraishi et al. 2009). A tethering molecule, DmCaBP1, has also been shown to be released by apoptotic cells (Okada et al. 2012), therefore masking PS alone may be insufficient to prevent macrophages from binding to apoptotic cells.

There are also a plethora of other potential explanations as to how apoptotic cells affect the migratory behaviour of macrophages. One hypothesis is that, as discussed in the previous chapter, increased numbers of apoptotic cells induces the expression of stress signalling in hemocytes, and that this may cause hemocyte inflammatory responses or indeed their general migration to be perturbed. One such stress signalling pathway is JNK signalling, which was also explored in the previous chapter. However as JNK signalling is generally not active in hemocytes in both controls and *simu* mutants, nor is it activated in hemocytes in response to wounds (Fig. 4.8), it is unlikely that disregulated JNK signalling explains the migratory defects seen in *simu* mutants. There are a range of other stress signalling pathways besides JNK which may be playing a role in disrupting hemocyte migratory behaviour in *simu* mutants, such as p38 MAPK, NF kappa B signalling, AKT or PI3K signalling, however these have not yet been explored and represent a line of future study.

Another possible mechanism is that apoptotic cells are altering the polarisation of macrophages to a more anti-inflammatory state, a process that is known to occur in vertebrate macrophages upon the phagocytosis of apoptotic cells (Szondy et al. 2017). It is also known that macrophage heterogeneity exists in vertebrate systems and that they possess a spectrum of polarisation states from the pro-inflammatory 'M1' phenotype to the anti-inflammatory and pro-resolving 'M2' phenotype (Mosser and Edwards 2008). The phenomenon of macrophage heterogeneity has yet to be identified in *Drosophila* however one important mediator of vertebrate macrophage polarisation are Reactive Oxygen Species (ROS), whose increased presence is associated with the promotion and function of 'M1' type macrophages, which are considered to be pro-inflammatory (Tan et al. 2016). When we examined hemocyte ROS levels in *simu* mutants, we

found that this was reduced compared to hemocytes in control embryos (Fig. 4.9). Therefore it is possible that the inflammatory state of hemocytes in *simu* mutants is being shifted to that of a more anti-inflammatory phenotype and that this is affecting the ability of hemocytes to mount inflammatory responses to wounds. However, in order to further confirm this, ROS levels in hemocytes in control embryos would have to be reduced, perhaps by knocking down expression of the NADPH oxidase Nox or by treating them with a ROS scavenging agent, to see whether this would reduce hemocyte inflammatory responses. To confirm that the reduction in ROS levels in *simu* mutants is due to the effect of apoptotic cells, those in which apoptosis has been removed (*simu*^{2}*;Df(3L)H99* embryos) would have to be compared to those in *simu*^{2} mutants. If the removal of apoptosis were to rescue ROS levels in hemocytes, then it is likely that apoptotic cells are somehow capable of reducing ROS levels in hemocytes. Unfortunately the appropriate crosses were not finished in time for me to examine this before the end of my PhD. Interestingly, a genome-wide microarray comparison of *simu*^{2} mutant and control embryos did in fact reveal a significant alteration in the expression profile of a range genes involved in cellular redox homeostasis (data not shown), further suggesting that the redox state of cells in *simu* mutants may be altered. However, I did not have time to validate these results by qPCR or to assess the affect of changes in the expression of any of these genes on hemocyte inflammatory responses in control embryos, therefore this represents an avenue of further study.

As many of the genes involved in macrophage polarisation in vertebrate systems are not expressed in *Drosophila*, it is difficult to assess the activation state of macrophages in this system. However, perhaps macrophage polarisation does exist in *Drosophila* but that the markers and mechanism governing this are different to vertebrate systems. It would be interesting to study whether apoptotic cells are capable of shifting macrophage polarisation states in *Drosophila* and this is something that other members of the lab are working towards identifying.

4.3.2 A cell-autonomous role for Simu in macrophage inflammatory responses

By wounding embryos in which Simu expression had been reduced specifically in hemocytes using RNAi knockdown, we were able to show that Simu is required cell-autonomously by hemocytes for their inflammatory migrations to wounds (Fig. 4.4). This is in contrast to general hemocyte motility, where Simu is not required cell-autonomously (Fig. 4.11), suggesting that the requirement for Simu by hemocytes is specific to inflammatory responses. In *simu*^{2} mutant embryos, the blocking of apoptosis is only partially able to rescue hemocyte recruitment to

wounds (Fig. 4.15), further suggesting that *simu*^{2} mutants also have a defect in hemocyte inflammatory responses that is not mediated by apoptotic cells.

As the apoptotic cell receptor Draper has also been shown to function as a receptor for the detection of wound cues (Evans et al. 2015), it is possible that Simu also has a role in this. Indeed, Simu has already been shown to act upstream of Draper in the phagocytosis of apoptotic cells (Kurant et al. 2008), therefore may also act in the same pathway as Draper during wound responses. When this was tested by examining wound response phenotypes in *simu;drpr* double mutants compared to the single mutants alone, we found that the double mutant wound phenotype was slightly but significantly more severe than *simu* mutant wound responses, but not those of *drpr* mutants (Fig. 4.16). This suggests that Simu and Draper may act in distinct pathways during hemocyte inflammatory responses. However, as Simu lacks an intracellular signalling domain (Kurant et al. 2008), it must work in concert with one or more other receptors to be able to induce an inflammatory response. As we have found that the apoptotic cell receptors Scab and βυ integrin are also required for hemocyte inflammatory responses to wounds (Chapter 6), it is possible that Simu may act in concert with them during inflammatory responses. Assessing the inflammatory responses in double mutants for *simu* and either of these receptors may shed light on this. Alternatively, Simu may be acting alongside an as yet unidentified receptor required for hemocyte inflammatory responses.

4.3.3 Recognition of necrotic cellular debris as a retention signal at wounds?

Analysis of hemocyte vacuolation at wounds showed that vacuolation in *simu* mutants was decreased (Fig. 4.17), and that Simu is required cell-autonomously in hemocytes for normal vacuolation at wounds (Fig. 4.17). This suggested that Simu is required in hemocytes for the normal engulfment of necrotic cellular debris at wounds.

PS is usually only found on the inner leaflet of the cell membrane, but during apoptosis is flipped to the outer membrane where it acts as an apoptotic ‘eat-me’ signal (Fadok et al. 2001). In the case of cellular necrosis, PS also becomes exposed due to the rupturing of the cellular membrane and is required for the engulfment of necrotic cells by macrophages (Brouckaert et al. 2004). As Simu has been shown to bind PS in the engulfment of apoptotic cells (Shklyar, Levy-Adam, et al. 2013), it is likely that Simu may also required for the efficient PS-dependent phagocytosis of necrotic cellular debris at wounds. The other apoptotic cell receptors identified in *Drosophila* have all been shown to be involved in the phagocytosis of other targets, in this case bacteria (Guillou et al. 2016; Nonaka et al. 2013; Hashimoto et al. 2009), therefore it is possibile that Simu may also be involved in the phagocytosis of other targets such as necrotic cells.

Furthermore, I would hypothesise that perhaps hemocyte binding of PS at wounds is required in order to retain hemocytes at wounds, as hemocytes lacking Simu, which has been shown to bind to PS (Shklyar, Levy-Adam, et al. 2013), show reduced retention at wounds (Fig. 4.15). The retention of inflammatory cells at sites of inflammation is an emerging field and it is now known that neutrophil reverse migration away from sites of inflammation represents an anti-inflammatory mechanism (Robertson et al. 2014; Mathias et al. 2006). The mechanisms of reverse migration of neutrophils away from sites of inflammation are now beginning to be understood in more detail, but it is thought that a combination of different mechanism may play a part in this, including signal desensitisation, the presence of repellent chemokines and the loss of cues which brought neutrophils to the inflammation site in the first place (Nourshargh et al. 2016). Although to my knowledge a role in the recognition or phagocytosis of cellular debris for macrophage retention at wounds has never been found. Again, this would be a rather difficult hypothesis to test as it is impossible to make a wound without inducing cellular necrosis. However, a foci of H_2O_2 could be generated artificially to mimic a wound lacking necrotic cellular debris, and macrophage retention at this locally generated signal could be assessed. This could be done by perhaps activating the H_2O_2 producing enzyme DUOX in a spatially regulated manner. Another approach would be to try and prevent hemocytes from being able to bind to PS at wounds. This was attempted by injecting the PS masking agent Annexin-V prior to wounding, however this had no significant affect on hemocyte wound densities at 60 minutes post-wound (data not shown). Alternatively, Simu may be involved in recognising a retention signal produced at wounds, however in *Drosophila*, whether retention signals are produced at sites of tissue damage and the identity of such signal is as yet unknown.

4.4 CONCLUSIONS

In this chapter we have shown that the accumulation of apoptotic cells in *Drosophila* embryos affects multiple aspects of macrophage migratory behaviour. By impairing the ability of both macrophages and glia to clear apoptotic cells using mutants for the apoptotic cell receptor Simu, we were able to cause apoptotic cells to accumulate in the vicinity of hemocytes. We show that the accumulation of apoptotic cells causes macrophage migration speeds to be slowed and also alters their ability to migrate to sites of tissue damage, which represents a dampening of macrophage inflammatory responses. Finally, we also show that Simu itself is required by macrophages for their normal inflammatory responses to wounds, and that it is also involved in their retention at sites of tissue damage, possibly through its interaction with necrotic cellular debris.

Chapter 5: Exploring the modulation of hemocyte inflammatory responses by apoptotic "find-me" cues

5.1 INTRODUCTION

In order for apoptotic cells to be cleared by professional phagocytes, the phagocytes must first be able to locate the whereabouts of the dying cells. For this to happen, it is thought that, at least in some organisms, apoptotic cells release chemotactic 'find-me' cues which phagocytes are able to sense and subsequently chemotax towards.

Several cues released by apoptotic cells that are capable of inducing chemotaxis of phagocytes have now been found, all using *in vitro* transmigration assays of monocytes and macrophages across a porous membrane towards supernatant taken from apoptotic cells (Gude et al. 2008; Truman et al. 2008; Lauber et al. 2003; Elliott et al. 2009). The first to be discovered was the phospholipid lysophosphatidylcholine (LPC), which was shown to be released by apoptotic cells upon Caspase activation and induced the transmigration of human monocytic cell lines, as well as primary human macrophages (Lauber et al. 2003). Sphingosine-1-phosphate (S-1-P) and fractalkine were also found to be released by apoptotic cells and induce chemotaxis of monocytes and/or macrophages (Gude et al. 2008; Truman et al. 2008). Truman *et al.* also demonstrated that the fractalkine receptor CX3CR1 was required by macrophages to chemotax towards its ligand, and went on to show a role for fractalkine and its receptor during recruitment of macrophages to apoptotic cells in a murine model – the first time "find-me" cues had been shown to function *in vivo* (Truman et al. 2008). Finally, the nucleotides ATP and UTP were also shown to be released by apoptotic cells, and act as chemoattractant cues for monocytes and macrophages both *in vitro* and *in vivo*, and that the nucleotide receptor $P2Y_2$ was required by macrophages to migrate towards the cue (Elliott et al. 2009). It is interesting to note that although these four separate studies used similar techniques to identify potential "find-me" cues, the cue identified in each case was unique. This is potentially due to the nature of the type of cell in which apoptosis was induced, and demonstrates the diversity of cues utilised by dying cells to attract phagocytes and the complexity that this adds to the process.

As migrating phagocytes come across a plethora of different chemokines during their journey to their desired destination, they must be able to prioritise cues to create a hierarchy of importance in order to reach their end target. An excellent example of this is neutrophil migration to sites of

infection. During their journey neutrophils must be able to prioritise so called 'end target' chemoattractants being released from the site of infection over endogenous chemoattractants that are encountered en-route to such sites. For example, neutrophils have been shown to prioritise migration towards bacterial and necrotic cell-derived fMLP over endogenous IL-8 (Campbell et al. 1997). It has also been shown that the p38 MAPK and PI3K/Akt signaling pathways are responsible for determining the hierarchy of responsiveness towards chemotactic cues, with p38 MAPK signaling mediating response to end target chemoattractants, whereas PI3K/Akt signaling mediates the response to intermediate ones (Heit et al. 2002). Furthermore, it has been shown that PTEN is the molecule responsible for prioritizing which chemoattractant neutrophils should respond to (Heit et al. 2008).

Drosophila hemocytes also possess the ability to prioritise competing chemotactic cues *in vivo*. As part of their developmental migration through the embryo, hemocytes migrate along the midline of the ventral embryo to form a continuous line of hemocytes by stage 13. From here they then migrate laterally and by stage 15, when they have reached their developmental destination within the embryo, they begin migrating randomly on the superficial surface of the VNC (Tepass et al. 1994; Wood et al. 2006). The chemoattractant ligands Pvf2 and Pvf3 are expressed in the CNS and are required to direct the migration of hemocytes along the midline of the VNC during developmental dispersal, and by stage 15 their expression is greatly decreased (Wood et al. 2006). Before stage 15 when these chemoattractants are down-regulated, hemocytes are unable to respond to sites of tissue damage due to their prioritisation of these developmental cues over H_2O_2 being produced at wounds (Moreira et al. 2010). However, when apoptosis is induced using UV-irradiation, hemocytes can be seen to be distracted from their developmental migration route and instead migrate towards and phagocytose apoptotic cells (Moreira et al. 2010). Therefore it seems that in *Drosophila* there is a hierarchy of prioritisation of cues by hemocytes, with apoptotic cells being the highest priority, followed by their developmental migration cues and finally those from wounds (Moreira et al. 2010).

As demonstrated in the previous chapter, increased numbers apoptotic cells such as in *simu* mutant embryos, causes a reduction in hemocyte migration to sites of tissue damage. Removal of apoptosis in these embryos using the *Df(3L)H99* genomic deletion rescues the ability of hemocytes to respond to such wound sites. Furthermore, induction of apoptosis in otherwise wild type embryos causes hemocyte wound responses to be reduced prior to the engulfment of the dying cells (Armitage and Evans, unpublished data). Apoptotic cells have also been shown to be able to distract hemocytes from their developmental migrations (Moreira et al. 2010). Together this data strongly suggests that hemocytes are able to prioritise migration to apoptotic cells over other chemoattractive cues, which led us to hypothesise that find-me cues released by apoptotic cells cause hemocytes to be distracted from migrating to wounds, instead prioritising

migration towards these cues. In an attempt to investigate this hypothesis, we sought to inject potential 'find-me' cues into the *Drosophila* embryo prior to wounding. We hypothesised that flooding the embryo with find-me cues in this way may be able to reduce the ability of hemocytes to migrate to wounds. As no such 'find-me' cues have been characterised in *Drosophila,* we turned to those that have been discovered in vertebrate systems and that have the potential to also act as 'find-me' cues in *Drosophila*. Therefore, the work in this chapter represents efforts to investigate whether established find-me cues have an evolutionarily-conserved role in the *Drosophila* embryo. It also showcases work I have done to set-up a novel experimental approach that could potentially be used to identify novel molecules released by apoptotic cells that modulate hemocyte behavior *in vivo*.

5.2 RESULTS

5.2.1 Injection of LPC prior to wounding has no affect on hemocyte inflammatory responses

The first known find-me cue to be tested was lysophosphatidylcholine (LPC), which was injected into embryos whose hemocytes were labelled using *UAS-GFP* expression under the control of the hemocyte specific *crq-GAL4* driver (*w;;crq-GAL4,UAS-GFP*).
In vitro LPC elicited the strongest migratory response of monocytes at a concentration of 20-30μM (Lauber et al. 2003). Therefore, as it is known that Latrunculin A, a chemical used to sequester monomeric actin, needs to be injected into *Drosophila* embryos at concentrations 40 times higher than those used *in vitro* studies (I. Evans, personal communication), each cue was injected at a concentration 40x higher than that shown to produce a maximal response *in vivo*, presumably as there is limited volume within the fly embryo to contain drug solutions. In order to visualise successful injection of LPC, and as a way of assessing the amount of LPC injected, fluorescent Dextran was also included in the injection solution.

As throughout this thesis, hemocyte inflammatory responses to wounds were assessed by quantifying the density of hemocytes present at wounds 60 minutes post-wounding. Compared to embryos injected with a control solution, there was no difference in the density of hemocytes recruited to sites of tissue damage when injected with LPC at a concentration of 1.6mM – 40 times the concentration shown to produce a maximal response in the original study identifying

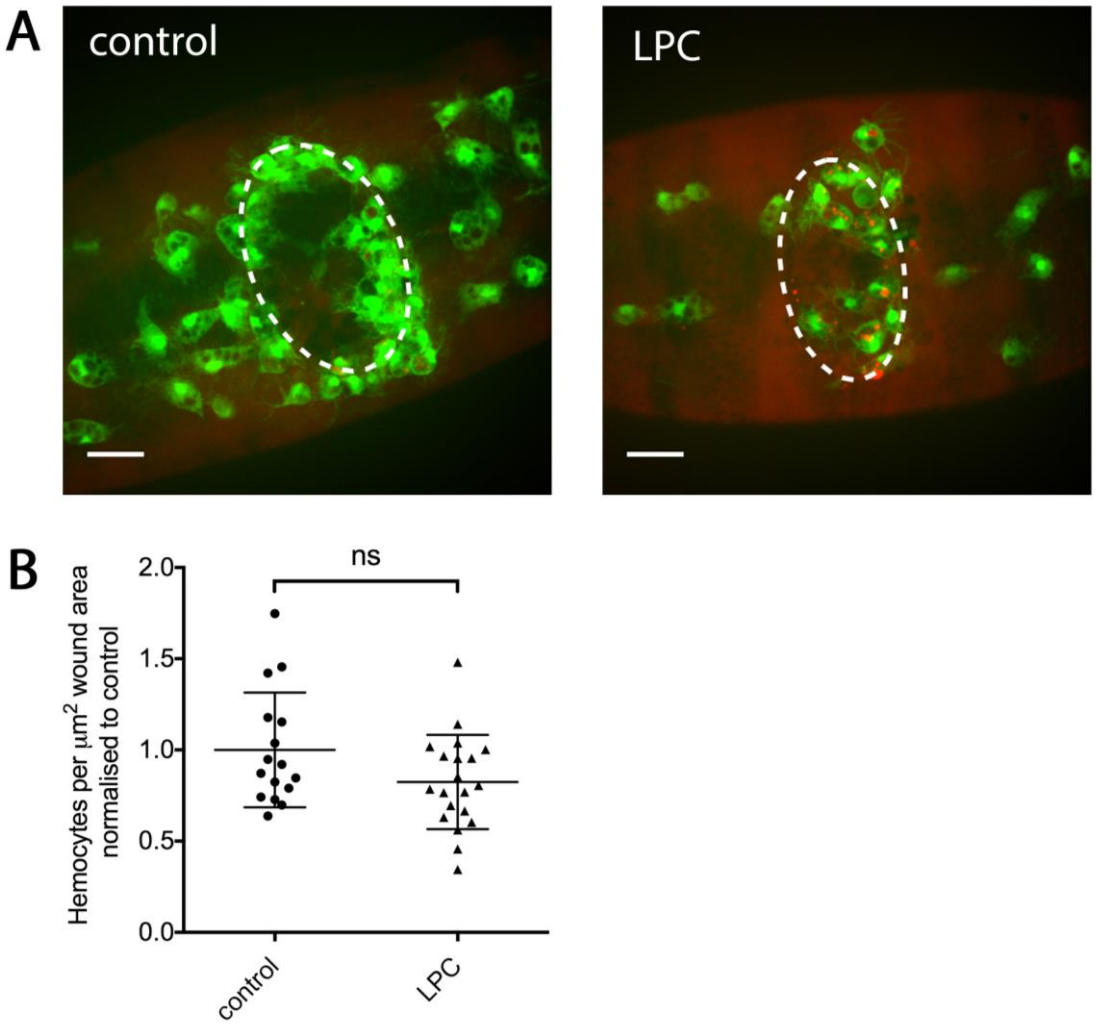

Figure 5.1: Injection of lysophosphatidylcholine into embryos prior to wounding has no effect on hemocyte inflammatory responses
(A) Representative stills of GFP-labelled hemocyte responses to wounds at 60 minutes post-wound in control and LPC injected embryos (both *w;;crq-GAL4,UAS-GFP*). Dextran (red) can also be seen in these embryos, indicating successful injection. In place of LPC, control embryos were injected with absolute ethanol diluted in PBS, as LPC was dissolved in ethanol prior to dilution in PBS. (B) Scatterplot of hemocyte wound responses per embryo shown as the number of hemocytes per μm^2 wound area at 60 minutes post-wounding normalised to the control average. Lines and error bars represent mean±SD; n=16 and 20 embryos for control and LPC injection respectively.
White dashed ovals represent wound perimeter; scale bars represent 20µm; statistical significance determined by Mann-Whitney test; ns= not significant.

LPC as a find-me cue (Lauber et al. 2003) (n=16 and 20 embryos for control and LPC injection respectively; p=0.140 via Mann-Whitney test; Fig. 5.1 A, B). This shows that the injection of LPC into embryos in this way, at the concentrations used in this experiment, does not prevent hemocytes from migrating to wounds. This suggests therefore that LPC may not be acting as a find-me cue in flies, although further evidence would be required to prove this.

5.2.2 Injection of sphingosine-1-phosphate prior to wounding has no effect on hemocyte inflammatory responses

Another identified apoptotic find-me cue is the bioactive lipid sphingosine-1-phosphate (S-1-P), which has been shown to be released by apoptotic cells and induce the migration of monocytes (Gude et al. 2008). Therefore we hypothesised that perhaps S-1-P injection prior to wounding may distract hemocytes from migrating to wounds. When we analysed the density of hemocytes at wounds 60 minutes post-wounding, we found that as with LPC injection, there was again no difference in the density of hemocytes at wounds between the control and embryos injected with 400nM S-1-P – 40 times the concentration shown to produce a maximal response in the original study identifying S-1-P as a find-me cue (Gude et al. 2008) (n=14 and 16 embryos for control and S-1-P injected embryos respectively; p=0.728 via Mann-Whitney test; Fig. 5.2). This shows that the injection of S-1-P into embryos in this way, at the concentrations used in this experiment, is not capable of distracting hemocytes from migrating to wounds. Therefore S-1-P may not be acting as a find-me cue in *Drosophila*, although more evidence would be required to definitively prove this.

5.2.3 Injection of non-hydrolysable ATP prior to wounding does not affect inflammatory responses

ATP has also been identified as a find-me cue capable of inducing the migration of monocytes and macrophages both *in vitro* and *in vivo* (Elliott et al. 2009). However, previous work in the lab has shown that the injection of ATP prior to wounding has no effect on hemocyte inflammatory responses (I. Evans, unpublished data). We hypothesised that one explanation as to why the injection of find-me cues does not seem to affect the inflammatory migration of hemocytes is that they are being degraded within the embryo before they have chance to have an effect (e.g. by aparase). ATP is hydrolysed by ATPase enzymes that break it down into ADP and phosphate, which can then be further broken down to AMP and adenosine. In order to address this we injected a form of ATP that cannot be hydrolysed (N-H ATP) at a concentration

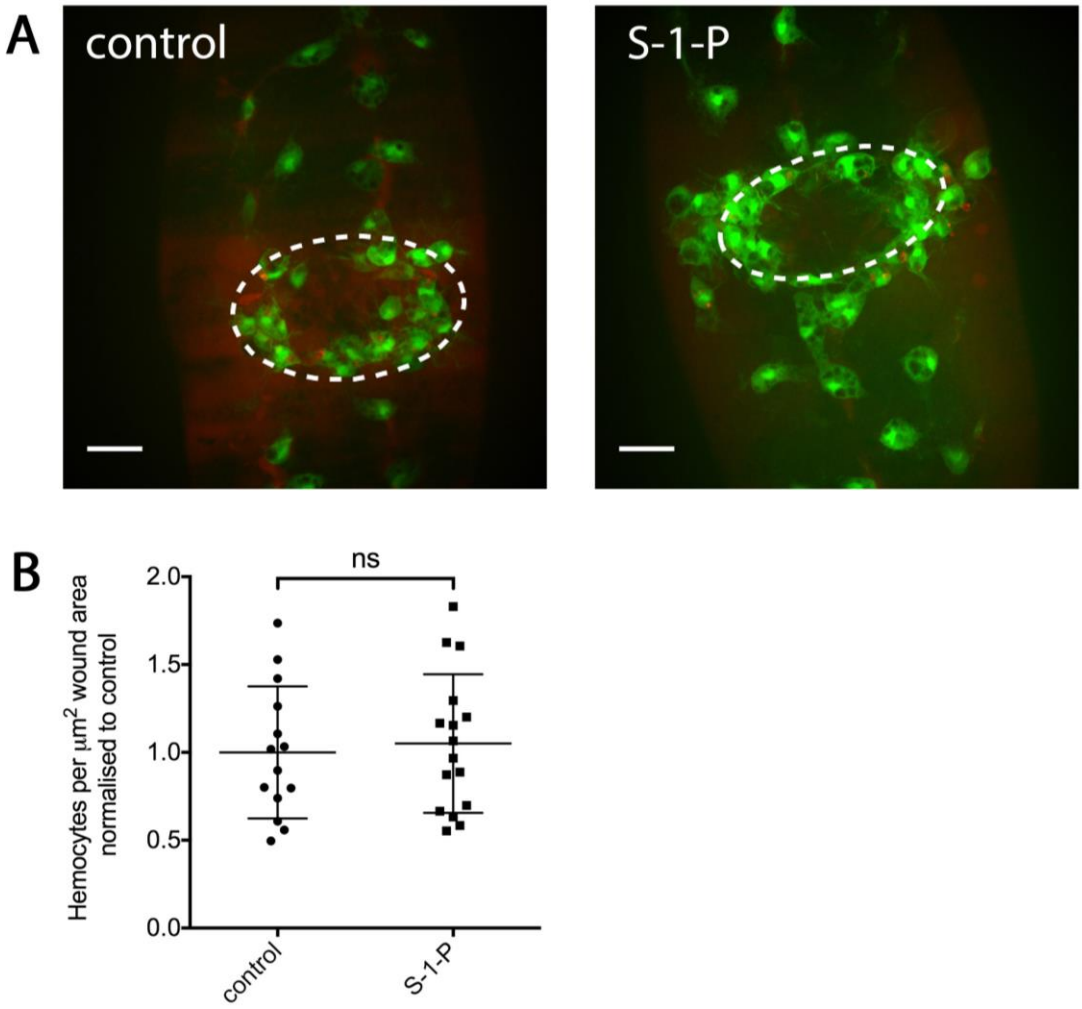

Figure 5.2: Injection of sphingosine-1-phosphate into embryos prior to wounding has no affect on hemocyte inflammatory responses

(A) Representative stills of GFP-labelled hemocyte responses to wounds at 60 minutes post-wound in control and sphingosine-1-phosphate (S-1-P) injected embryos (both *w;;crq-GAL4,UAS-GFP*). Dextran (red) can also be seen in these embryos, indicating successful injection In place of S-1-P, control embryos were injected with methanol diluted in PBS, as S-1-P was dissolved in methanol prior to dilution in PBS.

(B) Scatterplot of hemocyte wound responses per embryo shown as the number of hemocytes per μm^2 wound area at 60 minutes post-wounding normalised to the control average. Lines and error bars represent mean±SD; n=14 and 16 embryos for control and S-1-P injection respectively.

White dashed ovals represent wound perimeter; scale bars represent 20µm; statistical significance determined by Mann-Whitney test; ns= not significant.

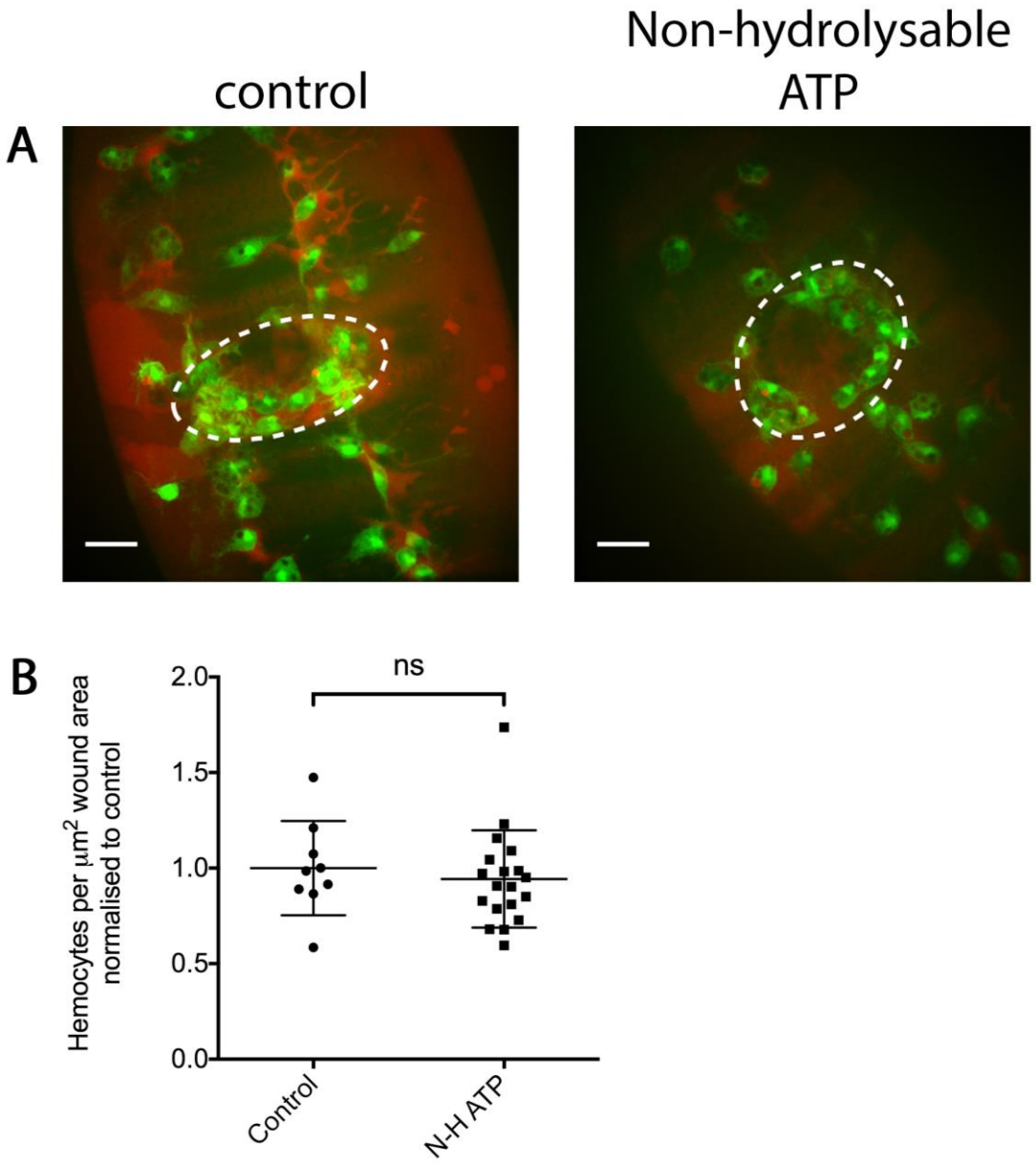

Figure 5.3: Injection of non-hydrolysable ATP into embryos prior to wounding has no affect on hemocyte inflammatory responses
(A) Representative stills of GFP-labelled hemocyte responses to wounds at 60 minutes post-wound in control and non-hydrolysable ATP injected embryos (both *w;;crq-GAL4,UAS-GFP*). Dextran (red) can also be seen in these embryos, indicating successful injection. In place of N-H ATP, control embryos were injected with MQH_2O in PBS, as N-H ATP was dissolved in MQH_2O prior to dilution in PBS. (B) Scatterplot of hemocyte wound responses per embryo shown as the number of hemocytes per μm^2 wound area at 60 minutes post-wounding normalized to the control average. Lines and error bars represent mean±SD; n=9 and 19 embryos for control and N-H ATP injection respectively.
White dashed ovals represent wound perimeter; scale bars represent 20μm; statistical significance determined by Mann-Whitney test; ns= not significant.

of 4μM (40 times the concentration shown to produce a maximal response in the original study identifying ATP as a find-me cue (Elliott et al. 2009)), and again examined the effect of this on hemocyte inflammatory responses (Fig. 5.3). When we did this we found again that there was no significant difference in hemocyte densities at wounds 60 minutes post-wounding when compared to controls (n=9 and 19 for control and N-H ATP injection respectively; p=0.410 via Mann-Whitney test; Fig. 5.3 A, B). This shows that the degradation of ATP does not explain why hemocyte inflammatory responses are not affected when ATP is injected prior to wounding. Furthermore, this suggests that ATP may not act as an apoptotic find-me cue in *Drosophila*, although more evidence is required to prove this.

Overall the injection of known vertebrate find-me cues prior to wounding does not prevent hemocytes from migrating to wounds. This suggests that vertebrate find-me cues do not act as such in *Drosophila*, therefore the find-me cues released by apoptotic cells in *Drosophila* may be distinct from those in vertebrates.

5.2.4 UV-irradiation induces apoptosis in *Drosophila* S2 cells

As none of the candidate find-me cues injected into embryos were able to perturb hemocytes from migrating to wounds, we sought to further investigate whether find-me cues were in fact capable of doing so, and developed a screen to attempt to identify novel cues. The find-me cues released by apoptotic cells in *Drosophila* have yet to be identified and our candidate approach suggests those identified in other systems are unlikely to be used in the fly embryo (Figures 5.1-5.3). However the fact that hemocytes are able to be distracted from their developmental migrations by the induction of apoptosis (Moreira et al. 2010) and the data presented elsewhere in this thesis suggests that they do exist in this system. One reason why the injection of known vertebrate find-me cues is unable to affect hemocyte inflammatory responses is that find-me cues in *Drosophila* are distinct from those in vertebrates. As an alternative approach to screen for novel cues, we hypothesised that apoptotic supernatants derived from cultures of apoptotic *Drosophila* S2 cells would contain find-me cues relevant to *Drosophila.* Therefore we established a protocol for Ultra Violet (UV)-induced S2 cell apoptosis in order to harvest apoptotic supernatants. The aim was then to inject this supernatant prior to wounding to investigate its effect on hemocyte inflammatory responses. Should the supernatants exhibit an anti-inflammatory effect the subsequent aims were to fractionate the supernatant to identify the critical molecules, which could then be investigated by RNAi of S2 cells prior to UV-induced cell death

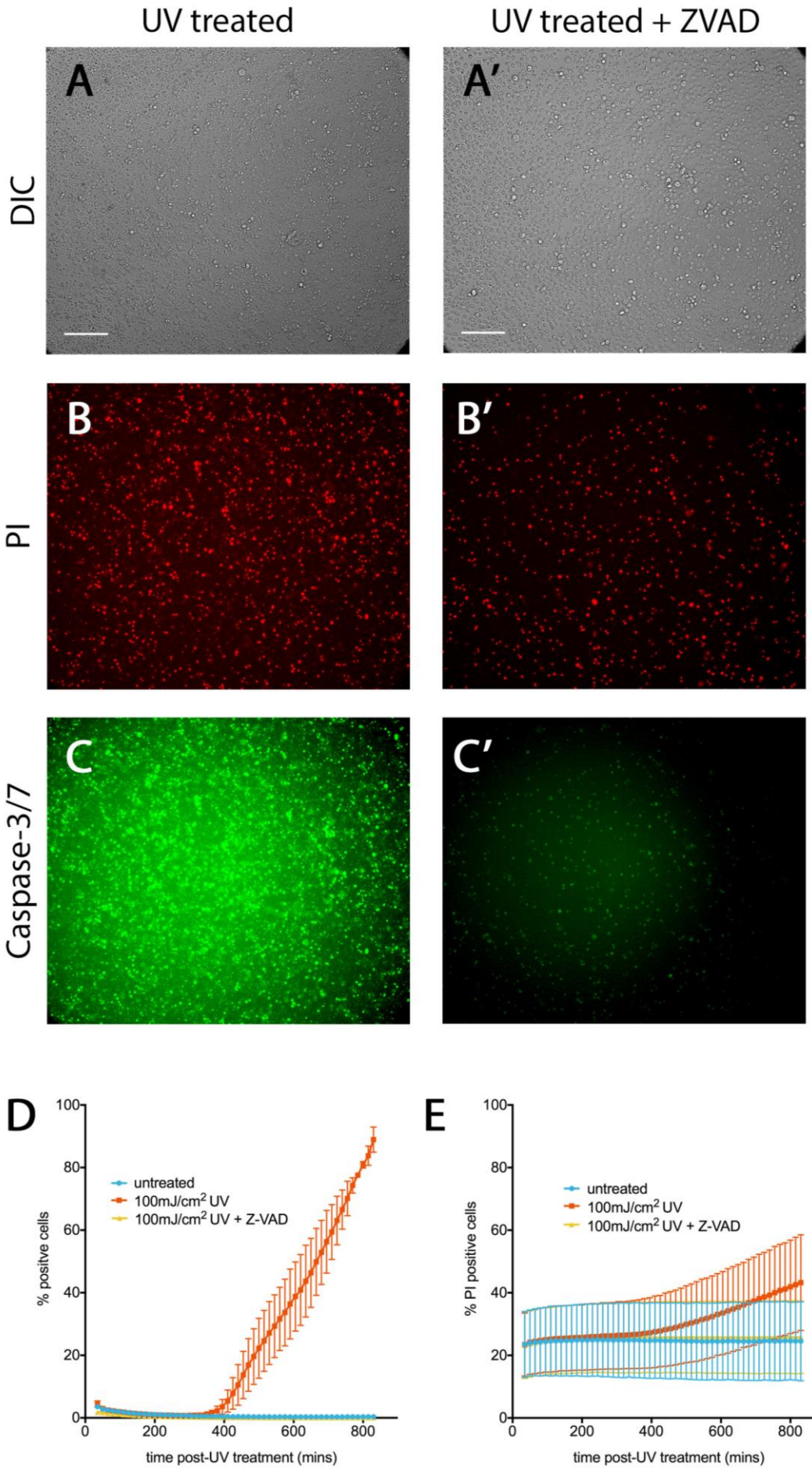
UV treated
UV treated + ZVAD
DIC
PI
Caspase-3/7
A
A′
B
B′
C
C′
D
E
untreated
100mJ/cm2 UV
100mJ/cm2 UV + Z-VAD
% positive cells
% PI positive cells
time post-UV treatment (mins)
0
20
40
60
80
100
200
400
600
800

Figure 5.4: UV-irradiation induces apoptosis and associated caspase activation in Drosophila S2 cells
(A and A') DIC images of S2 cells 800 minutes (13 ½ hours) post-UV irradiation, with or without the addition of the pan-caspase inhibitor ZVAD. Note the cellular blebbing in A compared to A', a hallmark of apoptosis which is prevented with the addition of ZVAD. (B and B') Propidium Iodide (PI) staining (red) of S2 cells 800 minutes (13 ½ hours) post-UV irradiation, with or without the addition of the pan-caspase inhibitor ZVAD. (C and C') CellEvent Caspase-3/7 indicator-positive cells (green) 800 minutes (13 ½ hours) post-UV irradiation, with or without the addition of the pan-caspase inhibitor ZVAD. Note the hugely increased number of green cells in C compared to C'. (D) Line graph of the percentage of CellEvent Caspase-3/7 indicator positive cells over time post-UV treatment (mins) in untreated cells (blue) and those that had been treated with 100mJ/cm^2 UV, with (yellow) or without the addition of ZVAD (orange). Data points and error bars represent mean±SD from two experimental repeats. (E) Line graph of the percentage of PI positive cells over time post-UV treatment (mins) in untreated cells (blue) and those that had been treated with 100mJ/cm^2 UV, with (yellow) or without the addition of ZVAD (orange). Data points and error bars represent mean±SD from two experimental repeats.

One widely used method of inducing apoptosis in cells is to treat them with UV radiation, a method which has also been shown to induce apoptosis in *Drosophila* S2 cells (Kiessling and Green 2006a). This allows for the induction of apoptosis without the need to treat the cells with apoptosis-inducing drugs, which if injected into embryos, may affect hemocyte behaviour. As 100mJ/cm^2 UVC was used to induce S2 cell apoptosis in the study by Kiessling and Green, we used this dose as a starting point to induce apoptosis (Kiessling and Green 2006b). When S2 cells were treated with either 0, 50, 100 or 200mJ/cm^2 UVC and left overnight, only those treated with 100 or 200mJ/cm^2 showed signs of cell blebbing – a hallmark of apoptosis (data not shown). This confirmed that, as published, 100mJ/cm^2 UVC was capable of inducing apoptosis in S2 cells (Kiessling and Green 2006b).

Since the release of apoptotic find-me cues seems to require the activation of Caspases (Lauber et al. 2003; Elliott et al. 2009; Gude et al. 2008), we wished to examine the timing of Caspase activation in S2 cells following UV-irradiation; this would also further confirm induction of apoptosis. To do this, S2 cells were treated with UV and the activation of caspases post-UV treatment was assessed using the CellEvent Caspase-3/7 Green Detection Reagent (Molecular Probes) – a substrate that becomes fluorescent green once cleaved by Caspase-3/7 and bound to DNA, indicating the activation of Caspases. Using this indicator we found that Caspases become active in S2 cells at around 6 ½ hours (400 minutes) post-UV irradiation and by around 13 hours approximately 80% of cells are Caspase positive (Fig. 5.4 C, D). Furthermore, the addition of the pan-Caspase inhibitor Z-VAD completely blocked the Caspase detection reagent from becoming fluorescent and also prevented cells from blebbing, suggesting that activated Caspases do indeed drive the observed increase in fluorescence (Fig. 5.4 A', C', D). To check that cells are not dying by necrosis using this method, propidium iodide (PI) staining post-UV

treatment was also assessed, as viable cells are impermeable to this agent and become permeable during necrosis, leading to the binding of PI to DNA. We found that the percentage of PI positive cells also began to increase at around the same time as Caspase activation (approximately 400 minutes post-UV treatment), however unlike the percentage of cells positive for Caspase activation, which rose by around 80% between 400 and 800 mins post-UV treatment (Fig. 5.4 D), the percentage of PI positive cells rose by only 15% in this time (Fig. 5.4 E). This suggests that treating cells with UV causes cells to die by apoptosis, but that this also triggers a low level of cellular necrosis, perhaps due to some apoptotic cells progressing to secondary necrosis.

Overall this assay shows that Caspase activation commences at around 6 ½ hours post UV-treatment and increases rapidly so that by 13 hours post-treatment around 80% of cells are Caspase-positive. Therefore, in order to inject embryos with supernatant from apoptotic cells with active Caspases, we will leave UV-treated cells for 13 hours before collecting the supernatant for injection.

5.2.5 Injection of apoptotic cell supernatant prior to wounding has no effect on hemocyte inflammatory responses

Once we had identified the time-course of Caspase activation post-UV irradiation of S2 cells, we wanted to inject the supernatant from such apoptotic cells to see whether a factor secreted by such cells was capable of distracting hemocytes from migrating to wounds. Our analysis showed that by 13 hours post-UV irradiation around 80% of S2 cells are Caspase positive (Fig. 5.4 D). Therefore, in order to leave the maximum amount of time possible for the secretion of potential find-me cues, we removed and injected the supernatant from apoptotic cells 13 hours post-UV irradiation.

When we injected embryos with apoptotic cell supernatant prior to wounding, and analysed hemocyte wound responses as previously, we again found that there was no significant reduction in inflammatory responses when compared to controls (n=7 and 10 embryos for control and apoptotic cell supernatant respectively; p=0.813 via Mann-Whitney test; Fig. 5.5 A, B). This suggests that the injection of apoptotic cell supernatants from this particular timepoint into embryos prior to wounding does not affect hemocyte inflammatory responses, perhaps because find-me cues are not capable of being prioritised over cues from sites of tissue damage by hemocytes. However there are a plethora of other potential explanations as to why this has no effect, as discussed below.

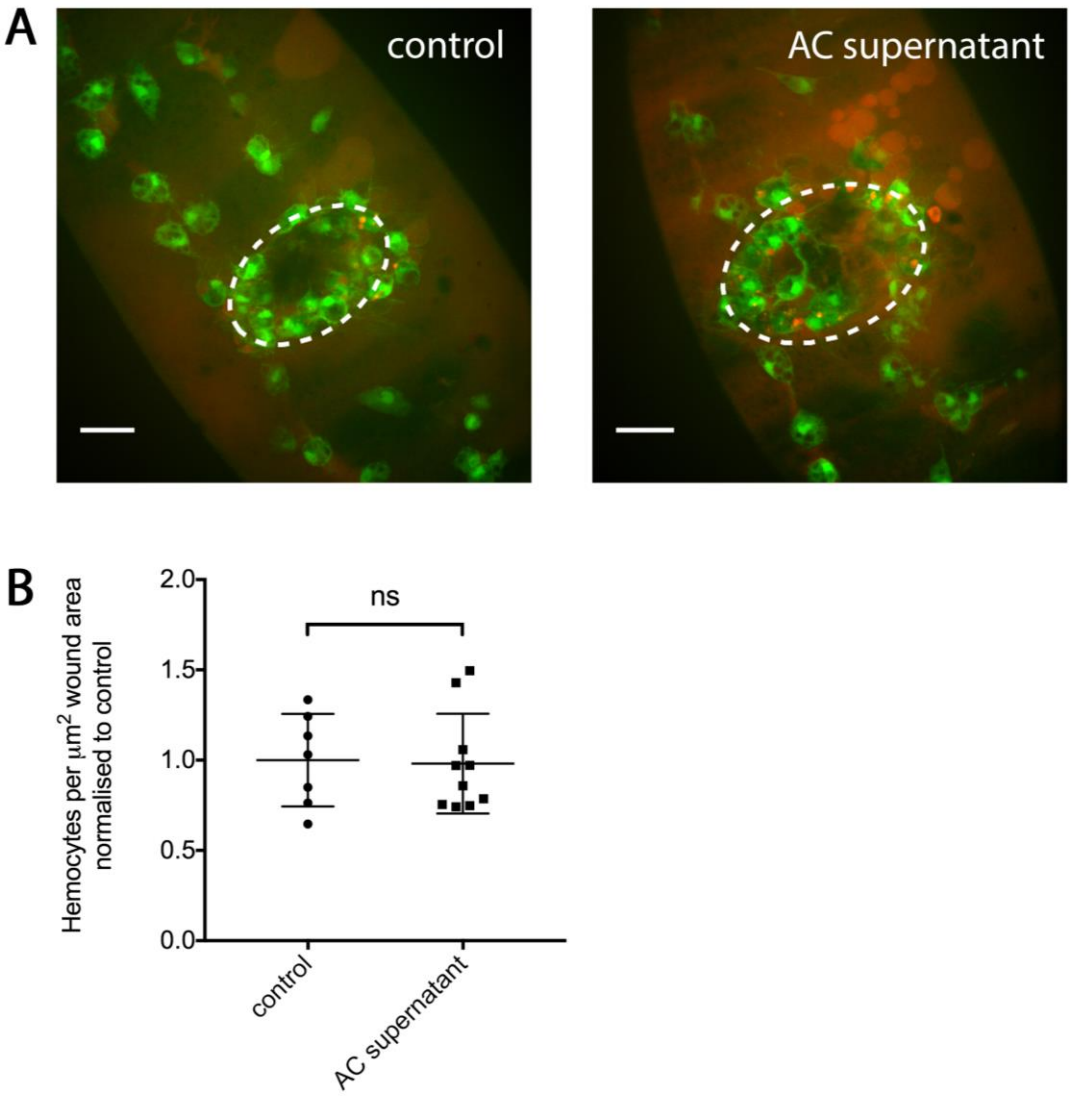

Figure 5.5: Injection of supernatant from apoptotic S2 cells into embryos prior to wounding has no affect on hemocyte inflammatory responses
(A) Representative stills of GFP-labelled hemocyte responses to wounds at 60 minutes post-wound in control and apoptotic cell supernatant (AC supernatant) injected embryos (both *w;;crq-GAL4,UAS-GFP*). Dextran (red) can also be seen in these embryos, indicating successful injection. Control embryos were injected with S2 cell media in place of supernatant from apoptotic cells. (B) Scatterplot of hemocyte wound responses per embryo shown as the number of hemocytes per μm^2 wound area at 60 minutes post-wounding normalized to the control average. Lines and error bars represent mean±SD; n=7 and 10 embryos for control and AC supernatant injection respectively.
White dashed ovals represent wound perimeter; scale bars represent 20µm; statistical significance determined by Mann-Whitney test; ns= not significant.

5.3 DISCUSSION

In an attempt to address the hypothesis that 'find-me' cues released by apoptotic cells are capable of distracting hemocytes from migrating to wounds, we injected known find-me cues from other organisms into *Drosophila* embryos prior to wounding to see whether this would reduce hemocyte inflammatory responses. We found that the injection of neither LPC, S-1-P, nor non-hydrolysable ATP, was able to suppress hemocyte inflammatory responses. The injection of supernatant taken from apoptotic S2 cells was also unable to distract hemocytes from migrating to wounds.

There are several reasons why injection of cues in this way did not result in decreased hemocyte inflammatory responses. Firstly, it may well be the case that hemocyte prioritisation of find-me cues released by apoptotic cells is not the reason why increased numbers of apoptotic cells reduces hemocyte inflammatory responses. As discussed in the previous chapter, there are many other possible mechanisms that might explain why a build-up of uncleared apoptotic cells may dampen hemocyte inflammatory responses. These range from the binding of apoptotic cells to hemocytes, the triggering downstream signaling cascades that suppress hemocyte inflammatory responses, to induction of stress signalling induced by the uncleared dying cells (see Chapter 4 discussion).

However, there are also a plethora of reasons why 'find-me' cue prioritisation by hemocytes may well still be the correct hypothesis as to why uncleared apoptotic cells suppress hemocyte inflammatory responses to wounds, but that the approach we used to test this may not work. Firstly, flooding embryos with potential 'find-me' cues may lead to receptor desensitization. This is a process whereby administration of high levels of agonist for a receptor leads to rapid attenuation of the signal triggered by the agonist and can lead to a down-regulation of the receptor, thus reducing the ability of cells to respond to a signal (Kelly et al. 2008). However, the fact that there are many uncleared apoptotic cells in *simu* mutants that are presumably secreting find-me cues that may be distracting hemocytes from migrating to wounds suggests that in *simu* mutants, desensitisation is not occurring. Therefore perhaps find-me cues are acting to produce a local gradient of chemotactic cues for hemocytes in *simu* mutants, and that flooding the embryos with cues does not produce this gradient, therefore does not distract hemocytes from migrating to wounds. Conversely, the concentration of cues injected may simply be too low to have an effect on hemocytes. Each cue was injected at a concentration 40x higher than that shown to produce a maximal response *in vivo*, as it is known that Latrunculin A, a chemical used to sequester monomeric actin, needs to be injected into *Drosophila* embryos at concentrations 40 times those used *in vitro* studies. However, this may not be the case for

these cues therefore a range of concentrations of each potential 'find-me' cue may need to be tested in order to identify a concentration that works. The cues may also be being degraded within the embryo before they have chance to have an anti-inflammatory affect on hemocytes, and cues may have to be continually produced to distract them from migrating to wounds. Alternatively, perhaps the exposure of hemocytes to apoptotic find-me cues needs to be more chronic to act in an anti-inflammatory way.

Therefore in order to validate the hypothesis that chemoattractive 'find-me' cues are prioritised over wound cues by macrophages, further tests would need to be carried out. One experiment that could be performed would be test this would be to use an *in vitro* system whereby macrophages are given the option to migrate towards two different cues. As hemocytes isolated from *Drosophila* do not migrate *in vitro*, vertebrate macrophages would need to be used. In this way the wound cue H_2O_2, which has shown to be required for the recruitment of inflammatory cells in both zebrafish and *Drosophila* ((Niethammer et al. 2009; Moreira et al. 2010), could be placed on one side of the macrophages and different potential find-me cues placed on the other to determine whether macrophages migrate preferentially towards find-me cues.

5.4 CONCLUSIONS

In this chapter we have shown that the injection of the known vertebrate find-me cues LPC and S-1-P, or a non-hydrolysable version of the find me cue ATP, is unable to prevent hemocytes from migrating to wounds. We have also developed an assay that may allow for the identification of novel find-me cues released by apoptotic cells in *Drosophila*. Overall, we have shown that injecting embryos with potential find-me cues does not induce an anti-inflammatory effect, which suggests that the distraction of hemocytes by find-me cues *in vivo*, as may be the case in *simu* mutants, is more complex than simply flooding the embryo with cues.

Chapter 6: Examining the role of apoptotic cell receptors in macrophage migratory behaviour

6.1 INTRODUCTION

In order for macrophages to phagocytose apoptotic cells, they must first be able to bind to dying cells through receptor-ligand interactions with so called 'eat-me' signals exposed on the surface of apoptotic cells (Barth et al. 2017). Aside from the apoptotic cell receptor Simu (Kurant et al. 2008), which has been discussed earlier, *Drosophila* have several other apoptotic cell receptors that have been identified.

One such known *Drosophila* apoptotic cell receptor is Draper (Drpr), a nimrod family protein and CED-1 homologue (Freeman et al. 2003; Manaka et al. 2004). This receptor was first identified to be involved in apoptotic cell clearance by glial cells in the CNS (Freeman et al. 2003), but has since been shown to also function as an apoptotic cell receptor in macrophages and follicular epithelial cells in *Drosophila* (Manaka et al. 2004; Etchegaray et al. 2012). However, more recently it has been suggested that Drpr is required not for the engulfment of apoptotic cells but for the maturation of phagosomes post-engulfment, as macrophages and glia in *drpr* mutants become full of apoptotic cells (Evans et al. 2015; Kurant et al. 2008). In glial cells, Drpr is required both for the engulfment of injured axons and the recruitment of glial projections towards injured axons in order for engulfment to occur (MacDonald et al. 2006), and it is also required for axonal pruning during pupal metamorphosis (Awasaki et al. 2006). Interestingly, several apoptotic cell-derived ligands for Drpr have been identified including the cell-surface 'eat-me' signals PS and Pret-a-porter (Kuraishi et al. 2009; Tung et al. 2013) and the secreted protein *Drosophila melanogaster* calcium-binding protein 1(DmCaBP1), which is thought to act as a bridging molecule between apoptotic cells and phagocytes (Okada et al. 2012). Aside from its role in apoptotic cell clearance, Drpr is also required for macrophage migration to sites of tissue damage (Evans et al. 2015), potentially acting as a receptor for damage at wounds. Macrophages in *Drosophila* embryos also need *drpr* to migrate at normal speeds (Evans et al. 2015). Therefore Draper has a diverse range of functions in *Drosophila* aside from its role in apoptotic cell clearance as originally identified, highlighting the potential of other receptors to possess multiple functions.

The first apoptotic cell receptor to be discovered in *Drosophila* was Croquemort (Crq), a homolog of the human scavenger receptor CD36 that is expressed specifically in hemocytes (Franc et al. 1996; Franc et al. 1999; Valerie A Fadok et al. 1998). The role of Crq as an apoptotic cell receptor was first shown by forcing expression of Crq in non-phagocytic COS-7 cells, which conferred them with the ability to bind to apoptotic cells specifically (Franc et al. 1996). It was then shown that Crq is required in *Drosophila* embryos for the efficient engulfment of apoptotic cells by macrophages as those in *crq* deficient embryos contain significantly fewer engulfed apoptotic cells (Franc et al. 1999). Interestingly, the expression of *crq* in macrophages seems to be regulated by the amount of apoptosis in *Drosophila*, as macrophages in embryos lacking apoptosis have reduced expression levels, whereas those in embryos with increased apoptosis have higher levels (Franc et al. 1999). Despite being shown to be a receptor for apoptotic cells, the ligand on the surface of apoptotic cells to which Crq binds has yet to be identified. Crq has also been shown to be required for the engulfment of bacteria, suggesting that it may act as a more general phagocytic receptor, as per Draper and Simu (see chapter 4), rather than being specific to apoptotic cells (Franc et al. 1999; Guillou et al. 2016). Interestingly, more recent work has provided evidence that, instead of being required for the engulfment of apoptotic cells, Crq is required for phagosome maturation post-engulfment in some cells at least (Han et al. 2014; Guillou et al. 2016).

Finally, beta-nu integrin (βυ) has also been identified as a phagocytic receptor for apoptotic cells in *Drosophila* embryonic macrophages (Nagaosa *et al*., 2011). The α subunit that forms a heterodimer with this β subunit to create a functional protein has since been suggested to be αPS3 (also known as Scab), as shown by their physical interaction as well as the reduced level of apoptotic cell phagocytosis upon reduced αPS3 expression (Nonaka *et al*., 2013). Similarly to Draper and Crq (Hashimoto et al. 2009; Franc et al. 1999; Guillou et al. 2016) integrin αPS3/βv has also been shown to involved in bacterial detection and engulfment as well as that of apoptotic cells (Nonaka *et al*., 2013). Like Crq, the ligand on apoptotic cells to which αPS3/βv integrin binds has yet to be identified, although it is thought that αPS3 binds to the ECM laminin proteins. Aside from their role in phagocytosis, both of these integrin subunits have been shown to have other functions, particularly in cell-cell adhesion. For example, Scab has been shown to have roles in wound healing (Campos et al. 2010) and dorsal closure (Homsy et al. 2006; Stark et al. 1997), as well as other aspects of embryonic morphogenesis (Stark et al. 1997), whilst Bv integrin is required for midgut migration during embryonic development (Devenport and Brown 2004).

In the previous chapter we showed that embryos mutant for the apoptotic cell receptor Simu exhibit reduced hemocyte inflammatory responses as well as decreased hemocyte migration speeds. This reduction in hemocyte speeds in this mutant is apoptotic cell dependent, and the

decreased ability of hemocytes to migrate to wounds is also partly associated to this. Besides the effect of apoptotic cells on hemocyte inflammatory migration to wounds in *simu* mutants, Simu itself seems to also be required for normal hemocyte inflammatory responses independent of apoptotic cells. This is not the first time that an apoptotic cell receptor has been shown to have a role in hemocyte inflammatory responses, as Draper has also been shown to be required for normal inflammatory migrations to wounds through its role in the detection of H_2O_2 from wounds (Evans et al. 2015). Interestingly, hemocytes in *drpr* mutants also have reduced hemocyte migration speeds (Evans et al. 2015). Therefore defects in apoptotic cell clearance associated with mutations in apoptotic cell receptors have been shown to alter hemocyte function and behaviour. In light of this, we decided to examine whether mutants for the other known apoptotic cell receptors Crq, Scab and βυ integrin also display these hemocyte migratory phenotypes, and whether any defects found may be explained by alterations in apoptotic cell clearance.

6.2 RESULTS

6.2.1 Hemocyte inflammatory responses to wounds are reduced in apoptotic cell receptor mutants

As we have previously shown that the apoptotic cell receptor Simu is required for normal hemocyte inflammatory responses (Chapter 4), and that the same is also true for the apoptotic cell receptor Draper (Evans et al. 2015), we sought to examine whether there was any role for the other known receptors, Scab, βυ integrin or Crq, in hemocyte inflammatory responses. To do this we wounded the ventral epithelium and examined the density of hemocytes present at the wound site 60 minutes post-wounding in these mutants (Fig. 6.1).

Firstly we examined hemocyte inflammatory responses in scb^2 mutant embryos, a hypomorphic allele of the *scb* gene that alters the amino acid sequence of its coding region (Nonaka et al. 2013) (Fig. 6.1 A). When we quantified the density of hemocytes at wounds 60 minutes post-wounding in control (*w;;crq-GAL4,UAS- GFP*) and scb^2 mutants (*w;*scb^2*;crq-GAL4,UAS-GFP*), we found that this was significantly decreased in scb^2 mutant embryos by approximately 50% (n= 18 and 16 embryos for control and scb^2 respectively; $p<0.0001$ via Mann-Whitney test; Fig. 6.1 B). This result suggests that *scb* is required for normal hemocyte inflammatory responses to wounds.

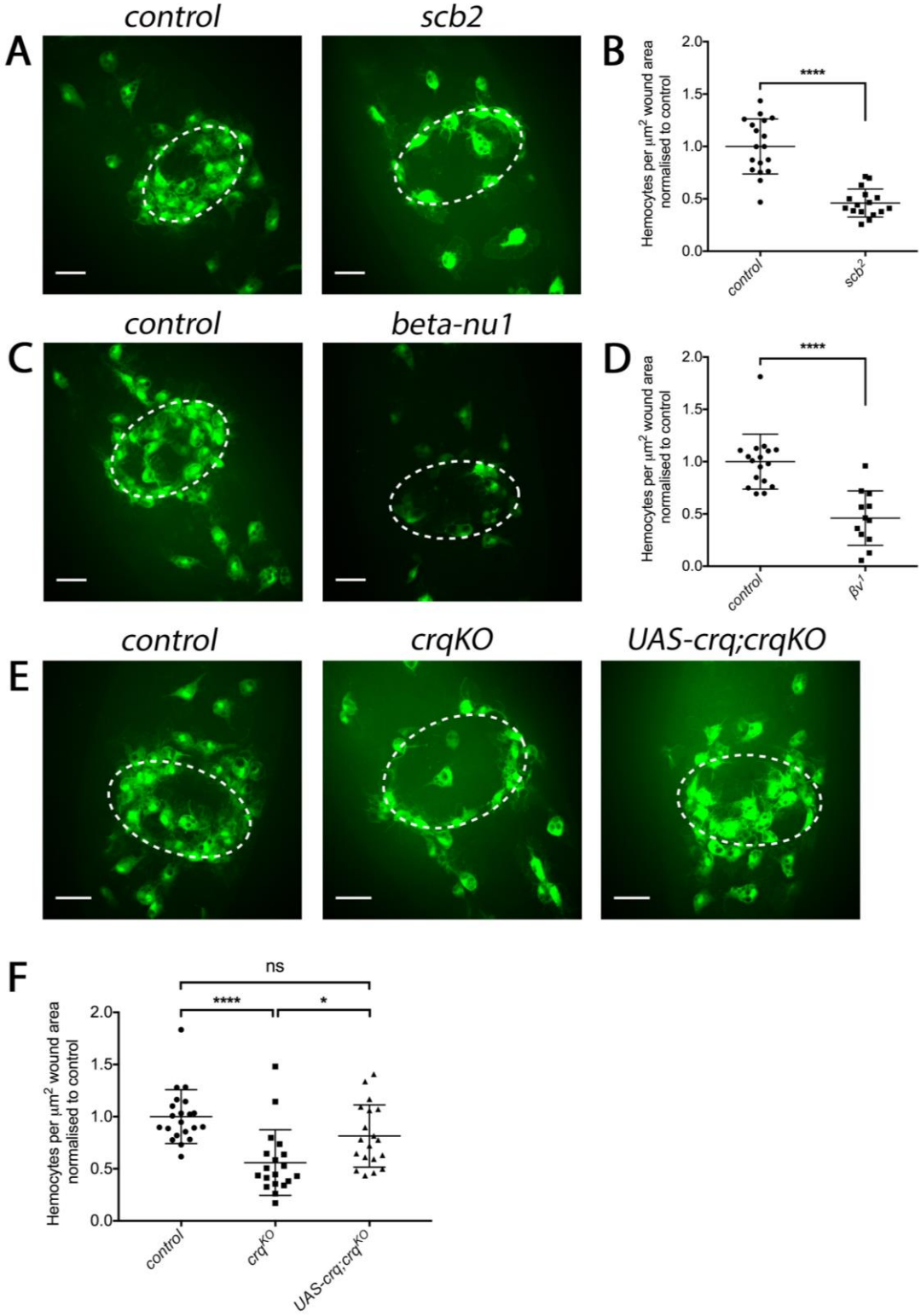
A
control
scb2
B
Hemocytes per µm² wound area normalised to control
****
control
scb2
C
control
beta-nu1
D
Hemocytes per µm² wound area normalised to control
****
control
βν1
E
control
crqKO
UAS-crq;crqKO
F
Hemocytes per µm² wound area normalised to control
ns
****
*
control
crqKO
UAS-crq;crqKO

Figure 6.1: Hemocyte inflammatory migrations to wounds are perturbed in *scb*^{2}, *βv*^{1} and *crq*^{KO} apoptotic cell receptor mutants
(A) Representative stills of GFP-labelled hemocyte responses to wounds at 60 minutes post-wound in control and *scb*^{2} mutant stage 15 embryos. (B) Scatterplot of hemocyte wound responses per embryo shown as the number of hemocytes per μm^{2} wound area at 60 minutes post-wounding normalized to the control average. Lines and error bars represent mean±SD; n=18 embryos for controls and n=16 for *scb*^{2} mutants. (C) Representative stills of GFP-labelled hemocyte responses to wounds at 60 minutes post-wound in control and *βv*^{1} mutant stage 15 embryos. (D) Scatterplot of hemocyte wound responses per embryo shown as the number of hemocytes per μm^{2} wound area at 60 minutes post-wounding normalised to the control average. Lines and error bars represent mean±SD; n=17 embryos for controls and n=12 for *βv*^{1} mutants. (E) Representative stills of GFP-labelled hemocyte responses to wounds at 60 minutes post-wound in control and *crq*^{KO} mutant stage 15 embryos, and in *crq*^{KO} mutants in which *crq* expression has been restored specifically in hemocytes (*w;UAS-crq;crq*^{KO}). (F) Scatterplot of hemocyte wound responses per embryo shown as the number of hemocytes per μm^{2} wound area at 60 minutes post-wounding normalized to the control average. Lines and error bars represent mean±SD; n=21, 19 and 19 embryos for control, *crq*^{KO} and *UAS-crq;crq*^{KO} respectively. White dashed ovals represent wound perimeter; scale bars represent 20μm; asterisks indicate statistical significance as determined by Mann-Whitney test (B and D) or Kruskal-Wallis one-way ANOVA with Dunn's multiple comparisons test (F); ****$p < 0.0001$, *$p<0.05$, ns= not significant.

Next we moved on to examine hemocyte inflammatory responses in *βv*^{1} mutant embryos, a null mutant allele of *βv* (Devenport and Brown 2004) (Fig. 6.1 C). When we compared the density of hemocytes at wounds 60 minutes post-wounding in *βv*^{1} mutant embryos (*w;βv*^{1}*;crq-GAL4,UAS-GFP*) compared to controls (*w;;crq-GAL4,UAS- GFP*) we found that this was significantly reduced, again by approximately 50% (n=17 and 12 embryos for control and *βv*^{1} respectively; $p<0.0001$ via Mann-Whitney test; Fig. 6.1 D). This suggests that, as well as Scab, *βv* integrin is also required for normal hemocyte inflammatory responses to wounds in *Drosophila* embryos. Finally, when we assessed inflammatory responses in *crq*^{KO} mutants (a *crq* knock-out which abolishes *crq* expression completely (Guillou et al. 2016)), we found that there was a significantly reduced density of hemocytes at wounds in *crq*^{KO} mutants (*w;crq*^{KO}*;crq-GAL4,UAS-GFP*) compared to controls (*w;;crq-GAL4,UAS- GFP*) (n= 21 and 19 embryos for control and *crq*^{KO} respectively; $p<0.0001$ via one-way ANOVA test (Fig. 6.1 E, F). This suggests that the apoptotic cell receptor Crq is also required for normal hemocyte inflammatory responses in the embryo. To further test whether Crq was required cell autonomously in hemocytes during their wound responses and confirm that the wound response defect was a result of loss of *crq* function, we also wounded *crq*^{KO} mutant embryos in which *crq* expression was restored specifically in hemocytes (*UAS-crq;crq*^{KO}*;crq-GAL4,UAS-GFP*) (Fig. 6.1 E). When we analysed wound responses in such embryos we found that the density of hemocytes at wounds after 60 minutes was significantly increased when compared to *crq*^{KO} mutants (n=19 *UAS-crq;crq*^{KO} embryos; p=0.0260 via Kruskall-Wallis one-way ANOVA), and that this response was also not significantly different compared to controls (p=0.138 via Kruskal-Wallis

one-way ANOVA test) (Fig. 6.1 F). Together this data shows that Crq is required specifically in hemocytes for their normal inflammatory responses to wounds.

Together this data suggests that, in addition to Simu (Chapter 4, Fig. 4.2) and Draper (Evans et al. 2015), all three of the remaining known apoptotic cell receptors (Scab, βυ integrin and Crq) are required in hemocyte inflammatory responses to wounds. This is a very intriguing result, as this suggests that all known apoptotic cell receptors play a role during hemocyte inflammatory responses, and also suggests that targeting apoptotic cell receptors may represent a novel therapeutic approach to treat inflammation.

6.2.2 Crq and Scab are required cell-autonomously by hemocytes for their normal inflammatory responses to wounds

Embryos mutant for the apoptotic cell receptors *crq*, βυ or *scb* exhibit decreased hemocyte inflammatory responses (Figure 6.1), therefore to test whether these genes are required cell-autonomously by hemocytes embryos in which either *crq* or *scb* expression was reduced specifically in hemocytes by RNAi knockdown (*w;UAS-crq RNAi;crq-GAL4,UAS-GFP* and *w;UAS-scab RNAi;crq-GAL4,UAS-GFP* respectively) were wounded and compared to controls (*w;;crq-GAL4,UAS-GFP*)[1]. When hemocyte wound responses were analysed by quantifying the density of hemocytes at the wound 60 minutes post-wounding, we found that this was significantly decreased in *crq RNAi* embryos compared to controls (n=18 and 10 embryos for control and *crq RNAi* respectively; p=0.0238 via Mann-Whitney test; Fig. 6.2 A, B). Supported by the earlier rescue of inflammatory responses in crq^{KO} mutants in which *crq* expression had been rescued specifically in hemocytes (Fig. 6.1 E, F), this result suggests that *crq* is required cell-autonomously by hemocytes during their inflammatory responses to wounds. It also suggests that the defect seen in crq^{KO} mutants is due specifically to the crq^{KO} mutation and not one in the genetic background of these mutants.

Similarly, when hemocyte inflammatory responses to wounds were analysed in the same way for control and *scb RNAi* embryos, we found that hemocyte densities at wounds were significantly decreased in *scb RNAi* compared to controls (n=16 and 14 embryos for control and *scb RNAi* respectively; p=0.0172 via Mann-Whitney test; Fig. 6.2 C, D). This suggests that *scb* is also required cell-autonomously by hemocytes for their efficient inflammatory responses to wounds. This result phenocopies the inflammatory defect seen in scb^{2} mutants, which provides

[1] Time constraints prevented hemocyte-specific knockdown of $βυ^{1}$ in time for submission, but this will be carried out in the future.

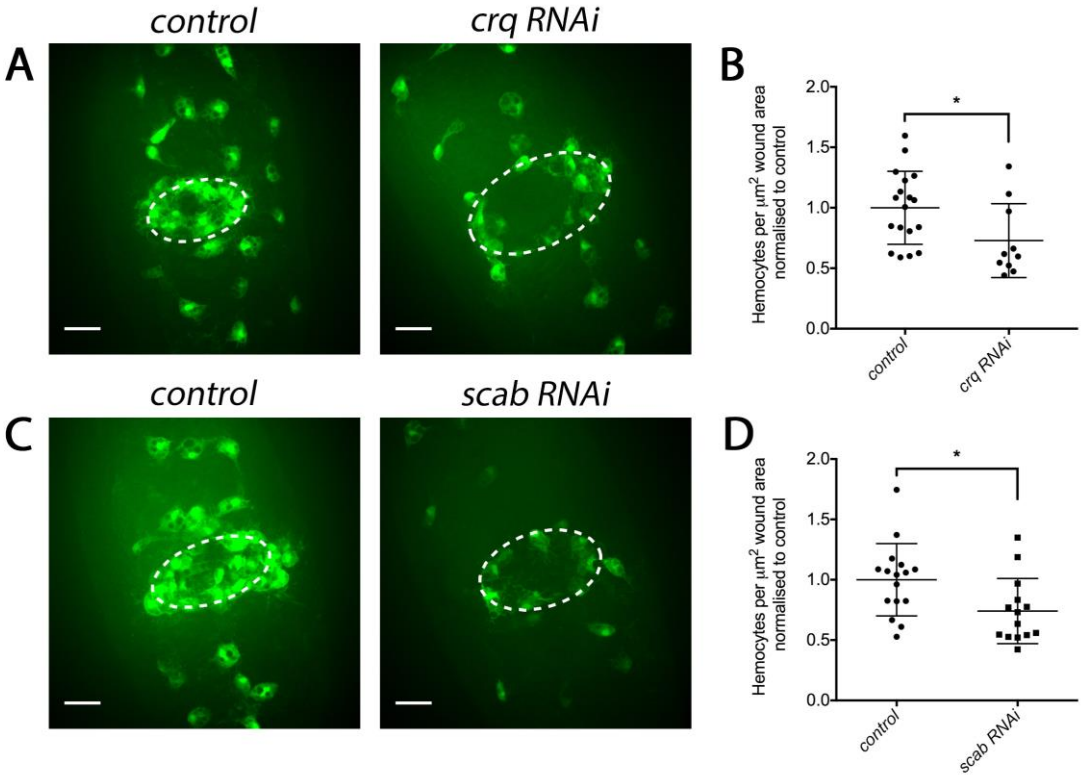

Figure 6.2: Hemocyte-specific RNAi knockdown of either *crq* or *scb* results in a wound response defect

(A) Representative stills of GFP-labelled hemocyte responses to wounds at 60 minutes post-wound in control stage 15 embryos and those in which *crq* expression has been reduced specifically in hemocytes using RNAi-mediated knockdown. (B) Scatterplot of hemocyte wound responses per embryo shown as the number of hemocytes per μm^2 wound area at 60 minutes post-wounding normalized to the control average. Lines and error bars represent mean±SD; n=18 embryos for controls and n=10 for *crq RNAi*. (C) Representative stills of GFP-labelled hemocyte responses to wounds at 60 minutes post-wound in control stage 15 embryos and those in which *scb* expression has been reduced specifically in hemocytes using RNAi knockdown. (D) Scatterplot of hemocyte wound responses per embryo shown as the number of hemocytes per μm^2 wound area at 60 minutes post-wounding normalized to the control average. Lines and error bars represent mean±SD; n=16 embryos for controls and n=14 for *scb RNAi*. White dashed ovals represent wound perimeter; scale bars represent 20μm; asterisks indicate statistical significance as determined by Mann-Whitney test; *$p < 0.05$.

evidence that it is not a background mutation in the genome of *scb*^{2} mutants that is causing the defect, but that it is specific to the *scb*^{2} mutation.

This data suggests that both *crq* and *scb* are required cell-autonomously by hemocytes for their inflammatory migrations to wounds. However, when comparing the inflammatory response defects in RNAi knockdowns compared to their respective zygotic mutants, we can see that these are less severe. Both *scb* and *crq* zygotic mutants have an approximately 50% reduction in their wound responses compared with around a 25% reduction upon RNAi knockdown. This discrepancy may be due to the incomplete knockdown of genes by RNAi, resulting in a weaker phenoctype.

6.2.3 Loss of apoptotic cell receptors perturbs hemocyte developmental dispersal

As we observed a reduction in the number of hemocytes present at wounds in *crq*^{KO}, *scb*^{2} and *βυ*^{1} mutants when compared to controls, we wanted to check that this was not due simply to a decrease in the number of hemocytes available to respond in the vicinity of the wound in stage 15 embryos. To assess this we counted the number of hemocytes present in the pre-wound images and calculated their density in this area of the embryo.
In *scb*^{2} mutants (*w;scb*^{2}*;crq-GAL4,UAS-GFP*) we found that hemocyte densities in this area were reduced by approximately 30% when compared to controls (*w;;crq-GAL4,UAS-GFP*) (n=21 and 19 embryos for control and *scb*^{2} respectively; $p<0.0001$ via Mann-Whitney test; Fig. 6.3 A, B). In order to test whether *scb* is required specifically in hemocytes for this, we also examined the density of hemocytes in this location in embryos in which *scb* expression was reduced specifically in hemocytes using RNAi knockdown (*w;UAS-scab RNAi;crq-GAL4,UAS-GFP*) (Fig. 6.3 C). When compared to controls (*w;;crq-GAL4,UAS-GFP*), the density of hemocytes in pre-wound images was again reduced by approximately 30% in *scab RNAi* embryos (n=14 and 41 embryos for control and *scab RNAi* respectively; $p<0.0001$ via Mann-Whitney test; Fig. 6.3 D). Together this shows that *scb* is required cell-autonomously by hemocytes for normal numbers of hemocytes to be present on the VNC in stage 15 embryos, and that *scb* may therefore be required for the normal developmental dispersal of hemocytes.
Next, we performed the same analysis on *βυ*^{1} mutants (*w; βυ*^{1}*;crq-GAL4,UAS-GFP*) and found a decrease in hemocyte densities of approximately 40% when compared to controls (*w;;crq-GAL4,UAS-GFP*) (n=18 and 17 embryos for control and *βυ*^{1} respectively; $p<0.0001$ via Mann-Whitney test; Fig. 6.3 E, F). This suggests that *βυ* integrin is also required for normal numbers of hemocytes to reach the VNC by embryonic stage 15.

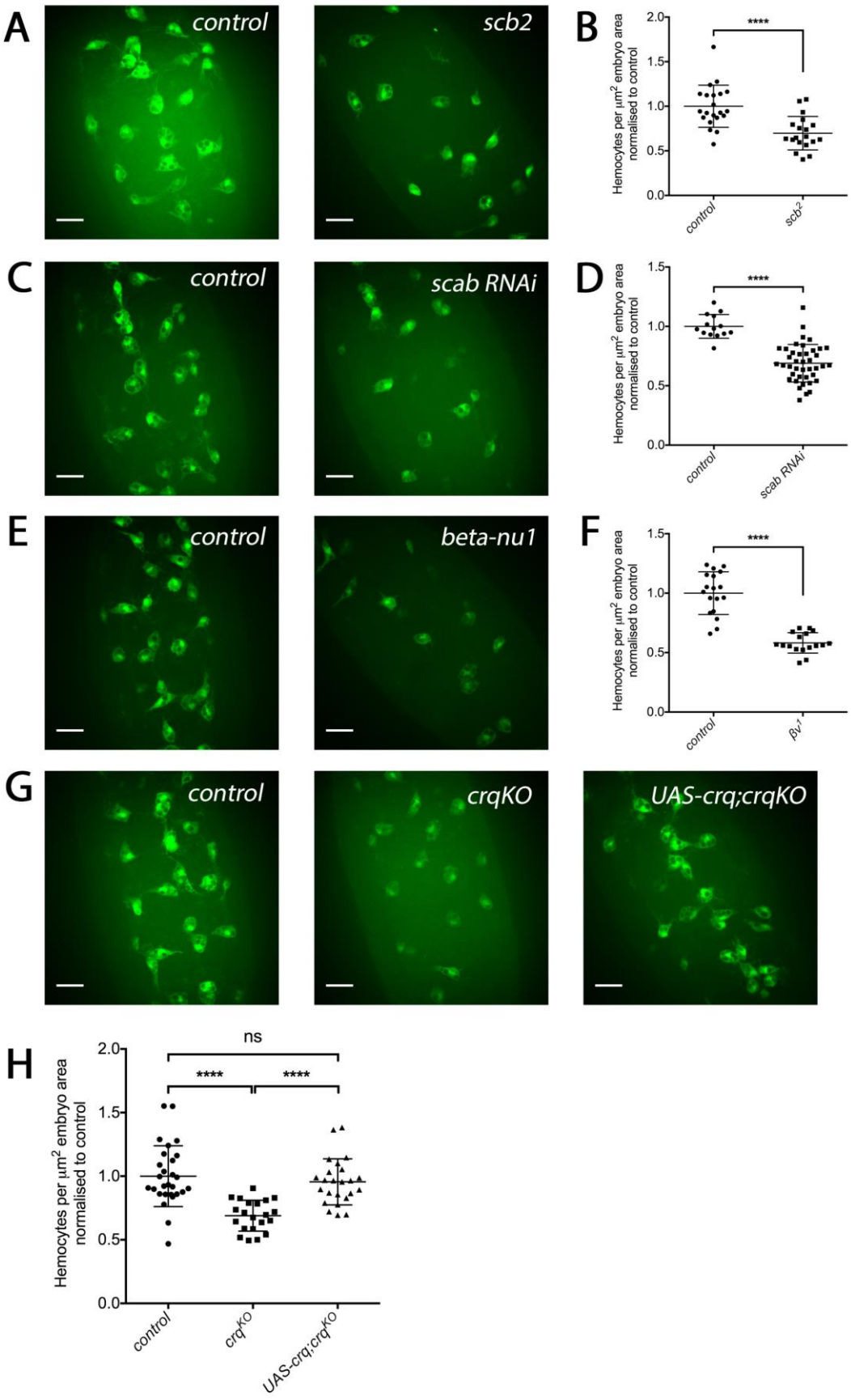
A
control
scb2
B
Hemocytes per µm² embryo area normalised to control
****
control
scb2
C
control
scab RNAi
D
Hemocytes per µm² embryo area normalised to control
****
control
scab RNAi
E
control
beta-nu1
F
Hemocytes per µm² embryo area normalised to control
****
control
βv1
G
control
crqKO
UAS-crq;crqKO
H
Hemocytes per µm² embryo area normalised to control
ns
****
****
control
crqKO
UAS-crq;crqKO

Figure 6.3: The apoptotic cell receptors *Scb*, *βv* and *Crq* are required for the presence of normal numbers of hemocytes on the superficial VNC
(A) Representative pre-wound stills of GFP-labelled hemocytes on the superficial VNC in control and scb^2 mutant stage 15 embryos, demonstrating a decrease in hemocyte density in this location in scb^2 mutants. (B) Scatterplot of hemocyte densities in stage 15 pre-wound images shown as the number of hemocytes per μm^2 embryo area normalized to the control average. Lines and error bars represent mean±SD; n=21 embryos for controls and n=19 for scb^2 mutants. (C) Representative pre-wound stills of GFP-labelled hemocytes on the superficial VNC in control stage 15 embryos, and those in which *scb* expression has been reduced specifically in hemocytes using RNAi knockdown (*scab RNAi*), demonstrating a decrease in hemocyte density in this location in *scab RNAi* embryos. (D) Scatterplot of hemocyte densities in stage 15 pre-wound images shown as the number of hemocytes per μm^2 embryo area normalized to the control average. Lines and error bars represent mean±SD; n=14 embryos for controls and n=41 for *scab RNAi*. (E) Representative pre-wound stills of GFP-labelled hemocytes on the superficial VNC in control and βv^1 mutant stage 15 embryos, demonstrating a decrease in hemocyte density in this location in βv^1 mutants. (F) Scatterplot of hemocyte densities in stage 15 pre-wound images shown as the number of hemocytes per μm^2 embryo area normalized to the control average. Lines and error bars represent mean±SD; n=18 embryos for controls and n=17 for βv^1 mutants. (G) Representative pre-wound stills of GFP-labelled hemocytes on the superficial VNC in control and crq^{KO} mutant stage 15 embryos, and in crq^{KO} mutants in which *crq* expression has been restored specifically in hemocytes (*UAS-crq;*crq^{KO}). This demonstrates that hemocyte density in this area is decreased in crq^{KO} mutants, but that this can be rescued by re-expressing *crq* specifically in hemocytes. (H) Scatterplot of hemocyte densities in stage 15 pre-wound images shown as the number of hemocytes per μm^2 embryo area normalized to the control average. Lines and error bars represent mean±SD; n=28, 21 and 24 embryos for control, crq^{KO} and *UAS-crq;*crq^{KO} respectively.

Finally, compared to pre-wound hemocyte densities in control embryos (*w;;crq-GAL4,UAS-GFP*), we also found that those in crq^{KO} mutants (*w;*crq^{KO}*;crq-GAL4,UAS-GFP*) were significantly decreased by approximately 30% (n=28 and 21 embryos for control and crq^{KO} mutants respectively; $p<0.0001$ via one-way ANOVA test; Fig. 6.3 G, H). To further test whether *crq* is required cell autonomously in hemocytes for normal numbers to be present on the VNC in stage 15 embryos, we also analysed pre-wound hemocyte density in crq^{KO} mutant embryos in which *crq* expression was rescued specifically in hemocytes (*UAS-crq;*crq^{KO}*;crq-GAL4,UAS-GFP*) (Fig. 6.3 G). When we compared hemocyte densities in these embryos with those in crq^{KO} mutants we found that this was significantly increased (n=24 *UAS-crq;*crq^{KO} embryos; $p<0.0001$ via one-way ANOVA test), and that this response was also not significant when compared to controls ($p=0.794$ via one-way ANOVA test) (Fig. 6.3 G, H). Together these results show that the number of hemocytes on the VNC in stage 15 embryos is reduced in *crq* mutants, but that this can be rescued by re-expressing *crq* specifically in hemocytes. This suggests a cell-autonomous role for Crq in hemocytes to ensure normal numbers reach the VNC.

Altogether this shows that hemocyte numbers are decreased in the wounding area in all three apoptotic cell receptor mutants tested when compared to controls. How these receptors are

involved in this process is yet to be elucidated, but it is possible that such receptors are required for the normal developmental dispersal of hemocytes during embryogenesis. In fact, it has already been shown that Scab is required for the normal developmental dispersal of hemocytes along the VNC, as in *scb* mutants hemocytes fail to migrate all the way along the midline of the VNC by stage 13 as would normally be expected (Comber et al. 2013). This delay in hemocyte migration in stage 13 *scb* mutants may explain why fewer hemocytes are present on the VNC at stage 15 embryos. The integrin βPS subunit (also called Myospheroid (Mys)) has also been shown to be required for the normal developmental dispersal of hemocytes in the embryos, with *mys* mutants showing a delay in the progression of hemocytes along the VNC midline in both stage 13 and 15 embryos (Comber et al. 2013). Therefore the beta integrin subunit βυ may also be required in this process, although this has yet to be tested. However, it is clear that hemocytes migrate sufficiently effectively as to be present along the entire midline of the VNC in stage 15 $\beta\upsilon^{1}$ mutant embryos (Fig. 6.3 E), therefore any defects in the progression of hemocyte along the ventral midline in $\beta\upsilon^{1}$ mutants are unlikely to be as severe as *mys* mutants. The reduced numbers of hemocytes present at the VNC is *crq* mutants may also be due to their reduced migration speeds (Fig. 6.5), which may lead to the delay of hemocyte developmental migrations, although this has not been tested.

In both *scb* and *βυ* mutants the wound response defect seems to be more pronounced than the reduction in hemocyte numbers at the VNC, for *crq* mutants however this difference seems less pronounced (Fig. 6.1 compared to Fig. 6.3). It is therefore possible that the wound response defect observed in these mutants is due solely to a decrease in the number of hemocytes in the wound vicinity rather than a decreased ability of hemocytes to migrate to wounds.

6.2.4 The percentage of hemocytes responding to wounds is decreased in *scb* and *βυ* mutants

In order to rule out that the inflammatory defects observed in *crq*, *scb* and *βυ* mutants were not solely due to decreased numbers of hemocytes at the VNC, we sought to characterise the ability of hemocytes to respond to wounds in more detail. To do this we observed hemocytes responding to wounds during time-lapse movies over a period of 58 minutes post-wound in control (*w;;crq-GAL4,UAS-GFP*), crq^{KO} (*w;*crq^{KO}*;crq-GAL4,UAS-GFP*), scb^{2} (*w;*scb^{2}*;crq-GAL4,UAS-GFP*) and $\beta\upsilon^{1}$ (*w;* $\beta\upsilon^{1}$*;crq-GAL4,UAS-GFP*) mutants, and calculated the percentage of hemocytes present in the frame of view at the beginning of the movie that actively migrate to the wound (Fig. 6.4). As hemocytes in embryos mutant for the apoptotic cell receptor Simu are more likely to leave the wound during this time (Chapter 4, Fig. 4.15), we also analysed the percentage of hemocyte leaving the wound in these apoptotic cell receptor mutants.

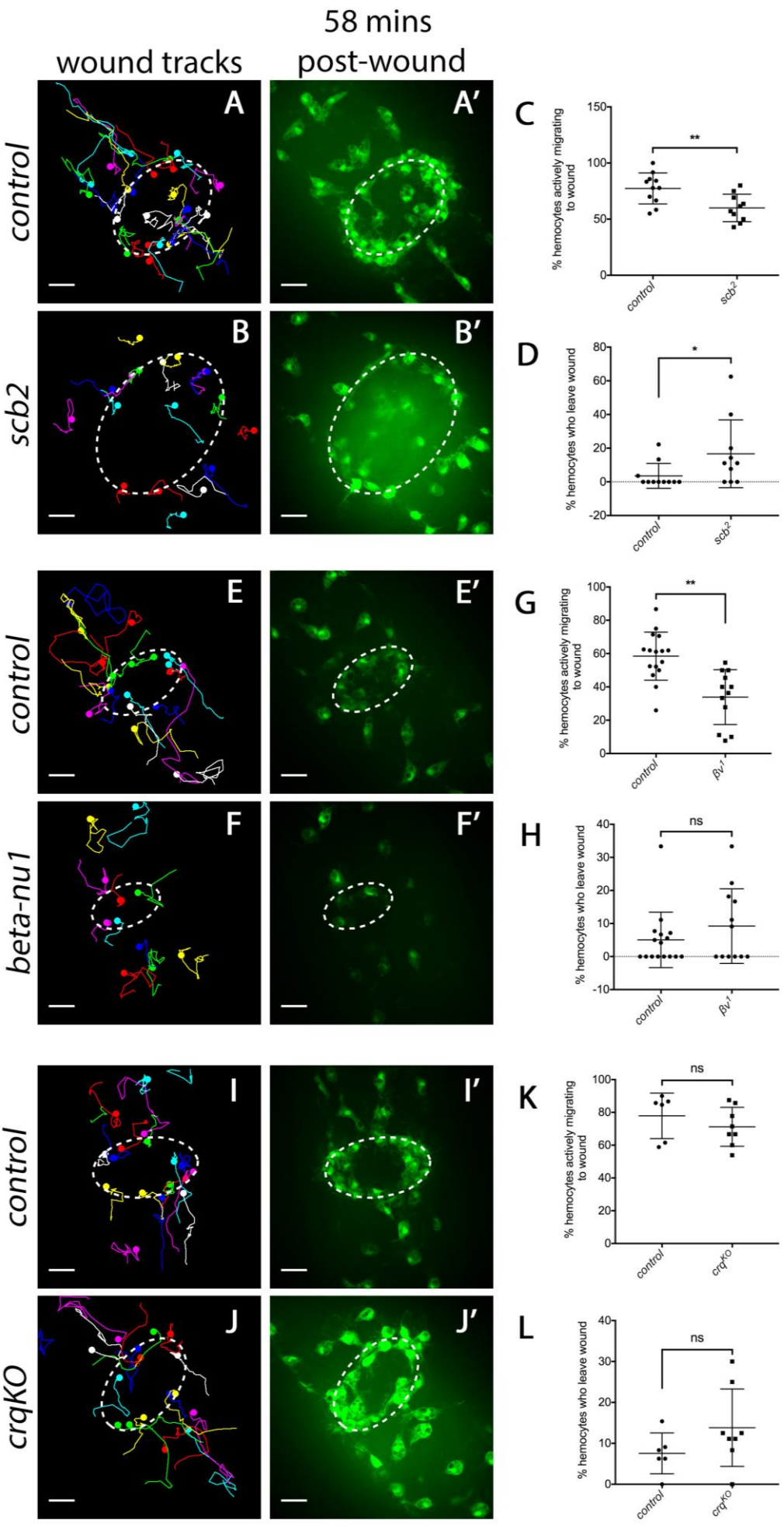
wound tracks
58 mins post-wound
control
scb2
control
beta-nu1
control
crqKO
A
A′
B
B′
C
D
E
E′
F
F′
G
H
I
I′
J
J′
K
L
% hemocytes actively migrating to wound
% hemocytes who leave wound
control
scb2
βν1
crqKO
**
*
ns

Figure 6.4: The percentage of hemocytes migrating to wounds during the 58-minute time period post-wounding is reduced in *scb*^{2}, *βv*^{1} and *crq*^{KO} mutants
(A) Representative tracks of hemocyte wound responses over 58 minutes from the time of wounding in control and *simu*^{2} mutant stage 15 embryos. Coloured lines represent the course of migration of each hemocyte tracked and coloured dots show the final position of hemocytes at 58 minutes post-wound. (B) Corresponding stills of GFP-labelled hemocytes at wounds 58 minutes post-wounding in control and *simu*^{2} embryos. (C) Scatterplot of the % of hemocytes present at t=0 minutes post-wound who actively migrate to the wound at any point during the wounding movie. Lines and error bars represent mean±SD; n=7 movies analysed for control embryos, n=9 for *simu*^{2} mutants.
White dashed ovals represent wound perimeter; scale bars represent 20μm; asterisks indicate statistical significance as determined by Mann-Whitney test; ***p < 0.001.

In *scb*^{2} mutants we found that the percentage of hemocytes actively migrating to wounds was significantly decreased by approximately 20% compared to controls (n=11 and 10 embryos for controls and *scb*^{2} respectively; p=0.0075 via Mann-Whitney test; Fig. 6.4 A-C). Interestingly, hemocytes in *scb*^{2} mutants were also 15% more likely to leave wounds when compared to those in controls (p=0.0487 via Mann-Whitney test; Fig. 6.4 D). Firstly this suggests that *scb* is required for the inflammatory migration of hemocytes to wounds, as although there are fewer hemocytes in the wounding area, a decreased percentage of these hemocytes are able to respond to wounds. However, this data also suggests that hemocyte retention at wounds is slightly perturbed in *scb* mutants, as hemocytes are more likely to migrate away from wounds in these mutants. As Scab is required for the normal migration of hemocytes along the ventral midline of the embryo (Comber et al. 2013), a process that involves the chemotaxis of hemocytes in response to Pvf chemoattractants (Wood et al. 2006), it may be the case that Scab is also required for the chemotaxis of hemocytes to wounds. However, *mys* mutants have severe defects in the migration of hemocytes along the ventral midline, but have normal numbers of hemocytes present at wounds 60 minutes post-wound (Comber et al. 2013), therefore this hypothesis is unlikely. It is possible that Scab may be acting as a receptor specifically required for hemocyte inflammatory recruitment. Therefore, unlike *mys*, *Scb* seems to have a distinct role in hemocyte inflammatory recruitment to wounds.

In *βv*^{1} mutants we found that the percentage of hemocyte migrating to wounds was significantly reduced by approximately 25% compared to controls (n=16 and 12 embryos for controls and *βv*^{1} respectively; p=0.0023 via Mann-Whitney test; Fig. 6.4 E-G), and this defect seemed more severe than in *scb* mutants (compare Fig. 6.4 A with Fig. 6.4 G). However, unlike in *scb* mutants, there was no significant difference in the percentage of hemocytes migrating away from wounds when compared to controls (p=0.411 via Mann-Whitney test; Fig. 6.4 H). This suggests that, like *scb*, *βv* integrin is also required in the inflammatory migration of hemocytes

to wounds, as although hemocyte numbers in the wounding area are decreased, the percentage of those hemocytes that respond to wounds is also decreased.

Finally, we found that unlike in *scb* and βv^1 mutants, the percentage of hemocytes responding to wounds in crq^{KO} mutants was no different to controls (n=4 and 8 embryos for control and crq^{KO} respectively; p=0.776 via Mann-Whitney test; Fig. 6.4 I-K). There also appears to be no defect in hemocyte retention at wounds in crq^{KO} mutants, as the percentage of hemocyte migrating away from wounds is comparable to controls (p=0.131 via Mann-Whitney test; Fig. 6.4 L). This suggests that hemocytes in *crq* mutant embryos are able to respond to wounds normally, but that there are simply fewer hemocytes in the vicinity of the wound. Therefore *crq* does not seem to be required for hemocyte inflammatory responses to wounds and the reduction in hemocytes at the wound is a consequence of reduced numbers of cells near the point of ablation.

6.2.5 Basal migration speeds of hemocytes in apoptotic cell receptor mutants

As we have shown that hemocyte basal migration speeds are reduced in *simu* mutants, and this has also shown to be the case in *drpr* mutants (Evans et al. 2015), we wanted to see whether mutants for the other known apoptotic cell receptors also displayed these defects. To do this we tracked the basal migrations of hemocytes in control (*w;;crq-GAL4,UAS-GFP*), crq^{KO} (*w;*crq^{KO}*;crq-GAL4,UAS-GFP*), scb^{01288} (*w;*scb^{01288}*;crq-GAL4,UAS-GFP*) and βv^1 (*w;* βv^1*;crq-GAL4,UAS-GFP*) mutant stage 15 embryos over a 60-minute time period using the Fiji manual tracking plug-in, and then calculated their average migration speeds (Fig. 6.5).

We found that hemocyte basal migration speeds in *scb* mutants were significantly reduced compared to controls, with hemocytes migrating at 1.25±0.22 μm/min and 1.86±0.11 μm/min respectively (n=9 and n=7 embryos for control and scb^{01288} respectively; p=0.0002 via Mann-Whitney test; Fig. 6.5 A, B). However, when we analysed hemocyte basal migration speeds in βv^1 mutants we found that these were not significantly different to controls, with hemocytes in controls migrating at 1.98±0.24 μm/min and those in βv^1 mutants migrating at 1.72±0.29 μm/min (n=10 embryos for both control and βv^1; p=0.0753 via Mann-Whitney test; Fig. 6.5 C, D). This suggests that *scb* is required for the normal migration of hemocytes but that *βυ* integrin is not, indicating that unlike has been suggested for apoptotic cell clearance (Nonaka et al. 2013) the Scab and βυ integrin subunits are unlikely to form a heterodimer that is required for hemocyte migration. Therefore as *Drosophila* only have one other β integrin subunit, *mys*, and that this has also been shown to be required for normal hemocyte migration speeds (Comber et al. 2013), it is likely that this is the β subunit interacting with Scab during hemocyte migrations.

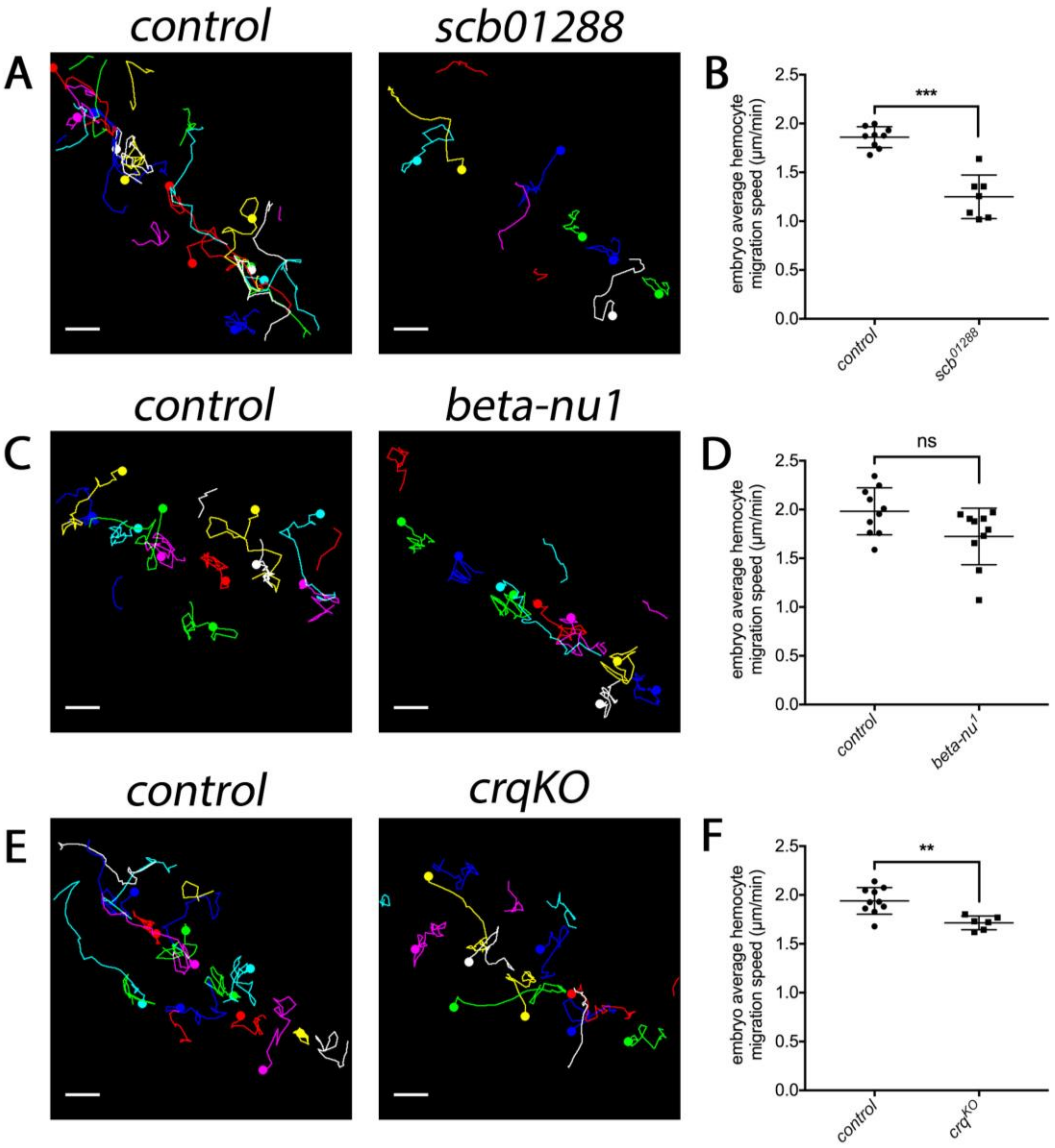

Figure 6.5: Hemocytes migrate at reduced speeds in *scb*^{01288} and *crq*^{KO} mutants, but not in *βv*^{1} mutants

(A) Representative tracks of hemocytes migrating on the superficial VNC over a 60-minute time period in control and *scb*^{01288} mutants. Coloured lines represent the course of migration of each hemocyte tracked and coloured dots show the final position of hemocytes. (B) Scatterplot of embryo average hemocyte migration speeds. Lines and error bar represent mean±SD; n=9 and 7 embryos for controls and *scb*^{01288} mutants respectively. (C) Representative tracks of hemocytes migrating on the superficial VNC over a 60-minute time period in control and *βv*^{1} mutants. Coloured lines represent the course of migration of each hemocyte tracked and coloured dots show the final position of hemocytes. (D) Scatterplot of embryo average hemocyte migration speeds. Lines and error bar represent mean±SD; n=10 embryos for both controls and *βv*^{1} mutants. (E) Representative tracks of hemocytes migrating on the superficial VNC over a 60-minute time period in control and *crq*^{KO} mutants. Coloured lines represent the course of migration of each hemocyte tracked and coloured dots show the final position of hemocytes. (F) Scatterplot of embryo average hemocyte migration speeds. Lines and error bar represent mean±SD; n=10 and 6 embryos for controls and *crq*^{KO} mutants respectively.

Finally, we found that hemocyte basal migration speeds in *crq*^{KO} mutants were decreased compared to controls, with control hemocytes migrating at an average speed of 1.94±0.14 μm/min and those in *crq*^{KO} mutants migrating at 1.72±0.07 μm/min (n=10 and 6 embryos for control and *crq*^{KO} respectively; p=0.003 via Mann-Whitney test; Fig. 6.5 E, F). This suggests that *crq* is required for normal hemocyte basal migration speeds. Interestingly, the mammalian homologue of Crq, CD36, has been shown to be involved in the migration of microglia in response to β-amyloid by signalling to proteins associated with focal adhesions (Stuart et al. 2007). Therefore it is not beyond the realms of possibility that Crq may be involved in hemocyte migration via regulation of the actin cytoskeleton.

6.2.6 Characterising apoptotic cell clearance in *crq*, *scab* and *βυ integrin* mutants *in vivo*

Crq, Scab and βυ integrin have all previously been reported to be required for the engulfment of apoptotic cells in *Drosophila* (Franc et al. 1999; Nagaosa et al. 2011; Nonaka et al. 2013), and as we have shown that apoptotic cells are capable of affecting hemocyte migratory behavior (Chapters 3 and 4), we wanted to assess apoptotic cell clearance in these mutants. To do this, control embryos as well as *scb*^{2}, *crq*^{KO} or *βυ*^{1} mutant embryos whose hemocytes were labelled using *UAS-GFP* expression under the control of the hemocyte specific *crq-GAL4* driver, were fixed and immunostained for cleaved DCP-1 (a downstream effector caspase cleaved during apoptosis (Song et al. 1997)) to label apoptotic cells and also for GFP to visualise hemocytes (Fig. 6.6 A, D, G). The number of untouched apoptotic cells surrounding hemocytes on the VNC in stage 15 embryos was then quantified by counting the number of cleaved DCP-1 positive particles that remained untouched by hemocytes. The engulfment of apoptotic cells by hemocytes was also quantified by counting the number of cleaved DCP-1 particles found within the hemocytes on the VNC in these embryos.

When comparing the average number of untouched apoptotic cells per embryo between controls and *crq*^{KO} mutants, we found that there was no significant difference between genotypes (n=4 and 5 embryos for control and *crq*^{KO} respectively; p>0.999 via Kruskall-Wallis one-way ANOVA test; Fig. 6.6 A, B). Furthermore, when we compared hemocyte engulfment of apoptotic cells in control and *crq*^{KO} mutants we again found that there was no significant difference despite there appearing to be a trend towards there being more apoptotic cells within hemocytes in *crq*^{KO} mutants (p=0.123 via Kruskal-Wallis one-way ANOVA test; Fig. 6.6 A, C). Interestingly in embryos in which *crq* expression had been rescued specifically in hemocytes in a *crq*^{KO} mutant background (*UAS-crq;crq*^{KO}*;crq-GAL4,UAS-GFP*) the trend towards an increase in engulfment was brought down again, however this was not statistically significant (n=5 and 4 embryos for *crq*^{KO} and *UAS-crq;crq*^{KO} respectively; p=0.172 via Kruskal-Wallis one-way

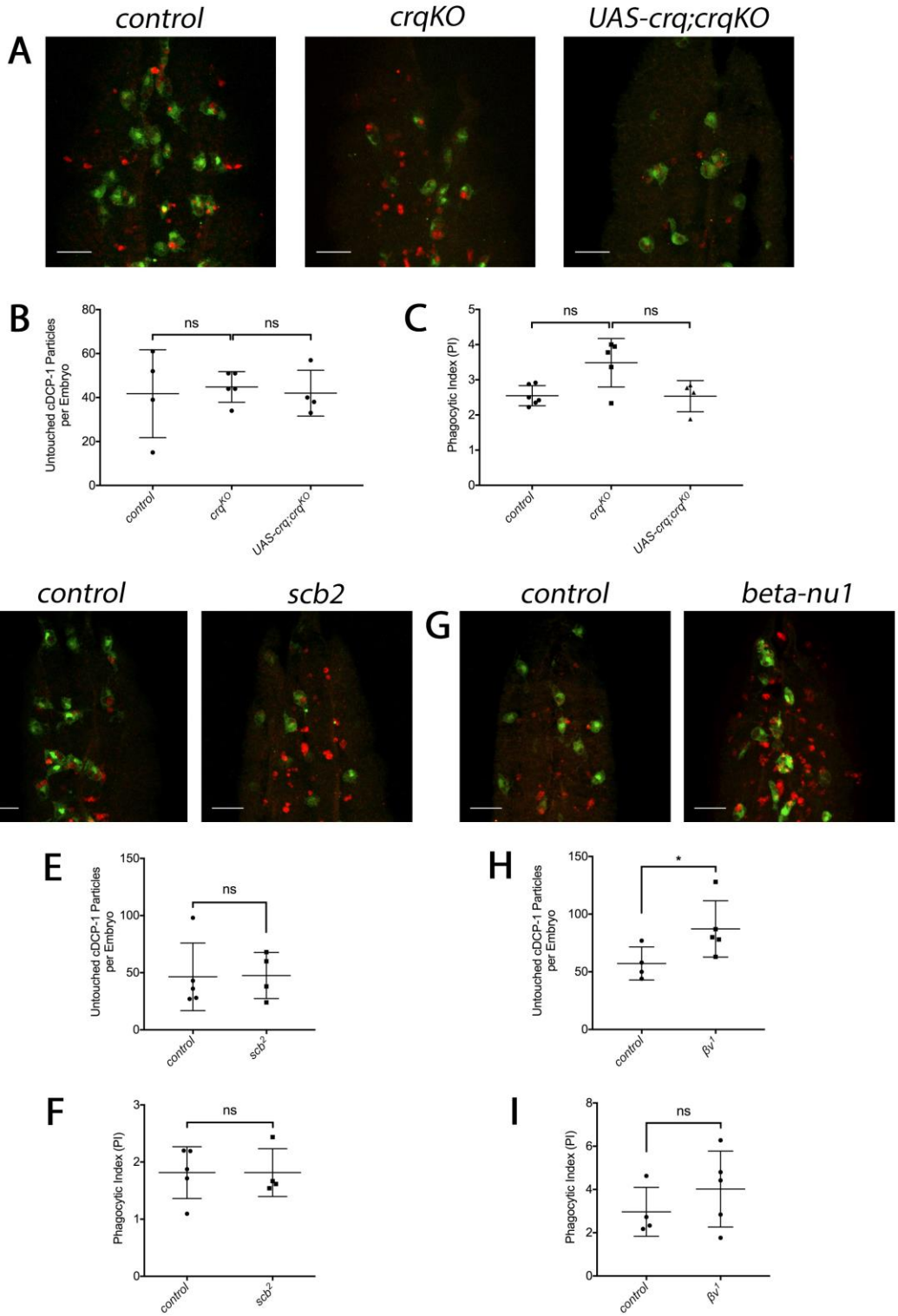
A
control
crqKO
UAS-crq;crqKO
B
Untouched cDCP-1 Particles per Embryo
ns
ns
control
crqKO
UAS-crq;crqKO
C
Phagocytic Index (PI)
ns
ns
control
crqKO
UAS-crq;crqKO
D
control
scb2
G
control
beta-nu1
E
Untouched cDCP-1 Particles per Embryo
ns
control
scb2
H
Untouched cDCP-1 Particles per Embryo
*
control
βν1
F
Phagocytic Index (PI)
ns
control
scb2
I
Phagocytic Index (PI)
ns
control
βν1

Figure 6.6: cDCP-1 staining in apoptotic cell receptor mutants reveals a defect in apoptotic cell clearance in βv^1 mutants

(A) Representative projections from confocal stacks of hemocytes (in green) and apoptotic cells (in red; cDCP-1) superficial to the VNC in control and crq^{KO} mutant fixed stage 15 embryos, as wells as in those in which *crq* expression has been restored specifically in hemocytes in a crq^{KO} mutant background (*UAS-crq;*crq^{KO}). (B) Scatterplot of the number of cDCP-1 particles that remain untouched by hemocytes in control, crq^{KO} and *UAS-crq;*crq^{KO} mutant embryos. Lines and error bars represent mean±SD; n=4, 5 and 4 embryos analysed for each of these genotypes respectively. (C) Scatterplot of the average number of DCP-1 particles engulfed per hemocyte, per embryo (referred to as the 'phagocytic index' (PI)). Lines and error bars represent mean±SD; n=6, 5 and 4 embryos analysed for each of the above genotypes respectively. (D) Representative projections from confocal stacks of hemocytes (in green) and apoptotic cells (in red; cDCP-1) superficial to the VNC in control and scb^2 mutant fixed stage 15 embryos. (E) Scatterplot of the number of cDCP-1 particles that remain untouched by hemocytes in control and scb^2 mutant embryos. Lines and error bars represent mean±SD; n=5 and 4 embryos analysed for control and scb^2 respectively. (F) Scatterplot of the average number of DCP-1 particles engulfed per hemocyte, per embryo (referred to as the 'phagocytic index' (PI)). Lines and error bars represent mean±SD; n=5 and 4 embryos analysed for control and scb^2 respectively. (G) Representative projections from confocal stacks of hemocytes (in green) and apoptotic cells (in red; cDCP-1) superficial to the VNC in control and βv^1 mutant fixed stage 15 embryos. (E) Scatterplot of the number of cDCP-1 particles that remain untouched by hemocytes in control and βv^1 mutant embryos. Lines and error bars represent mean±SD; n=4 and 5 embryos analysed for control and βv^1 respectively. (F) Scatterplot of the average number of DCP-1 particles engulfed per hemocyte, per embryo (referred to as the 'phagocytic index' (PI)). Lines and error bars represent mean±SD; n=4 and 5 embryos analysed for control and βv^1 respectively.

Note: analysis of apoptotic cell clearance in apoptotic cell receptor mutants was done in concert with Sharadha, a masters student in the lab.

ANOVA test; Fig. 6.6 A, C) Together this analysis suggests that there are no defects in apoptotic cell clearance by hemocytes on the VNC in stage 15 *crq* null embryos. This is in contrast to in the head of the embryo, where *crq* has been shown to be required for apoptotic cell clearance by hemocytes (Franc et al. 1999). As at the VNC apoptotic cells appear to be cleared by both hemocytes and glia, it may be the case that any hemocyte-specific defects in apoptotic cell clearance in *crq* mutants are disguised due to glial cells phagocytosing many of the apoptotic cells that would otherwise be cleared by hemocytes. This seems possible, as in *repo* mutants where glial cell phagocytosis of apoptotic cells is severely disrupted, hemocytes phagocytose increased numbers of apoptotic cells, and therefore this relationship may also work the other way around. This is something that could be checked in order to fully assess the role of Crq in hemocyte apoptotic cell clearance.

Next we assessed the role of Scab in the clearance of apoptotic cells by hemocytes. When the average number of untouched apoptotic cells in control and scb^2 mutant embryos was compared we found that again, there was no significant difference between the two genotypes (n=5 and 4 embryos for control and scb^2 respectively; p=0.905 via Mann-Whitney test; Fig. 6.6 D, E). In addition, when we compared the engulfment of apoptotic cells by hemocytes in control and scb^2

mutant embryos we found that, as in *crq* mutants, there was no significant difference in the average number of cleaved DCP-1 particles within hemocytes (n=5 and 4 embryos for control and scb^2 respectively; p=0.730 via Mann-Whitney test; Fig. 6.6 D, F). This analysis suggests that Scab is not required for the efficient engulfment of apoptotic cells by hemocytes, at least in hemocytes on the VNC in stage 15 embryos. Although, as mentioned above, perhaps any hemocyte-specific defects are being hidden by an upregulation in phagocytic activity by glia, therefore glial cell clearance would also need to be checked to assess this.

Finally, we moved on to assess the the last remaining known apoptotic cell receptor, βυ integrin, and its role in hemocyte apoptotic cell clearance. When we compared the average number of untouched cleaved DCP-1 particles in control and $\beta\upsilon^1$ mutant embryos we found that, in contrast to crq^{KO} and scb^2 mutants, there was a significant increase in $\beta\upsilon^1$ mutants (n=4 and 5 embryos for control and $\beta\upsilon^1$ respectively; p=0.0317 via Mann-Whitney test; Fig. 6.6 G, H). However, when we analysed the engulfment of apoptotic cells by hemocytes we found no significant difference in the average number of cleaved DCP-1 particles within hemocytes between $\beta\upsilon^1$ mutants and controls (n=4 and 5 embryos for control and $\beta\upsilon^1$ respectively; p=0.413 via Mann-Whitney test; Fig. 6.6 G, I). Together this analysis suggests that there is a defect in apoptotic cell clearance in $\beta\upsilon$ mutants, as there is a slight but significant build-up of untouched apoptotic cells in these mutants whilst engulfment remains the same as controls. However, we cannot rule out that there is more cell death in the embryo in $\beta\upsilon$ mutants that is leading to increased numbers of apoptotic cells being seen. If this was the case however, and if βυ integrin does not play a role in apoptotic cell clearance, you might expect to see increased numbers of engulfed apoptotic cells in hemocytes in $\beta\upsilon$ mutants due to the increased numbers of apoptotic cells for them to clear.

Taken together this data shows that the efficient clearance of apoptotic cells at the superficial VNC in stage 15 embryos does not require Scab or Crq, but does require βυ integrin. Therefore, it seems that there is some redundancy in the role of previously identified apoptotic cell receptors in hemocyte apoptotic cell clearance, as removing any one of these individual receptors has no effect on the number of apoptotic cells engulfed by hemocytes. It would be interesting to generate flies mutant for more than one apoptotic cell receptor to see how this affects apoptotic cell clearance in the embryo. As the clearance of apoptotic cells by hemocytes is a highly dynamic process, assessing the ability of hemocytes to clear apoptotic cells from fixed samples has some serious drawbacks. For example it is impossible to quantify the rate at which hemocytes phagocytose apoptotic cells, and it is very difficult to comment on how they interact with the apoptotic cells. Some studies have used the injection of the PS-binding agent Annexin V to examine apoptotic cell clearance live *in vivo* (Shklyar, Shklover, et al. 2013; Shklyar et al. 2014), however this has its drawbacks as Annexin V potentially disrupts the

binding of apoptotic cell receptors to PS and therefore may interfere with phagocytosis. Very recently a study was published describing new *Drosophila* fly lines expressing fluorescent Caspase activation markers to allow for real-time visualisation of apoptosis and it's clearance *in vivo* (Schott et al. 2017). Unfortunately these were not available to me during my studies however they are likely to be of great use in future studies.

6.2.7 Crq is required cell-autonomously to prevent a build-up of engulfed apoptotic cells in hemocytes located in the head

In the original studies that identified Crq as an apoptotic cell receptor, the engulfment of apoptotic cells by hemocytes was examined in the head region of the embryo (Franc et al. 1999). Therefore to rule out that the reason we identified no role for *crq* in apoptotic cell clearance by hemocytes was due to differences in the location of hemocytes, we examined the engulfment of apoptotic cells in the head region of embryos in which *crq* expression had been reduced specifically in hemocytes using RNAi mediated knockdown of *crq*. To do this we fixed and stained stage 15 embryos for GFP (to label hemocytes) and cleaved DCP-1 (to label apoptotic cells) and counted the number of apoptotic cells within hemocytes in the head region of control (*w;;crq-GAL4,UAS-GFP*) and *crq RNAi* embryos (*w;UAS-crq RNAi;crq-GAL4,UAS-GFP*).

Interestingly and somewhat unexpectedly, hemocytes located in the head of *crq RNAi* embryos seemed to contain increased numbers of apoptotic cells when compared to controls (n=59 and 39 hemocytes from a minimum of 6 embryos per genotype for control and *crq RNAi* respectively; $p<0.0001$ via Mann-Whitney test; Fig. 6.7 A, B). To ensure that this defect was not specific to *crq RNAi* embryos and was indeed due to the location that the hemocytes are in, we also assessed the engulfment of apoptotic cells at the VNC in these embryos. As is also the case in crq^{KO} mutant embryos, we found that hemocytes at the VNC in *crq RNAi* embryos contained similar numbers of apoptotic cells when compared to controls (n=87 and 37 hemocytes from a minimum of 3 embryos per genotype for control and *crq RNAi* respectively; $p=0.126$ via Mann-Whitney test; Fig. 6.7 C).

Firstly this suggests that, at least when located in the head region of the embryo, instead of being required for engulfment of apoptotic cells, *crq* seems to potentially be required for the processing and degradation of apoptotic cells post-engulfment. This is not the first time that this relationship has been shown, as in epidermal cell-mediated clearance of dendrite debris *crq* also seems not to be required for engulfment, but for the maturation of phagosomes (Han et al. 2014). Indeed, in embryos lacking *crq* expression, pupal epidermal cells contained vacuoles that

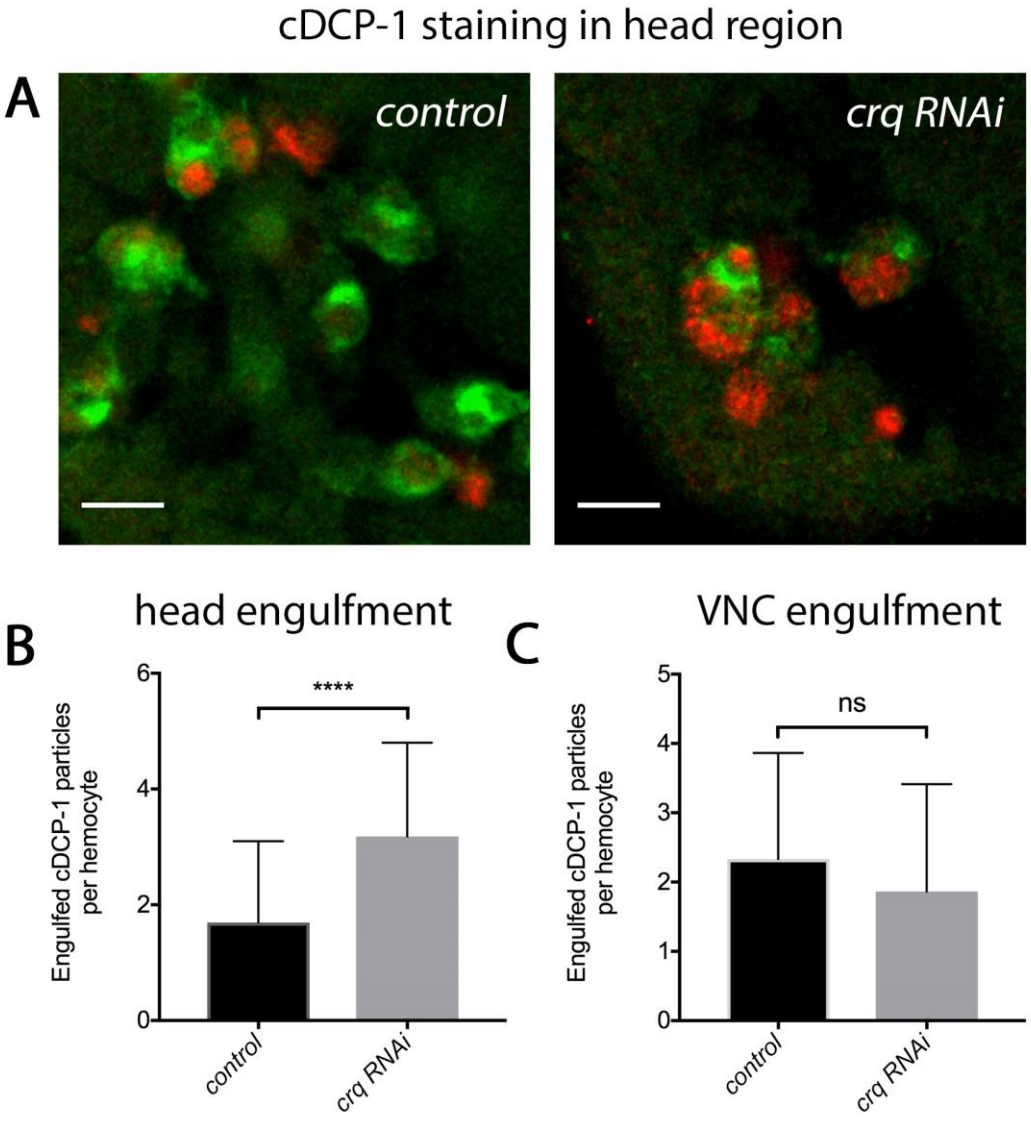

Figure 6.7: Hemocyte-specific RNAi knockdown of *crq* results in an accumulation of cDCP-1 particles inside hemocytes located in the head

(A) Representative slices from confocal stacks of hemocytes (in green) and apoptotic cells (in red; cDCP-1) located in the head region of control and *crq RNAi* stage 15 embryos. (B) Bar graph of the number of cDCP-1 particles engulfed per hemocyte located in the head of embryos. Bars are error bars represent mean±SD; n=59 and 39 hemocytes from a minimum of 6 embryos per genotype for control and *crq RNAi* respectively. (C) Bar graph of the number of cDCP-1 particles engulfed per hemocyte located on the superficial VNC. Bars are error bars represent mean±SD; n=87 and 37 hemocytes from a minimum of 3 embryos per genotype for control and *crq RNAi* respectively.

Scale bars represent 10μm; asterisks indicate statistical significance as determined by Mann-Whitney test; ****$p < 0.0001$ and ns= not significant.

appeared much larger due to the fusion of phagosomes, suggesting a role for *crq* in the prevention of this fusion (Han et al. 2014). This data also highlights that apoptotic cell clearance by hemocytes varies according to their location within the embryo. The weight of the burden of apoptotic cell clearance on hemocytes may also depend on which other phagocytes are available to aid in the clearance of apoptotic cells. For example, at the VNC, hemocytes are in very close contact with phagocytic glial cells and are likely to work in concert to clear apoptotic cells in this area (Shklyar et al. 2014). Perhaps in the head of the embryo, hemocytes are not in such close contact with glia therefore have to work alone in clearing-up apoptotic cells. This may explain why a build-up of apoptotic cells is seen within the hemocytes in the head of the embryo when this does not occur in those at the VNC. In any case our data suggests that *crq* is not required for the engulfment of apoptotic cells, and presumably other apoptotic cell receptors are mediating engulfment in this case.

6.2.8 Blocking apoptosis in *βv integrin* mutants fails to rescue hemocyte inflammatory responses

In Chapter 4 we showed that apoptotic cells are capable of affecting hemocyte inflammatory migrations to wounds. Therefore as we identified a defect in apoptotic cell clearance in βv^1 mutants, and these mutants also have a severe defect in their hemocyte inflammatory responses to wounds, we sought to remove apoptosis in these mutants to see whether this might rescue this defect. To do this we wounded βv^1 mutant embryos that also contained the genomic deletion *Df(3L)H99* (*w;*βv^1*;Df(3L)H99, crq-GAL4,UAS-GFP*), which blocks all developmental apoptosis in the embryo (White et al. 1994).

As previously, to assess the inflammatory response of hemocytes, we quantified the density of hemocytes present at the wound at 60 minutes post-wounding. When we did this we found that, compared to βv^1 mutants alone (*w;*βv^1*;crq-GAL4,UAS-GFP*), the density of hemocytes in βv^1*;Df(3L)H99* was no different (n=16 and 13 embryos for βv^1 and βv^1*;Df(3L)H99* respectively; p=0.423 via Mann-Whitney test; Fig. 6.8 A, B). Furthermore, as we have observed previously (Chapter 4, Fig. 4.13), we also found that there was a significant reduction in hemocytes inflammatory responses in *Df(3L)H99* embryos (*w;;Df(3L)H99,crq-GAL4,UAS-GFP*) compared to controls (*w;;crq-GAL4,UAS-GFP*) (n=18 and 12 embryos for control and *Df(3L)H99* respectively; p=0.0116 via Mann-Whitney test; Fig. 6.8 A, B). This shows that the removal of apoptosis in a βv^1 mutant background does not rescue the inflammatory response defect; therefore it is unlikely that the defect in hemocyte inflammatory responses in βv^1 is due to the presence of increased numbers of untouched apoptotic cells.

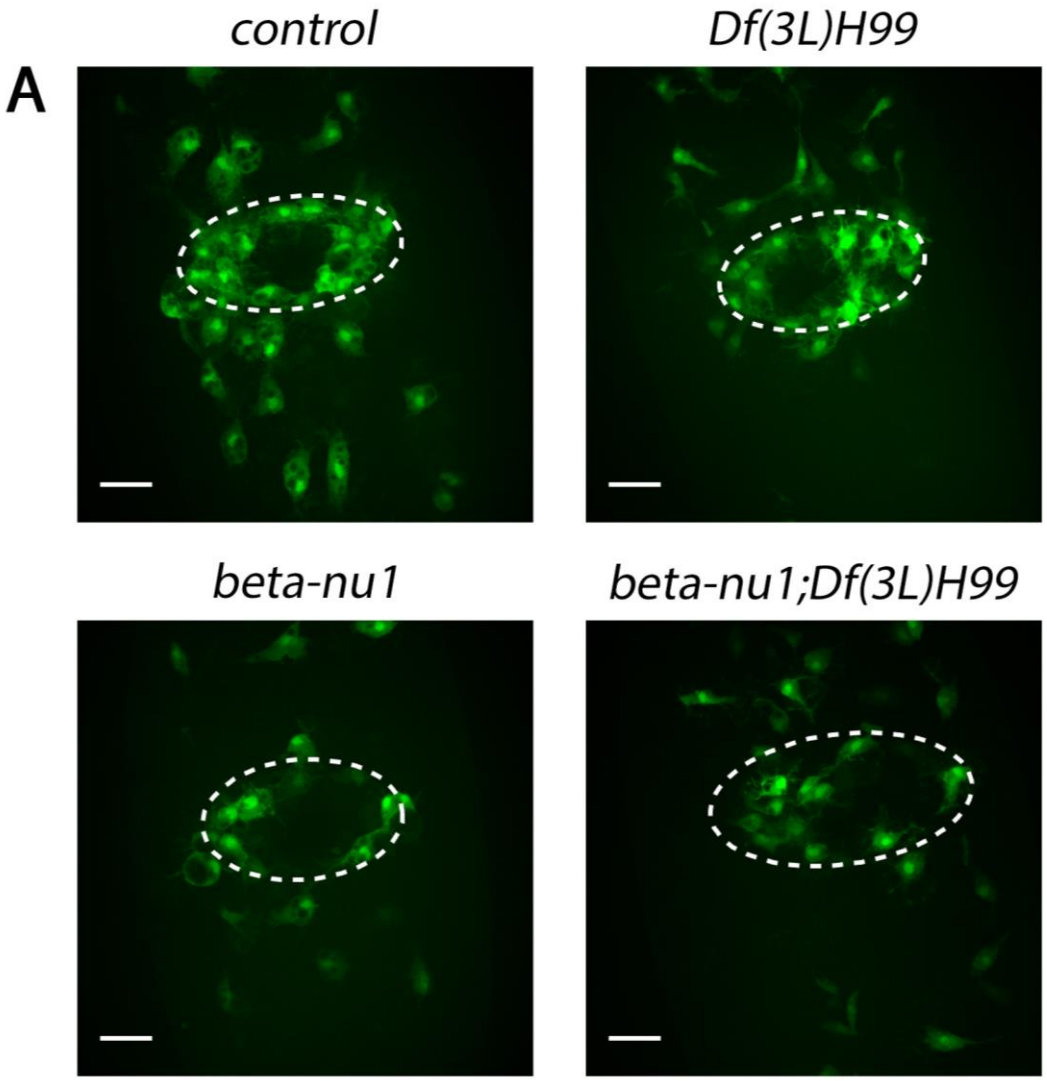
A
control
Df(3L)H99
beta-nu1
beta-nu1;Df(3L)H99

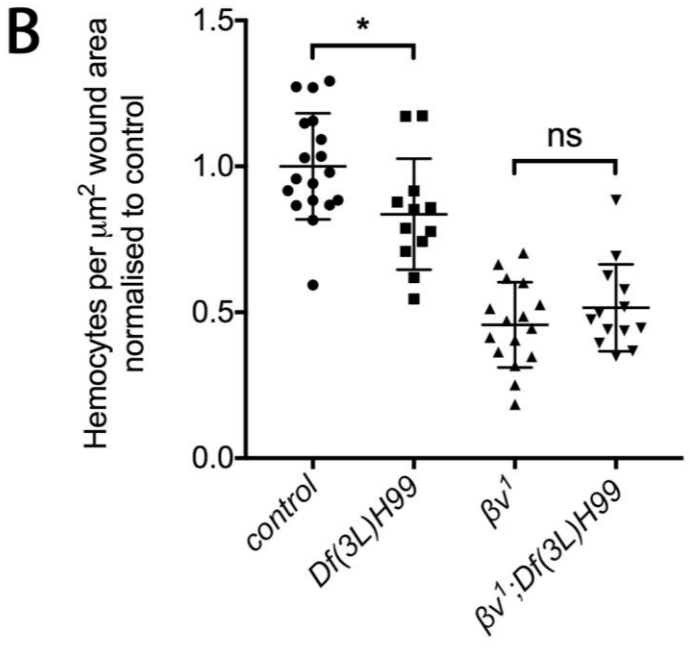
B
Hemocytes per µm2 wound area normalised to control
1.5
1.0
0.5
0.0
*
ns
control
Df(3L)H99
βv1
βv1;Df(3L)H99

Figure 6.8: Blocking apoptosis using the *Df(3L)H99* genomic deletion is unable to rescue macrophage wound responses in βv^1 mutants
(A) Representative stills of GFP-labelled hemocyte responses to wounds at 60 minutes post-wound in control, *Df(3L)H99*, βv^1, and βv^1;*Df(3L)H99* mutant stage 15 embryos. (B) Scatterplot of hemocyte wound responses per embryo shown as the number of hemocytes per μm^2 wound area at 60 minutes post-wounding normalized to the control average. Lines and error bars represent mean±SD; n=18, 12, 16 and 13 embryos per genotype for the above genotypes respectively.
White dashed ovals represent wound perimeter; scale bars represent 20μm; asterisks indicate statistical significance as determined by Mann-Whitney test; *p < 0.05 and ns= not significant.

6.2.9 Blocking apoptosis in *scb* and *crq* mutants confirms wound response defect is not due to apoptotic cells

In order to be absolutely confident that the wound response defects observed in both *scb* and *crq* mutant were not due to any defects in apoptotic cell clearance that we might have missed in our analysis of fixed embryos, we wounded both of these mutants in which all developmental apoptosis had been blocked using the *Df(3L)H99* genomic deletion as above. Firstly, compared to scb^{01288} mutants alone (*w;*scb^{01288}*;crq-GAL4,UAS-GFP*), we found that the density of hemocytes at wounds 60 minutes post-wounding in scb^{01288} mutant embryos in which apoptosis had been blocked using *Df(3L)H99* (*w;*scb^{01288}*;Df(3L)H99,crq-GAL4,UAS-GFP*) were no different, with both genotypes showing a reduction in hemocyte density of around 55% compared to controls (n=16 and 8 embryos for scb^{01288} and scb^{01288}*;Df(3L)H99* respectively; p=0.742 via Mann-Whitney test; Fig. 6.9 A, B). Therefore blocking apoptosis has no obvious affect on *scb* mutant hemocyte wound responses, suggesting that the inflammatory response defect observed in these mutants is not due to the presence of apoptotic cells.

Similarly, when apoptosis was blocked in a crq^{KO} mutant background using *Df(3L)H99* (*w;*crq^{KO}*;Df(3L)H99,crq-GAL4,UAS-GFP*) there was no difference in hemocyte wound responses compared to crq^{KO} mutants alone (*w;*crq^{KO}*;crq-GAL4,UAS-GFP*) (n=16 and 17 embryos for crq^{KO} and crq^{KO}*;Df(3L)H99* respectively; p=0.986 via Mann-Whitney test; Fig. 6.9 C, D). This therefore suggests that the wound response defect observed in crq^{KO} mutants cannot be rescued by removing apoptosis, therefore the defect is unlikely to be due to the presence of apoptotic cells in these mutants.

Together this data shows that, even if we have somehow missed a defect in hemocyte apoptotic cell clearance in *scb* and *crq* mutant embryos, either at the VNC or elsewhere in the embryo, it

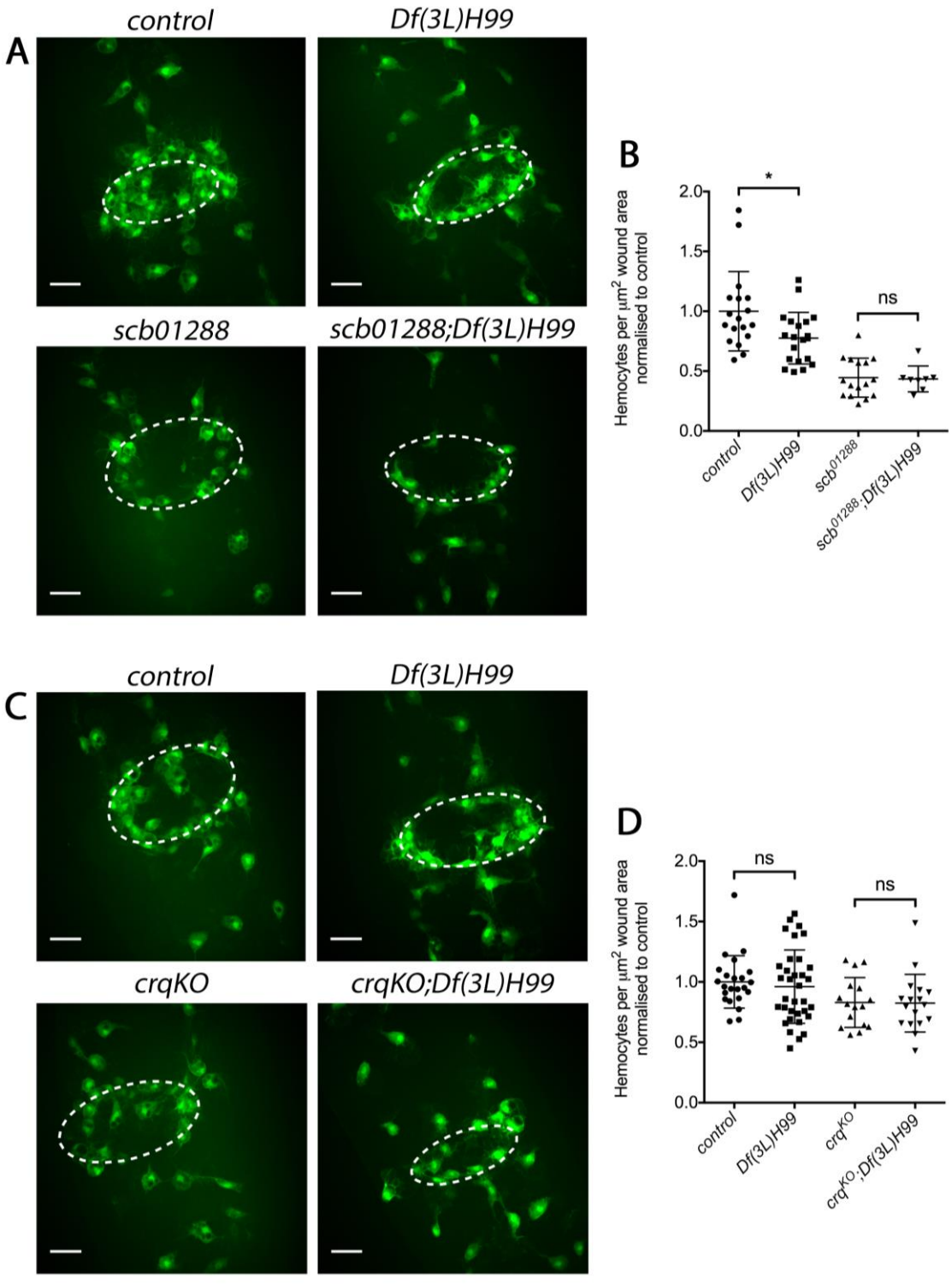
A
control
Df(3L)H99
scb01288
scb01288;Df(3L)H99
B
Hemocytes per µm² wound area normalised to control
*
ns
control
Df(3L)H99
scb01288
scb01288;Df(3L)H99
C
control
Df(3L)H99
crqKO
crqKO;Df(3L)H99
D
Hemocytes per µm² wound area normalised to control
ns
ns
control
Df(3L)H99
crqKO
crqKO;Df(3L)H99

Figure 6.9: Blocking apoptosis in *scb* and *crq* mutants fails to rescue their wound response defects
(A) Representative stills of GFP-labelled hemocyte responses to wounds at 60 minutes post-wound in control, *Df(3L)H99*, scb^{01288}, and scb^{01288}*;Df(3L)H99* mutant stage 15 embryos. (B) Scatterplot of hemocyte wound responses per embryo shown as the number of hemocytes per μm^2 wound area at 60 minutes post-wounding normalized to the control average. Lines and error bars represent mean±SD; n=18, 20, 16 and 8 embryos per genotype for the above genotypes respectively. (C) Representative stills of GFP-labelled hemocyte responses to wounds at 60 minutes post-wound in control, *Df(3L)H99*, crq^{KO}, and crq^{KO}*;Df(3L)H99* mutant stage 15 embryos. (D) Scatterplot of hemocyte wound responses per embryo shown as the number of hemocytes per μm^2 wound area at 60 minutes post-wounding normalized to the control average. Lines and error bars represent mean±SD; n=23, 34, 16 and 17 embryos per genotype for the above genotypes respectively.
White dashed ovals represent wound perimeter; scale bars represent 20μm; asterisks indicate statistical significance as determined by Mann-Whitney test; *p < 0.05 and ns= not significant.

seems unlikely that their respective wound response defects are due to the presence of apoptotic cells. Therefore hemocyte wound response defects are likely due to factors unrelated to apoptosis.

6.2.10 Apoptotic cells are not responsible for reduced hemocyte speeds in *scb* and *crq* mutants

In order to be absolutely confident that the hemocyte migratory defects observed in *scb* and *crq* mutants are not due to any defects in apoptotic cell clearance that we might have missed in our analysis of fixed embryos, we analysed hemocyte migration speeds in both of these mutants in which all developmental apoptosis had been blocked using the *Df(3L)H99* genomic deletion as above. As *βυ* mutants do not have a significant defect in hemocyte migration speeds, we did not perform this test on these mutants.

Firstly, when compared to hemocyte migration speeds in scb^{01288} mutant embryos alone (*w;*scb^{01288}*;crq-GAL4,UAS-GFP*), those in scb^{01288}*;Df(3L)H99* embryos (*w;*scb^{01288}*;crq-GAL4,UAS-GFP*) migrated at similar speeds (n=7 and 3 embryos for scb^{01288} and scb^{01288}*;Df(3L)H99* respectively; p=0.117 via Mann-Whitney test). This result suggests that it is unlikely that apoptotic cells in scb^{01288} mutants are the cause of reduced hemocyte migration speeds in these mutants. Also, compared to crq^{KO} mutants alone (*w;*crq^{KO}*;crq-GAL4,UAS-GFP*), hemocyte migration speeds in crq^{KO}*;Df(3L)H99* embryos (*w;*crq^{KO}*;Df(3L)H99,crq-GAL4,UAS-GFP*) were no different (n=6 and 5 embryos for crq^{KO} and crq^{KO}*;Df(3L)H99*

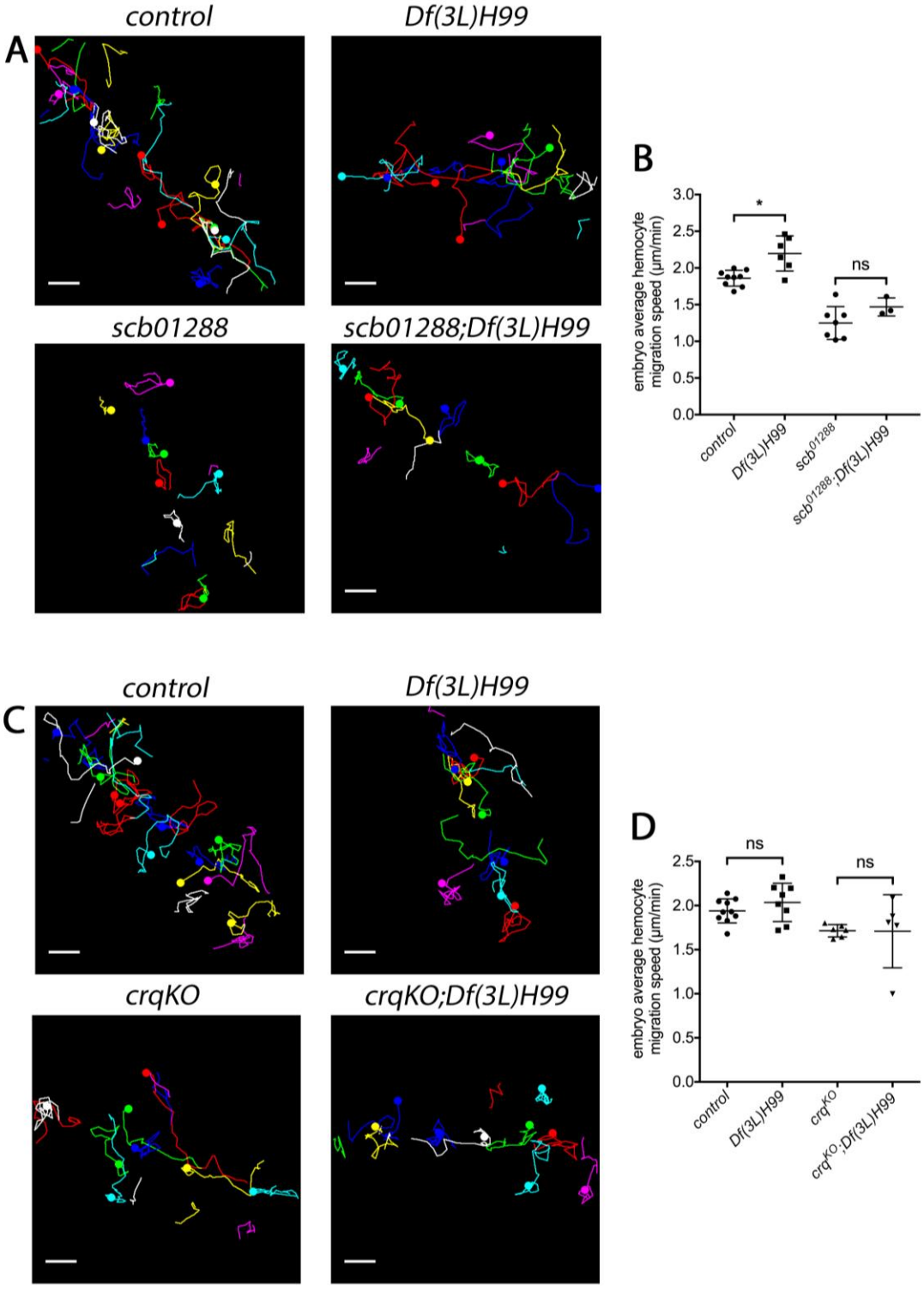
A
control
Df(3L)H99
scb01288
scb01288;Df(3L)H99
B
embryo average hemocyte migration speed (µm/min)
3.0
2.5
2.0
1.5
1.0
0.5
0.0
*
ns
control
Df(3L)H99
scb01288
scb01288;Df(3L)H99
C
control
Df(3L)H99
crqKO
crqKO;Df(3L)H99
D
embryo average hemocyte migration speed (µm/min)
2.5
2.0
1.5
1.0
0.5
0.0
ns
ns
control
Df(3L)H99
crqKO
crqKO;Df(3L)H99

Figure 6.10: Blocking apoptosis in *scb* and *crq* mutants fails to rescue hemocyte migration speeds
(A) Representative tracks of hemocytes migrating on the superficial VNC over a 60-minute time period in control, *Df(3L)H99*, scb^{01288} and scb^{01288}*;Df(3L)H99* mutants. Coloured lines represent the course of migration of each hemocyte tracked and coloured dots show the final position of hemocytes. (B) Scatterplot of embryo average hemocyte migration speeds. Lines and error bar represent mean±SD; n=9, 6, 7 and 3 embryos for the above genotypes respectively.
(C) Representative tracks of hemocytes migrating on the superficial VNC over a 60-minute time period in control, *Df(3L)H99*, crq^{KO}, and crq^{KO}*;Df(3L)H99* mutants. Coloured lines represent the course of migration of each hemocyte tracked and coloured dots show the final position of hemocytes. (D) Scatterplot of embryo average hemocyte migration speeds. Lines and error bar represent mean±SD; n=10, 8, 6 and 5 embryos for the above genotypes respectively.
Scale bars represent 20μm; asterisks indicate statistical significance as determined by Mann-Whitney test; *p < 0.05 and ns= not significant.

respectively; p=0.178 via Mann-Whitney test; Fig 6.9 C, D). This suggests that the migratory defect observed in crq^{KO} mutants is not due to the presence of apoptotic cells.

We can therefore be confident that the reduced migration speeds of hemocytes in both scb^{01288} and crq^{KO} mutant embryos are not due to any defects in apoptotic cell clearance. This suggests that hemocyte migrations speeds are reduced by a factor unrelated to apoptosis in these mutants.

6.3 DISCUSSION

In this chapter we have shown that the apoptotic cell receptors Scab, βυ integrin and Crq are required for normal hemocyte inflammatory responses to wounds, and that at least in the case of Scab and Crq, these receptors are required cell-autonomously for this response. We also show that Scab, βυ integrin and Crq are all required for normal numbers of hemocytes to reach the superficial VNC by stage 15 of embryonic development, and that again for Scab and Crq at least, this is a cell-autonomous role. We then go on to show that both Crq and Scab are required for hemocytes to migrate at normal speeds, but that βυ integrin does not seem to be required for this behaviour. Finally we show that hemocytes mutant for either *scb* or *crq* exhibit no apparent defects in their clearance of apoptotic cells on the VNC in stage 15 embryos, but that there does seem to be a slight build-up of uncleared apoptotic cells in *βυ* mutants.

6.3.1 Are previously identified apoptotic cell receptors actually required for apoptotic cell clearance?

Croquemort has previously been shown to be required for the engulfment of apoptotic cells in *Drosophila* embryos (Franc et al. 1999). However, we were unable to reproduce this using the assays presented in this chapter (Fig. 6.6), albeit using a different mutant and measuring clearance in a different region of the embryo. In the original studies, Crq was found to be required for phagocytosis of apoptotic cells by hemocytes in the head of embryos that were anywhere between stage 11 and 16 of embryonic development (Franc et al. 1999). As the amount of apoptosis that can be found within tissues of the embryo changes dramatically through embryonic development (Abrams et al. 1993), the number of apoptotic cells detected and therefore the number of engulfed apoptotic cells may differ quite substantially. For example, if by chance the majority of control embryos in their study were stage 13/14, when high numbers of apoptotic cells can be found in the head (Abrams et al. 1993), and their embryos lacking Crq were mostly stage 11/12 when fewer can be found (Abrams et al. 1993), then this may give the false impression that Crq is required for engulfment when in fact there are simply fewer apoptotic cells in the latter due to timing differences. Therefore, examining apoptotic cell clearance in specifically staged embryos (stage 15) is likely a more appropriate and accurate approach. Also, as the original studies examined apoptotic cell clearance in hemocytes in the head of embryos (Franc et al. 1999), whereas we looked at those on the superficial VNC, differences in apoptosis in these different areas of the embryo may also contribute to the differences in clearance seen. In an attempt to address this possibility, we examined the engulfment of apoptotic cells by hemocytes in the head of stage 15 embryos in which *crq* expression had been reduced specifically in hemocytes using RNAi-mediated knockdown. Interestingly, this analysis showed that there were an increased number of apoptotic cells within hemocytes in the head of *crq RNAi* embryos compared to controls, adding to the increasing amount of data suggesting that Crq is required not for the engulfment of apoptotic cells per-se, but for their degradation post-engulfment (Han et al. 2014; Guillou et al. 2016). Another reason for the difference between our study and the published data may be due to the differences in apoptotic cell markers used - cleaved DCP-1 versus 7-AAD (Franc et al. 1999). Finally, as at the time of the original study a *crq* mutant allele was not available, Crq was first identified as an apoptotic cell receptor in embryos with two genomic deletions overlapping the *crq* locus (Franc et al. 1999), as opposed to the crq^{KO} null allele used in our analysis. Although hemocyte-specific re-expression of *crq* was able to partially rescue the engulfment of apoptotic cells in the over-lapping deficiency embryos, it seemed that engulfment still remained reduced compared to controls (Franc et al. 1999), suggesting that the removal of other genes in such embryos may be contributing to the decrease in apoptotic cell engulfment observed. Overall, I believe that our assay of hemocyte apoptotic cell clearance, examining hemocytes in a

very specific location using embryos at specific stages of embryonic development with the specific removal of *crq*, represents a more accurate way of assessing the role of Crq in apoptotic cell clearance than that published originally (Franc et al. 1999).

In contrast to published data (Nonaka et al. 2013), we also found no evidence of a requirement for Scab in apoptotic cell clearance in *Drosophila* embryos using our assay. In the original study that identified *scab* as necessary for efficient phagocytosis of apoptotic cells by hemocytes, apoptotic cell clearance was assessed by first homogenising stage 16 embryos. Cell suspensions were then fixed and stained to identify hemocytes and apoptotic cells via TUNEL staining and anti-Crq staining, respectively. Phagocytosis of apoptotic cells was then assessed by quantifying the percentage of hemocytes that contained apoptotic cells (Nonaka et al. 2013; Nagaosa et al. 2011). This analysis showed that hemocytes from *scab* mutant embryos and from those in which Scab expression had been knocked down specifically in hemocytes using RNAi had decreased numbers of apoptotic cells within them (Nonaka et al. 2013). However, isolating hemocytes from embryos in this way is a very destructive process that may disrupt hemocyte biology by, for example, potentially activating stress signalling or causing downstream signalling stimulated by the presence of damage signals caused by embryo homogenisation. Also, analysing apoptotic cell clearance by quantifying the percentage of hemocytes that have engulfed apoptotic cells is less detailed than quantifying the number of engulfed apoptotic cells per hemocyte. For example, hemocytes from *scab* mutant embryos identified as having phagocytosed apoptotic cells in the study by Nonaka *et al.* may have engulfed many more compared to those in control embryos, but this will not have been picked up by this analysis (Nonaka et al. 2013). Furthermore, it seems likely that there is some redundancy in the role of apoptotic cell receptors in apoptotic cell clearance. For example, in *simu* mutants, there is a build-up of uncleared apoptotic cells seemingly due to the inefficient clearance by both hemocytes and glia, however hemocytes in these mutants do still contain apoptotic cells, highlighting redundancy in the system.

6.3.2 A role for the integrin subunits Scab and βυ in hemocyte migratory behaviour

In *scab* and *βυ integrin* mutant embryos there is also a decrease in the number of hemocytes at the wound 60 minutes post-wounding (Fig. 6.1). Hemocyte numbers at the VNC are also reduced in both of these mutants, however those hemocytes that are present in the wounding area are less able to migrate to wounds when compared to controls (Fig. 6.4). In *βυ integrin* mutants, hemocytes do not migrate at reduced speeds (Fig. 6.5), therefore slowed migration is unlikely to account for the inflammatory defect. Furthermore, in embryos mutant for the βPS

integrin *mys* hemocytes migrate more slowly, but hemocyte numbers at the wound 60 minutes post-wounding are normal in these mutants (Comber et al. 2013), suggesting that the slowed hemocyte migration observed in *scab* mutants is unlikely to account for the inflammatory response defect. Altogether our data suggests that *scab* and *βυ integrin* are required for normal hemocyte inflammatory responses to wounds, and Scab at least is required cell-autonomously by hemocytes. Time constraints precluded analysis of *βυ integrin* in a tissue-specific manner, therefore a hemocyte-specific role for βυ integrin in hemocyte inflammatory responses has yet to be confirmed.

But what role do Scab and βυ integrin play in hemocyte inflammatory responses to wounds? Scab is an orthologue of the human integrin α4 subunit, which has been shown to be required for the chemotaxis of macrophages towards chemoattractants such as Osteopontin (Lund et al. 2013), although this ligand does not seem to be present in *Drosophila*. Studies examining the chemotaxis of neutrophils showed that the integrin α4 subunit as well as the integrin LFA-1 was required for their chemotaxis towards the chemoattractant fLMP, but that blocking integrin α4 using antibodies did not affect the speed of migration, suggesting that integrin α4 is required specifically during chemotaxis and not general migration (Heit et al. 2005). They also showed that the role of integrin α4 in chemotaxis is specific to fMLP and that it was not involved in chemotaxis towards IL-8 (Heit et al. 2005). Therefore *in vitro* models of vertebrate leukocyte migration suggest a role for the vertebrate homologue of Scab in chemotaxis towards specific ligands. It is possible therefore that Scab is somehow involved in hemocyte chemotaxis towards wounds. As βυ integrin is thought to be the beta subunit that forms a heterodimer with the alpha subunit Scab to create a functional protein (Nonaka et al. 2013), βυ integrin may also be required for the chemotaxis of hemocytes to wounds.

We also showed that hemocyte migration speeds are slowed in *scab* mutant embryos, and that this defect was unrelated to apoptosis (Figs. 6.5 and 6.10). Integrins are important during the migration of cells, as they represent the link between the extracellular matrix components on which they migrate and the intracellular actin network (Huttenlocher and Horwitz 2011). Integrin transmembrane receptors are heterodimeric in nature, with both an α subunit and a β subunit required to associate non-covalently in order to form a functioning integrin receptor. In mammals 8 different β subunits and 18 α subunits have been identified, whereas *Drosophila* possess fewer of both subunit types, with only 2 β and 5 α subunits (reference). Integrins are essential components of cellular focal adhesions; protein complexes linking cells to the extracellular matrix that represent signalling centres mediating cellular interaction with the ECM. Therefore, integrins as well as extracellular matrix components are important players in cellular migration.

Indeed, several roles for integrins have been identified in *Drosophila* hemocyte migration. Firstly, it is known that the α integrin subunit Inflated (αPS2) is required for the penetration of hemocytes into the germband during their developmental migration in the embryo (Siekhaus et al. 2010). The PDZ-GEF Dizzy has also been found to be important in hemocyte migration, and it is thought that this is due to its ability to control integrin-dependent adhesion through Rap-1 mediated control of the βPS integrin *mys* function (Huelsmann et al. 2006). Indeed, as already mentioned, hemocytes in *mys* mutant embryos migrate at slower speeds than controls and also have defects in hemocyte developmental migration, most notably along the ventral midline of the embryo (Comber et al. 2013). They also show that the α integrin subunits αPS1 and αPS3 (Scab) are required for the normal migration of hemocyte along the ventral midline by embryonic stage 13, and that this migration is delayed in mutants for these subunits (Comber et al. 2013). In this study they also go on to show that *mys* is required in hemocytes for normal contact inhibition during hemocyte migration, a factor that controls the dispersal and distribution of hemocytes in the *Drosophila* embryo (Stramer et al. 2010), with hemocytes remaining in contact with each other for longer periods of time (Comber et al. 2013). Finally they also showed that *mys* is required for the normal separation of the VNC from the epidermis (Comber et al. 2013), a process that is known to be required for the migration of hemocytes along the ventral midline (Evans et al. 2010). Therefore the normal migration of hemocytes has been shown to be dependent on βPS, and αPS1, 2 and 3 (Scab), however a role for βv integrin has not been identified until now.

As mentioned earlier, integrins have important roles in the linking of cells to the extracellular matrix (ECM) through which they migrate, which allows communication between the cell and its surroundings. In *Drosophila*, hemocytes are known to deposit ECM components during their migration (Olofsson and Page 2005). It is also known that the lack of the ECM component laminin causes the failure of hemocyte migration along the VNC (Urbano et al. 2009), and that hemocytes also require laminin to migrate at normal speeds and respond normally to wounds (Sánchez-Sánchez et al. 2017). Furthermore, it has been shown that hemocytes themselves produce and secrete laminins to regulate their own migration (Sánchez-Sánchez et al. 2017). As many of the integrin subunits in *Drosophila* have been shown to bind to laminin, the interaction between integrins and laminins is important in cell migration (Urbano et al. 2011). Therefore as the ligand to which Scab binds is thought to be laminin (Hynes and Zhao 2000), it may well be the case that Scab is required for normal hemocyte migration through this interaction.

Chapter 7: Final discussion

Many chronic inflammatory diseases such as COPD, atherosclerosis and systemic lupus erythematosus are associated with the build-up of apoptotic cells (Szondy et al. 2014). There are also high amounts of apoptosis at sights of inflammation. As macrophages are important players in the inflammatory response, from the initiation to the resolving of inflammation as well as having key roles during the inflammatory process, and as they are present at sites of pathology and can exacerbate disease progression, it is important to understand how these cells function when faced with increased levels of apoptosis. To date much of the research on how apoptotic cells impact macrophage function has focused on the anti-inflammatory effects of efferocytosis as well as the mechanisms leading to the failed clearance of apoptotic cells in some chronic inflammatory conditions (Szondy et al. 2017). However there is still much to be discovered about how apoptotic cells affect the behaviour and function of macrophages, particularly *in vivo*.

The purpose of this PhD project was to investigate how apoptotic cells affect macrophage function *in vivo* using *Drosophila melanogaster*, and more specifically how they affect macrophage migratory behaviour, a relationship that has only recently come to our attention (Evans et al. 2013). In particular two studies suggest a causal link between the build-up of apoptotic cells and defective macrophage migration. The first showed that the build-up of apoptotic cells within macrophages in SCAR mutant *Drosophila* embryos causes macrophage migration speeds to be slowed (Evans et al. 2013), and similarly the second shows the same relationship but this time in a zebrafish model of lysosomal disorders (Berg et al. 2016). The work presented in this thesis has expanded our knowledge on the affects of apoptotic cells on various aspects of macrophage migration.

In order to study how the clearance of apoptotic cells affects macrophage migratory behaviour *in vivo*, two different models of perturbed apoptotic cell clearance were used. By perturbing the ability of glial cells to clear apoptotic cells, as is the case in *repo* mutant embryos, the number of apoptotic cells for macrophages to clear was increased, which resulted in macrophages becoming full of apoptotic cells. Conversely, when the clearance of apoptotic cells by both macrophages and glial cells was disrupted, as is the case in *simu* mutants, this resulted in an accumulation of apoptotic cells that remained uncleared by phagocytes. In each of these models both the inflammatory migration of macrophages to sites of tissue damage as well as their speed of migration under homeostatic conditions were inhibited. The rescue of the percentage of macrophages migrating to wounds upon blocking all developmental apoptosis in *simu* mutants suggested that apoptotic cells were capable of having an anti-inflammatory effect on

macrophages prior to them being engulfed. Wound responses in *repo* mutants could not be rescued by removing apoptosis, as there seems to be a defect in macrophage inflammatory responses that is independent of apoptotic cells in these embryos, possibly due to defects in glial cells, which is interesting in itself. In both of these models of perturbed apoptotic cell clearance, the migration speeds of macrophages could be rescued by the removal of apoptosis, which further proves that pathological levels of apoptotic cells perturb macrophage migration.

The mechanism of how apoptotic cells exert their anti-inflammatory affect prior to being engulfed was examined, but was unable to be identified. It was hypothesised that "find-me" cues released by uncleared apoptotic cells are capable of distracting macrophages from migrating to wounds, however this was unable to be proved using the assay of find-me cue injection. Until the identity of the find-me cues released by apoptotic cells in *Drosophila* are identified, this hypothesis is very hard to prove, and this represents a very important area of future research.

7.1 Pathological levels of apoptotic cells as regulators of the inflammatory migration of macrophages to sites of tissue damage

The work presented in this thesis has highlighted a previously unknown role for apoptotic cells in the modulation of macrophage migration to sites of tissue damage. Although it is well understood that the phagocytosis of apoptotic cells by macrophages induces an anti-inflammatory phenotype which aids in the resolution of inflammation (Szondy et al. 2017; Voll et al. 1997; Valerie A. Fadok et al. 1998), how apoptotic cells affect the function and behaviour of macrophages *in vivo* is incompletely understood. The rescue of inflammatory responses by blocking developmental apoptosis in *simu* mutants (a model with greatly increased numbers of apoptotic cells that remain untouched by phagocytes), in concert with further studies from other members of the lab showing that hemocyte wound responses are reduced during the acute induction of apoptosis prior to apoptotic cells being engulfed (Armitage and Evans, unpublished data), suggests that apoptotic cells are capable of exerting their anti-inflammatory effect prior to being engulfed by macrophages.

Despite examining a variety of potential mechanisms as to how uncleared apoptotic cells may be exerting their affects on the migration of macrophages, a definitive mechanism is yet to be identified. As macrophages in the *Drosophila* embryo seem to prioritise their migration to

apoptotic cells over other chemotactic cues, and macrophages are able to be distracted from their normal routes of developmental dispersal by the induction of apoptosis (Moreira et al. 2010), it seems likely that chemoattractive cues released by apoptotic cells may be able to distract macrophages from migrating to sites of tissue damage in *Drosophila*. The chemoattractants released by apoptotic cells in *Drosophila* that lead to the recruitment of macrophages are yet to be discovered, however the distraction mentioned above indicates that they are present (Moreira et al. 2010). In contrast several 'find-me' cues released by apoptotic cells have been shown to induce monocyte/macrophage chemotaxis in vertebrate systems, which have been shown to be lysophosphatidylcholine (LPC) (Lauber et al. 2003), sphingosine-1-phosphate (S-1-P) (Gude et al. 2008), fractalkine (Truman et al. 2008) and the nucleotides ATP and UTP (Elliott et al. 2009). However, the injection of some of these cues into the *Drosophila* embryo failed to affect macrophage inflammatory responses, suggesting that the acute exposure of *Drosophila* macrophages to vertebrate find-me cues does not distract them from migrating to sites of tissue damage. The injection of supernatant from apoptotic *Drosophila* S2 cells also failed to reduce macrophage wound responses; therefore we were unable to prove a link between apoptotic cell-derived chemoattractants and the inhibition of inflammatory responses.

7.1.2 ROS as mediators of hemocyte inflammatory responses?

However we were able to show that, in *simu* mutant embryos where the number of uncleared apoptotic cells is greatly increased, macrophages exhibit decreased levels of reactive oxygen species (ROS). In contrast, in embryos in which increased numbers of apoptotic cells can be found within macrophages, macrophage ROS levels are normal. Recent data from microarray studies comparing gene expression in control and *simu* mutant embryos have also revealed the differential expression of genes involved in cellular redox homeostasis (data not shown). Together this suggests that the build-up of uncleared apoptotic cells affects the redox status of macrophages.

It has previously been shown that the incubation of activated macrophages with apoptotic cells quenches the production of ROS by vertebrate macrophages *in vitro*, and that this seems to be dependent of PS exposure by apoptotic cells (Serinkan et al. 2005). Interestingly, inhibition of the NADPH oxidase ROS-producing enzyme in neutrophils leads to their decreased ability to chemotax (Hattori et al. 2010). Critically, this study also showed that neutrophils from mice lacking NADPH oxidase activity showed defective recruitment to sites of inflammation, suggesting a link between decreased ROS production and defective inflammatory recruitment (Hattori et al. 2010). ROS have also been shown to produced downstream of integrin

engagement, and these ROS mediate integrin signalling to control cellular spreading and adhesion (Chiarugi et al. 2003). ROS have also been implicated in the control of cellular migration through their regulation of the actin cytoskeleton (Xu et al. 2017). Furthermore, the ROS H_2O_2 has been shown to be produced at wounds (Moreira et al. 2010) and induces the spreading of *Drosophila* hemocytes (Comber 2014) – a process that requires integrins and is involved in cell migration (reviewed by Holly et al. 2000).

Together this presents us with a potential model of how unclearead apoptotic cells may be able to inhibit macrophage inflammatory migrations to sites of tissue damage. I would suggest that, through an as yet unidentified mechanism, uncleared apoptotic cells cause macrophage ROS production to be decreased, which in turn reduces the ability of macrophages to migrate towards sites of inflammation, possibly through the prevention of cellular spreading. As we have also shown that the integrin subunits αPS3 (Scab) and βυ are required for normal hemocyte inflammatory responses to wounds, it would be interesting to examine whether these link in to this process somewhere.

7.2 Increased numbers of apoptotic cells affect the migration speeds of macrophages *in vivo*

The examination of macrophage migration speeds in two novel models of increased apoptosis, coupled with the rescue of migration speeds by the removal of apoptosis, have shown that apoptotic cells are capable of reducing the speed of macrophage migration when their numbers are increased. This is in line with previous studies showing that the accumulation of apoptotic cells within macrophages reduce macrophage migration speeds (Berg et al. 2016; Evans et al. 2013). Therefore it is now clear that the efficient clearance and degradation of apoptotic cells is essential to regulate the migratory capability of macrophages. As macrophage migration is a fundamental aspect of their function, this has implications for apoptotic cells in regulating the function of macrophages in vivo.

The mechanisms by which apoptotic cells reduce the migration speeds of macrophages have yet to be identified, and as discussed in Chapters 3 and 4, there are a plethora of potential hypotheses as to how they might be doing this. Therefore elucidating these mechanisms represent a very interesting line of future work. It would certainly be interesting to see, as is the case with macrophage wound responses, whether the acute induction of apoptosis in the *Drosophila* embryo before apoptotic cells have been engulfed is also capable of inducing a migratory phenotype defect. This would help to separate whether apoptotic cells have to be

engulfed to have an effect on macrophage migration, which would have implications on which hypotheses to follow.

7.3 Modulation of macrophage wound retention as an anti-inflammatory mechanism in *Drosophila*

A surprising discovery made during the work contained within this thesis was the identification of the apoptotic cell receptor Simu, as well as the αPS3 integrin subunit Scab, as transmembrane proteins required for the retention of macrophages at wounds. To my knowledge, this was the first time that any factor has been implicated as a molecule required for macrophage wound retention in *Drosophila*. As Simu is known to bind to phosphatidylserine (PS) on apoptotic cells (Shklyar, Levy-Adam, et al. 2013), a potential mechanism of Simu-mediated macrophage retention is the receptor-ligand interaction between Simu and PS exposed by necrotic cellular debris at wounds, which is supported by my finding that Simu is required for the engulfment of debris at wounds. Therefore an interesting potential retention signal may be the interaction of macrophages with cellular debris located at sites of tissue damage.

Although this data is extremely exciting, more work needs to be done to definitively prove the link between macrophage-necrotic cell interactions and inflammatory retention. It would be very interesting to examine whether PS receptors also mediate the retention of macrophages or indeed neutrophils at sites of inflammation in vertebrate systems such as zebrafish or mice, and if so, whether therapies targeting PS receptors may represent a novel therapeutic approach to combat inflammation.

7.3.1 A potential role for macrophage adhesion as a retention signal

It is interesting to note that Eater, a Nimrod family protein of which Simu is also a member, has been shown to be required for macrophages to form sessile patches in *D*rosophila larvae, indicating a role in macrophage adhesion (Bretscher et al. 2015). Infact, the adhesion of hemocytes upon infection and injury is a hallmark of insect cellular innate immune responses (Strand 2008). As macrophages at wounds seem to form connections between themselves and with the surrounding tissue at wounds, and macrophage-macrophage adhesion may act in the recruitment of macrophages to wounds (Babcock et al. 2008), perhaps macrophage adhesion represents a retention mechanism at wounds. The finding that the αPS3 integrin Scab is also required for the normal retention of macrophages at wounds supports this idea, as it is well

known that integrins are very important in cellular adhesion. Therefore perhaps both Simu and Scab are required for macrophage retention at wounds in *Drosophila*. It would be interesting to examine the wounding movies in *simu* and *scb* mutants in more detail, and perhaps quantifying other parameters, such as the amount of time macrophages stay in contact with each other and the different cells at the wound, would allow us to get a better of idea as to whether there are any cell-cell interaction defects at wounds in these mutants. It line with its role in the formation of hemocyte sessile patches (Bretscher et al. 2015), it would also be interesting to see whether Eater has a role in macrophage retention at wounds in *Drosophila*.

The identification of genes required for macrophage retention at wounds in *Drosophila* has identified this system as a potential novel model to study this aspect of inflammatory biology. Indeed along with its high genetic tractability, and as it is an excellent system for high-resolution *in vivo* live imaging, it would be a very strong model organism to study this highly dynamic process.

7.4 Novel roles for integrins in macrophage inflammatory responses in *Drosophila*

Whilst attempting to rescue the inflammatory responses of macrophages by un-coupling the binding of apoptotic cells to their receptors and thus disrupting downstream signalling, we made the surprise discovery that both the integrin subunits βυ and αPS3 seem to be required for the normal recruitment of macrophages to wounds in *Drosophila* embryos. Although it has been previously shown that βPS integrin (Mys) is required for the recruitment of hemocytes to wounds at a normal rate, the number of hemocytes present at wounds 60 minutes post-wounding was no different to controls (Comber et al. 2013). As it was shown that the percentage of hemocytes responding to wounds in both *Scab* and *βυ integrin* mutants was decreased, and the number present at wounds 60 minutes post-wounding was decreased, this is the first time that integrins have been shown to play a role in the active migration of hemocytes to sites of tissue damage.

In vertebrate systems, extensive research has been carried out on the role of integrins in leukocyte trafficking during inflammatory recruitment, particularly during their adhesion and extravasation. As discussed in chapter 6, there are a range of possible roles played by integrins during hemocyte inflammatory responses, however further investigation is required to determine the exact role of integrins in hemocyte wound responses.

Bibliography

Abercrombie, M. and Heaysman, J.E.M., 1953. Observations on the social behaviour of cells in tissue culture: I. Speed of movement of chick heart fibroblasts in relation to their mutual contacts [Online]. *Experimental Cell Research*, 5(1), pp.111–131. Available from: http://www.sciencedirect.com/science/article/pii/0014482753900986.

Abercrombie, M., Heaysman, J.E.M., and Pegrum, S.M., 1971. The locomotion of fibroblasts in culture: IV. Electron microscopy of the leading lamella [Online]. *Experimental Cell Research*, 67(2), pp.359–367. Available from: http://www.sciencedirect.com/science/article/pii/0014482771904204.

Abercrombie, M., Joan, E., Heaysman, M., and Pegrum, S.M., 1970. The locomotion of fibroblasts in culture: II. 'Ruffling' [Online]. *Experimental Cell Research*, 60(3), pp.437–444. Available from: http://www.sciencedirect.com/science/article/pii/0014482770905379.

Abrams, J.M., White, K., Fessler, L.I., and Steller, H., 1993. Programmed cell death during Drosophila embryogenesis [Online]. *Development*, 117(1), p.29 LP-43. Available from: http://dev.biologists.org/content/117/1/29.abstract.

Abreu-Blanco, M.T., Verboon, J.M., Liu, R., Watts, J.J., and Parkhurst, S.M., 2012. Drosophila embryos close epithelial wounds using a combination of cellular protrusions and an actomyosin purse string [Online]. *Journal of Cell Science*, 125(24), p.5984 LP-5997. Available from: http://jcs.biologists.org/content/125/24/5984.abstract.

Agaisse, H., Petersen, U.M., Boutros, M., Mathey-Prevot, B., and Perrimon, N., 2003. Signaling role of hemocytes in Drosophila JAK/STAT-dependent response to septic injury. *Developmental Cell*, 5(3), pp.441–450.

Ait-Oufella, H., Kinugawa, K., Zoll, J., Simon, T., Boddaert, J., Heeneman, S., Blanc-Brude, O., Barateau, V., Potteaux, S., Merval, R., Esposito, B., Teissier, E., Daemen, M.J., Lesèche, G., Boulanger, C., Tedgui, A., and Mallat, Z., 2007. Lactadherin deficiency leads to apoptotic cell accumulation and accelerated atherosclerosis in mice. *Circulation*, 115(16), pp.2168–2177.

Akakura, S., Kar, B., Singh, S., Cho, L., Tibrewal, N., Sanokawa-Akakura, R., Reichman, C., Ravichandran, K.S., and Birge, R.B., 2005. C-terminal SH3 domain of CrkII regulates the assembly and function of the DOCK180/ELMO Rac-GEF [Online]. *Journal of Cellular Physiology*, 204(1), pp.344–351. Available from: http://dx.doi.org/10.1002/jcp.20288.

Alfonso, T.B. and Jones, B.W., 2002. gcm2 Promotes Glial Cell Differentiation and Is Required with glial cells missing for Macrophage Development in Drosophila [Online]. *Developmental Biology*, 248(2), pp.369–383. Available from: http://www.sciencedirect.com/science/article/pii/S0012160602907402.

Awasaki, T., Tatsumi, R., Takahashi, K., Arai, K., Nakanishi, Y., Ueda, R., and Ito, K., 2006. Essential Role of the Apoptotic Cell Engulfment Genes draper and ced-6 in Programmed Axon Pruning during Drosophila Metamorphosis. *Neuron*, 50(6), pp.855–867.

Ayyaz, A., Li, H., and Jasper, H., 2015. Hemocytes control stem cell activity in the Drosophila intestine [Online]. *Nature cell biology*, 17(6), pp.736–748. Available from: http://www.ncbi.nlm.nih.gov/pmc/articles/PMC4449816/.

Babcock, D.T., Brock, A.R., Fish, G.S., Wang, Y., Perrin, L., Krasnow, M. a, and Galko, M.J., 2008. Circulating blood cells function as a surveillance system for damaged tissue in Drosophila larvae. *Proceedings of the National Academy of Sciences of the United States of America*, 105(29), pp.10017–10022.

Barolo, S., Castro, B., and Posakony, J.W., 2004. New Drosophila transgenic reporters: Insulated P-element vectors expressing fast-maturing RFP. *BioTechniques*, 36(3), pp.436–442.

Barth, N.D., Marwick, J.A., Vendrell, M., Rossi, A.G., and Dransfield, I., 2017. The 'Phagocytic Synapse' and Clearance of Apoptotic Cells [Online]. *Frontiers in Immunology*, 8, p.1708. Available from:

https://www.frontiersin.org/article/10.3389/fimmu.2017.01708.

Barzik, M., Kotova, T.I., Higgs, H.N., Hazelwood, L., Hanein, D., Gertler, F.B., and Schafer, D.A., 2005. Ena/VASP proteins enhance actin polymerization in the presence of barbed end capping proteins. *Journal of Biological Chemistry*, 280(31), pp.28653–28662.

Bedard, K., Szabo, E., Michalak, M., and Opas, M.B.T.-I.R. of C., 2005. Cellular Functions of Endoplasmic Reticulum Chaperones Calreticulin, Calnexin, and ERp57. In: *A Survey of Cell Biology*. Academic Press, pp.91–121. Available from: http://www.sciencedirect.com/science/article/pii/S0074769605450044.

Bellingan, G.J., Caldwell, H., Howie, S.E., Dransfield, I., and Haslett, C., 1996. In vivo fate of the inflammatory macrophage during the resolution of inflammation: inflammatory macrophages do not die locally, but emigrate to the draining lymph nodes. [Online]. *The Journal of Immunology*, 157(6), p.2577 LP-2585. Available from: http://www.jimmunol.org/content/157/6/2577.abstract.

Berg, R.D., Levitte, S., O'Sullivan, M.P., O'Leary, S.M., Cambier, C.J., Cameron, J., Takaki, K.K., Moens, C.B., Tobin, D.M., Keane, J., and Ramakrishnan, L., 2016. Lysosomal Disorders Drive Susceptibility to Tuberculosis by Compromising Macrophage Migration [Online]. *Cell*, 165(1), pp.139–152. Available from: http://www.sciencedirect.com/science/article/pii/S0092867416301362.

Bernardoni, R., Kammerer, M., Vonesch, J.-L., and Giangrande, A., 1999. Gliogenesis Depends on glide/gcm through Asymmetric Division of Neuroglioblasts [Online]. *Developmental Biology*, 216(1), pp.265–275. Available from: http://www.sciencedirect.com/science/article/pii/S0012160699995118.

Bernardoni, R., Vivancos, V., and Giangrande, a, 1997. Glide/Gcm Is Expressed and Required in the Scavenger Cell Lineage. *Developmental biology*, 191(1), pp.118–130.

Bhatia, V.K., Yun, S., Leung, V., Grimsditch, D.C., Benson, G.M., Botto, M.B., Boyle, J.J., and Haskard, D.O., 2007. Complement C1q reduces early atherosclerosis in low-density lipoprotein receptor-deficient mice [Online]. *American Journal of Pathology*, 170(1), pp.416–426. Available from: http://dx.doi.org/10.2353/ajpath.2007.060406.

Bloor, J.W. and Kiehart, D.P., 2001. zipper Nonmuscle Myosin-II Functions Downstream of PS2 Integrin in Drosophila Myogenesis and Is Necessary for Myofibril Formation [Online]. *Developmental Biology*, 239(2), pp.215–228. Available from: http://www.sciencedirect.com/science/article/pii/S001216060190452X.

Bökel, C. and Brown, N.H., 2002. Integrins in development: Moving on, responding to, and sticking to the extracellular matrix. *Developmental Cell*, 3(3), pp.311–321.

Bossing, T., Udolph, G., Doe, C.Q., and Technau, G.M., 1996. The Embryonic Central Nervous System Lineages ofDrosophila melanogaster: I. Neuroblast Lineages Derived from the Ventral Half of the Neuroectoderm [Online]. *Developmental Biology*, 179(1), pp.41–64. Available from: http://www.sciencedirect.com/science/article/pii/S0012160696902407.

Breitsprecher, D., Kiesewetter, A.K., Linkner, J., Vinzenz, M., Stradal, T.E.B., Small, J.V., Curth, U., Dickinson, R.B., and Faix, J., 2011. Molecular mechanism of Ena/VASP-mediated actin- filament elongation [Online]. *The EMBO Journal*, 30(3), p.456 LP-467. Available from: http://emboj.embopress.org/content/30/3/456.abstract.

Bretscher, A.J., Honti, V., Binggeli, O., Burri, O., Poidevin, M., Kurucz, É., Zsámboki, J., Andó, I., and Lemaitre, B., 2015. The Nimrod transmembrane receptor Eater is required for hemocyte attachment to the sessile compartment in Drosophila melanogaster [Online]. *Biology Open*, 4(3), p.355 LP-363. Available from: http://bio.biologists.org/content/4/3/355.abstract.

Brophy, M.L., Dong, Y., Wu, H., Rahman, H.N.A., Song, K., and Chen, H., 2017. Eating the Dead to Keep Atherosclerosis at Bay [Online]. *Frontiers in Cardiovascular Medicine*, 4(January). Available from: http://journal.frontiersin.org/article/10.3389/fcvm.2017.00002/full.

Brouckaert, G., Kalai, M., Krysko, D. V, Saelens, X., Vercammen, D., Ndlovu, `Matladi, Haegeman, G., D'Herde, K., and Vandenabeele, P., 2004. Phagocytosis of Necrotic Cells by Macrophages Is Phosphatidylserine Dependent and Does Not Induce Inflammatory Cytokine Production [Online]. D. Drubin, ed. *Molecular Biology of the Cell*, 15(3), pp.1089–1100. Available from: http://www.ncbi.nlm.nih.gov/pmc/articles/PMC363082/.

Brückner, K., Kockel, L., Duchek, P., Luque, C.M., Rørth, P., and Perrimon, N., 2004. The PDGF/VEGF Receptor Controls Blood Cell Survival in Drosophila [Online]. *Developmental Cell*, 7(1), pp.73–84. Available from: http://www.sciencedirect.com/science/article/pii/S1534580704002072.

Brugnera, E., Haney, L., Grimsley, C., Lu, M., Walk, S.F., Tosello-Trampont, A.-C., Macara, I.G., Madhani, H., Fink, G.R., and Ravichandran, K.S., 2002. Unconventional Rac-GEF activity is mediated through the Dock180–ELMO complex [Online]. *Nature Cell Biology*, 4, p.574. Available from: http://dx.doi.org/10.1038/ncb824.

Bryant, R.E., DesPrez, R.M., VanWay, M.H., and Rogers, D.E., 1966. STUDIES ON HUMAN LEUKOCYTE MOTILITY [Online]. *The Journal of Experimental Medicine*, 124(3), p.483 LP-499. Available from: http://jem.rupress.org/content/124/3/483.abstract.

Bugyi, B. and Carlier, M.-F., 2010. Control of Actin Filament Treadmilling in Cell Motility [Online]. *Annual Review of Biophysics*, 39(1), pp.449–470. Available from: https://doi.org/10.1146/annurev-biophys-051309-103849.

Campbell, G., Goring, H., Lin, T., Spana, E., Andersson, S., Doe, C.Q., and Tomlinson, A., 1994. RK2, a glial-specific homeodomain protein required for embryonic nerve cord condensation and viability in Drosophila [Online]. *Development*, 120(10), pp.2957–2966. Available from: http://dev.biologists.org/content/120/10/2957.abstract.

Campbell, J.J., Foxman, E.F., and Butcher, E.C., 1997. Chemoattractant receptor cross talk as a regulatory mechanism in leukocyte adhesion and migration. *European Journal of Immunology*, 27(10), pp.2571–2578.

Campos, I., Geiger, J.A., Santos, A.C., Carlos, V., and Jacinto, A., 2010. Genetic Screen in Drosophila melanogaster Uncovers a Novel Set of Genes Required for Embryonic Epithelial Repair [Online]. *Genetics*, 184(1), pp.129–140. Available from: http://www.ncbi.nlm.nih.gov/pmc/articles/PMC2815911/.

Carlson, S.D., Juang, J., Hilgers, S.L., and Garment, M.B., 2000. Arriers of the. , pp.151–174.

Chabaud, M., Heuze, M.L., Bretou, M., Vargas, P., Maiuri, P., Solanes, P., Maurin, M., Terriac, E., Le Berre, M., Lankar, D., Piolot, T., Adelstein, R.S., Zhang, Y., Sixt, M., Jacobelli, J., Benichou, O., Voituriez, R., Piel, M., and Lennon-Dumenil, A.M., 2015. Cell migration and antigen capture are antagonistic processes coupled by myosin II in dendritic cells. *Nature Communications*, 6(May), pp.1–16.

Chatterjee, N. and Bohmann, D., 2012. A Versatile ΦC31 Based Reporter System for Measuring AP-1 and Nrf2 Signaling in Drosophila and in Tissue Culture [Online]. *PLOS ONE*, 7(4), p.e34063. Available from: https://doi.org/10.1371/journal.pone.0034063.

Chen, D., Jian, Y., Liu, X., Zhang, Y., Liang, J., Qi, X., Du, H., Zou, W., Chen, L., Chai, Y., Ou, G., Miao, L., Wang, Y., and Yang, C., 2013. Clathrin and AP2 Are Required for Phagocytic Receptor-Mediated Apoptotic Cell Clearance in Caenorhabditis elegans [Online]. *PLOS Genetics*, 9(5), p.e1003517. Available from: https://doi.org/10.1371/journal.pgen.1003517.

Chen, J., Xie, C., Tian, L., Hong, L., Wu, X., and Han, J., 2010. Participation of the p38 pathway in Drosophila host defense against pathogenic bacteria and fungi [Online]. *Proceedings of the National Academy of Sciences of the United States of America*, 107(48), pp.20774–20779. Available from: http://www.ncbi.nlm.nih.gov/pmc/articles/PMC2996427/.

Chen, P., Nordstrom, W., Gish, B., and Abrams, J.M., 1996. grim, a novel cell death gene in Drosophila. [Online]. *Genes & Development* , 10(14), pp.1773–1782. Available from: http://genesdev.cshlp.org/content/10/14/1773.abstract.

Chiarugi, P., Pani, G., Giannoni, E., Taddei, L., Colavitti, R., Raugei, G., Symons, M., Borrello, S., Galeotti, T., and Ramponi, G., 2003. Reactive oxygen species as essential mediators of cell adhesion: the oxidative inhibition of a FAK tyrosine phosphatase is required for cell adhesion [Online]. *The Journal of Cell Biology*, 161(5), pp.933–944. Available from: http://www.ncbi.nlm.nih.gov/pmc/articles/PMC2172955/.

Chistiakov, D.A., Bobryshev, Y. V., and Orekhov, A.N., 2016. Macrophage-mediated cholesterol handling in atherosclerosis. *Journal of Cellular and Molecular Medicine*, 20(1), pp.17–28.

Cho, N.K., Keyes, L., Johnson, E., Heller, J., Ryner, L., Karim, F., and Krasnow, M.A., 2002.

Developmental Control of Blood Cell Migration by the Drosophila VEGF Pathway [Online]. *Cell*, 108(6), pp.865–876. Available from: http://www.sciencedirect.com/science/article/pii/S0092867402006761.

Clark, R.I., Woodcock, K.J., Geissmann, F., Trouillet, C., and Dionne, M.S., 2011. Multiple TGF-β Superfamily Signals Modulate the Adult Drosophila Immune Response [Online]. *Current Biology*, 21(19), pp.1672–1677. Available from: http://www.ncbi.nlm.nih.gov/pmc/articles/PMC3191266/.

Comber, K., 2014. *Investigation into the Molecular Mechanisms Governing Drosophila Embryonic Hemocyte Migration in vivo*. University of Bath.

Comber, K., Huelsmann, S., Evans, I., Sánchez-Sánchez, B.J., Chalmers, A., Reuter, R., Wood, W., and Martín-Bermudo, M.D., 2013. A dual role for the βPS integrin myospheroid in mediating Drosophila embryonic macrophage migration [Online]. *Journal of Cell Science*, 126(15), pp.3475–3484. Available from: http://www.ncbi.nlm.nih.gov/pmc/articles/PMC3730248/.

Cook, R.K., Christensen, S.J., Deal, J.A., Coburn, R.A., Deal, M.E., Gresens, J.M., Kaufman, T.C., and Cook, K.R., 2012. The generation of chromosomal deletions to provide extensive coverage and subdivision of the Drosophila melanogaster genome [Online]. *Genome Biology*, 13(3), p.R21. Available from: https://doi.org/10.1186/gb-2012-13-3-r21.

Cooper, J.A. and Sept, D.B.T.-I.R. of C. and M.B., 2008. New Insights into Mechanism and Regulation of Actin Capping Protein. In: Academic Press, pp.183–206. Available from: http://www.sciencedirect.com/science/article/pii/S1937644808006047.

Cordero, J.B., Macagno, J.P., Stefanatos, R.K., Strathdee, K.E., Cagan, R.L., and Vidal, M., 2010. Oncogenic Ras Diverts a Host TNF Tumor Suppressor Activity into Tumor Promoter [Online]. *Developmental Cell*, 18(6), pp.999–1011. Available from: http://www.sciencedirect.com/science/article/pii/S1534580710002509.

Crozatier, M. and Meister, M., 2007. Drosophila haematopoiesis [Online]. *Cellular Microbiology*, 9(5), pp.1117–1126. Available from: http://dx.doi.org/10.1111/j.1462-5822.2007.00930.x.

Cuttell, L., Vaughan, A., Silva, E., Escaron, C.J., Lavine, M., Van Goethem, E., Eid, J.P., Quirin, M., and Franc, N.C., 2008. Undertaker, a Drosophila Junctophilin, Links Draper-Mediated Phagocytosis and Calcium Homeostasis. *Cell*, 135(3), pp.524–534.

Davis, J.R., Huang, C.-Y., Zanet, J., Harrison, S., Rosten, E., Cox, S., Soong, D.Y., Dunn, G.A., and Stramer, B.M., 2012. Emergence of embryonic pattern through contact inhibition of locomotion [Online]. *Development*, 139(24), p.4555 LP-4560. Available from: http://dev.biologists.org/content/139/24/4555.abstract.

Davis, J.R., Luchici, A., Mosis, F., Thackery, J., Salazar, J.A., Mao, Y., Dunn, G.A., Betz, T., Miodownik, M., and Stramer, B.M., 2015. Inter-cellular forces orchestrate contact inhibition of locomotion [Online]. *Cell*, 161(2), pp.361–373. Available from: http://dx.doi.org/10.1016/j.cell.2015.02.015.

Demedts, I.K., Demoor, T., Bracke, K.R., Joos, G.F., and Brusselle, G.G., 2006. Role of apoptosis in the pathogenesis of COPD and pulmonary emphysema [Online]. *Respiratory Research*, 7(1), p.53. Available from: http://www.ncbi.nlm.nih.gov/pmc/articles/PMC1501017/.

Devenport, D. and Brown, N.H., 2004. Morphogenesis in the absence of integrins: mutation of both Drosophila β subunits prevents midgut migration [Online]. *Development*, 131(21), p.5405 LP-5415. Available from: http://dev.biologists.org/content/131/21/5405.abstract.

van den Eijnde, S.M., Boshart, L., Baehrecke, E.H., De Zeeuw, C.I., Reutelingsperger, C.P.M., and Vermeij-Keers, C., 1998. Cell surface exposure of phosphatidylserine during apoptosis is phylogenetically conserved [Online]. *Apoptosis*, 3(1), pp.9–16. Available from: https://doi.org/10.1023/A:1009650917818.

Elliott, M.R., Chekeni, F.B., Trampont, P.C., Lazarowski, E.R., Kadl, A., Walk, S.F., Park, D., Woodson, R.I., Ostankovich, M., Sharma, P., Lysiak, J.J., Harden, T.K., Leitinger, N., and Ravichandran, K.S., 2009. Nucleotides released by apoptotic cells act as a find-me signal to promote phagocytic clearance [Online]. *Nature*, 461(7261), pp.282–286. Available from: http://www.nature.com/doifinder/10.1038/nature08296 [Accessed 24 August 2017].

Elliott, M.R. and Ravichandran, K.S., 2010. Clearance of apoptotic cells: implications in health and disease [Online]. *The Journal of Cell Biology*, 189(7), p.1059 LP-1070. Available from: http://jcb.rupress.org/content/189/7/1059.abstract.

Ellis, R.E., Jacobson, D.M., and Horvitz, H.R., 1991. Genes required for the engulfment of cell corpses during programmed cell death in Caenorhabditis elegans. [Online]. *Genetics*, 129(1), p.79 LP-94. Available from: http://www.genetics.org/content/129/1/79.abstract.

Etchegaray, J.I., Timmons, A.K., Klein, A.P., Pritchett, T.L., Welch, E., Meehan, T.L., Li, C., and McCall, K., 2012. Draper acts through the JNK pathway to control synchronous engulfment of dying germline cells by follicular epithelial cells [Online]. *Development (Cambridge, England)*, 139(21), pp.4029–4039. Available from: http://www.ncbi.nlm.nih.gov/pmc/articles/PMC3472587/.

Evans, C.J., Hartenstein, V., and Banerjee, U., 2003. Thicker Than Blood: Conserved Mechanisms in Drosophila and Vertebrate Hematopoiesis [Online]. *Developmental Cell*, 5(5), pp.673–690. Available from: http://www.sciencedirect.com/science/article/pii/S1534580703003356.

Evans, I.R., Ghai, P.A., Urbančič, V., Tan, K.L., and Wood, W., 2013. SCAR/WAVE-mediated processing of engulfed apoptotic corpses is essential for effective macrophage migration in Drosophila. *Cell Death and Differentiation*, 20(5), pp.709–720.

Evans, I.R., Hu, N., Skaer, H., and Wood, W., 2010. Interdependence of macrophage migration and ventral nerve cord development in Drosophila embryos [Online]. *Development*, 137(10), pp.1625–1633. Available from: http://dx.doi.org/10.1242/dev.046797%5Cnhttp://dev.biologists.org/content/137/10/1625.short%5Cnhttp://www.ncbi.nlm.nih.gov/pubmed/20392742%5Cnhttp://dev.biologists.org/content/137/10/1625.full.pdf%5Cnhttp://dev.biologists.org/cgi/doi/10.1242/dev.046797.

Evans, I.R., Rodrigues, F.S.L.M., Armitage, E.L., and Wood, W., 2015. Draper/CED-1 Mediates an Ancient Damage Response to Control Inflammatory Blood Cell Migration In Vivo. [Online]. *Current biology : CB*, 25(12), pp.1606–12. Available from: http://linkinghub.elsevier.com/retrieve/pii/S0960982215004881%5Cnhttp://www.ncbi.nlm.nih.gov/pubmed/26028435.

Evans, I.R. and Wood, W., 2014. Drosophila blood cell chemotaxis [Online]. *Current Opinion in Cell Biology*, 30, pp.1–8. Available from: http://www.sciencedirect.com/science/article/pii/S0955067414000441.

Fadok, V.A., Bratton, D.L., Konowal, A., Freed, P.W., Westcott, J.Y., and Henson, P.M., 1998. Macrophages that have ingested apoptotic cells in vitro inhibit proinflammatory cytokine production through autocrine/paracrine mechanisms involving TGF-??, PGE2, and PAF. *Journal of Clinical Investigation*, 101(4), pp.890–898.

Fadok, V.A., De Cathelineau, A., Daleke, D.L., Henson, P.M., and Bratton, D.L., 2001. Loss of phospholipid asymmetry and surface exposure of phosphatidylserine is required for phagocytosis of apoptotic cells by macrophages and fibroblasts. *Journal of Biological Chemistry*, 276(2), pp.1071–1077.

Fadok, V.A., Voelker, D.R., Campbell, P.A., Cohen, J.J., Bratton, D.L., and Henson, P.M., 1992. Exposure of phosphatidylserine on the surface of apoptotic lymphocytes triggers specific recognition and removal by macrophages. [Online]. *The Journal of Immunology*, 148(7), p.2207 LP-2216. Available from: http://www.jimmunol.org/content/148/7/2207.abstract.

Fadok, V.A., Warner, M.L., Bratton, D.L., and Henson, P.M., 1998. CD36 Is Required for Phagocytosis of Apoptotic Cells by Human Macrophages That Use Either a Phosphatidylserine Receptor or the Vitronectin Receptor (α_vβ₃) [Online]. *The Journal of Immunology*, 161(11), p.6250 LP-6257. Available from: http://www.jimmunol.org/content/161/11/6250.abstract.

Ferrante, A.W., Reinke, R., and Stanley, E.R., 1995. Shark, a Src homology 2, ankyrin repeat, tyrosine kinase, is expressed on the apical surfaces of ectodermal epithelia. [Online]. *Proceedings of the National Academy of Sciences of the United States of America*, 92(6), pp.1911–1915. Available from: http://www.ncbi.nlm.nih.gov/pmc/articles/PMC42392/.

Franc, N.C., Dimarcq, J.L., Lagueux, M., Hoffmann, J., and Ezekowitz, R.A.B., 1996.

Croquemort, a novel drosophila hemocyte/macrophage receptor that recognizes apoptotic cells. *Immunity*, 4(5), pp.431–443.

Franc, N.C., Heitzler, P., Ezekowitz, R.A.B., and White, K., 1999. Requirement for Croquemort in Phagocytosis of Apoptotic Cells in Drosophila [Online]. *Science*, 284(5422), pp.1991–1994. Available from: http://www.jstor.org.sheffield.idm.oclc.org/stable/2898169.

Freeman, M.R., Delrow, J., Kim, J., Johnson, E., and Doe, C.Q., 2003. Unwrapping Glial Biology [Online]. *Neuron*, 38(4), pp.567–580. Available from: http://www.sciencedirect.com/science/article/pii/S0896627303002897 [Accessed 29 March 2016].

Fullard, J.F., Kale, A., and Baker, N.E., 2009. Clearance of apoptotic corpses [Online]. *Apoptosis*, 14(8), pp.1029–1037. Available from: https://doi.org/10.1007/s10495-009-0335-9.

Gardai, S.J., McPhillips, K.A., Frasch, S.C., Janssen, W.J., Starefeldt, A., Murphy-Ullrich, J.E., Bratton, D.L., Oldenborg, P.A., Michalak, M., and Henson, P.M., 2005. Cell-surface calreticulin initiates clearance of viable or apoptotic cells through trans-activation of LRP on the phagocyte. *Cell*, 123(2), pp.321–334.

Ghosh, S., Singh, A., Mandal, S., and Mandal, L., 2015. Active Hematopoietic Hubs in Drosophila Adults Generate Hemocytes and Contribute to Immune Response [Online]. *Developmental Cell*, 33(4), pp.478–488. Available from: http://dx.doi.org/10.1016/j.devcel.2015.03.014.

Giesen, K., Hummel, T., Stollewerk, A., Harrison, S., Travers, A., and Klambt, C., 1997. Glial development in the Drosophila CNS requires concomitant activation of glial and repression of neuronal differentiation genes [Online]. *Development*, 124(12), p.2307 LP-2316. Available from: http://dev.biologists.org/content/124/12/2307.abstract.

van Goethem, E., Silva, E.A., Xiao, H., and Franc, N.C., 2012. The Drosophila TRPP cation channel, PKD2 and Dmel/Ced-12 act in genetically distinct pathways during apoptotic cell clearance. *PLoS ONE*, 7(2).

Gold, K.S. and Brückner, K., 2014. Drosophila as a model for the two myeloid blood cell systems in vertebrates [Online]. *Experimental hematology*, 42(8), pp.717–727. Available from: http://www.ncbi.nlm.nih.gov/pmc/articles/PMC5013032/.

Goyal, L., McCall, K., Agapite, J., Hartwieg, E., and Steller, H., 2000. Induction of apoptosis by Drosophila reaper, hid and grim through inhibition of IAP function [Online]. *The EMBO Journal*, 19(4), pp.589–597. Available from: http://www.ncbi.nlm.nih.gov/pmc/articles/PMC305597/.

Granderath, S., Stollewerk, A., Greig, S., Goodman, C.S., O'Kane, C.J., and Klambt, C., 1999. loco encodes an RGS protein required for Drosophila glial differentiation [Online]. *Development*, 126(8), p.1781 LP-1791. Available from: http://dev.biologists.org/content/126/8/1781.abstract.

Grether, M.E., Abrams, J.M., and Agapite, J., 1995. The head involution defective gene of Drosophila melanogaster functmns in programmed cell death. *Genes & Development*, 9, pp.1694–1708.

Gude, D.R., Alvarez, S.E., Paugh, S.W., Mitra, P., Yu, J., Griffiths, R., Barbour, S.E., Milstien, S., and Spiegel, S., 2008. Apoptosis induces expression of sphingosine kinase 1 to release sphingosine-1-phosphate as a "come-and-get-me" signal. [Online]. *FASEB journal : official publication of the Federation of American Societies for Experimental Biology*, 22(8), pp.2629–38. Available from: http://www.ncbi.nlm.nih.gov/pubmed/18362204 [Accessed 24 August 2017].

Guillou, A., Troha, K., Wang, H., Franc, N.C., and Buchon, N., 2016. The Drosophila CD36 Homologue croquemort Is Required to Maintain Immune and Gut Homeostasis during Development and Aging [Online]. *PLOS Pathogens*, 12(10), p.e1005961. Available from: https://doi.org/10.1371/journal.ppat.1005961.

Gupton, S.L. and Waterman-Storer, C.M., 2006. Spatiotemporal Feedback between Actomyosin and Focal-Adhesion Systems Optimizes Rapid Cell Migration [Online]. *Cell*, 125(7), pp.1361–1374. Available from: http://www.sciencedirect.com/science/article/pii/S0092867406007197.

Halter, D.A., Urban, J., Rickert, C., Ner, S.S., Ito, K., Travers, A.A., and Technau, G.M., 1995.

The homeobox gene repo is required for the differentiation and maintenance of glia function in the embryonic nervous system of Drosophila melanogaster [Online]. *Development*, 121(2), pp.317–332. Available from: http://dev.biologists.org/content/121/2/317.abstract.

Hamon, Y., Trompier, D., Ma, Z., Venegas, V., Pophillat, M., Mignotte, V., Zhou, Z., and Chimini, G., 2006. Cooperation between Engulfment Receptors: The Case of ABCA1 and MEGF10. R. Insall, ed. *PLoS ONE*, 1(1), p.e120.

Han, C., Song, Y., Xiao, H., Wang, D., Franc, N.C., Jan, L.Y., and Jan, Y.-N., 2014. Epidermal Cells Are the Primary Phagocytes in the Fragmentation and Clearance of Degenerating Dendrites in Drosophila [Online]. *Neuron*, 81(3), pp.544–560. Available from: http://www.sciencedirect.com/science/article/pii/S0896627313010891.

Hashimoto, Y., Tabuchi, Y., Sakurai, K., Kutsuna, M., Kurokawa, K., Awasaki, T., Sekimizu, K., Nakanishi, Y., and Shiratsuchi, A., 2009. Identification of Lipoteichoic Acid as a Ligand for Draper in the Phagocytosis of Staphylococcus aureus by Drosophila Hemocytes [Online]. *The Journal of Immunology*, 183(11), pp.7451–7460. Available from: http://www.jimmunol.org/cgi/doi/10.4049/jimmunol.0901032.

Hattori, H., Subramanian, K.K., Sakai, J., Jia, Y., Li, Y., Porter, T.F., Loison, F., Sarraj, B., Kasorn, A., Jo, H., Blanchard, C., Zirkle, D., McDonald, D., Pai, S.-Y., Serhan, C.N., and Luo, H.R., 2010. Small-molecule screen identifies reactive oxygen species as key regulators of neutrophil chemotaxis [Online]. *Proceedings of the National Academy of Sciences*, 107(8), p.3546 LP-3551. Available from: http://www.pnas.org/content/107/8/3546.abstract.

HEGYI, L., SKEPPER, J.N., CARY, N.A.T.R.B., and MITCHINSON, M.J., 1996. FOAM CELL APOPTOSIS AND THE DEVELOPMENT OF THE LIPID CORE OF HUMAN ATHEROSCLEROSIS [Online]. *The Journal of Pathology*, 180(4), pp.423–429. Available from: http://dx.doi.org/10.1002/(SICI)1096-9896(199612)180:4%3C423::AID-PATH677%3E3.0.CO.

Heino, T.I., Kärpänen, T., Wahlström, G., Pulkkinen, M., Eriksson, U., Alitalo, K., and Roos, C., 2001. The Drosophila VEGF receptor homolog is expressed in hemocytes [Online]. *Mechanisms of Development*, 109(1), pp.69–77. Available from: http://www.sciencedirect.com/science/article/pii/S092547730100510X.

Heit, B., Colarusso, P., and Kubes, P., 2005. Fundamentally different roles for LFA-1, Mac-1 and α₄-integrin in neutrophil chemotaxis [Online]. *Journal of Cell Science*, 118(22), p.5205 LP-5220. Available from: http://jcs.biologists.org/content/118/22/5205.abstract.

Heit, B., Robbins, S.M., Downey, C.M., Guan, Z., Colarusso, P., Miller, J.B., Jirik, F.R., and Kubes, P., 2008. PTEN functions to 'prioritize' chemotactic cues and prevent 'distraction' in migrating neutrophils. *Nature Immunology*, 9(7), pp.743–752.

Heit, B., Tavener, S., Raharjo, E., and Kubes, P., 2002. An intracellular signaling hierarchy determines direction of migration in opposing chemotactic gradients. *Journal of Cell Biology*, 159(1), pp.91–102.

Hochreiter-Hufford, A. and Ravichandran, K.S., 2013. Clearing the dead: Apoptotic cell sensing, recognition, engulfment, and digestion. *Cold Spring Harbor Perspectives in Biology*, 5(1).

Hodge, S., Hodge, G., Scicchitano, R., Reynolds, P.N., and Holmes, M., 2003. Alveolar macrophages from subjects with chronic obstructive pulmonary disease are deficient in their ability to phagocytose apoptotic airway epithelial cells. *Immunology and Cell Biology*, 81(4), pp.289–296.

Hoffmann, P.R., deCathelineau, A.M., Ogden, C.A., Leverrier, Y., Bratton, D.L., Daleke, D.L., Ridley, A.J., Fadok, V.A., and Henson, P.M., 2001. Phosphatidylserine (PS) induces PS receptor–mediated macropinocytosis and promotes clearance of apoptotic cells [Online]. *The Journal of Cell Biology*, 155(4), p.649 LP-660. Available from: http://jcb.rupress.org/content/155/4/649.abstract.

Holly, S.P., Larson, M.K., and Parise, L. V, 2000. Multiple Roles of Integrins in Cell Motility [Online]. *Experimental Cell Research*, 261(1), pp.69–74. Available from: http://www.sciencedirect.com/science/article/pii/S0014482700950407.

Homsy, J.G., Jasper, H., Peralta, X.G., Wu, H., Kiehart, D.P., and Bohmann, D., 2006. JNK signaling coordinates integrin and actin functions during Drosophila embryogenesis [Online]. *Developmental Dynamics*, 235(2), pp.427–434. Available from: http://dx.doi.org/10.1002/dvdy.20649.

Hosoya, T., Takizawa, K., Nitta, K., and Hotta, Y., 1995. Glial cells missing: A binary switch between neuronal and glial determination in drosophila. *Cell*, 82(6), pp.1025–1036.

Hsu, T.Y. and Wu, Y.C., 2010. Engulfment of Apoptotic Cells in C. elegans Is Mediated by Integrin α/SRC Signaling [Online]. *Current Biology*, 20(6), pp.477–486. Available from: http://dx.doi.org/10.1016/j.cub.2010.01.062.

Huelsmann, S., Hepper, C., Marchese, D., Knöll, C., and Reuter, R., 2006. The PDZ-GEF Dizzy regulates cell shape of migrating macrophages via Rap1 and integrins in the Drosophila embryo [Online]. *Development*, 133(15), p.2915 LP-2924. Available from: http://dev.biologists.org/content/133/15/2915.abstract.

Huttenlocher, A. and Horwitz, A.R., 2011. Integrins in Cell Migration [Online]. *Cold Spring Harbor Perspectives in Biology*, 3(9), p.a005074. Available from: http://www.ncbi.nlm.nih.gov/pmc/articles/PMC3181029/.

Huynh, M.N., Fadok, V.A., and Henson, P.M., 2002. Phosphatidylserine-dependent ingestion of apoptotic cells promotes TGF- β 1 secretion and the resolution of inflammation. *The Journal of clinical investigation*, 109(1), pp.41–50.

Hynes, R.O. and Zhao, Q., 2000. The Evolution of Cell Adhesion [Online]. *The Journal of Cell Biology*, 150(2), p.F89 LP-F96. Available from: http://jcb.rupress.org/content/150/2/F89.abstract.

Johnson, G.L. and Nakamura, K., 2007. The c-Jun Kinase/Stress-activated Pathway: Regulation, Function and Role in Human Disease [Online]. *Biochimica et biophysica acta*, 1773(8), pp.1341–1348. Available from: http://www.ncbi.nlm.nih.gov/pmc/articles/PMC1995559/.

Johnson, S., Michalak, M., Opas, M., and Eggleton, P., 2001. The ins and outs of calreticulin: from the ER lumen to the extracellular space [Online]. *Trends in Cell Biology*, 11(3), pp.122–129. Available from: http://www.sciencedirect.com/science/article/pii/S0962892401019262.

Jones, B.W., Fetter, R.D., Tear, G., and Goodman, C.S., 1995. Glial Cells Missing: a Genetic Switch That Controls Glial Versus Neuronal Fate. *Cell*, 82(6), pp.1013–1023.

Juncadella, I.J., Kadl, A., Sharma, A.K., Shim, Y.M., Hochreiter-Hufford, A., Borish, L., and Ravichandran, K.S., 2012. Apoptotic cell clearance by bronchial epithelial cells critically influences airway inflammation [Online]. *Nature*, 493, p.547. Available from: http://dx.doi.org/10.1038/nature11714.

Jung, S.-H., Evans, C.J., Uemura, C., and Banerjee, U., 2005. The Drosophila lymph gland as a developmental model of hematopoiesis [Online]. *Development*, 132(11), p.2521 LP-2533. Available from: http://dev.biologists.org/content/132/11/2521.abstract.

Kelly, E., Bailey, C.P., and Henderson, G., 2008. Agonist-selective mechanisms of GPCR desensitization [Online]. *British Journal of Pharmacology*, 153(Suppl 1), pp.S379–S388. Available from: http://www.ncbi.nlm.nih.gov/pmc/articles/PMC2268061/.

Kiessling, S. and Green, D.R., 2006a. Cell survival and proliferation in Drosophila S2 cells following apoptotic stress in the absence of the APAF-1 homolog, ARK, or downstream caspases [Online]. *Apoptosis*, 11(4), pp.497–507. Available from: https://doi.org/10.1007/s10495-006-5341-6.

Kiessling, S. and Green, D.R., 2006b. Cell survival and proliferation in Drosophila S2 cells following apoptotic stress in the absence of the APAF-1 homolog, ARK, or downstream caspases. *Apoptosis*, 11(4), pp.497–507.

Kinchen, J.M., 2010. A model to die for: signaling to apoptotic cell removal in worm, fly and mouse [Online]. *Apoptosis*, 15(9), pp.998–1006. Available from: https://doi.org/10.1007/s10495-010-0509-5.

Kinchen, J.M., Cabello, J., Klingele, D., Wong, K., Feichtinger, R., Schnabel, H., Schnabel, R., and Hengartner, M.O., 2005. Two pathways converge at CED-10 to mediate actin rearrangement and corpse removal in C. elegans [Online]. *Nature*, 434, p.93. Available

from: http://dx.doi.org/10.1038/nature03263.
Kinchen, J.M., Doukoumetzidis, K., Almendinger, J., Stergiou, L., Tosello-Trampont, A., Sifri, C.D., Hengartner, M.O., and Ravichandran, K.S., 2008. A pathway for phagosome maturation during engulfment of apoptotic cells [Online]. *Nature Cell Biology*, 10, p.556. Available from: http://dx.doi.org/10.1038/ncb1718.
Kinchen, J.M. and Ravichandran, K.S., 2008. Phagosome maturation: going through the acid test [Online]. *Nature Reviews Molecular Cell Biology*, 9, p.781. Available from: http://dx.doi.org/10.1038/nrm2515.
Kinne, R.W., Stuhlmüller, B., and Burmester, G.-R., 2007. Cells of the synovium in rheumatoid arthritis. Macrophages [Online]. *Arthritis Research & Therapy*, 9(6), p.224. Available from: http://www.ncbi.nlm.nih.gov/pmc/articles/PMC2246244/.
Klaes, A., Menne, T., Stollewerk, A., Scholz, H., and Klämbt, C., 1994. The Ets transcription factors encoded by the Drosophila gene pointed direct glial cell differentiation in the embryonic CNS [Online]. *Cell*, 78(1), pp.149–160. Available from: http://www.sciencedirect.com/science/article/pii/0092867494905819.
Klambt, C., 1993. The Drosophila gene pointed encodes two ETS-like proteins which are involved in the development of the midline glial cells [Online]. *Development*, 117(1), p.163 LP-176. Available from: http://dev.biologists.org/content/117/1/163.abstract.
Kolaczkowska, E. and Kubes, P., 2013. Neutrophil recruitment and function in health and inflammation [Online]. *Nature Reviews Immunology*, 13, p.159. Available from: http://dx.doi.org/10.1038/nri3399.
Kornbluth, S. and White, K., 2005. Apoptosis in Drosophila: neither fish nor fowl (nor man, nor worm) [Online]. *Journal of Cell Science*, 118(9), p.1779 LP-1787. Available from: http://jcs.biologists.org/content/118/9/1779.abstract.
Krause, M. and Gautreau, A., 2014. Steering cell migration: lamellipodium dynamics and the regulation of directional persistence [Online]. *Nature Reviews Molecular Cell Biology*, 15, p.577. Available from: http://dx.doi.org/10.1038/nrm3861.
Kuraishi, T., Manaka, J., Kono, M., Ishii, H., Yamamoto, N., Koizumi, K., Shiratsuchi, A., Lee, B.L., Higashida, H., and Nakanishi, Y., 2007. Identification of calreticulin as a marker for phagocytosis of apoptotic cells in Drosophila. *Experimental Cell Research*, 313(3), pp.500–510.
Kuraishi, T., Nakagawa, Y., Nagaosa, K., Hashimoto, Y., Ishimoto, T., Moki, T., Fujita, Y., Nakayama, H., Dohmae, N., Shiratsuchi, A., Yamamoto, N., Ueda, K., Yamaguchi, M., Awasaki, T., and Nakanishi, Y., 2009. Pretaporter, a Drosophila protein serving as a ligand for Draper in the phagocytosis of apoptotic cells [Online]. *EMBO Journal*, 28(24), pp.3868–3878. Available from: http://dx.doi.org/10.1038/emboj.2009.343.
Kurant, E., Axelrod, S., Leaman, D., and Gaul, U., 2008. Six-Microns-Under Acts Upstream of Draper in the Glial Phagocytosis of Apoptotic Neurons. *Cell*, 133(3), pp.498–509.
Kurkulos, M., Weinberg, J.M., Pepling, M.E., and Mount, S.M., 1991. Polyadenylylation in copia requires unusually distant upstream sequences. [Online]. *Proceedings of the National Academy of Sciences*, 88(8), p.3038 LP-3042. Available from: http://www.pnas.org/content/88/8/3038.abstract.
Lanot, R., Zachary, D., Holder, F., and Meister, M., 2001. Postembryonic Hematopoiesis in Drosophila [Online]. *Developmental Biology*, 230(2), pp.243–257. Available from: http://www.sciencedirect.com/science/article/pii/S0012160600901234.
Lauber, K., Bohn, E., Kröber, S.M., Xiao, Y., Blumenthal, S.G., Lindemann, R.K., Marini, P., Wiedig, C., Zobywalski, A., Baksh, S., Xu, Y., Autenrieth, I.B., Schulze-Osthoff, K., Belka, C., Stuhler, G., and Wesselborg, S., 2003. Apoptotic Cells Induce Migration of Phagocytes via Caspase-3-Mediated Release of a Lipid Attraction Signal [Online]. *Cell*, 113(6), pp.717–730. Available from: http://linkinghub.elsevier.com/retrieve/pii/S0092867403004227 [Accessed 24 August 2017].
Laudanna, C., Kim, J.Y., Constantin, G., and Butcher, E.C., 2002. Rapid leukocyte integrin activation by chemokines. *Immunological Reviews*, 186, pp.37–46.
Lauffenburger, D.A. and Horwitz, A.F., 1996. Cell migration: A physically integrated molecular process. *Cell*, 84(3), pp.359–369.

Lebestky, T., Chang, T., Hartenstein, V., and Banerjee, U., 2000. Specification of Drosophila Hematopoietic Lineage by Conserved Transcription Factors [Online]. *Science*, 288(5463), p.146 LP-149. Available from: http://science.sciencemag.org/content/288/5463/146.abstract.

Lemaitre, B. and Hoffmann, J., 2007. The Host Defense of Drosophila melanogaster [Online]. *Annual Review of Immunology*, 25(1), pp.697–743. Available from: https://doi.org/10.1146/annurev.immunol.25.022106.141615.

Li, Y., Lee, P.Y., and Reeves, W.H., 2010. Monocyte and Macrophage Abnormalities in Systemic Lupus Erythematosus [Online]. *Archivum Immunologiae et Therapiae Experimentalis*, 58(5), pp.355–364. Available from: https://doi.org/10.1007/s00005-010-0093-y.

Van Lint, P. and Libert, C., 2007. Chemokine and cytokine processing by matrix metalloproteinases and its effect on leukocyte migration and inflammation [Online]. *Journal of Leukocyte Biology*, 82(6), pp.1375–1381. Available from: http://www.jleukbio.org/cgi/doi/10.1189/jlb.0607338.

Logan, M.A., Hackett, R., Doherty, J., Sheehan, A., Speese, S.D., and Freeman, M.R., 2012. Negative regulation of glial engulfment activity by Draper terminates glial responses to axon injury. *Nature Neuroscience*, 15(5), pp.722–730.

Lu, N. and Zhou, Z., 2012. Chapter eight - Membrane Trafficking and Phagosome Maturation During the Clearance of Apoptotic Cells. In: K. W. B. T.-I. R. of C. and M. B. Jeon, ed. Academic Press, pp.269–309. Available from: http://www.sciencedirect.com/science/article/pii/B9780123943040000130.

Lund, S.A., Wilson, C.L., Raines, E.W., Tang, J., Giachelli, C.M., and Scatena, M., 2013. Osteopontin mediates macrophage chemotaxis via ??4 and ??9 integrins and survival via the ??4 integrin. *Journal of Cellular Biochemistry*, 114(5), pp.1194–1202.

MacDonald, J.M., Beach, M.G., Porpiglia, E., Sheehan, A.E., Watts, R.J., and Freeman, M.R., 2006. The Drosophila Cell Corpse Engulfment Receptor Draper Mediates Glial Clearance of Severed Axons [Online]. *Neuron*, 50(6), pp.869–881. Available from: http://www.sciencedirect.com/science/article/pii/S0896627306003199.

MacDonald, J.M., Doherty, J., Hackett, R., and Freeman, M.R., 2013. The c-Jun kinase signaling cascade promotes glial engulfment activity through activation of draper and phagocytic function [Online]. *Cell Death and Differentiation*, 20(9), pp.1140–1148. Available from: http://www.ncbi.nlm.nih.gov/pmc/articles/PMC3741495/.

Maderna, P. and Godson, C., 2003. Phagocytosis of apoptotic cells and the resolution of inflammation [Online]. *Biochimica et Biophysica Acta (BBA) - Molecular Basis of Disease*, 1639(3), pp.141–151. Available from: http://www.sciencedirect.com/science/article/pii/S0925443903001467.

Makhijani, K., Alexander, B., Tanaka, T., Rulifson, E., and Bruckner, K., 2011. The peripheral nervous system supports blood cell homing and survival in the Drosophila larva [Online]. *Development*, 138(24), pp.5379–5391. Available from: http://dev.biologists.org/cgi/doi/10.1242/dev.067322.

Manaka, J., Kuraishi, T., Shiratsuchi, A., Nakai, Y., Higashida, H., Henson, P., and Nakanishi, Y., 2004. Draper-mediated and phosphatidylserine-independent phagocytosis of apoptotic cells by Drosophila hemocytes/macrophages. *Journal of Biological Chemistry*, 279(46), pp.48466–48476.

Mathias, J.R., Perrin, B.J., Liu, T.-X., Kanki, J., Look, A.T., and Huttenlocher, A., 2006. Resolution of inflammation by retrograde chemotaxis of neutrophils in transgenic zebrafish [Online]. *Journal of Leukocyte Biology*, 80(6), pp.1281–1288. Available from: http://dx.doi.org/10.1189/jlb.0506346.

Matsuda, M., Ota, S., Tanimura, R., Nakamura, H., Matuoka, K., Takenawa, T., Nagashima, K., and Kurata, T., 1996. Interaction between the amino-terminal SH3 domain of CRK and its natural target proteins. *Journal of Biological Chemistry*, 271(24), pp.14468–14472.

Meier, B., Zielinski, A., Weber, C., Arcizet, D., Youssef, S., Franosch, T., Rädler, J.O., and Heinrich, D., 2011. Chemotactic cell trapping in controlled alternating gradient fields [Online]. *Proceedings of the National Academy of Sciences*, 108(28), p.11417 LP-11422. Available from: http://www.pnas.org/content/108/28/11417.abstract.

Miyanishi, M., Tada, K., Koike, M., Uchiyama, Y., Kitamura, T., and Nagata, S., 2007. Identification of Tim4 as a phosphatidylserine receptor. *Nature*, 450(7168), pp.435–439.

Moreira, S., Stramer, B., Evans, I., Wood, W., and Martin, P., 2010. Prioritization of Competing Damage and Developmental Signals by Migrating Macrophages in the Drosophila Embryo [Online]. *Current Biology*, 20(5), pp.464–470. Available from: http://dx.doi.org/10.1016/j.cub.2010.01.047.

Mosser, D.M. and Edwards, J.P., 2008. Exploring the full spectrum of macrophage activation [Online]. *Nature reviews. Immunology*, 8(12), pp.958–969. Available from: http://www.ncbi.nlm.nih.gov/pmc/articles/PMC2724991/.

Mullins, R.D., Heuser, J.A., and Pollard, T.D., 1998. The interaction of Arp2/3 complex with actin: Nucleation, high affinity pointed end capping, and formation of branching networks of filaments [Online]. *Proceedings of the National Academy of Sciences*, 95(11), pp.6181–6186. Available from: http://www.pnas.org/cgi/doi/10.1073/pnas.95.11.6181.

Murray, P.J. and Wynn, T.A., 2011. Protective and pathogenic functions of macrophage subsets [Online]. *Nature Reviews Immunology*, 11, p.723. Available from: http://dx.doi.org/10.1038/nri3073.

Nagaosa, K., Okada, R., Nonaka, S., Takeuchi, K., Fujita, Y., Miyasaka, T., Manaka, J., Ando, I., and Nakanishi, Y., 2011. Integrin βv-mediated phagocytosis of apoptotic cells in Drosophila embryos. *Journal of Biological Chemistry*, 286(29), pp.25770–25777.

Nagel, B.M., Bechtold, M., Rodriguez, L.G., and Bogdan, S., 2017. Drosophila WASH is required for integrin-mediated cell adhesion, cell motility and lysosomal neutralization [Online]. *Journal of Cell Science*, 130(2), p.344 LP-359. Available from: http://jcs.biologists.org/content/130/2/344.abstract.

Ni, J.-Q., Liu, L.-P., Binari, R., Hardy, R., Shim, H.-S., Cavallaro, A., Booker, M., Pfeiffer, B.D., Markstein, M., Wang, H., Villalta, C., Laverty, T.R., Perkins, L.A., and Perrimon, N., 2009. A Drosophila Resource of Transgenic RNAi Lines for Neurogenetics [Online]. *Genetics*, 182(4), p.1089 LP-1100. Available from: http://www.genetics.org/content/182/4/1089.abstract.

Niethammer, P., Grabher, C., Look, A.T., and Mitchison, T.J., 2009. A tissue-scale gradient of hydrogen peroxide mediates rapid wound detection in zebrafish [Online]. *Nature*, 459(7249), pp.996–999. Available from: http://dx.doi.org/10.1038/nature08119.

Nonaka, S., Nagaosa, K., Mori, T., Shiratsuchi, A., and Nakanishi, Y., 2013. Integrin ??pS3/??-mediated Phagocytosis of Apoptotic Cells and Bacteria in Drosophila. *Journal of Biological Chemistry*, 288(15), pp.10374–10380.

Nourshargh, S., Renshaw, S.A., and Imhof, B.A., 2016. Reverse Migration of Neutrophils: Where, When, How, and Why? [Online]. *Trends in Immunology*, 37(5), pp.273–286. Available from: http://dx.doi.org/10.1016/j.it.2016.03.006.

O'Reilly, P., Gaggar, A., and Blalock, J.E., 2008. Interfering with extracellular matrix degradation to blunt inflammation [Online]. *Current opinion in pharmacology*, 8(3), pp.242–248. Available from: http://www.ncbi.nlm.nih.gov/pmc/articles/PMC2491454/.

Okada, R., Nagaosa, K., Kuraishi, T., Nakayama, H., Yamamoto, N., Nakagawa, Y., Dohmae, N., Shiratsuchi, A., and Nakanishi, Y., 2012. Apoptosis-dependent externalization and involvement in apoptotic cell clearance of DmCaBP1, an endoplasmic reticulum protein of Drosophila. *Journal of Biological Chemistry*, 287(5), pp.3138–3146.

Olofsson, B. and Page, D.T., 2005. Condensation of the central nervous system in embryonic Drosophila is inhibited by blocking hemocyte migration or neural activity [Online]. *Developmental Biology*, 279(1), pp.233–243. Available from: http://www.sciencedirect.com/science/article/pii/S0012160604008711.

Oppenheim, R.W., 1991. Cell Death During Development of the Nervous System [Online]. *Annual Review of Neuroscience*, 14(1), pp.453–501. Available from: https://doi.org/10.1146/annurev.ne.14.030191.002321.

Park, D., Tosello-Trampont, A.C., Elliott, M.R., Lu, M., Haney, L.B., Ma, Z., Klibanov, A.L., Mandell, J.W., and Ravichandran, K.S., 2007. BAI1 is an engulfment receptor for apoptotic cells upstream of the ELMO/Dock180/Rac module. *Nature*, 450(7168), pp.430–434.

Park, S.-Y., Jung, M.-Y., Lee, S.-J., Kang, K.-B., Gratchev, A., Riabov, V., Kzhyshkowska, J.,

and Kim, I.-S., 2009. Stabilin-1 mediates phosphatidylserine-dependent clearance of cell corpses in alternatively activated macrophages [Online]. *Journal of Cell Science*, 122(18), pp.3365–3373. Available from: http://jcs.biologists.org/cgi/doi/10.1242/jcs.049569.

Pasic, L., Kotova, T., and Schafer, D.A., 2008. Ena/VASP proteins capture actin filament barbed ends. *Journal of Biological Chemistry*, 283(15), pp.9814–9819.

Pastor-Pareja, J.C., Wu, M., and Xu, T., 2008. An innate immune response of blood cells to tumors and tissue damage in Drosophila [Online]. *Disease Models & Mechanisms*, 1(2–3), pp.144–154. Available from: http://www.ncbi.nlm.nih.gov/pmc/articles/PMC2562178/.

Penberthy, K.K. and Ravichandran, K.S., 2016. Apoptotic cell recognition receptors and scavenger receptors [Online]. *Immunological Reviews*, 269(1), pp.44–59. Available from: http://dx.doi.org/10.1111/imr.12376.

Pollard, J.W., 2004. Tumour-educated macrophages promote tumour progression and metastasis [Online]. *Nature Reviews Cancer*, 4, p.71. Available from: http://dx.doi.org/10.1038/nrc1256.

Poon, I.K.H., Lucas, C.D., Rossi, A.G., and Ravichandran, K.S., 2014. Apoptotic cell clearance: basic biology and therapeutic potential [Online]. *Nature reviews. Immunology*, 14(3), pp.166–180. Available from: http://www.ncbi.nlm.nih.gov/pmc/articles/PMC4040260/.

Rämet, M., Lanot, R., Zachary, D., and Manfruelli, P., 2002. JNK Signaling Pathway Is Required for Efficient Wound Healing in Drosophila [Online]. *Developmental Biology*, 241(1), pp.145–156. Available from: http://www.sciencedirect.com/science/article/pii/S0012160601905020.

Ratheesh, A., Belyaeva, V., and Siekhaus, D.E., 2015. Drosophila immune cell migration and adhesion during embryonic development and larval immune responses [Online]. *Current Opinion in Cell Biology*, 36, pp.71–79. Available from: http://www.sciencedirect.com/science/article/pii/S0955067415000782.

Razzell, W., Evans, I.R., Martin, P., and Wood, W., 2013. Calcium Flashes Orchestrate the Wound Inflammatory Response through DUOX Activation and Hydrogen Peroxide Release [Online]. *Current Biology*, 23(5), pp.424–429. Available from: http://www.ncbi.nlm.nih.gov/pmc/articles/PMC3629559/.

Rehorn, K.P., Thelen, H., Michelson, a M., and Reuter, R., 1996. A molecular aspect of hematopoiesis and endoderm development common to vertebrates and Drosophila. *Development (Cambridge, England)*, 122(12), pp.4023–4031.

Ridley, A.J., 2001. Rho GTPases and cell migration [Online]. *Journal of Cell Science*, 114(15), p.2713 LP-2722. Available from: http://jcs.biologists.org/content/114/15/2713.abstract.

Ridley, A.J., 2011. Life at the leading edge [Online]. *Cell*, 145(7), pp.1012–1022. Available from: http://dx.doi.org/10.1016/j.cell.2011.06.010.

Robertson, A.L., Holmes, G.R., Bojarczuk, A.N., Burgon, J., Loynes, C.A., Chimen, M., Sawtell, A.K., Hamza, B., Willson, J., Walmsley, S.R., Anderson, S.R., Coles, M.C., Farrow, S.N., Solari, R., Jones, S., Prince, L.R., Irimia, D., Rainger, G.E., Kadirkamanathan, V., Whyte, M.K.B., and Renshaw, S.A., 2014. A Zebrafish Compound Screen Reveals Modulation of Neutrophil Reverse Migration as an Anti-Inflammatory Mechanism [Online]. *Science Translational Medicine*, 6(225), p.225ra29 LP-225ra29. Available from: http://stm.sciencemag.org/content/6/225/225ra29.abstract.

Rogulja-Ortmann, A., Lüer, K., Seibert, J., Rickert, C., and Technau, G.M., 2007. Programmed cell death in the embryonic central nervous system of Drosophila melanogaster [Online]. *Development*, 134(1), p.105 LP-116. Available from: http://dev.biologists.org/content/134/1/105.abstract.

Romero, S., Le Clainche, C., Didry, D., Egile, C., Pantaloni, D., and Carlier, M.F., 2004. Formin is a processive motor that requires profilin to accelerate actin assembly and associated ATP hydrolysis. *Cell*, 119(3), pp.419–429.

Rougerie, P., Miskolci, V., and Cox, D., 2013. Generation of membrane structures during phagocytosis and chemotaxis of macrophages: role and regulation of the actin cytoskeleton [Online]. *Immunological Reviews*, 256(1), pp.222–239. Available from: http://dx.doi.org/10.1111/imr.12118.

Sánchez-Sánchez, B.J., Urbano, J.M., Comber, K., Dragu, A., Wood, W., Stramer, B., and Martín-Bermudo, M.D., 2017. Drosophila Embryonic Hemocytes Produce Laminins to

Strengthen Migratory Response. *Cell Reports*, 21(6), pp.1461–1470.
Schmidt, H., Rickert, C., Bossing, T., Vef, O., Urban, J., and Technau, G.M., 1997. The Embryonic Central Nervous System Lineages ofDrosophila melanogaster [Online]. *Developmental Biology*, 189(2), pp.186–204. Available from: http://www.sciencedirect.com/science/article/pii/S0012160697986607.
Schott, S., Ambrosini, A., Barbaste, A., Benassayag, C., Gracia, M., Proag, A., Rayer, M., Monier, B., and Suzanne, M., 2017. A fluorescent toolkit for spatiotemporal tracking of apoptotic cells in living Drosophila tissues [Online]. *Development*, 144(20), p.3840 LP-3846. Available from: http://dev.biologists.org/content/144/20/3840.abstract.
Schrijvers, D.M., De Meyer, G.R.Y., Kockx, M.M., Herman, A.G., and Martinet, W., 2005. Phagocytosis of apoptotic cells by macrophages is impaired in atherosclerosis. *Arteriosclerosis, Thrombosis, and Vascular Biology*, 25(6), pp.1256–1261.
Schwabe, T., Bainton, R.J., Fetter, R.D., Heberlein, U., and Gaul, U., 2005. GPCR signaling is required for blood-brain barrier formation in Drosophila. *Cell*, 123(1), pp.133–144.
Segawa, K. and Nagata, S., 2015. An Apoptotic 'Eat Me' Signal: Phosphatidylserine Exposure [Online]. *Trends in Cell Biology*, 25(11), pp.639–650. Available from: https://www.sciencedirect.com/science/article/pii/S0962892415001531 [Accessed 7 January 2018].
Serinkan, B.F., Gambelli, F., Potapovich, A., Babu, H., Di Giuseppe, M., Ortiz, L.A., Fabisiak, J.P., and Kagan, V.E., 2005. Apoptotic cells quench reactive oxygen and nitrogen species and modulate TNF-α/TGF-β1 balance in activated macrophages: Involvement of phosphatidylserine-dependent and -independent pathways [1]. *Cell Death and Differentiation*, 12(8), pp.1141–1144.
Shen, Q., He, B., Lu, N., Conradt, B., Grant, B.D., and Zhou, Z., 2013. Phagocytic receptor signaling regulates clathrin and epsin-mediated cytoskeletal remodeling during apoptotic cell engulfment in C. elegans [Online]. *Development*, 140(15), p.3230 LP-3243. Available from: http://dev.biologists.org/content/140/15/3230.abstract.
Shimonaka, M., Katagiri, K., Nakayama, T., Fujita, N., Tsuruo, T., Yoshie, O., and Kinashi, T., 2003. Rap1 translates chemokine signals to integrin activation, cell polarization, and motility across vascular endothelium under flow [Online]. *The Journal of Cell Biology*, 161(2), p.417 LP-427. Available from: http://jcb.rupress.org/content/161/2/417.abstract.
Shklyar, B., Levy-Adam, F., Mishnaevski, K., and Kurant, E., 2013. Caspase Activity Is Required for Engulfment of Apoptotic Cells [Online]. *Molecular and Cellular Biology*, 33(16), pp.3191–3201. Available from: http://www.ncbi.nlm.nih.gov/pmc/articles/PMC3753910/.
Shklyar, B., Sellman, Y., Shklover, J., Mishnaevski, K., Levy-Adam, F., and Kurant, E., 2014. Developmental regulation of glial cell phagocytic function during Drosophila embryogenesis. *Developmental Biology*, 393(2), pp.255–269.
Shklyar, B., Shklover, J., and Kurant, E., 2013. Live Imaging of Apoptotic Cell Clearance during Drosophila Embryogenesis [Online]. *Journal of Visualized Experiments : JoVE*, (78), p.50151. Available from: http://www.ncbi.nlm.nih.gov/pmc/articles/PMC3855923/.
Siekhaus, D., Haesemeyer, M., Moffitt, O., and Lehmann, R., 2010. RhoL controls invasion and Rap1 localization during immune cell transmigration in Drosophila [Online]. *Nature Cell Biology*, 12(6), pp.605–610. Available from: http://dx.doi.org/10.1038/ncb2063.
Sims, D., Duchek, P., and Baum, B., 2009. PDGF/VEGF signaling controls cell size in Drosophila [Online]. *Genome Biology*, 10(2), p.R20. Available from: https://doi.org/10.1186/gb-2009-10-2-r20.
Sluss, H.K., Han, Z., Barrett, T., Davis, R.J., and Ip, Y.T., 1996. A JNK signal transduction pathway that mediates morphogenesis and an immune response in Drosophila. [Online]. *Genes & Development*, 10(21), pp.2745–2758. Available from: http://www.genesdev.org/cgi/doi/10.1101/gad.10.21.2745.
Song, Z., McCall, K., and Steller, H., 1997. DCP-1, a Drosophila Cell Death Protease Essential for Development [Online]. *Science*, 275(5299), pp.536–540. Available from: http://www.jstor.org.sheffield.idm.oclc.org/stable/2891807.
Sonnenfeld, M.J. and Jacobs, J.R., 1995. Macrophages and glia participate in the removal of

apoptotic neurons from the Drosophila embryonic nervous system [Online]. *The Journal of Comparative Neurology*, 359(4), pp.644–652. Available from: http://dx.doi.org/10.1002/cne.903590410.

Stark, K.A., Yee, G.H., Roote, C.E., Williams, E.L., Zusman, S., and Hynes, R.O., 1997. A novel alpha integrin subunit associates with betaPS and functions in tissue morphogenesis and movement during Drosophila development. [Online]. *Development (Cambridge, England)*, 124(22), pp.4583–94. Available from: http://www.ncbi.nlm.nih.gov/pubmed/9409675.

Stork, T., Bernardos, R., and Freeman, M.R., 2012. Analysis of glial cell development and function in Drosophila. *Cold Spring Harbor Protocols*, 7(1), pp.1–17.

Stramer, B., Moreira, S., Millard, T., Evans, I., Huang, C.-Y., Sabet, O., Milner, M., Dunn, G., Martin, P., and Wood, W., 2010. Clasp-mediated microtubule bundling regulates persistent motility and contact repulsion in Drosophila macrophages in vivo [Online]. *The Journal of Cell Biology*, 189(4), p.681 LP-689. Available from: http://jcb.rupress.org/content/189/4/681.abstract.

Stramer, B., Wood, W., Galko, M.J., Redd, M.J., Jacinto, A., Parkhurst, S.M., and Martin, P., 2005. Live imaging of wound inflammation in Drosophila embryos reveals key roles for small GTPases during in vivo cell migration [Online]. *The Journal of Cell Biology*, 168(4), p.567 LP-573. Available from: http://jcb.rupress.org/content/168/4/567.abstract.

Strand, M.R., 2008. The insect cellular immune response [Online]. *Insect Science*, 15(1), pp.1–14. Available from: http://dx.doi.org/10.1111/j.1744-7917.2008.00183.x.

Stuart, L.M., Bell, S.A., Stewart, C.R., Silver, J.M., Richard, J., Goss, J.L., Tseng, A.A., Zhang, A., El, J.B., and Moore, K.J., 2007. CD36 Signals to the Actin Cytoskeleton and Regulates Microglial Migration via a p130Cas Complex * □. , 282(37), pp.27392–27401.

Su, H.P., Nakada-Tsukui, K., Tosello-Trampont, A.C., Li, Y., Bu, G., Henson, P.M., and Ravichandran, K.S., 2002. Interaction of CED-6/GULP, an adapter protein involved in engulfment of apoptotic cells with CED-1 and CD91/low density lipoprotein receptor-related protein (LRP). *Journal of Biological Chemistry*, 277(14), pp.11772–11779.

Suraneni, P., Rubinstein, B., Unruh, J.R., Durnin, M., Hanein, D., and Li, R., 2012. The Arp2/3 complex is required for lamellipodia extension and directional fibroblast cell migration [Online]. *The Journal of Cell Biology*, 197(2), pp.239–251. Available from: http://www.ncbi.nlm.nih.gov/pmc/articles/PMC3328382/.

Szondy, Z., Garabuczi, É., Joós, G., Tsay, G.J., and Sarang, Z., 2014. Impaired Clearance of Apoptotic Cells in Chronic Inflammatory Diseases: Therapeutic Implications [Online]. *Frontiers in Immunology* , 5, p.354. Available from: https://www.frontiersin.org/article/10.3389/fimmu.2014.00354.

Szondy, Z., Sarang, Z., Kiss, B., Garabuczi, É., and Köröskényi, K., 2017. Anti-inflammatory Mechanisms Triggered by Apoptotic Cells during Their Clearance [Online]. *Frontiers in Immunology*, 8, p.909. Available from: http://www.ncbi.nlm.nih.gov/pmc/articles/PMC5539239/.

Takeshima, H., Komazaki, S., Nishi, M., Iino, M., and Kangawa, K., 2000. Junctophilins: A Novel Family of Junctional Membrane Complex Proteins [Online]. *Molecular Cell*, 6(1), pp.11–22. Available from: http://www.sciencedirect.com/science/article/pii/S1097276505000055.

Tan, H.-Y., Wang, N., Li, S., Hong, M., Wang, X., and Feng, Y., 2016. The Reactive Oxygen Species in Macrophage Polarization: Reflecting Its Dual Role in Progression and Treatment of Human Diseases [Online]. *Oxidative Medicine and Cellular Longevity*, 2016, pp.1–16. Available from: http://www.hindawi.com/journals/omcl/2016/2795090/.

Tauzin, S., Starnes, T.W., Becker, F.B., Lam, P., and Huttenlocher, A., 2014. Redox and Src family kinase signaling control leukocyte wound attraction and neutrophil reverse migration [Online]. *The Journal of Cell Biology*, 207(5), p.589 LP-598. Available from: http://jcb.rupress.org/content/207/5/589.abstract.

Tepass, U., Fessler, L.I., Aziz, A., and Hartenstein, V., 1994. Embryonic origin of hemocytes and their relationship to cell death in Drosophila [Online]. *Development*, 120(7), p.1829 LP-1837. Available from: http://dev.biologists.org/content/120/7/1829.abstract.

Thorp, E., Cui, D., Schrijvers, D.M., Kuriakose, G., and Tabas, I., 2008. Mertk receptor mutation reduces efferocytosis efficiency and promotes apoptotic cell accumulation and plaque necrosis in atherosclerotic lesions of Apoe-/- mice. *Arteriosclerosis, Thrombosis, and Vascular Biology*, 28(8), pp.1421–1428.

Truman, L.A., Ford, C.A., Pasikowska, M., Pound, J.D., Wilkinson, S.J., Dumitriu, I.E., Melville, L., Melrose, L.A., Ogden, C.A., Nibbs, R., Graham, G., Combadiere, C., and Gregory, C.D., 2008. CX3CL1/fractalkine is released from apoptotic lymphocytes to stimulate macrophage chemotaxis [Online]. *Blood*, 112(13), pp.5026–5036. Available from: http://www.ncbi.nlm.nih.gov/pubmed/18799722 [Accessed 24 August 2017].

Tucker, P.K., Evans, I.R., and Wood, W., 2011. Ena drives invasive macrophage migration in Drosophila embryos [Online]. *Disease Models & Mechanisms*, 4(1), p.126 LP-134. Available from: http://dmm.biologists.org/content/4/1/126.abstract.

Tung, T.T., Nagaosa, K., Fujita, Y., Kita, A., Mori, H., Okada, R., Nonaka, S., and Nakanishi, Y., 2013. Phosphatidylserine recognition and induction of apoptotic cell clearance by Drosophila engulfment receptor Draper [Online]. *The Journal of Biochemistry*, 153(5), pp.483–491. Available from: http://dx.doi.org/10.1093/jb/mvt014.

Urbano, J.M., Domínguez-Giménez, P., Estrada, B., and Martín-Bermudo, M.D., 2011. PS Integrins and Laminins: Key Regulators of Cell Migration during Drosophila Embryogenesis [Online]. C. Gonzalez, ed. *PLoS ONE*, 6(9), p.e23893. Available from: http://www.ncbi.nlm.nih.gov/pmc/articles/PMC3174947/.

Urbano, J.M., Torgler, C.N., Molnar, C., Tepass, U., López-Varea, A., Brown, N.H., de Celis, J.F., and Martín-Bermudo, M.D., 2009. Drosophila laminins act as key regulators of basement membrane assembly and morphogenesis [Online]. *Development*, 136(24), p.4165 LP-4176. Available from: http://dev.biologists.org/content/136/24/4165.abstract.

Verboon, J.M., Rahe, T.K., Rodriguez-Mesa, E., and Parkhurst, S.M., 2015. Wash functions downstream of Rho1 GTPase in a subset of Drosophila immune cell developmental migrations [Online]. R. Fehon, ed. *Molecular Biology of the Cell*, 26(9), pp.1665–1674. Available from: http://www.ncbi.nlm.nih.gov/pmc/articles/PMC4436778/.

Vieira, O. V, Botelho, R.J., and Grinstein, S., 2002. Phagosome maturation: aging gracefully [Online]. *Biochemical Journal*, 366(3), p.689 LP-704. Available from: http://www.biochemj.org/content/366/3/689.abstract.

Voll, R.E., Herrmann, M., Roth, E.A., Stach, C., Kalden, J.R., and Girkontaite, I., 1997. Immunosuppressive effects of apoptotic cells [Online]. *Nature*, 390(6658), pp.350–351. Available from: http://www.nature.com/doifinder/10.1038/37022.

Van Vré, E.A., Ait-Oufella, H., Tedgui, A., and Mallat, Z., 2012. Apoptotic cell death and efferocytosis in atherosclerosis. *Arteriosclerosis, Thrombosis, and Vascular Biology*, 32(4), pp.887–893.

van der Wal, A., 1999. Atherosclerotic plaque rupture – pathologic basis of plaque stability and instability [Online]. *Cardiovascular Research*, 41(2), pp.334–344. Available from: http://cardiovascres.oxfordjournals.org/cgi/doi/10.1016/S0008-6363(98)00276-4.

Wang, X., Wu, Y.-C., Fadok, V.A., Lee, M.-C., Gengyo-Ando, K., Cheng, L.-C., Ledwich, D., Hsu, P.-K., Chen, J.-Y., Chou, B.-K., Henson, P., Mitani, S., and Xue, D., 2003. Cell Corpse Engulfment Mediated by C. elegans Phosphatidylserine Receptor Through CED-5 and CED-12 [Online]. *Science*, 302(5650), p.1563 LP-1566. Available from: http://science.sciencemag.org/content/302/5650/1563.abstract.

Wang, Y., Luo, G., Chen, J., Jiang, R., Zhu, J., Hu, N., Huang, W., Cheng, G., Jia, M., Su, B., Zhang, N., and Cui, T., 2017. Cigarette smoke attenuates phagocytic ability of macrophages through down-regulating Milk fat globule-EGF factor 8 (MFG-E8) expressions. *Scientific Reports*, 7(February), pp.1–12.

Weavers, H., Evans, I.R., Martin, P., and Wood, W., 2016. Corpse Engulfment Generates a Molecular Memory that Primes the Macrophage Inflammatory Response [Online]. *Cell*, 165(7), pp.1658–1671. Available from: http://www.ncbi.nlm.nih.gov/pmc/articles/PMC4912690/.

White, K., Grether, M.E., Abrams, J.M., Young, L., Farrell, K., and Steller, H., 1994. Genetic

control of programmed cell death in Drosophila. [Online]. *Science*, 264(5159), pp.677–83. Available from: http://www.ncbi.nlm.nih.gov/pubmed/8171319.

White, K., Tahaoglu, E., and Steller, H., 1996. Cell Killing by the Drosophila Gene reaper [Online]. *Science*, 271(5250), p.805 LP-807. Available from: http://science.sciencemag.org/content/271/5250/805.abstract.

Wood, W., Faria, C., and Jacinto, A., 2006. Distinct mechanisms regulate hemocyte chemotaxis during development and wound healing in Drosophila melanogaster. *Journal of Cell Biology*, 173(3), pp.405–416.

Wood, W. and Jacinto, A., 2007. Drosophila melanogaster embryonic haemocytes: Masters of multitasking. *Nature Reviews Molecular Cell Biology*, 8(7), pp.542–551.

Wu, H.-H., Bellmunt, E., Scheib, J.L., Venegas, V., Burkert, C., Reichardt, L.F., Zhou, Z., Farinas, I., and Carter, B.D., 2009. Glial Precursors Clear Sensory Neuron Corpses during Development via Jedi-1, an Engulfment Receptor [Online]. *Nature neuroscience*, 12(12), pp.1534–1541. Available from: http://www.ncbi.nlm.nih.gov/pmc/articles/PMC2834222/.

Xiong, W.C., Okano, H., Patel, N.H., Blendy, J.A., and Montell, C., 1994. repo encodes a glial-specific homeo domain protein required in the Drosophila nervous system. *Genes & development*, 8(8), pp.981–994.

Xu, Q., Huff, L.P., Fujii, M., and Griendling, K.K., 2017. Redox regulation of the actin cytoskeleton and its role in the vascular system [Online]. *Free Radical Biology and Medicine*, 109, pp.84–107. Available from: http://www.sciencedirect.com/science/article/pii/S0891584917301284.

Yeh, E., Gustafson, K., and Boulianne, G.L., 1995. Green fluorescent protein as a vital marker and reporter of gene expression in Drosophila. [Online]. *Proceedings of the National Academy of Sciences of the United States of America*, 92(15), pp.7036–7040. Available from: http://www.ncbi.nlm.nih.gov/pmc/articles/PMC41466/.

Yoo, S.K., Starnes, T.W., Deng, Q., and Huttenlocher, A., 2011. Lyn is a redox sensor that mediates leukocyte wound attraction in vivo [Online]. *Nature*, 480(7375), pp.109–112. Available from: http://dx.doi.org/10.1038/nature10632.

Yu, X., Odera, S., Chuang, C.H., Lu, N., and Zhou, Z., 2006. C. elegans Dynamin Mediates the Signaling of Phagocytic Receptor CED-1 for the Engulfment and Degradation of Apoptotic Cells. *Developmental Cell*, 10(6), pp.743–757.

Ziegenfuss, J.S., Biswas, R., Avery, M.A., Hong, K., Sheehan, A.E., Yeung, Y.-G., Stanley, E.R., and Freeman, M.R., 2008. Draper-dependent glial phagocytic activity is mediated by Src and Syk family kinase signalling [Online]. *Nature*, 453, p.935. Available from: http://dx.doi.org/10.1038/nature06901.

Appendix 1: Standard *Drosophila* medium and DABCO recipes

Standard *Drosophila* medium is prepared by according to the following recipe:

1 litre cold tap water

80g medium cornmeal

18g dried yeast

10g soya flour

80g malt extract

40g molasses

8g agar

25ml nipagin in absolute ethanol

4ml propionic acid

DABCO recipe: 1g DABCO (sigma) + 4ml 10x PBS + 36ml glycerol

Appendix 2: Fly lines generated for research

Chapter 3

Figure	Description	Genotype
3.1	control	*w;;crq-GAL4,UAS-GFP*
	repo^{03702}	*w;;repo^{03702},crq-GAL4,UAS-GFP*
3.2	control	*w;;crq-GAL4,UAS-GFP*
	repo^{03702}	*w;;repo^{03702},crq-GAL4,UAS-GFP*
3.3 A, B, E, F, G, H	control	*w;;crq-GAL4,UAS-GFP*
	repo^{03702}	*w;;repo^{03702},crq-GAL4,UAS-GFP*
3.3 C, D	control	*w;;crq-GAL4,UAS-nuclear red stinger*
	repo^{03702}	*w;;repo^{03702},crq-GAL4,UAS-nuclear red stinger*
3.4	control	*w;;crq-GAL4,UAS-GFP*
	repo^{03702}	*w;;repo^{03702},crq-GAL4,UAS-GFP*
3.5	control	*w;TRE-eGFP;crq-GAL4,UAS-nuclear red stinger*
	repo^{03702}	*w;TRE-eGFP;repo^{03702},crq-GAL4,UAS-nuclear red stinger*
3.6	control	*w;;crq-GAL4,UAS-nuclear red stinger*
	repo^{03702}	*w;;repo^{03702},crq-GAL4,UAS-nuclear red stinger*
3.7	control	*w;;crq-GAL4,UAS-GFP*
	repo^{03702}	*w;;repo^{03702},crq-GAL4,UAS-GFP*
	crq^{KO};repo^{03702}	*w;crq^{KO};repo^{03702},crq-GAL4,UAS-GFP*
	scb^{2};repo^{03702}	*w;scb^{2};repo^{03702},crq-GAL4,UAS-GFP*

	simu^{2};repo^{03702}	*w;simu^{2};repo^{03702},crq-GAL4,UAS-GFP*
	βυ^{1};repo^{03702}	*w;βυ^{1};repo^{03702},crq-GAL4,UAS-GFP*
3.8	control	*w;;crq-GAL4,UAS-GFP*
	p38a RNAi	*w;UAS-p38a RNAi;crq-GAL4,UAS-GFP*
	repo^{03702}	*w;;repo^{03702},crq-GAL4,UAS-GFP*
	p38a RNAi;repo^{03702}	*w;UAS-p38a RNAi;repo^{03702},crq-GAL4,UAS-GFP*
3.9	control	*w;;crq-GAL4,UAS-GFP*
	repo^{03702}	*w;;repo^{03702},crq-GAL4,UAS-GFP*
3.10	*control*	*w;srp-GAL4,UAS-GFP/srp-GAL4,UAS-nuclear red stinger*
	Df(3L)H99	*w;srp-GAL4,UAS-GFP/srp-GAL4,UAS-nuclear red stinger;Df(3L)H99*
	repo^{03702}	*w;srp-GAL4,UAS-GFP/srp-GAL4,UAS-nuclear red stinger;repo^{03702}*
	repo^{03702};Df(3L)H99	*w;srp-GAL4,UAS-GFP/srp-GAL4,UAS-nuclear red stinger;repo^{03702},Df(3L)H99*
3.11	*control*	*w;srp-GAL4,UAS-GFP/srp-GAL4,UAS-nuclear red stinger*
	Df(3L)H99	*w;srp-GAL4,UAS-GFP/srp-GAL4,UAS-nuclear red stinger;Df(3L)H99*
	repo^{03702}	*w;srp-GAL4,UAS-GFP/srp-GAL4,UAS-nuclear red stinger;repo^{03702}*
	repo^{03702};Df(3L)H99	*w;srp-GAL4,UAS-GFP/srp-GAL4,UAS-nuclear red stinger;repo^{03702},Df(3L)H99*
3.12	*control*	*w;srp-GAL4,UAS-GFP/srp-GAL4,UAS-nuclear red stinger*
	Df(3L)H99	*w;srp-GAL4,UAS-GFP/srp-GAL4,UAS-nuclear red stinger;Df(3L)H99*
	repo^{03702}	*w;srp-GAL4,UAS-GFP/srp-GAL4,UAS-nuclear red stinger;repo^{03702}*
	repo^{03702};Df(3L)H99	*w;srp-GAL4,UAS-GFP/srp-GAL4,UAS-nuclear red stinger;repo^{03702},Df(3L)H99*

Chapter 4

Figure	Description	Genotype
4.1	control	*w;;crq-GAL4,UAS-GFP*
	simu^2	*w;simu^2;crq-GAL4,UAS-GFP*
4.2	control	*w;;crq-GAL4,UAS-GFP*
	simu^2	*w;simu^2;crq-GAL4,UAS-GFP*
4.3	control	*w;;crq-GAL4,UAS-GFP*
	simu^2/+	*w;simu^2/+;crq-GAL4,UAS-GFP*
	Df(2L)BSC253/+	*w;Df(2L)BSC253/+;crq-GAL4,UAS-GFP*
	simu^2/Df(2L)BSC253	*w;simu^2/Df(2L)BSC253;crq-GAL4,UAS-GFP*
4.4	control	*w;;crq-GAL4,UAS-GFP*
	simu RNAi	*w;UAS-simu RNAi;crq-GAL4,UAS-GFP*
4.5	control	*w;srp-GAL4,UAS-nuclear red stinger/+;crq-GAL4,UAS-GFP/+*
	UAS-simu	*w;srp-GAL4,UAS-nuclear red stinger/+;UAS-simu/crq-GAL4,UAS-GFP*
	simu^2	*w;simu^2,srp-GAL4,UAS-nuclear red stinger/simu^2;crq-GAL4,UAS-GFP/+*
	simu^2;UAS-simu	*w;simu^2,srp-GAL4,UAS-nuclear red stinger/simu^2;UAS-simu/crq-GAL4,UAS-GFP*
4.6 A, A',B, B', D, E	control	*w;;crq-GAL4,UAS-GFP*
	simu^2	*w;simu^2;crq-GAL4,UAS-GFP*
4.6 C, C', F	control	*w;;crq-GAL4,UAS-nuclear red stinger*
	simu^2	*w;simu^2;crq-GAL4,UAS-nuclear red stinger*
4.7	control	*w;;crq-GAL4,UAS-GFP*
	simu^2	*w;simu^2;crq-GAL4,UAS-GFP*

4.8	control	*w;TRE-eGFP;crq-GAL4,UAS-nuclear red stinger*
	simu^{2}	*w;TRE-eGFP,simu^{2};crq-GAL4,UAS-nuclear red stinger*
4.9	control	*w;;crq-GAL4,UAS-nuclear red stinger*
	simu^{2}	*w;simu^{2};crq-GAL4,UAS-nuclear red stinger*
4.10	control	*w;;crq-GAL4,UAS-GFP*
	simu^{2}	*w;simu^{2};crq-GAL4,UAS-GFP*
4.11	control	*w;;crq-GAL4,UAS-GFP*
	simu RNAi	*w;UAS-simu RNAi;crq-GAL4,UAS-GFP*
4.12	control	*w;;crq-GAL4,UAS-GFP*
	Df(3L)H99	*w;;Df(3L)H99,crq-GAL4,UAS-GFP*
	simu^{2}	*w;simu^{2};crq-GAL4,UAS-GFP*
	simu^{2};Df(3L)H99	*w;simu^{2};Df(3L)H99,crq-GAL4,UAS-GFP*
4.13	control	*w;;crq-GAL4,UAS-GFP*
	Df(3L)H99	*w;;Df(3L)H99,crq-GAL4,UAS-GFP*
	simu^{2}	*w;simu^{2};crq-GAL4,UAS-GFP*
	simu^{2};Df(3L)H99	*w;simu^{2};Df(3L)H99,crq-GAL4,UAS-GFP*
4.14	control	*w;;crq-GAL4,UAS-GFP*
	Df(3L)H99	*w;;Df(3L)H99,crq-GAL4,UAS-GFP*
	simu^{2}	*w;simu^{2};crq-GAL4,UAS-GFP*
	simu^{2};Df(3L)H99	*w;simu^{2};Df(3L)H99,crq-GAL4,UAS-GFP*
4.15	control	*w;;crq-GAL4,UAS-GFP*
	Df(3L)H99	*w;;Df(3L)H99,crq-GAL4,UAS-GFP*
	simu^{2}	*w;simu^{2};crq-GAL4,UAS-GFP*
	simu^{2};Df(3L)H99	*w;simu^{2};Df(3L)H99,crq-GAL4,UAS-GFP*
4.16	control	*w;p{srp-GMA}*
	drpr$^{\Delta 5}$	*w;p{srp-GMA}; drpr$^{\Delta 5}$*
	simu^{2}	*w;simu^{2},p{srp-GMA}*

	simu^{2};drpr$^{\Delta 5}$	*w;simu^{2},p{srp-GMA}; drpr$^{\Delta 5}$*
4.17 A-C	*Df(3L)H99*	*w;;Df(3L)H99,crq-GAL4,UAS-GFP*
	simu^{2}	*w;simu^{2};crq-GAL4,UAS-GFP*
4.17 D-F	*Df(3L)H99*	*w;;Df(3L)H99,crq-GAL4,UAS-GFP*
	simu RNAi;Df(3L)H99	*w;UAS-simu RNAi;Df(3L)H99,crq-GAL4,UAS-GFP*

Chapter 5

Figure	**Description**	**Genotype**
5.1	control	*w;;crq-GAL4,UAS-GFP*
	LPC	*w;;crq-GAL4,UAS-GFP*
5.2	control	*w;;crq-GAL4,UAS-GFP*
	S-1-P	*w;;crq-GAL4,UAS-GFP*
5.3	control	*w;;crq-GAL4,UAS-GFP*
	N-H ATP	*w;;crq-GAL4,UAS-GFP*
5.5	control	*w;;crq-GAL4,UAS-GFP*
	AC supernatant	*w;;crq-GAL4,UAS-GFP*

Chapter 6

Figure	**Description**	**Genotype**
6.1	control	*w;;crq-GAL4,UAS-GFP*
	scb^{2}	*w;scb^{2};crq-GAL4,UAS-GFP*
	βv^{1}	*w;βv^{1};crq-GAL4,UAS-GFP*

	crq^{KO}	*w;crq^{KO};crq-GAL4,UAS-GFP*
	UAS-crq;crq^{KO}	*UAS-crq;crq^{KO};crq-GAL4,UAS-GFP*
6.2	control	*w;;crq-GAL4,UAS-GFP*
	crq RNAi	*w;UAS-crq RNAi;crq-GAL4,UAS-GFP*
	scab RNAi	*w;UAS-scab RNAi;crq-GAL4,UAS-GFP*
6.3	control	*w;;crq-GAL4,UAS-GFP*
	scb^{2}	*w;scb^{2};crq-GAL4,UAS-GFP*
	scab RNAi	*w;UAS-scab RNAi;crq-GAL4,UAS-GFP*
	βv^{1}	*w;βv^{1};crq-GAL4,UAS-GFP*
	crq^{KO}	*w;crq^{KO};crq-GAL4,UAS-GFP*
	UAS-crq;crq^{KO}	*UAS-crq;crq^{KO};crq-GAL4,UAS-GFP*
6.4	control	*w;;crq-GAL4,UAS-GFP*
	scb^{2}	*w;scb^{2};crq-GAL4,UAS-GFP*
	βv^{1}	*w;βv^{1};crq-GAL4,UAS-GFP*
	crq^{KO}	*w;crq^{KO};crq-GAL4,UAS-GFP*
6.5	control	*w;;crq-GAL4,UAS-GFP*
	scb^{2}	*w;scb^{2};crq-GAL4,UAS-GFP*
	βv^{1}	*w;βv^{1};crq-GAL4,UAS-GFP*
	crq^{KO}	*w;crq^{KO};crq-GAL4,UAS-GFP*
6.6	control	*w;;crq-GAL4,UAS-GFP*
	crq^{KO}	*w;crq^{KO};crq-GAL4,UAS-GFP*
	UAS-crq;crq^{KO}	*UAS-crq;crq^{KO};crq-GAL4,UAS-GFP*
	scb^{2}	*w;scb^{2};crq-GAL4,UAS-GFP*
	βv^{1}	*w;βv^{1};crq-GAL4,UAS-GFP*
6.7	control	*w;;crq-GAL4,UAS-GFP*
	crq RNAi	*w;UAS-crq RNAi;crq-GAL4,UAS-GFP*
6.8	control	*w;;crq-GAL4,UAS-GFP*
	Df(3L)H99	*w;;Df(3L)H99,crq-GAL4,UAS-GFP*
	βv^{1}	*w;βv^{1};crq-GAL4,UAS-GFP*

	βv^1;Df(3L)H99	*w;βv^1;Df(3L)H99,crq-GAL4,UAS-GFP*
6.9	control	*w;;crq-GAL4,UAS-GFP*
	Df(3L)H99	*w;;Df(3L)H99,crq-GAL4,UAS-GFP*
	scb^{01288}	*w;scb^{01288};crq-GAL4,UAS-GFP*
	scb^{01288};Df(3L)H99	*w;scb^{01288};Df(3L)H99,crq-GAL4,UAS-GFP*
	crq^{KO}	*w;crq^{KO};crq-GAL4,UAS-GFP*
	crq^{KO};Df(3L)H99	*w;crq^{KO};Df(3L)H99,crq-GAL4,UAS-GFP*
6.10	control	*w;;crq-GAL4,UAS-GFP*
	Df(3L)H99	*w;;Df(3L)H99,crq-GAL4,UAS-GFP*
	scb^{01288}	*w;scb^{01288};crq-GAL4,UAS-GFP*
	scb^{01288};Df(3L)H99	*w;scb^{01288};Df(3L)H99,crq-GAL4,UAS-GFP*
	crq^{KO}	*w;crq^{KO};crq-GAL4,UAS-GFP*
	crq^{KO};Df(3L)H99	*w;crq^{KO};Df(3L)H99,crq-GAL4,UAS-GFP*